Designing main group compounds for small molecule activation





Xiongfei Zheng

The Queen's College

Thesis submitted for the Degree of Doctor of Philosophy

October 2022

Acknowledgment

There is a Chinese saying describing time flies like a white horse went past through a gap. Four years spent in Oxford still feels like a dream where all these magic of science happens. Shifting from Material Science to Inorganic Chemistry was proved to be a right choice. I started to observe the objective world with a more in-depth way. 13 lab books, 1400 reactions, 50 novel structures, thousands of days and nights staying in front of my fumehood, and numerus failures have led me to this stage of graduation. And I know that graduation only represents the end of staying in this lab, but never means the termination of seeking the truth. Although being held up by the pandemic, I am glad that most of the experimental work was done nicely, and I can tell everyone a few stories about the chemistry that I have been doing during the past four years. I know that I can not finish these works alone and I would like to express my appreciations to everyone who is always supporting me during this journey.

First and foremost, I would like to thank my supervisor, Professor Simon Aldridge, for taking me into this group. His patience and encouragements have guided me through the exploration in chemistry. Also, he is one of the smartest people I have ever met. He can always find an amazing idea behind these subtle reactions and makes a persuasive punchline for writing the stories. This thesis can not be completed without his supervision and help.

I would like to thank my gorgeous labmates as well for accompanying me through the days. Dr. Andrey Protchenko, Dr. Ying Lu, Dr. Ying Kai Loh, Dr. Maria Fuentes-Dominguez, Dr. Ili Zulkifly, Dr. Matthew Roy, Dr. Alexa, Caise, Dr. Mathias Ellwanger, Dr. Yuwen Wang, Dr. Joe Boronski, Dr. Caitilin McManus, Dr. Anna Booth, Mr. Andreas Heilman, Mr. Simon Tholke, Mr. Agamemnon Crumpton, Mr. Aisling Roper, Mr. Lewis Wales, Mr. Liam Griffin, thank you all for your help in the lab. Among them, I would like to give my highest respect to Dr. Andrey Protchenko who have devoted himself into this field. The techniques he works

with the crystals and glasswares are the thing I can never look up. And the attitude he treats with the reactions and chemicals is the thing I should learn about. I love the stories he told me about his life in Moscow and Sussex and I wish him good health.

Lastly, I would like to thank my parents Jie Zheng and Mei Zhang, for their everlasting support mentally and financially. They taught me to be a man with integrity and honest, and there is nothing I can give them in return. I will always love them.

Abstract

This thesis reports on work aimed at designing main group compounds for small molecule activation, and includes studies of the reactivities of Frustrated Lewis Pairs (FLPs), low valent group 13 (gallium) compounds and low oxidation state group 14 compounds of tin and germanium towards H_2 and CO.

Chapter 3 discusses the synthesis of several xanthene and acridine based FLPs which can activate H_2 and CO reversibly. For the xanthene-based P/B FLP, H_2 can be activated under high pressure (4 atm), and the acridine-based bis-borane FLP systems are capable of capturing gaseous carbon monoxide. In the case of the $-BAr^f_2$ system CO uptake can be shown by VT-NMR studies to occur reversibly.

In Chapter 4, we report on the development of a mono-anionic phosphino-amide ligand based on a xanthene backbone, together with the synthesis of the corresponding Ga(I) complex, (PON)Ga, as a probe of its coordination properties in low valent main group chemistry.

In Chapter 5, we use a boryl substituted tin halide as a precursor to synthesize low oxidation state tin compounds. Here we describe the formation of formally Sn^I and Sn^0 compounds and their transformation into $[B]_4Sn_6$ ([B] = $(HCNDipp)_2B$); the mechanism has been studied by DFT methods and shown to proceed via a bisborylstannavinylidene intermediate. Moreover, we also isolated the tin cyclobutadiene dianion analogue of tin $K_2[B]_4Sn_4$ which can react with benzoic acid to give a neutral Sn_4 ring $[B]_4Sn_4H_2$. DFT studies shows that $K_2[B]_4Sn_4$ is not aromatic but the putative dication $[[B]_4Sn_4]^{2+}$ could be aromatic.

In Chapter 6, we used $K_2[B]_2Ge_2$ as nucleophile to react with LiI and catBBr, generating two planar digermene species $Li_2[B]_2Ge_2$ and [B]BcatGeGeBcat[B]. The latter was found to react with CO to form a boryl/borylcarboxylate stabilized digermyne, $[B]CO_2Ge_2[B]$; the

mechanism for the formation of [B]CO_2Ge_2[B] is proposed to proceed through a bisborylgermavinylidene intermediate. $K_2[B]_2Ge_2$ can also react with electrophile (IPrMe)$GeCl_2$ to form a Ge_3 unit which dimerizes on carbene abstraction leading to the formation of a $[B]_4Ge_6$ cluster, the germanium analogue of $[B]_4Sn_6$.

List of Abbreviations

The following abbreviations will be employed throughout this thesis

Ad = admantyl

Ar = aryl

Cy = *cyclo*-hexyl

DFT = Density Functional Theory

Dipp = 2,6-di-*iso*-propylphenyl

DMAP = 4-dimethylaminopyridine

ESD = estimated standard deviation

Et = ethyl

Hex = hexyl

h = hour(s)

hν = photon

HOMO = highest occupied molecular orbital

I^{i}PrMe = (^{i}PrNC(CH$_3$)$_2$)$_2$C:

^{i}Pr = *iso*-propyl

LA = Lewis acid

LB = Lewis base

LUMO = lowest unoccupied molecular orbital

Me = methyl

Mes = mesityl, 2,4,6-trimethylphenyl

NMR = nuclear magnetic resonance

Ph = phenyl

TMS = trimethylsilyl

ppm = parts per million

R = aliphatic group (unless otherwise stated)

rt = room temperature

^{t}Bu = *tert*-butyl

THF = tetrahydrofuran

Trip = 2,4,6-tri-*iso*-propylphenyl

[B] = $(HCNDipp)_2B$

Table of Contents

Chapter 1: Introduction **1**

1.1 Background 1

1.2 Frustrated Lewis Pairs (FLPs) for small molecule activation 2

1.2.1 Interaction between Lewis acid and Lewis base centres 3

1.2.2 Transition state of H_2 activation by FLPs 5

1.2.3 FLPs for catalytic processes 9

1.3 Low valent main group compounds for small molecule activation 10

1.3.1 Carbenes 11

1.3.2 Heavier carbene analogues and their reactivity 13

1.3.3 Low Valent Group 13 compounds and their reactivity 19

1.4 Multiple bonds for small molecule activation 25

1.4.1 Bonding in dimetallenes and dimetallynes 26

1.4.2 Reactivity of dimetallenes and dimetallynes 30

1.4.3 Vinylidenes 34

1.5 References 37

Chapter 2: General methods **45**

2.1 Spectroscopic and analytical techniques 45

2.2 References 47

Chapter 3: Designing FLPs for small molecule activation **48**

3.1 Introduction 48

3.2 Results and Discussion 51

3.3 Conclusions 62

3.4 Synthesis and characterization of novel compounds 63

3.5 References 75

Chapter 4: Low valent group 13 species supported by a mono anionic ligand 77

4.1 Introduction 77

4.2 Results and Discussion 78

4.3 Conclusions 86

4.4 Syntheses and characterization of novel compounds 87

4.5 References 96

Chapter 5: Low oxidation state boryl-tin compounds 99

5.1 Introduction 99

5.2 Results and Discussion 101

5.3 Conclusions 111

5.4 Synthesis and characterization of novel compounds 112

5.5 References 122

Chapter 6: Low oxidation state boryl-germanium compounds 122

6.1 Introduction 122

6.2 Results and Discussion 123

6.3 Conclusions 138

6.4 Synthesis and characterization of novel compounds 139

6.5 Computational Details 145

6.6 References 145

Chapter 1 Introduction

1.1 Background

Main group chemistry has traditionally been compared unfavourably with transition metal systems in terms of the availability of useful (industrially applicable) patterns of reactivity.[1] Transition metal complexes are widely used in catalytic processes, usually having partially occupied *d*-orbitals and small energy separations between frontier orbitals (HOMO-LUMO gap, Figure 1.1).[1] However, over the past few decades, key discoveries have revealed several types of main group compound that can behave like transition metal complexes on the basis of similar frontier orbital symmetries and narrow HOMO-LUMO gaps. Widely used industrial processes are often catalysed by transition metal compounds, which can be expensive and often toxic. While many main group compounds are not typically associated with these problems,[2] the further development of main group chemistry to allow *s* and *p*-block compounds to be used in small molecule activation and catalysis is necessary.

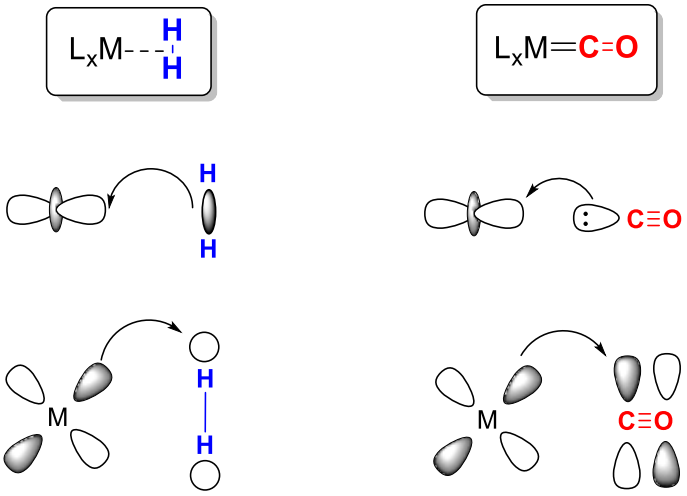


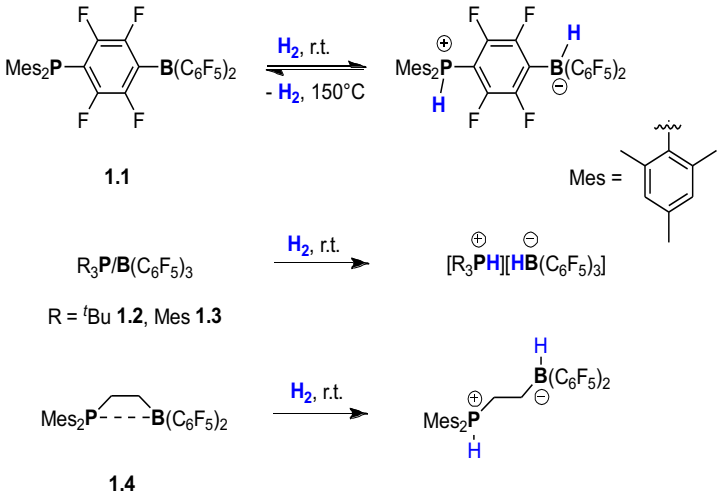
Figure 1.1 *Modes of interaction of transition metals reacting with H_2 and CO.*

For "typical" main group compounds, the *s* or *p* orbitals are either fully occupied or empty and are far apart energetically, making them unsuitable to interact with small molecules like CO,

C_2H_4 or H_2. Recent findings, however, have shown that main group compounds can be synthesized as stable species which can overcome these drawbacks. For example, Frustrated Lewis Pairs,[3] stable low-valent derivatives with open coordination sites,[4] and other compounds which for many years were thought to be short-lived or non-existent, have been shown not only to be isolable, but also to behave like transition metal systems in undergoing oxidative addition, reductive elimination, insertion reactions etc.

1.2 Frustrated Lewis Pairs (FLPs) for small molecule activation

The combination of sterically encumbered donors (Lewis bases) and acceptors (Lewis acids) which are unquenched by coordinate bond formation (known as FLPs), have drawn much attention for their abilities to activate small molecules and for the development of metal-free protocols for catalytic processes. Stephan *et al.* discovered that *p*-$(Mes_2PH)C_6F_4(BH(C_6F_5)_2)$ could reversibly release H_2 to yield *p*-$(Mes_2P)C_6F_4(B(C_6F_5)_2)$ (**1.1**, Scheme 1.1).[5] A key feature of the reaction is the steric prevention of the formation of a stable Lewis acid-base adduct, which permits the synergic interaction of the empty borane 2*p* orbital and the phosphine lone pair orbital with the H_2 molecule. The donor-acceptor reactivity of FLPs fulfils a similar function to the frontier orbitals of transition metals, in that the σ bond of H_2 interacts with the borane, accompanied by electron donation from the phosphine to the σ^* orbital of H_2. These processes ultimately lead to the cleavage of H_2, forming H^+ at phosphorus and H^- at boron.



Scheme 1.1 *Examples of the reversible H_2 activation by metal free FLPs.*

It is not only intramolecular FLPs that can activate H_2. The simple combination of $B(C_6F_5)_3/PR_3$ (R = ^{t}Bu **1.2** or Mes **1.3**) with H_2 can also yield the corresponding phosphonium/hydridoborate salts.[6] Subsequently Erker *et al*. reported an intramolecular ethylene bridged phosphine/borane FLP **1.4** that can also activate H_2 (Scheme 1.2.1).[7] Since these initial findings, FLPs have been shown to activate/capture a wide range of small molecules including CO_2, CO, SO_2, N_2O, NO,[8-13] olefins,[14] alkynes,[15] C-H bonds,[16] and other unsaturated substrates. Although the range of species exhibiting FLP reactivity has been extended to transition metals,[17] rare earth metals,[18] group 1 and 2 metals,[19-20] and classical Lewis acid-base adducts,[21] this thesis will mainly be concerned with "traditional" group 13/15 FLPs.

1.2.1 Interaction between Lewis acid and Lewis base centres

When talking about FLPs, the question rises as to how 'frustrated' the Lewis acid and Lewis base centres need to be for useful reactivity. The FLP report by Brown *et al.* in 1942[22] showed that no typical Lewis acid/base adduct was formed between 2,6-lutidine and trimethylborane, while the 2,6-lutidine-trifluoroborane adduct was readily formed. In this case, the more

sterically demanding methyl groups (compared with fluorine) help protect the Lewis acid centre and make it 'frustrated' during the reaction with the Lewis base. These results have also posed the question of how Lewis acids/bases interact in active FLPs. Further computational chemistry studies have probed the Lewis acid/base interaction. For example, the $^{t}Bu_3P/B(C_6F_5)_3$ pair **1.2** is proposed to form an associated "complex" by non-covalent $C_6F_5\cdots{}^{t}Bu$ interactions (Figure 1.2), allowing a H_2 molecule to enter the pocket between P and B centres. Molecular dynamics simulations have suggested that only ca. 2 % of the $^{t}Bu_3P/B(C_6F_5)_3$ compounds are associated with each other in toluene at any given time at room temperature.[23] NMR spectroscopy techniques were applied to probe the association of the $Mes_3P/B(C_6F_5)_3$ pair **1.3** in solution in which no preferential Lewis acid/base orientation is favoured, suggesting association via weak secondary dispersion interactions rather than Lewis acid/base interactions.[24]

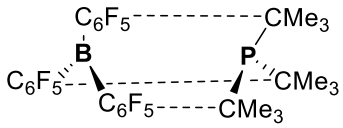


Figure 1.2 *Non-covalent $C_6F_5\cdots{}^{t}Bu$ interactions in intermolecular FLP* ***1.2****.*

Further studies were conducted using intramolecular FLPs. This type of FLP features a single molecule containing both the acidic and basic sites. The initially reported ethylene bridged P/B FLP **1.4**[7] was calculated to have a closed heterocyclic four-membered-ring structure with a weak P···B interaction. (- 6.1(10.7) kcal mol^{-1} compared to the open gauche form) (Figure 1.3).[25] The vicinal N/B FLP **1.5** has a short N-B distance (1.824(6) Å) in the solid state and the ^{11}B signal is at 9.1 ppm in solution, indicating that **1.5** is an intramolecular adduct (Figure 1.3).[26] The two sets of ^{19}F NMR signals observed for **1.5** slowly merge into one set upon warming to 363 K, implying the presence of homotopic C_6F_5 substituents. The N-B dissociation process was monitored by VT-NMR which revealed a Gibbs activation energy of $\Delta G^{\ddagger}$(298 K)

= 13.2 ± 0.2 kcal mol^{-1}. Similarly, the activation barriers determined for the chiral N/B FLP **1.6** and P/B FLP **1.7** were shown to be $\Delta G^{\ddagger}$(318 K) = 13.8 ± 0.2 kcal mol^{-1} and $\Delta G^{\ddagger}$(298 K) = 12.1 ± 0.3 kcal mol^{-1}, respectively. These data shows the N-B and P-B interactions are labile and rapid dissociate for these vicinal intramolecular FLPs, making subsequent reactivity towards small molecules viable.

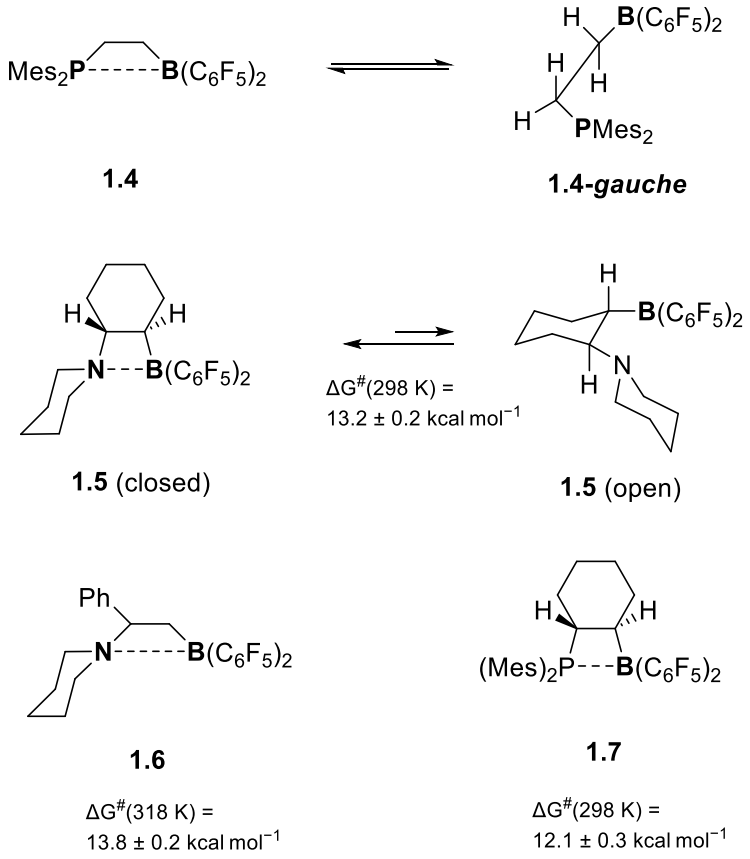


Figure 1.3 *"Frustration" in vicinal FLPs.*

1.2.2 Transition state of H_2 activation by FLPs

The reactions between $B(C_6F_5)_3/PR_3$ (R = ^{t}Bu **1.2** or Mes **1.3**) and H_2 were used as models to study the mechanism of heterolytic hydrogen splitting.[6] Side-on interaction of H_2 with the Lewis acid BR_3 (R = C_6F_5, C_6H_5) to form a $BR_3\cdots H_2$ "adduct" results in polarization of H_2, a subsequent protonation of the phosphine results in the formation of a phosphonium/hydridoborate salt. However, no evidence was found to support the formation of

such $BR_3\cdots H_2$ complexes even at low temperature (190 K) and elevated pressure of H_2 (ca. 4 atm). The alternative $PR_3\cdots H_2$ interaction can only be observed in a argon matrix.[27] Single-point SCS-MP2/cc-pVTZ energy calculations were applied to characterize the possible reaction pathways and intermediates.[28] A weakly bound $^tBu_3P\cdots B(C_6F_5)_3$ "adduct" was identified as a minimum with a P···B distance at 4.2 Å, held together by multiple C-H···F hydrogen bonds and dispersion interactions. When combined with H_2, a transition state in which H_2 interacts with both active centres of the FLP was found, lying only +10.4 kcal mol^{-1} higher in energy. Above the ground state, in the transition state structure, the H_2 molecule is nearly aligned with the P···B axis and the H-H bond is slightly elongated, which suggests an early transition state (ET model) for H-H bond cleavage. (Figure 1.4)

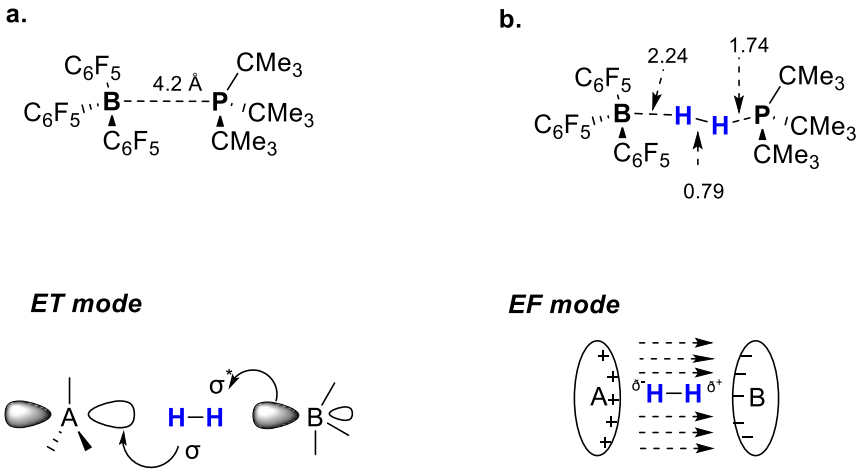


Figure 1.4 *(Upper) a. Pre-organization of* ***1.2*** *before H_2 activation. b. Transition state of H_2 entering into the 'pocket' of FLP. (Lower) Electron Transfer and Electron Field modes describing the activation of H_2 (A = Lewis acid; B = Lewis base).*

A conceptually different mechanistic scenario was proposed by Grimme *et al.*[25] It was proposed that the FLPs possess a significant electric field (EF) (Figure 1.4), such that the process of H_2 being exposed the FLP cavity leads to a heterolytic cleavage process that is almost barrierless. Pápai *et al.*[29] then examined the structural and electronic rearrangements and the EFs along the H_2 splitting pathways for a representative set of reactions, finding that a

simple electric-field-based model provides predictions that are very different from the computed features, even for the initial stages of the reaction. For example, strong EFs only show up in spherical regions rather than the "cavities" of the FLPs, and although the bond order of an H_2 molecule decreases in the EF, the change is much smaller than the values calculated in the presence of FLP components (and not strong enough to cleave H_2). Also, in the TS for cleavage, the angles between the orientation of H-H axis and the EF vector are calculated to be ca. 45° (on average) while they should be parallel if polarized by the EF. While in the ET model, Natural Bond Orbital (NBO) analysis confirms that the donor/acceptor interactions involve the $\sigma^*(H_2)/\sigma(H_2)$ orbitals. The H–H bond order decreases due to the population of the $\sigma^*(H_2)$ and depletion of the $\sigma(H_2)$ orbitals. At the same time, overlap between the donor orbital and $\sigma^*(H_2)$, as well as between the acceptor orbital and $\sigma(H_2)$, account for the formation of the B–H and H–A bonds and for the appearance of charges on the components of intermolecular donor/acceptor systems (Figure 1.5).[30]

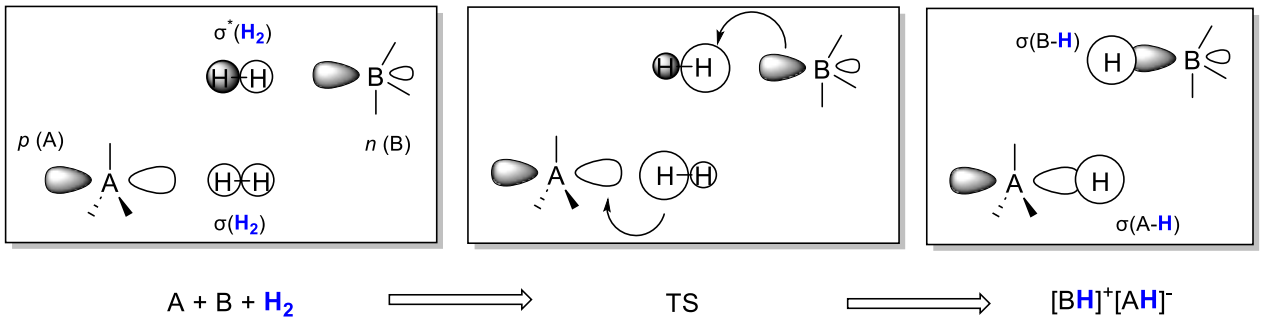
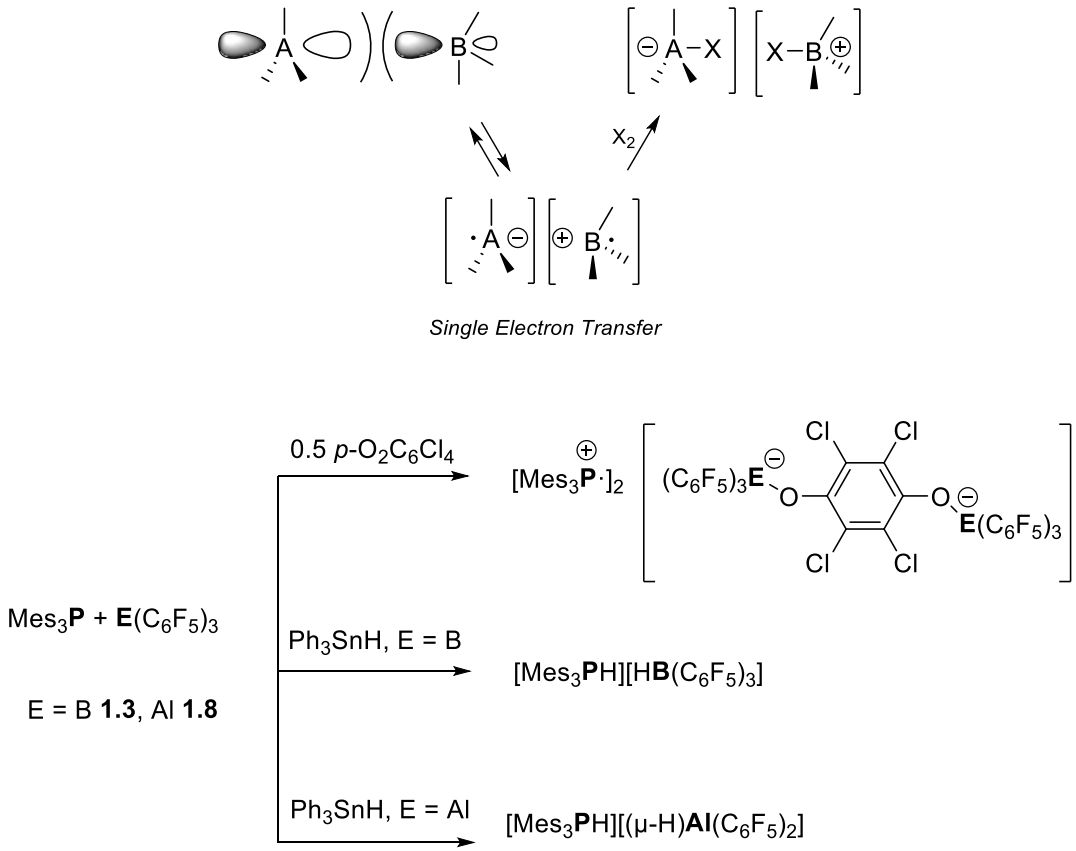


Figure 1.5 *ET mode interpretation for polarization and cleavage of H_2 and the formation of new hydrogenated product.*

In 2017, Stephan *et al.*[31] proposed a radical mechanism for FLP reactivity. They found that the reactions of $Mes_3P/E(C_6F_5)_3$ (E = B **1.3**, Al **1.8**) with *p*-$O_2C_6Cl_4$ gave the intermediates $[Mes_3P]^{\cdot}{}_2[(C_6F_5)_3EOC_6Cl_4OE(C_6F_5)_3]$ (E = B, Al), which supported a mechanism proceeding via a single-electron transfer (SET) process (Scheme 1.2). This SET proposal was further

supported by the reactions of $Mes_3P/E(C_6F_5)_3$ (E = B, Al) with Ph_3SnH, which yield $[Mes_3PH][HB(C_6F_5)_3]$ and $[Mes_3PH][(\mu\text{-}H)Al(C_6F_5)_2]$, respectively, together with $Ph_3SnSnPh_3$ (Scheme 1.2). The radical species generated by combining $Mes_3P/Al(C_6F_5)_3$ also give a room-temperature EPR spectrum consisting of a doublet resonance with a *g* value of 2.0089 and a hyperfine coupling constant of 238 G (attributed to the coupling of an unpaired electron to the phosphorus centre, and consistent with known triarylphosphine cations).[32-33]



Scheme 1.2 *(upper) Proposed mechanism for the activation of a generic substrate by FLPs via a SET process; (lower) Reactivity of $Mes_3P/E(C_6F_5)_3$ (E = B **1.3**, Al **1.8**) towards p-$O_2C_6Cl_4$ and Ph_3SnH.*

1.2.3 FLPs for catalytic processes

The rapid evolution of FLPs has led to the study of metal-free hydrogenation catalysis for various unsaturated organic substrates, including imines,[34] enamines,[35] silyl enol ethers,[36] olefins,[37] alkynes etc.[38,39] Using imines as an example, the mechanism for the hydrogenation process includes initial protonation of the basic organic substrate to generate an iminium ion intermediate which is then reduced by the hydridoborate component of the FLP-H_2 activated compound. (Figure 1.6)

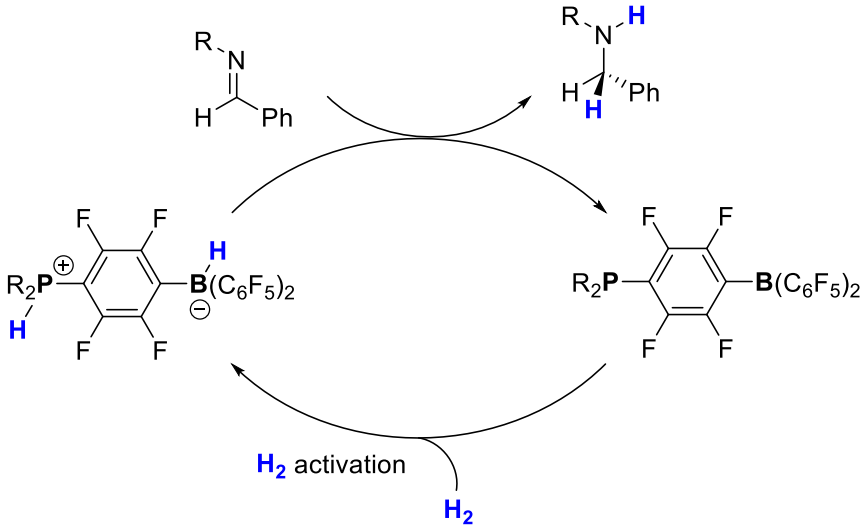
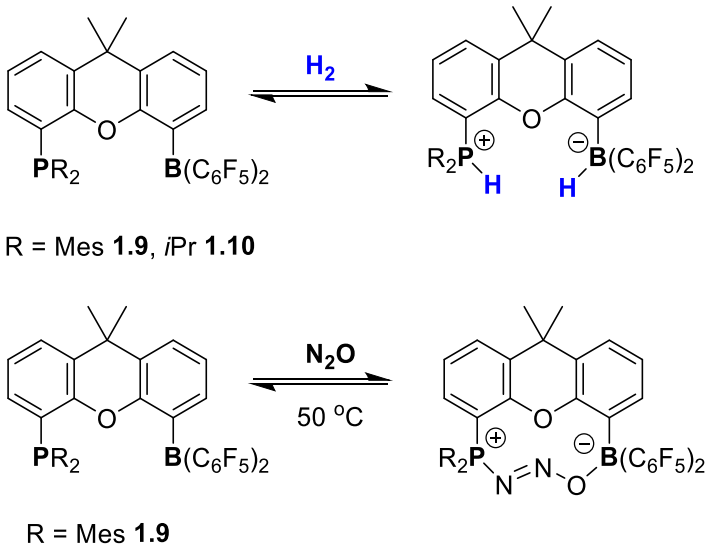


Figure 1.6 *Catalytic cycle for imine hydrogenation using FLP* ***1.1****.*

Reversibility in H_2 and other small molecule capture and release is a key requirement in potential applications of FLPs such as sensing and catalysis.[26, 34-35, 40] Such behaviour needs ΔG^o to be relatively close to zero, as well as the activation barriers in both directions ($\Delta G^{\ddagger}$) to be low. By using geometrically constrained FLPs system in which the Lewis acid and base are pre-organized onto a common backbone scaffold, the magnitude of $\Delta S^{\ddagger}$ can be lowered.[41]

Previous research[8,42] in our group showed a series of single component FLPs using a dimethylxanthene backbone that can be applied for small molecule capture, with the additional finding that through tuning of both the thermodynamics of activation ($\Delta G^o = -7.9$ kJ mol^{-1} at

295 K) and the degree of pre-organization, reversibility for H_2 and nitrous oxide capture can be achieved close to room temperature. (Scheme 1.3) By applying a pre-organized xanthene supported FLP, and tuning the acidity and basicity of the Lewis acid and base centres, controllable small molecule activation can then be achieved. More detailed exploration of this idea is reported in Chapter 3.



Scheme 1.3 *Xanthene based P/B FLPs for reversible H_2 and N_2O activation.*

1.3 Low valent main group compounds for small molecule activation

The presence of an element with an unusual valence state in a compound can suggest interesting structural or chemical features. For main group systems, the relative stability of lower oxidation and valence states within a given group tends to increase upon descending the group, a phenomenon which is generally referred to as the 'inert pair effect'. The combination of low coordination number, incompletely filled orbitals and available electrons make compounds containing these elements in low oxidation states or valence states significantly more reactive than their higher oxidation state relatives. For example, a low oxidation state can enable a typically electrophilic group 13 compound to act as an electron donor.[43-45] The basic structural and chemical properties of low oxidation state main group compounds have led to their use as

catalysts and as precursors for the formation other novel materials.[46] For example, Radosevich *et al*. developed a planar, trivalent phosphorus compound that is shown to undergo reversible two-electron redox cycling (P^{III}/P^{V}), enabling its use as catalyst for a transfer hydrogenation reactions.[47]

Historically, low valent main group compounds have proved hard to isolate, but recent studies in stabilising high reactive systems both kinetically (by using bulky ligands) and thermodynamically (by using π electron donating substituents) have allowed many examples to be accessed (e.g. carbenes[48] and their heavier congeners).[4]

1.3.1 Carbenes

Carbenes are defined as neutral compounds of divalent carbon in which the carbon atom possesses only six valence electrons. The two unshared electrons may either be paired and located in an sp^2 orbital (singlet state) or occupy two separate orbitals with parallel spins (triplet state, Figure 1.7).[49] In order to be of widespread synthetic utility,[48] carbenes need to be designed so that the singlet state is more stable than the more reactive diradical triplet state. In 1988, Bertrand *et al*.[50] used an adjacent phosphorus fragment to access the first isolable carbene $(TMS_2NP)(SiMe_3)C$: **1.11**, which was followed by the isolation of a stable cyclic imidazole-2-ylidene carbene $(HCNAd)_2C$: **1.12** by Arduengo *et al*.[51] in 1991. (Figure 1.7) Subsequently, numerous stable carbenes have been reported. Among them, N-heterocyclic carbenes ($(HCNR)_2C$:) represent the most widely investigated class in transition metal chemistry,[52-53] organo-catalysis,[54] main group chemistry etc.[55]

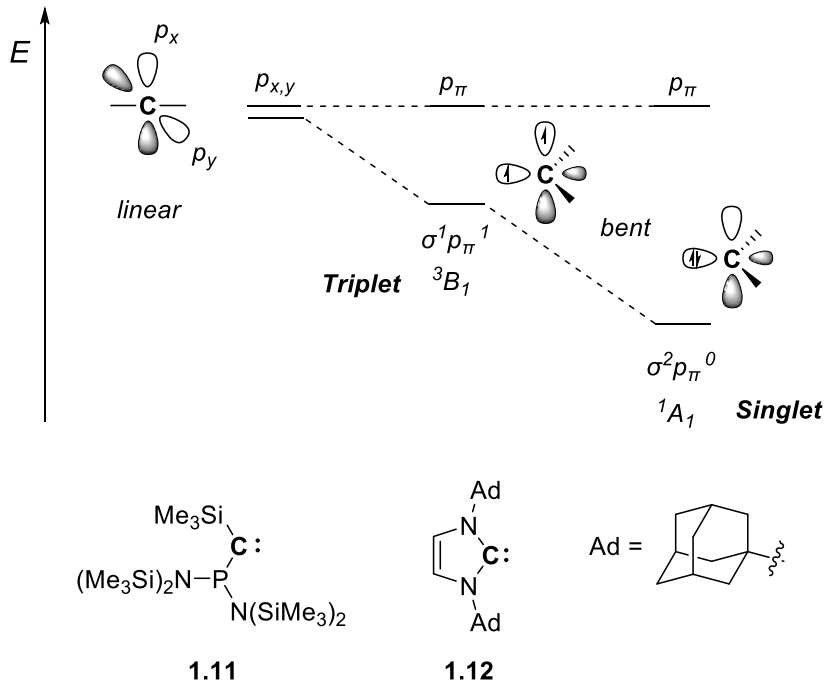


Figure 1.7 *(Upper) Frontier orbitals and possible electron configurations for a carbene, (Lower) Isolable acyclic carbene* ***1.11*** *and N-heterocyclic carbene* ***1.12****.*

Electronically, the σ-electron withdrawing and π-electron donating effects of the α nitrogens within a cyclic framework help stabilize the HOMO (lone pair) and destabilize the LUMO (unoccupied p_π), respectively (Figure 1.8). Thus, the energy separations between the HOMO and the LUMO and between the singlet and triplet ground states are increased. In addition to NHCs, Bertrand *et al.*[56] have synthesized cyclic(alkyl)amino carbenes (CAACs) which can be viewed as NHCs in which one of the amino substituents has been replaced by CR'$_2$. Substitution of the electronegative nitrogen makes the carbene more electron rich and also enhances the π acceptor abilities compared to NHCs (CAACs are both stronger nucleophiles and electrophiles). As such, CAACs have different chemical properties to NHCs (e.g. CAACs readily activate H_2, CO and NH_3),[48,57-58] and there are significant differences in the electronic structures of the corresponding main group element adducts with NHCs. For example, the reduction of the tetrabromo diborane $LBBr_2BBr_2L$ (L = IDipp, **1.13**, or CAAC, **1.14**) by sodium naphthalenide (Scheme 1.4) leads to the formation of species of the type LBBL.

(IDipp)BB(IDipp), **1.15**, formed in this way is the first example of a B-B triple bond, featuring a short bond length of 1.449(3) Å, while the (CAAC)BB(CAAC) system **1.16** has a longer B-B distance of 1.449(3) Å and a shorter B-C bond (1.458(2) Å, cf. 1.495(3) Å for (IDipp)BB(IDipp)), illustrating the enhanced π accepting abilities of CAACs.[59-60]

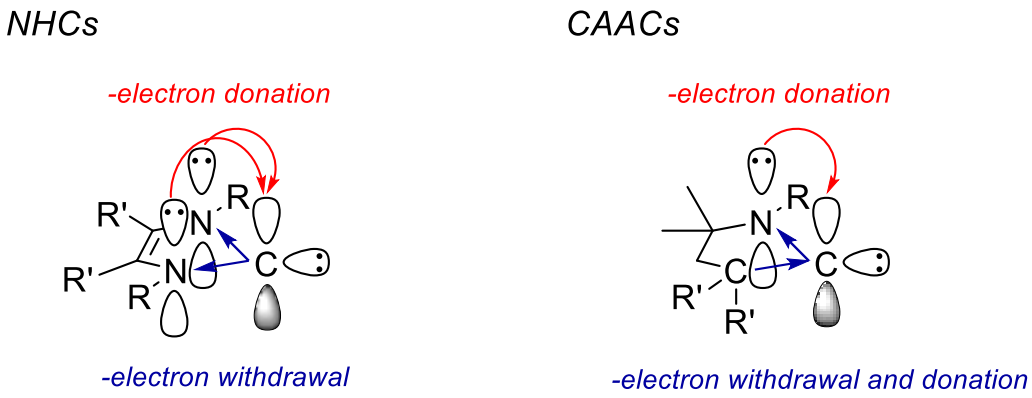
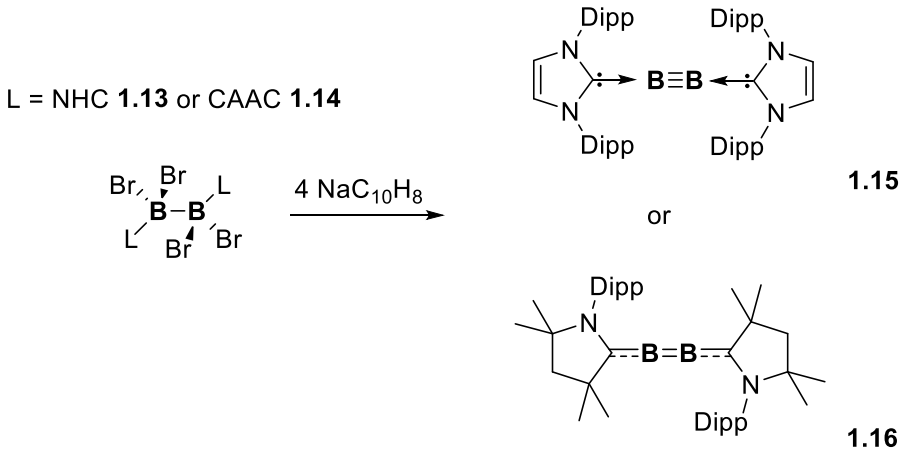


Figure 1.8 *Schematic representation of electronic effects in NHCs and CAACs.*



Scheme 1.4 *Reduction of NHC and CAAC supported diboranes and their divergent products.*

1.3.2 Heavier carbene analogues and their reactivity

In contrast to carbon, the heavier group 14 atoms prefer the ns^2np^2 valence electron configurations in their divalent species as opposed to *sp* orbital hybridization.[61] Since the two electrons remain as a singlet pair in the *ns* orbital, the ground states of the parent metallylenes

H_2M are singlets (ΔE_{ST} = 16.7 kcal mol^{-1} (Si), 21.8 kcal mol^{-1} (Ge), 24.8 kcal mol^{-1} (Sn), 34.8 kcal mol^{-1} (Pb)), while H_2C is a ground state triplet (ΔE_{ST} = −14.0 kcal mol^{-1}).[62] Metallylenes, therefor have a vacant *p* orbital (highly reactive for accepting electrons to make the element centre fulfil "octet rule") and a lone pair of valence orbitals which make them more reactive than expected. Thus, for example, SiH_2 can only be isolated below 77 K and polymerizes at elevated temperatures.[63-65] In order to stabilize a stable metallylene, thermodynamic (mesomeric effects intramolecular coordination through heteroatoms such as N, O, P, etc.) and / or kinetic methods (to avoid self-oligomerization and attack by external nucleophiles) are required (Figure 1.9).[66-76]

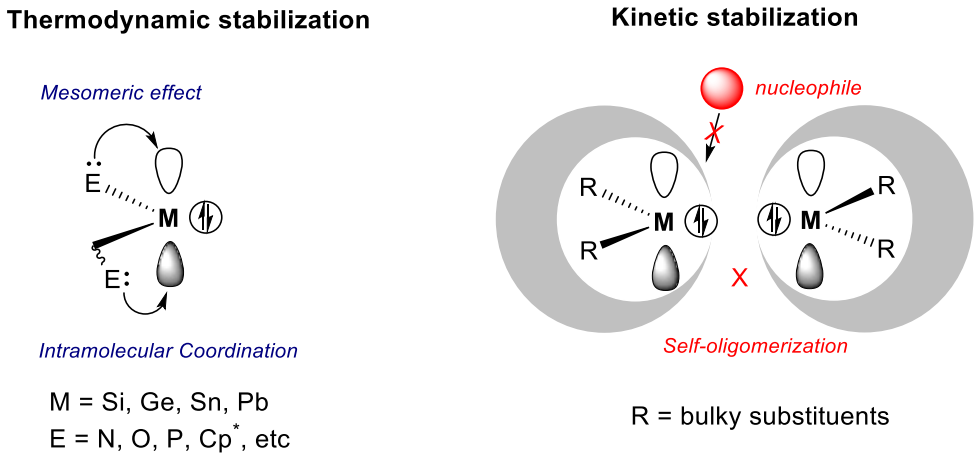
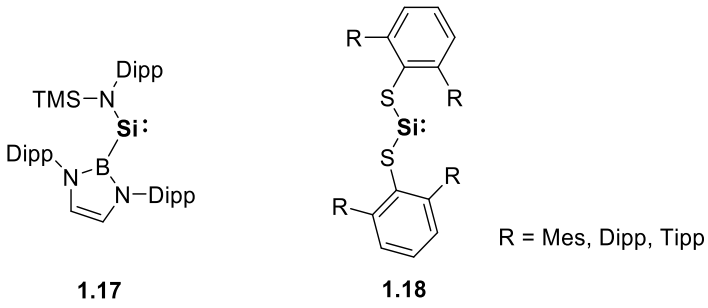


Figure 1.9 *Stabilization strategies for metallyenes.*

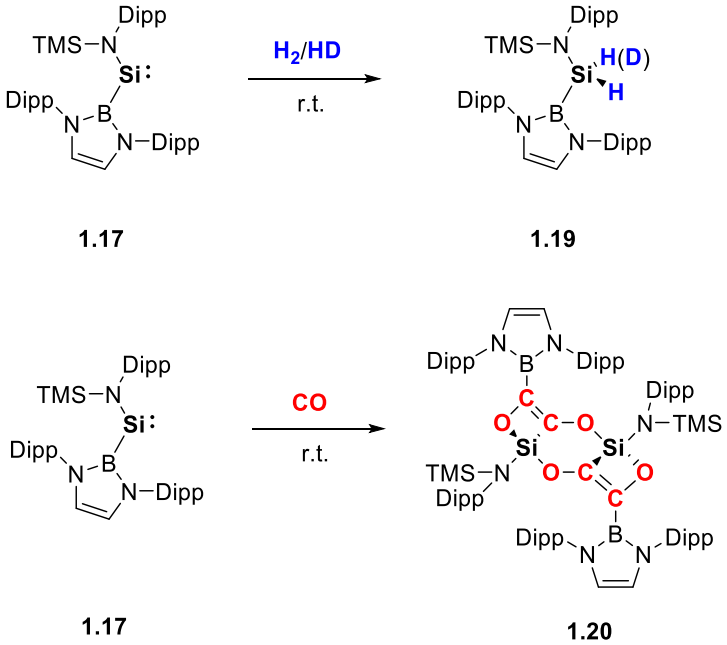
Among these systems, a number of acyclic metallylenes have shown both workable stability and interesting reactivity toward small molecules. Such systems possess a lower lying excited electronic state (more electrophilic, due to the free rotation of the stabilizing substituents, amido groups for example),[77] and are more nucleophilic (wider RER angles increase the *p* character of the lone pair)[77] than their cyclic systems, providing coordinative and oxidative flexibility. In 2012, our group[74] and the Power group[78] reported two back-to-back examples of two-coordinate stable silylenes **1.17** and **1.18** (Figure 1.10). By employing a strong sigma donor boryl ligand, silylene **1.17** was shown to possess a wider R-Si-R angle (109.7(1)°) than

1.18 (90.519(19)°), and a small singlet-triplet gap (24.8 kcal mol^{-1}). **1.17** can readily react with H_2/HD to form the Si(IV) oxidative addition product **1.19** at ambient temperature (Scheme 1.5). Interestingly, computational results show that the homoleptic bis(boryl)germylene $[(HCNDipp)_2B]_2Ge$ and bis(boryl)silylene $[(HCNDipp)_2B]_2Si$ compounds have prohibitively low singlet-triplet gaps (4.3 and -0.06 kcal mol^{-1}). Silylene **1.17** can also react with CO, forming a reductively coupled CO compound featuring two Si(IV) centres linked together as part of a central six-membered $Si_2C_2O_2$ ring **1.20**.[79]



1.17 **1.18**

Figure 1.10 *First two examples of acyclic two-coordinated silylene.*



Scheme 1.5 *Boryl substituted silylene **1.17** reacts with H_2/HD and CO at ambient temperature.*

Several isoelectronic ligands including N-heterocyclic boryloxy (NHBO), N-heterocyclic imine (NHI) and N-heterocyclic olefin (NHO) donors have been exploited to stabilize low valent silicon species and their heavier congeners which are stable at room temperature (Figure 1.11).[75-76, 80-83] However, these metallylenes are electronically "too protected" by the ligands and are generally not so reactive. Although there are also examples of transient species such as (NHI)[(TMS)$_3$Si]Si: which activate H_2[84], most of the examples of silylenes systems do not readily react with H_2 or CO.

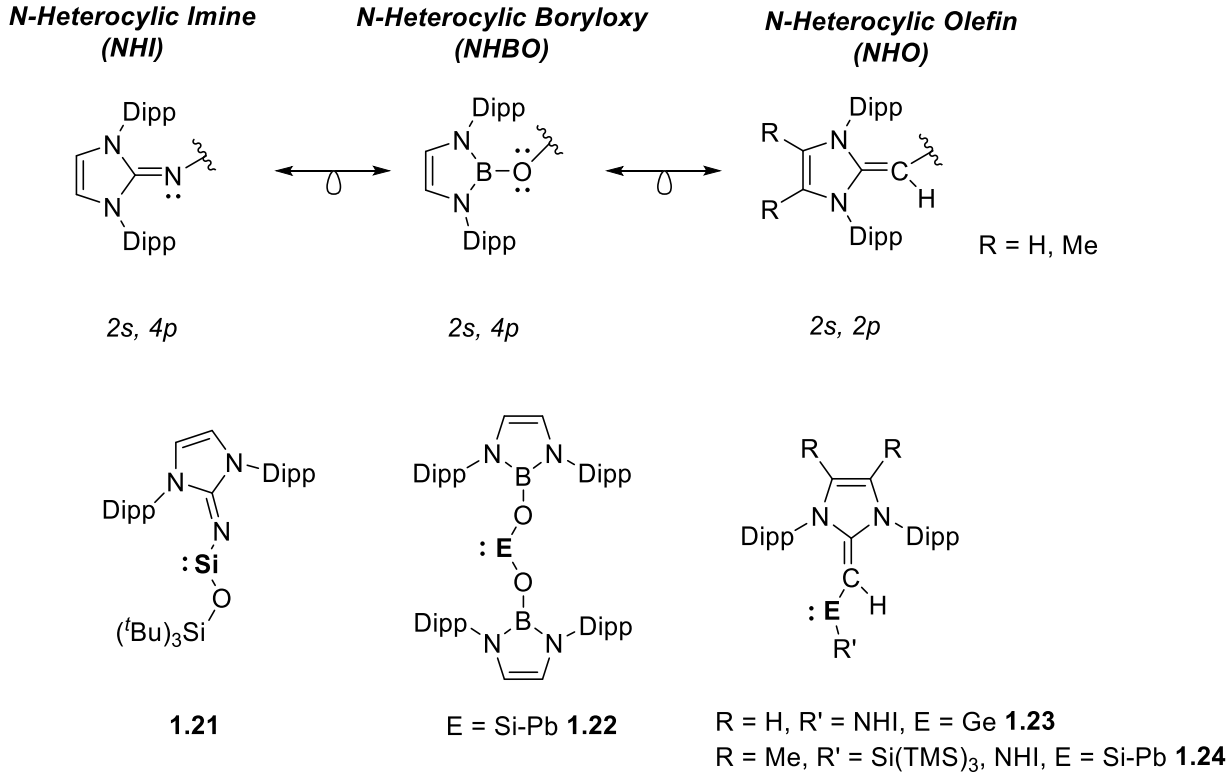
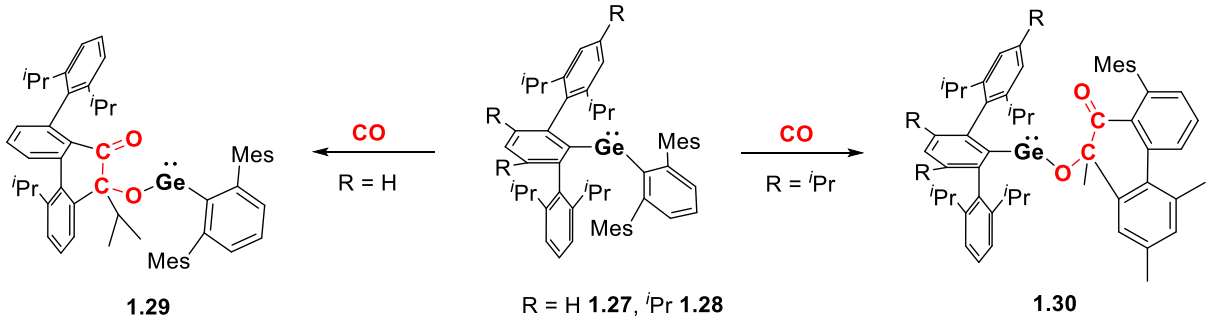


Figure 1.11 *(Upper) Isoelectronic relationship between NHI, NHBO and NHO ligands, (Lower) Selected examples of NHI, NHBO and NHO supported metallylenes.*

By employing terphenyl ligands, Power *et al.*[85] have synthesized two stable diaryl-germylenes (**1.25** and **1.26**) which can activate CO and form the insertion compounds **1.27** and **1.28** (Scheme 1.6). The proposed mechanism includes initial formation of a germaketene, followed by stepwise insertion of two CO molecules into the C-Ge bond and oxygen migration to form

the carbene Ar''C(O)COGeAr', which then undergoes a C-C bond activation with one of the aryl substituents (Figure 1.12). Noticeably, DFT calculations show that the germaketene features a pyramidal germanium centre with a weak Ge-CO interaction in which the CO molecule sits approximately perpendicular to the GeC_2 plane, rather than a "normal" structure containing trigonal-planar germanium and a strong Ge=C double bond.



Scheme 1.6 *Activation of CO by terphenyl stabilized germylenes to give CO coupling and insertion products.*

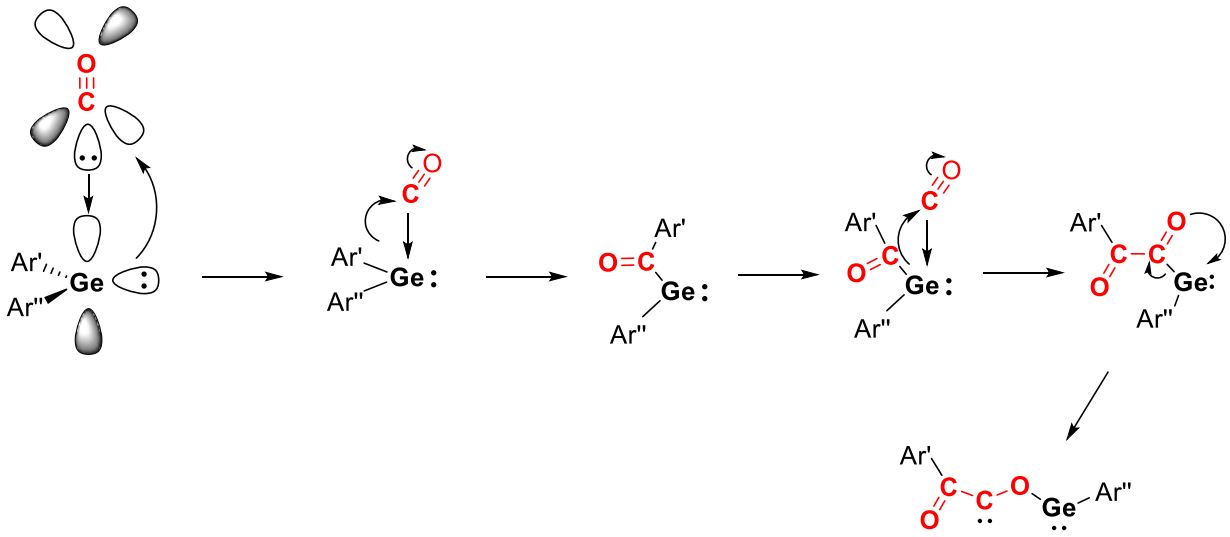


Figure 1.12 *Mechanism of the CO insertion and coupling by a diarylgermylene; the carbene generated in the last step inserts into the C-C bond at the ortho position of the aryl groups to generate* ***1.27*** *and* ***1.28****.*

Previously elusive, in 2020, the Schulz[86] and Inoue[87] groups reported two examples of organosilicon-carbonyl complexes, synthesized via exposure of a transient silylene to 1 atm of CO (Figure 1.13). In each case, the CO moiety of the carbonyl complex is not coplanar with the RSiR' plane. It is worth noting that silylene H_2Si and diorganosilylenes R_2Si (R = alkyl, Cp*) react with CO to give non-covalent adducts R_2Si–CO that are only stable under cryogenic matrix isolation conditions in solid argon.[88-90] The uncomplexed silaketenes are transition structures for the degenerate interconversion of the silicon carbonyl complexes. Thus, the carbonyl complex **1.31** is 6.9 kcal mol^{-1} more stable than the relevant silaketene. (Figure 1.13)

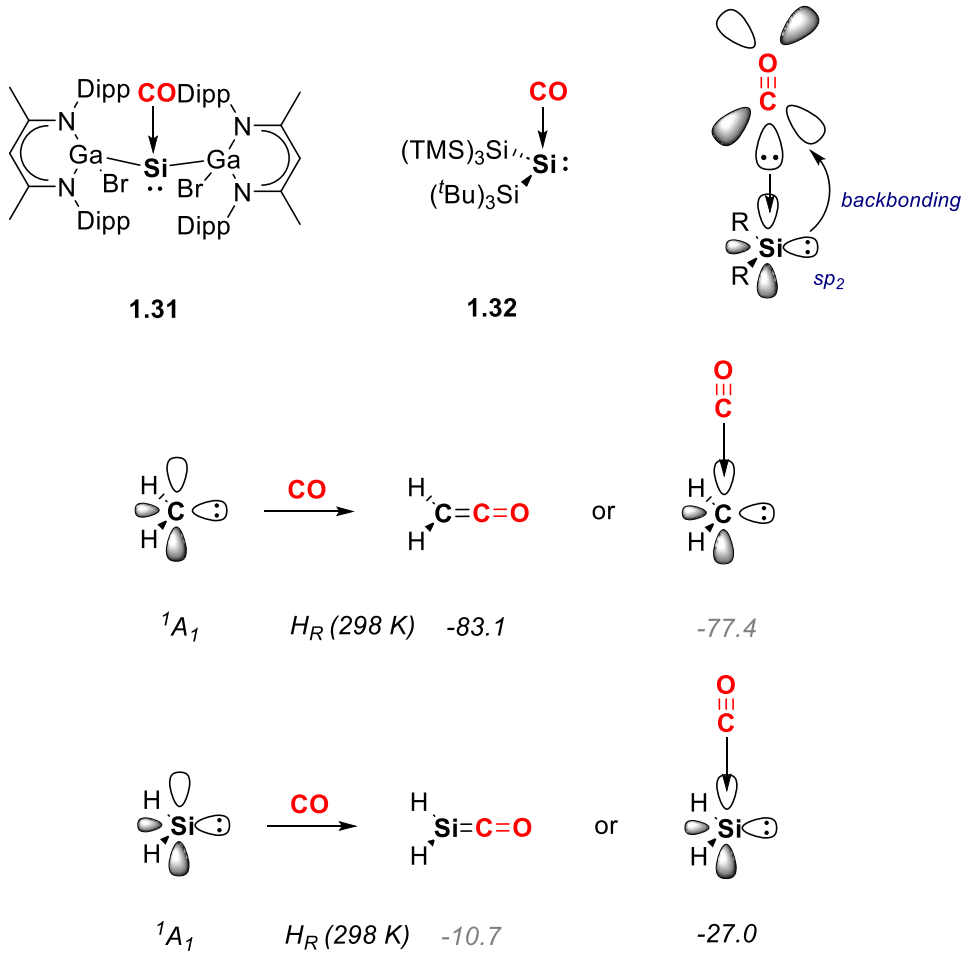
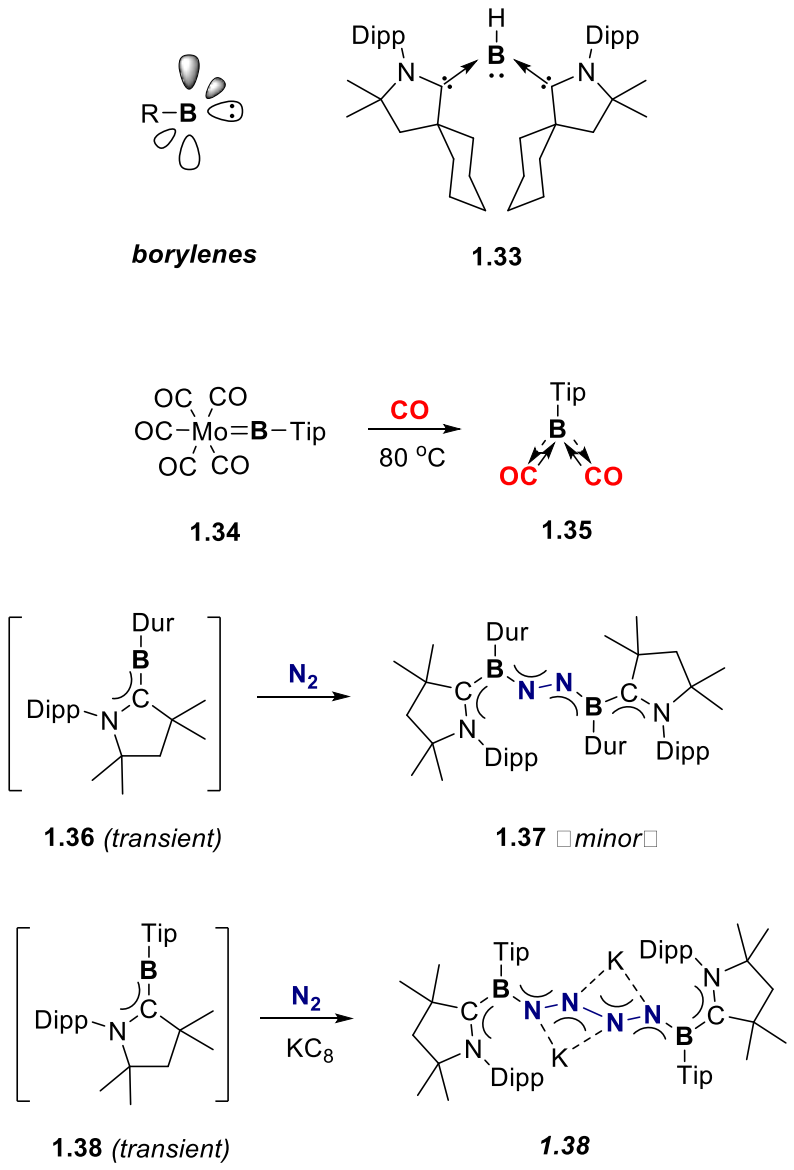


Figure 1.13 *(upper) Binding mode of CO complexes* ***1.31*** *and* ***1.32,*** *(lower) calculated energies for carbene and silylene CO complexes.*

1.3.3 Low valent group 13 compounds and their reactivity

In contrast to carbenes, all borylenes studied computationally have a singlet ground state. Calculations show that the singlet triplet gaps for $(Me_3Si)B$ and BF are 8.2 kcal mol^{-1} (lowest) and 78.7 kcal mol^{-1} (highest), respectively.[91-92] The HOMO is a nonbonding lone pair with *sp* character, whereas the LUMO and LUMO+1 are the two empty p_π-type orbitals that are often degenerate.[93] Free borylenes (RB) have only been spectroscopically characterized in the gas phase or in matrices at low temperature. Bertrand *et al*. have reported the CAAC-stabilized parent borylene $(CAAC)_2BH$ **1.33**.[94] By employing amido and other sigma donors, other examples of stable borylenes were successfully synthesized, such as $(CAAC)[(Me_3Si)_2N]B$, $(NHC)(^iPr_2N)B$, etc.[93] Borylenes show high reactivity towards small molecule substrates. For example, a transient borylene generated from $Mo(CO)_5$BTip **1.34**, reacts with CO at 80 °C to form the borylene dicarbonyl complex $TipB(CO)_2$ **1.35**.[95] Nitrogen can even be fixed/reductively coupled by a transient CAAC-supported transient borylene ((CAAC)BR, R = Dur **1.36**, Tip **1.37**) at room temperature,[96-97] and can be further converted to ammonium chloride by several cycles of reduction and protonation (Scheme 1.7).[98] In a similar way to transition metals, the borylene is able to accept the σ-electrons from N_2 into an empty sp^2 orbital at boron, while the lone pair in the *p* orbital of boron can then backdonate to the π^* orbital of nitrogen. (Figure 1.14)



Scheme 1.7 *Borylenes and their reactivity towards CO and* N_2.

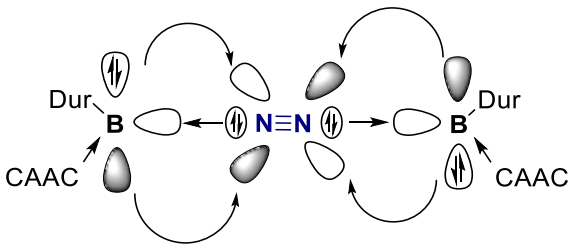


Figure 1.14 *The binding mode of borylene* ***1.36*** *with* N_2.

The isolation of neutral low valent aluminium compounds including the tetrameric complex $[(Cp^*Al)_4]$ **1.39**,[99] Nacnac ligand stabilized monomeric aluminylene **1.40**,[43] bulkier

cyclopentadienyl derivative **1.41**,[100] CAAC supported parent aluminylene **1.42**,[101] terphenyl group supported ^{IPr}TerAl: **1.43**,[102] and carbazolyaluminylene **1.44**,[103-104] has yielded another set of group 13 compounds which readily react with small molecules (Figure 1.15).[105]

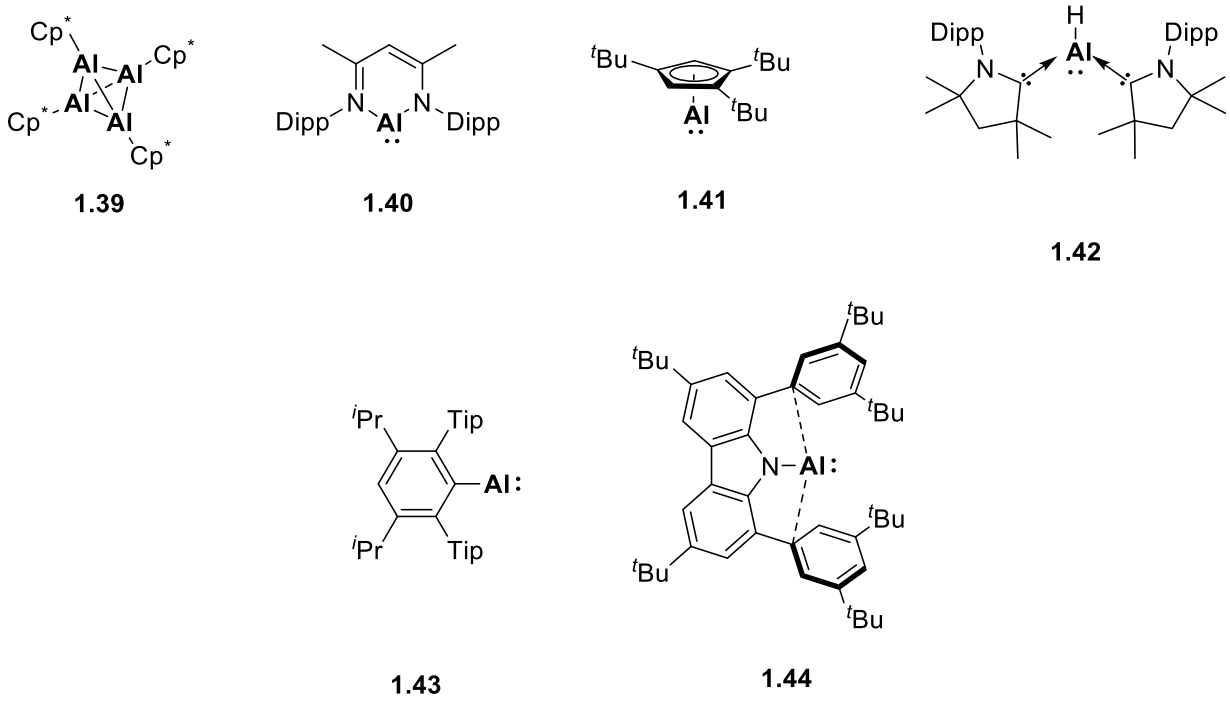


Figure 1.15 *Selected examples of neutral aluminium(I) compounds.*

Remarkably, in 1999 Schmidbaur *et al*.[106] isolated an anionic potassium gallyl supported by the diazabutadiene ligand **1.45**. Yamashita and Nozaki *et al*. then reported the first nucleophilic boryl compound ([(HCNDipp)$_2$B]Li·DME)$_2$ and monomer [(HCNDipp)$_2$B]Li·2THF ([(HCNDipp)$_2$B] = boryl) **1.46**,[45] which can be regarded as isoelectronic analogues of stable N-heterocyclic carbenes. The solid state structure of **1.46** reveals a B-Li bond of 2.291(6) Å, i.e. slightly longer than the sum of the covalent radii (2.11 Å).[107] Unlike conventional boron-containing reagents which are usually considered as electrophiles, the boron centre in **1.46** shows unusual nucleophilicity, and **1.46** can react with electrophiles to make B-R bonds (R = Me, *n*-Bu, Bn, etc).[45] In 2018, our group then reported the first anionic nucleophilic aluminium compound K$_2$[(NON)Al]$_2$ (NON = 4,5-bis(2,6diisopropylanilido)-2,7-di-tert-butyl-9,9-

dimethylxanthene) **1.47**,[44] which displays unprecedented reactivity in the formation of aluminium-element covalent bonds and in the C-H oxidative addition of benzene. The complex utilizes a xanthene-based, strongly electron-donating diamido ligand bearing bulky Dipp groups to stabilize the low valent aluminium centre, and can activate small molecules like H_2 and benzene. When using 2,2,2-cryptand to capture the potassium cation, this compound gives rise to an even more reactive monomeric aluminyl compound which can effect the reversible cleavage of the C-C bond in benzene at room temperature, thereby providing a route to functionalized acyclic compounds from benzene.[108] The structure of $K_2[(NON)Al]_2$ in the solid state is shown to be a centrosymmetric dimer, featuring two formally anionic $[(NON)Al]^-$ units held together through flanking potassium-arene contacts. The non-bonded Al···Al separation (6.627(1) Å) is more than double the length of the formal Al-Al single bond in $[(NON)Al]_2$ (2.646(1) Å). Comparably, boryl potassium **1.48**[109] was synthesized using boryl lithium and $K\{N(SiMe_3)_2\}$, which features a dimeric structure in which two formally anionic diazaboryl units are held together by a pair of K^+ counterions. The lithium aluminyl compound **1.49**[110] was synthesized by the salt metathesis reaction between $K_2[(NON)Al]_2$ and LiI, revealing a monomeric structure in the solid state and having a long Al-Li contact (2.750(4) Å, cf. 2.49 Å for the sum of the respective covalent radii).

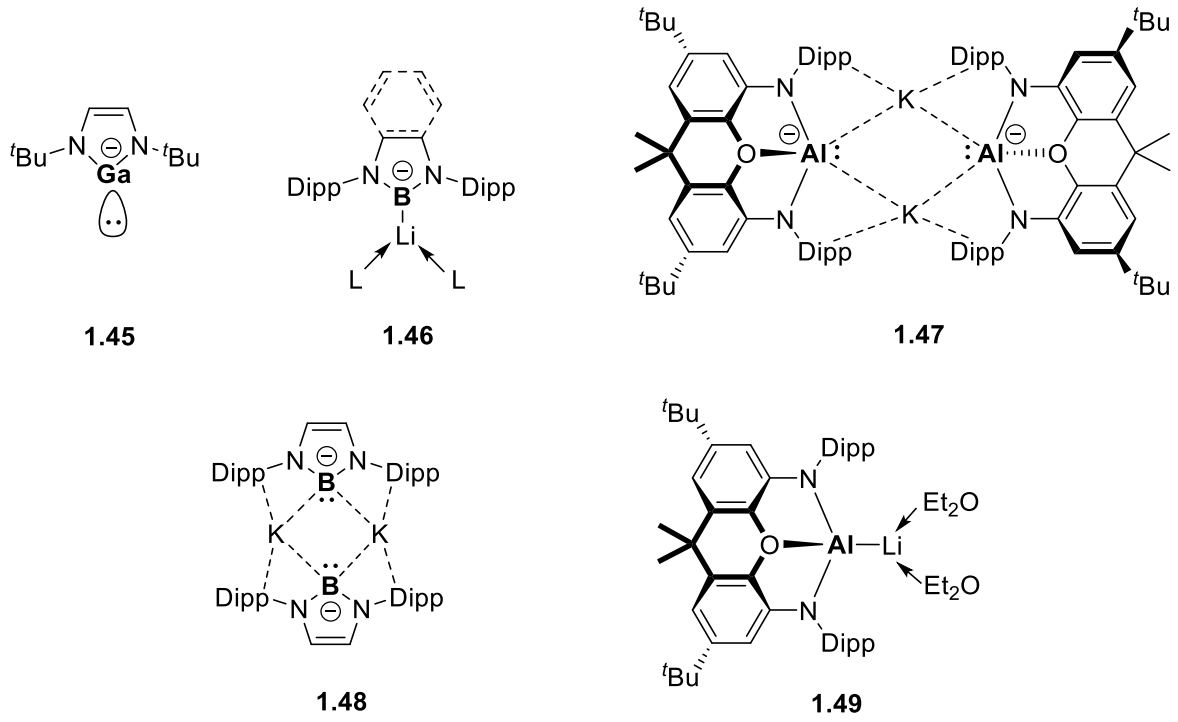
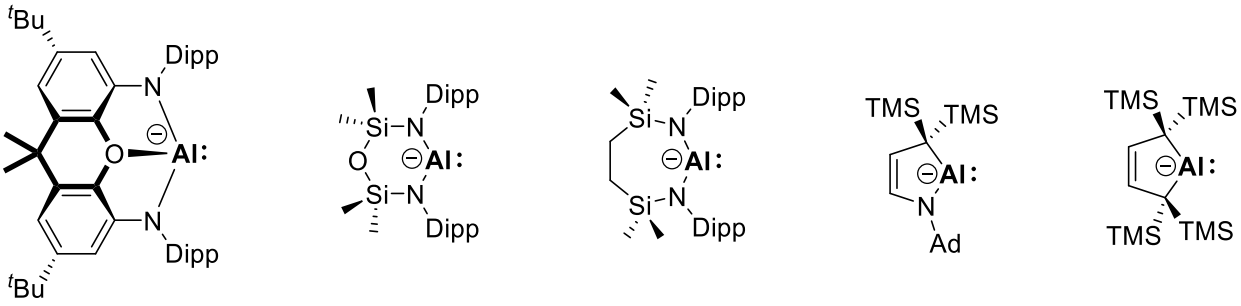


Figure 1.16 *Examples of nucleophilic low valent group 13 compounds.*

A number of examples of nucleophilic aluminyl species have subsequently been reported, featuring amido/alkyl substituents and five/six/seven membered rings to stabilize the low valent aluminium centre **1.51-1.54**.[111-115] These aluminyl anions possess broadly similar HOMO-LUMO energy gaps, and the HOMO corresponds to a lone pair at the aluminium centre.[116] However while the empty p_z orbital for **1.50-1.52** is centred in the LUMO+3 (LUMO+1 for **1.53)**, **1.50** has a much lower lying p_z orbital derived from the reduced N-to-Al π donation from the amido substituents. In contrast to **1.51** and **1.52**, the amido substituents in **1.50** do not lie coplanar with the AlN_2 unit. This non-planar geometry is required for the aluminium centre to be accommodated in the xanthene scaffold of **1.50**, and the resulting effect on the N to Al π donation finds precedent in the anti-Bredt carbene systems reported by Bertrand et al.[117] Using xanthene-based ligands to support low valent main group species is discussed more in detail in Chapter 4.

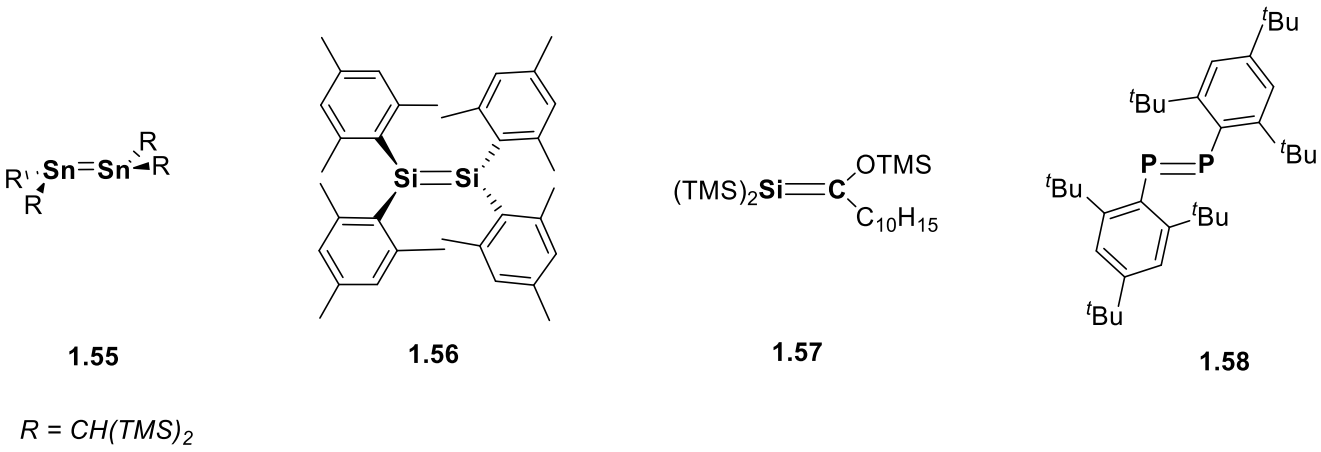


1.50 **1.51** **1.52** **1.53** **1.54**

Figure 1.17 *Selected examples of nucleophilic aluminyl anions.*

1.4 Multiple bonds for small molecule activation

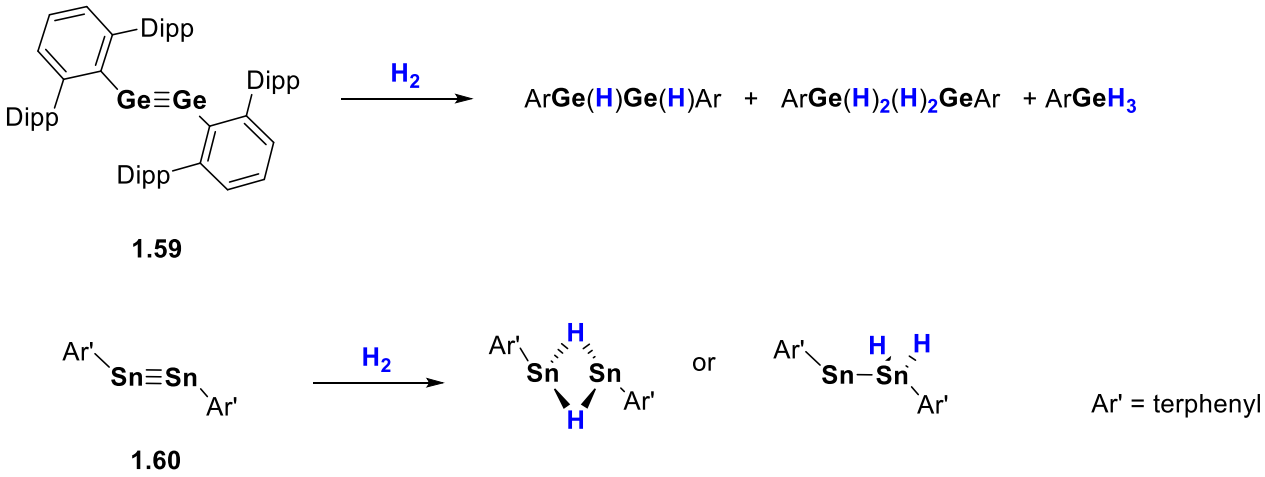
The "double-bond rule" asserted that heavier *p* block elements cannot form stable multiple bonds.[65, 118-119] This assertion was widely accepted until Lappert *et al*. reported the first isolable distannylene **1.55** in 1976,[120] followed shortly afterwards by West's disilene,[64] Brook's silaethene,[121] and Yoshifuji's diphosphene (Figure 1.18).[122] Dimetallenes and dimetallynes combine the reactivity of electron-rich multiple bonds and the unique electronic properties of low valent main group compounds, while dinuclear complexes could also benefit from the cooperative effects of two E atoms.[123] This combination at the outset made them promising candidates for the activation of small molecules. For example, H_2 activation by terphenyl supported Ge^I, **1.59**[124] and Sn^I, **1.60**[125] compounds of the type ArEEAr (E = Ge, Sn, Ar = Terphenyl) was the first such process to be reported for a main group compound (Scheme 1.8). The key interaction involves donation from the σ-orbital of H_2 into the LUMO of ArEEAr, and synergic electron donation from the π-HOMO orbital of the Ge/Sn species into the σ^*-orbital of H_2. As such, it is similar in many aspects to the process of H_2 activation by transition metals.



1.55 **1.56** **1.57** **1.58**

R = CH(TMS)$_2$

Figure 1.18 *Examples of dimetallene and related compounds.*



1.59

1.60

Scheme 1.8 *Reaction of dimetallyne* ***1.60*** *with H_2.*

1.4.1 Bonding in dimetallenes and dimetallynes

The heavier direct analogues of alkenes and alkynes, dimetallenes and dimetallynes ($R_2E{=}ER_2$, REER, E = Si, Ge, Sn Pb), favour trans-bent structures rather than the planar E_2H_4 or linear HEEH (e.g. ethylene, acetylene) systems seen for carbon. To form a "standard" E-E multiple bond, the significant Pauli repulsion between the occupied orbitals or the excitation into the singlet or quartet state needs to be overcome.[1] Therefore an alternative double donor-acceptor interaction is energetically favoured in which the lone pair of electrons is donated into the vacant *p* orbital of the partner. Quantum chemical probes using two monomeric H_2E or HE

fragment show that the heavier tetrylenes possess a singlet ground state (ΔE_{ST} = 16.7 kcal mol^{-1} (Si), 21.8 kcal mol^{-1} (Ge), 24.8 kcal mol^{-1} (Sn), 34.8 kcal mol^{-1} (Pb)), while methylene (H_2C) has a ground state triplet (ΔE_{ST} = −14.0 kcal mol^{-1}),[62] is capable of forming a planar structure (Figure 1.19). In triply bonded compounds, alkynes possess *sp*-hybridized carbon atoms in the quartet ground state, resulting in three covalent bonds and a linear structure. For dimetallynes the doublet HE units are not able to form covalent triple bonds.[126-129] In both cases, significant Pauli repulsion between the occupied orbitals or the excitation into the quartet state would need to be overcome in order to form a "standard" E-E multiple bond. Therefore a double donor-acceptor interaction is energetically favoured.[126-129]

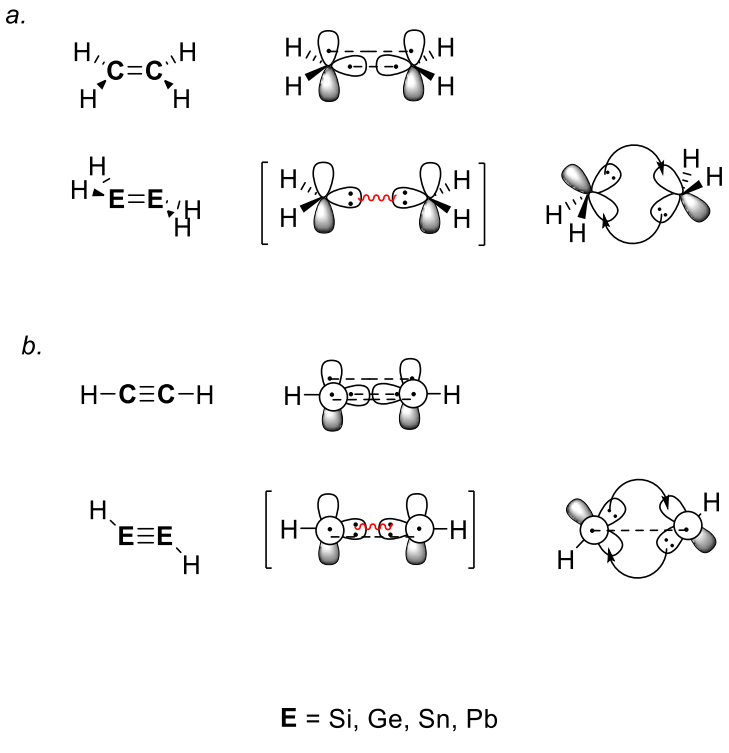


Figure 1.19 *Ethylene (a) and acetylene (b): covalent bonding descriptions and their relevant CGMT models*

For dimetallenes R_2EER_2, the increasing deviation from a planar double bond on descending group 14 can be interpreted in terms of the increasing stability of the singlet ground state, leading to more significant *trans*-bending and weakening of the E=E bond.[130-131] This in turn

can be understood by second order Jahn-Teller mixing (Figure 1.20, upper). The frontier orbitals involved in the E=E double bond of the planar structure having D_{2h} symmetry are the σ, π, π^* and σ^* orbitals. If the molecule undergoes a deformation to afford a molecule of C_{2h} symmetry, the molecular orbitals have the designations σ, n_-, n_+ and σ^*. The mixing of n_-/σ^* and σ/n_+ pairs is then allowed by symmetry, which results in a lowering of the energy of the σ- and π-bonding orbitals.

A similar effect can be seen for dimetallynes, which can also be understood as stemming from second order Jahn-Teller mixing (Figure 1.20, lower).[130] For REER systems which adopt a linear geometry ($D_{\infty h}$), the molecular orbitals consist of a *σ*-bonding orbital, two degenerate π-bonding orbitals and their corresponding antibonding combinations. The orbitals do not mix because of the orthogonal geometry they adopt with respect to one another. The *trans*-bending distortion produces a geometry with C_{2h} symmetry, in which the degeneracy of the π and π^* orbitals is recovered, and a new occupied orbital of lone pair character (*n*-) is generated. Formerly symmetry forbidden σ/π^* and π/σ^* mixing is allowed in the *trans*-bent case, thus lowering the energy of σ- and π-bonding orbitals through a second order Jahn-Teller mixing. On descending the group, the trans-bending becomes more favourable because of E-E π-bonding character decreases and lone pair character on E increases.[130, 132]

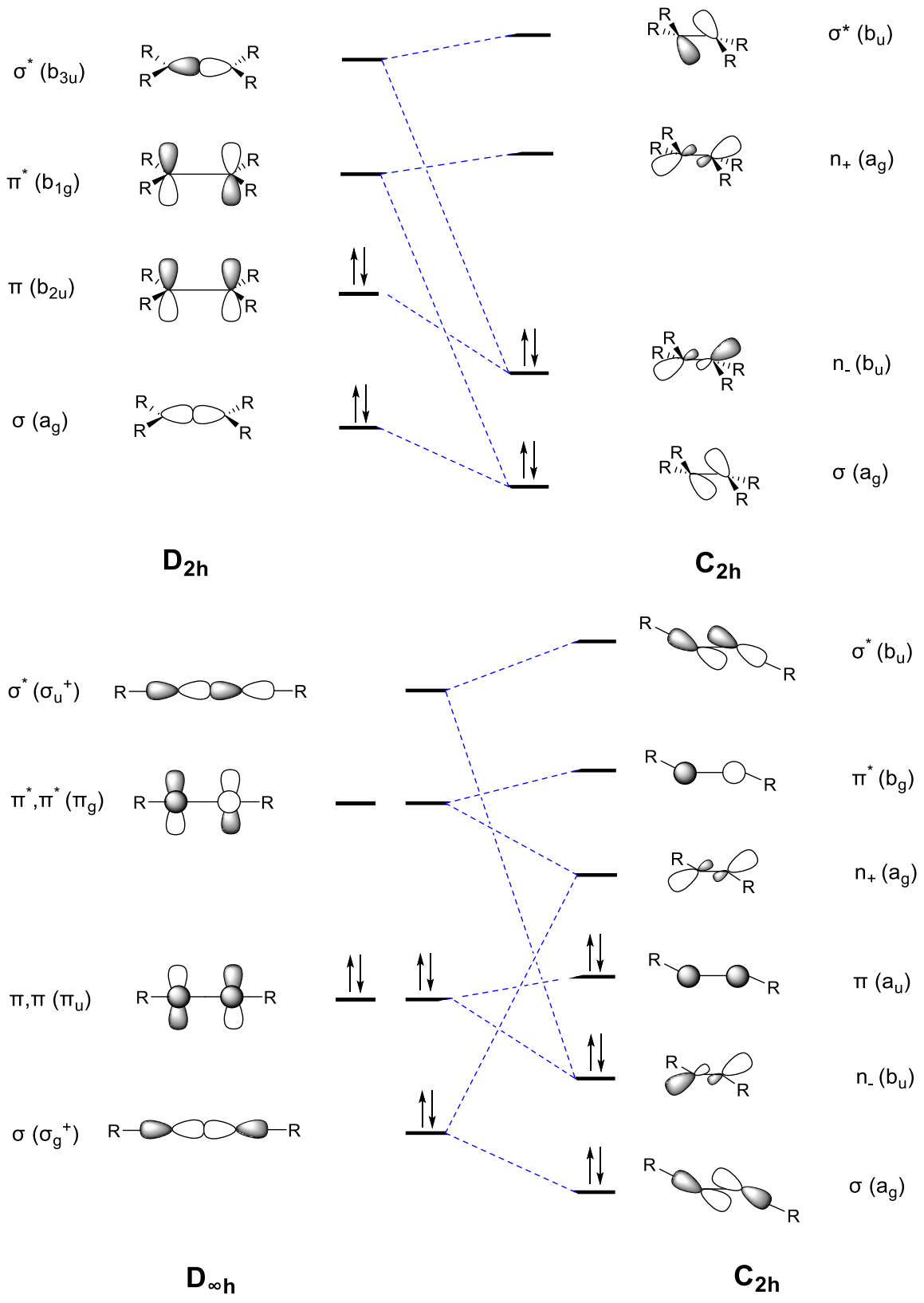
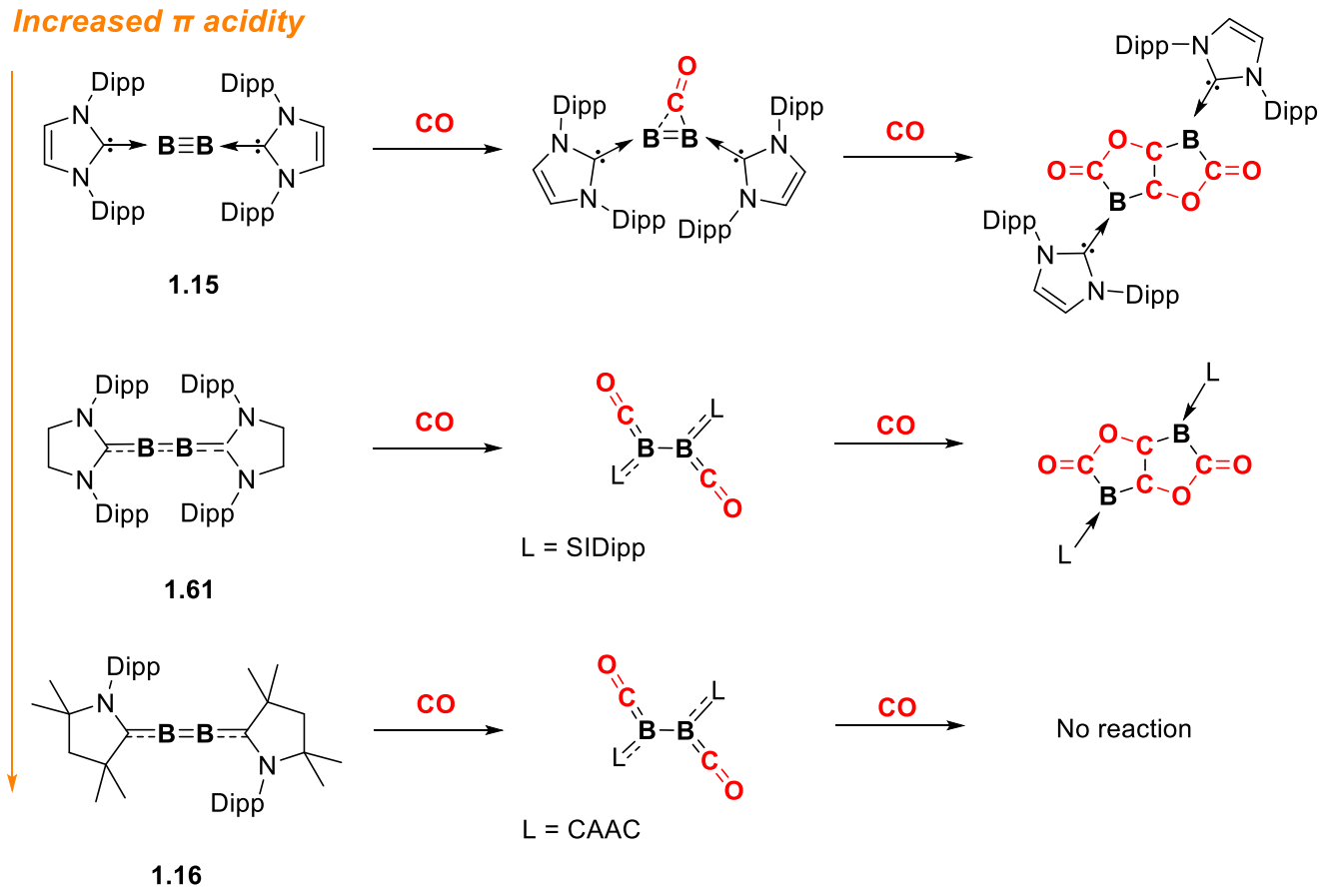


Figure 1.20 *Orbital schemes showing the second order Jahn–Teller distortions in R_2EER_2 (upper) and REER systems (lower) (E = Si, Ge, Sn, Pb).*

1.4.2 Reactivity of dimetallenes and dimetallynes

In terms of reactivity, homonuclear group 13 bonds are generally found to react readily with small molecules. For example, the reactivity of diboryne compounds can be influenced by the π acidity of the supporting ligands.[133-135] CO coupling was observed for NHC-stabilized diborynes **1.15** and **1.61**, but **1.15** and **1.61** do not react with hydrogen. By contrast, CAAC-stabilized **1.16** effects the activation of hydrogen at room temperature and the coordination of CO at both boron centres (Scheme 1.9).



Scheme 1.9 *Diboryne reactivity towards CO.*

The Inoue group has subsequently reported two NHC stabilized dialumenes **1.62**[136] and **1.63** (Figure 1.21).[137] Silyl substituted **1.62** adopts a *trans*-planar geometry while aryl substituted **1.63** features a *trans*-bent and twisted geometry. Due to the increased flexibility in **1.63**, facile

hydrogen activation is achievable (**1.62** shows no reactivity with H_2), yielding both the *cis* and *trans* isomers of a 1,2-dihydro-dialumane. The reactivity of heavier E (group 13) multiple bonds (E = Ga-Tl)[138-140] are limited to a few examples. Digallene Ar'GaGaAr' (Ar' = 2,6-$Dipp_2C_6H_3$) can activate hydrogen and ammonia,[141] while the related dithallene readily dissociates to its monomeric form.[140]



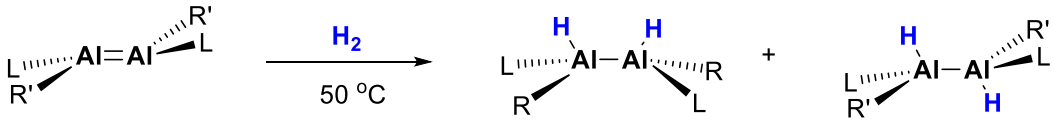
1.62

R = SiMe^{t}Bu$_2$
L = IPr

1.63

R = Tipp
L = IPr

Figure 1.21 *NHC-stabilized dialumenes* ***1.62*** *and* ***1.63****.*



1.63

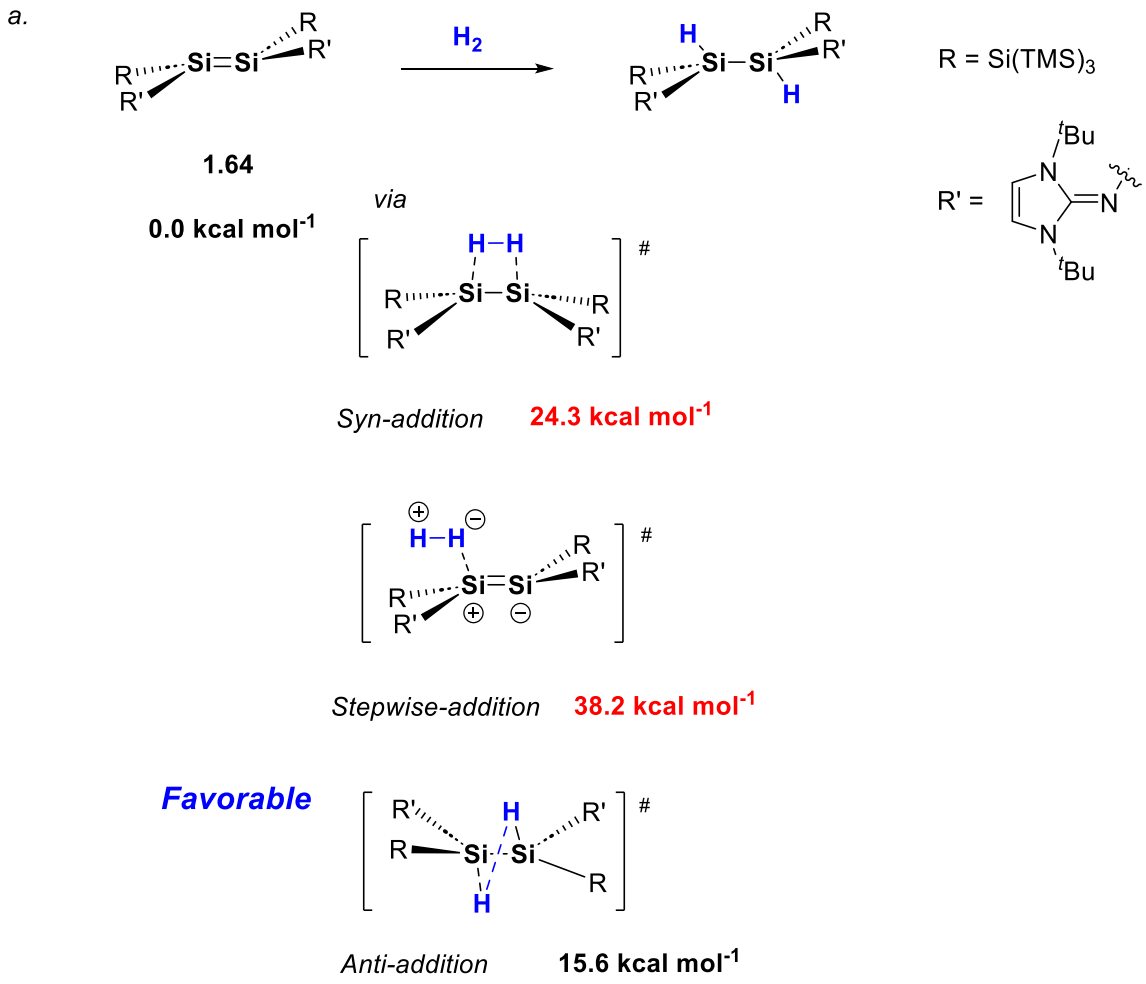
R = Tipp
L = IPr

cis

trans

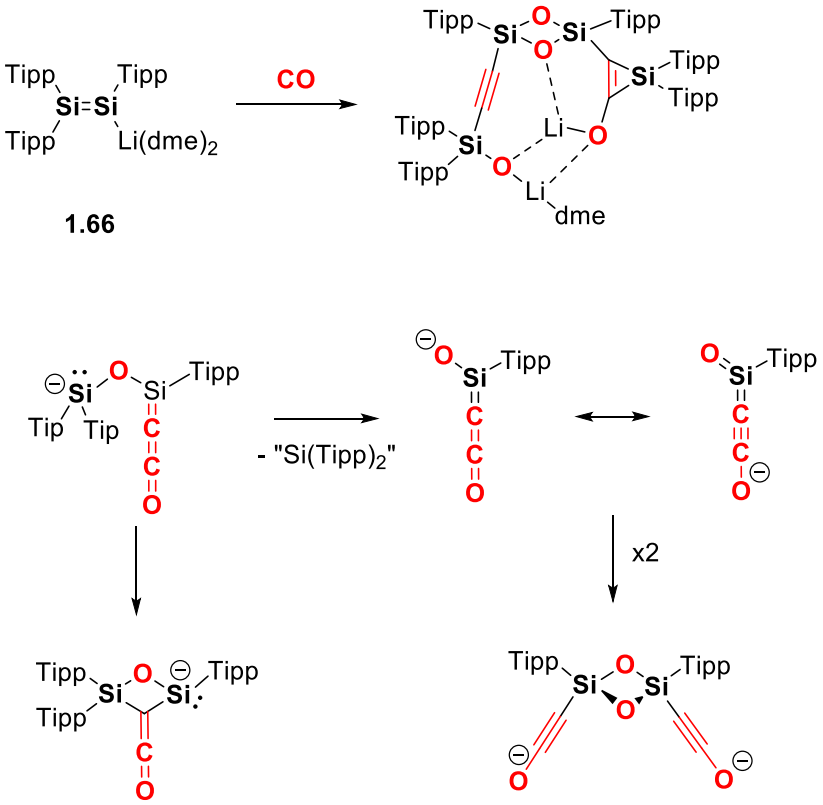
Scheme 1.10 *Reaction of dialumene* ***1.63*** *with H_2 to form cis and trans hydrogenated products.*

A highly *trans*-bent NHI-stabilized disilene **1.64** was found to react with hydrogen to form a 1,2-disilane via net *anti*-addition, in contrast to alkene hydrogenation where *syn*-addition is favoured.[142] Computational analysis shows that twisted pre-organisation of the central Si=Si bond leads to a lower barrier for the accommodation of hydrogen than *syn*-addition or a stepwise addition process. Another example of hydrogen activation by a disilene was reported by Iwamoto, and results in the formation of trihydriodisilane and hydroborane fragments via the initial cleavage of the Si-B bond (Scheme 1.11).[143]



Scheme 1.11 *(a) The reaction of NHI-supported disilene* ***1.64*** *with H_2 showing the favoured transition state, (b) Addition of H_2 to a disilene with elimination of borane.*

Activation of CO by group 14 multiple bonds was developed by the Scheschkewitz group;[144-146] the terphenyl substituted disilenide **1.66** can cleave CO and form a C-C bond via the two-fold addition of CO to the disilenide forming a silylenoid by elimination of silylene $Trip_2Si$, which then dimerizes in head-to-tail fashion. The final step involves a two-fold reaction of $Trip_2Si$ with one molecule of silylene inserting into one of terminal alkynyl C–O bonds and another molecule undergoing [1+2] cyclization with the CC triple bond.

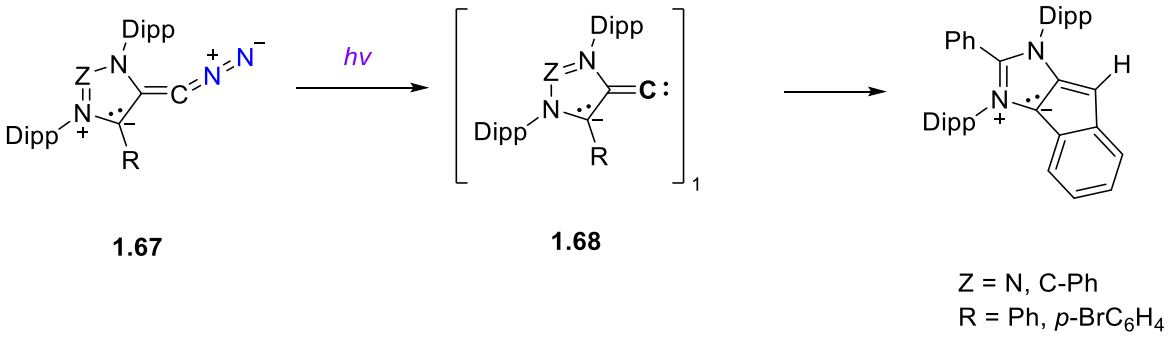


Scheme 1.12 *Proposed mechanism of the reaction of disilenide* ***1.66*** *with CO.*

1.4.3 Vinylidenes

In contrast to the alkyne isomer, vinylidenes ($H_2C=C$) have been observed only transiently with a lifetime of 10^{-12} seconds, as a result of 1,2-migration of a hydrogen atom to generate ethyne being highly exothermic and occuring with a very low energy barrier (about 2.4 kcal mol^{-1}).[147-150] Besides well-known metal vinylidene complexes,[151] free singlet vinylidenes ($R_2C=C$) are

proposed as building blocks in a series of organic reactions (e.g. Seyferth-Gilbert homologation).[152] The first ground-state triplet vinylidene **1.68** was characterized by Hansmann *et al.* by irradiating **1.67** in a frozen toluene solution and employing EPR to characterize the photolysis products (Scheme 1.13).[153] Vinylidene isomers are found to lie relatively low in energy in the case of heavier analogues of ethyne, E_2H_2 (E = Si-Pb).[154-155] Strategies of using N-heterocyclic carbene to stabilize heavier vinylidenes were developed by Scheschkewitz *et al*. **1.69**[156] and by Filippou *et al*. **1.70.**[157] A genuine base-free germanium analogue of vinylidene **1.71** was made by our group in 2016 in which the bulky and electron-donating boryl ligand was employed to support the Ge_2 unit at room temperature (Figure 1.22).[158] Noticeably, $\{(HCNDipp)_2B\}_2GeGe$ **1.71** can be accessed by the two-electron oxidation of the Ge^0 compound $K_2[(HCNDipp)_2BGeGe(HCNDipp)_2B]$ **1.72**, which reveals the labile nature of 1,2-boryl migration from the digermyne to digermavinylidene (Scheme 1.14). $\{(HCNDipp)_2B\}_2GeGe$ was found to react with H_2 at elevated temperature or high pressure (4 atm) H_2, forming the 1,2-dihydridogermane **1.73**. Further design and exploration of the heavier group 14 multiple bonds is discussed in Chapters 5 and 6.



1.67 **1.68**

Scheme 1.13 *Photolytic generation of a transient ground-state triplet vinylidene,* ***1.68****.*

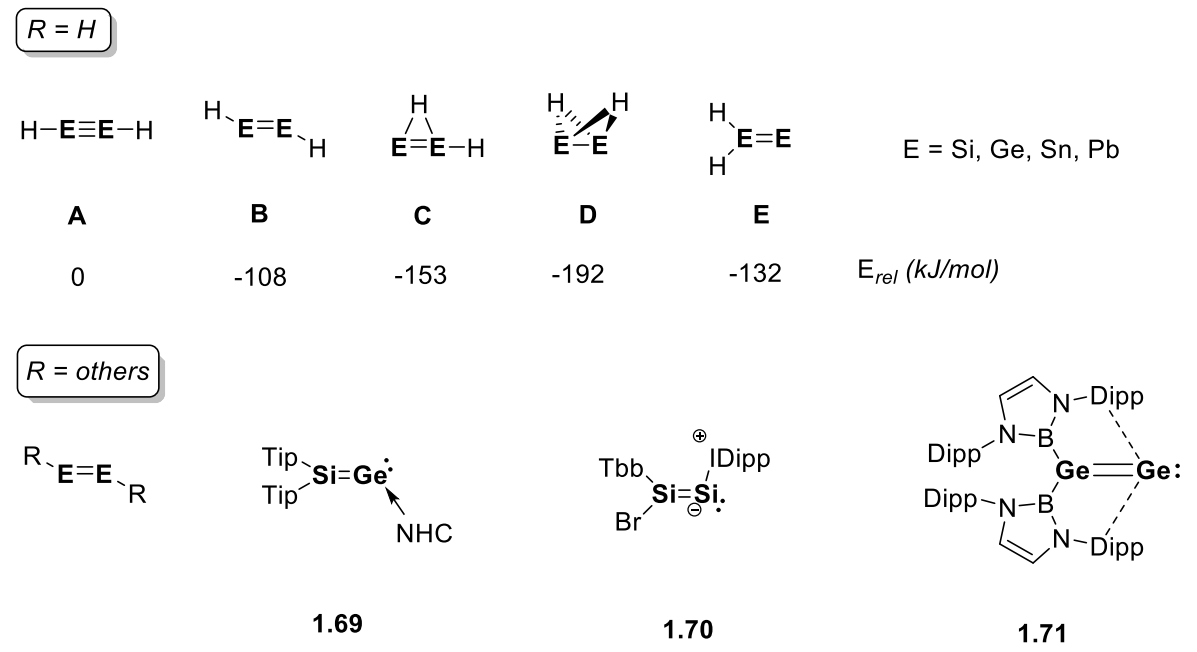
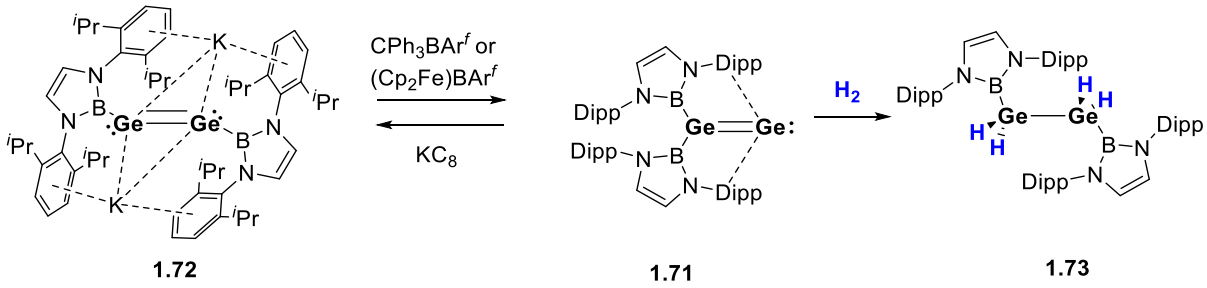


Figure 1.22 *Examples of heavier analogues of vinylidenes.*



Scheme 1.14 *Synthesis of digermavinylidene* ***1.71*** *and its reactivity towards* H_2.

1.5 References

1. Power, P. P., Main-group elements as transition metals. *Nature* **2010,** *463*, 171.
2. Wilkins, L. C.; Melen, R. L., Enantioselective Main Group Catalysis: Modern Catalysts for Organic Transformations. *Coord. Chem. Rev.* **2016,** *324*, 123-139.
3. Stephan, D. W., Frustrated Lewis pairs: a new strategy to small molecule activation and hydrogenation catalysis. *Dalton Trans.* **2009,** (17), 3129-3136.
4. Mizuhata, Y.; Sasamori, T.; Tokitoh, N., Stable Heavier Carbene Analogues. *Chem. Rev.* **2009,** *109* (8), 3479-3511.
5. Welch, G. C.; Juan, R. R. S.; Masuda, J. D.; Stephan, D. W., Reversible, metal-free hydrogen activation. *Science* **2006,** *314* (5802), 1124-1126.
6. Welch, G. C.; Stephan, D. W., Facile Heterolytic Cleavage of Dihydrogen by Phosphines and Boranes. *J. Am. Chem. Soc.* **2007,** *129* (7), 1880-1881.
7. Spies, P.; Erker, G.; Kehr, G.; Bergander, K.; Fröhlich, R.; Grimme, S.; Stephan, D. W., Rapid intramolecular heterolytic dihydrogen activation by a four-membered heterocyclic phosphane–borane adduct. *Chem. Commun.* **2007,** (47), 5072-5074.

8. Mo, Z.; Kolychev, E. L.; Rit, A.; Campos, J.; Niu, H.; Aldridge, S., Facile reversibility by design: tuning small molecule capture and activation by single component frustrated Lewis pairs. *J. Am. Chem. Soc.* **2015,** *137* (38), 12227-12230.
9. Kelly, M. J.; Gilbert, J.; Tirfoin, R.; Aldridge, S., Frustrated Lewis Pairs as Molecular Receptors: Colorimetric and Electrochemical Detection of Nitrous Oxide. *Angew. Chem., Int. Ed.* **2013,** *52* (52), 14094-14097.
10. Zheng, X.; Zulkifly, I.; Heilmann, A.; McManus, C.; Aldridge, S., Colorimetric Metal-Free Detection of Carbon Monoxide: Reversible CO Uptake by a BNB Frustrated Lewis Pair. *Angew. Chem., Int. Ed.* **2021,** *60* (30), 16416-16419.
11. Sajid, M.; Klose, A.; Birkmann, B.; Liang, L. Y.; Schirmer, B.; Wiegand, T.; Eckert, H.; Lough, A. J.; Frohlich, R.; Daniliuc, C. G.; Grimme, S.; Stephan, D. W.; Kehr, G.; Erker, G., Reactions of phosphorus/boron frustrated Lewis pairs with SO_2. *Chem. Sci.* **2013,** *4* (1), 213-219.
12. Sajid, M.; Lawzer, A.; Dong, W.; Rosorius, C.; Sander, W.; Schirmer, B.; Grimme, S.; Daniliuc, C. G.; Kehr, G.; Erker, G., Carbonylation Reactions of Intramolecular Vicinal Frustrated Phosphane/Borane Lewis Pairs. *J. Am. Chem. Soc.* **2013,** *135* (49), 18567-18574.
13. Stephan, D. W.; Erker, G., Frustrated Lewis pair chemistry of carbon, nitrogen and sulfur oxides. *Chem. Sci.* **2014,** *5* (7), 2625-2641.
14. McCahill, J. S. J.; Welch, G. C.; Stephan, D. W., Reactivity of "Frustrated Lewis Pairs": Three-Component Reactions of Phosphines, a Borane, and Olefins. *Angew. Chem., Int. Ed.* **2007,** *46* (26), 4968-4971.
15. Dureen, M. A.; Stephan, D. W., Terminal Alkyne Activation by Frustrated and Classical Lewis Acid/Phosphine Pairs. *J. Am. Chem. Soc.* **2009,** *131* (24), 8396-8397.
16. Légaré, M.-A.; Courtemanche, M.-A.; Rochette, É.; Fontaine, F.-G., Metal-free catalytic C-H bond activation and borylation of heteroarenes. *Science* **2015,** *349* (6247), 513-516.
17. Flynn, S. R.; Wass, D. F., Transition Metal Frustrated Lewis Pairs. *ACS Catal.* **2013,** *3* (11), 2574-2581.
18. Guan, Y.; Lu, E.; Xu, X., Rare-earth mediated dihydrogen activation and catalytic hydrogenation. *J. Rare Earths* **2021,** *39* (9), 1017-1023.
19. Xu, M.; Jupp, A. R.; Qu, Z.-W.; Stephan, D. W., Alkali Metal Species in the Reversible Activation of H_2. *Angew. Chem., Int. Ed.* **2018,** *57* (34), 11050-11054.
20. Brand, S.; Pahl, J.; Elsen, H.; Harder, S., Frustrated Lewis Pair Chemistry with Magnesium Lewis Acids. *Eur. J. Inorg. Chem.* **2017,** *2017* (36), 4187-4195.
21. Johnstone, T. C.; Wee, G. N. J. H.; Stephan, D. W., Accessing Frustrated Lewis Pair Chemistry from a Spectroscopically Stable and Classical Lewis Acid-Base Adduct. *Angew. Chem., Int. Ed.* **2018,** *57* (20), 5881-5884.
22. Brown, H. C.; Schlesinger, H. I.; Cardon, S. Z., Studies in Stereochemistry. I. Steric Strains as a Factor in the Relative Stability of Some Coördination Compounds of Boron. *J. Am. Chem. Soc.* **1942,** *64* (2), 325-329.
23. Bakó, I.; Stirling, A.; Bálint, S.; Pápai, I., Association of frustrated phosphine–borane pairs in toluene: molecular dynamics simulations. *Dalton Trans.* **2012,** *41* (30), 9023-9025.
24. Rocchigiani, L.; Ciancaleoni, G.; Zuccaccia, C.; Macchioni, A., Probing the Association of Frustrated Phosphine–Borane Lewis Pairs in Solution by NMR Spectroscopy. *J. Am. Chem. Soc.* **2014,** *136* (1), 112-115.
25. Grimme, S.; Kruse, H.; Goerigk, L.; Erker, G., The Mechanism of Dihydrogen Activation by Frustrated Lewis Pairs Revisited. *Angew. Chem., Int. Ed.* **2010,** *49* (8), 1402-1405.
26. Schwendemann, S.; Fröhlich, R.; Kehr, G.; Erker, G., Intramolecular frustrated N/B lewis pairs by enamine hydroboration. *Chem. Sci.* **2011,** *2* (9), 1842-1849.
27. Moroz, A.; Sweany, R. L.; Whittenburg, S. L., Van der Waals complexes between Lewis bases and molecular hydrogen in argon matrixes. *J. Phys. Chem.* **1990,** *94* (4), 1352-1357.
28. Rokob, T. A.; Hamza, A.; Stirling, A.; Soós, T.; Pápai, I., Turning Frustration into Bond Activation: A Theoretical Mechanistic Study on Heterolytic Hydrogen Splitting by Frustrated Lewis Pairs. *Angew. Chem., Int. Ed.* **2008,** *47* (13), 2435-2438.
29. Rokob, T. A.; Bakó, I.; Stirling, A.; Hamza, A.; Pápai, I., Reactivity Models of Hydrogen Activation by Frustrated Lewis Pairs: Synergistic Electron Transfers or Polarization by Electric Field? *J. Am. Chem. Soc.* **2013,** *135* (11), 4425-4437.

30. Hamza, A.; Stirling, A.; András Rokob, T.; Pápai, I., Mechanism of hydrogen activation by frustrated Lewis pairs: A molecular orbital approach. *Int. J. Quantum Chem.* **2009,** *109* (11), 2416-2425.
31. Liu, L.; Cao, L. L.; Shao, Y.; Menard, G.; Stephan, D. W., A Radical Mechanism for Frustrated Lewis Pair Reactivity. *Chem* **2017,** *3* (2), 259-267.
32. Ménard, G.; Hatnean, J. A.; Cowley, H. J.; Lough, A. J.; Rawson, J. M.; Stephan, D. W., C–H Bond Activation by Radical Ion Pairs Derived from R3P/Al(C6F5)3 Frustrated Lewis Pairs and N_2O. *J. Am. Chem. Soc.* **2013,** *135* (17), 6446-6449.
33. Pan, X.; Chen, X.; Li, T.; Li, Y.; Wang, X., Isolation and X-ray Crystal Structures of Triarylphosphine Radical Cations. *J. Am. Chem. Soc.* **2013,** *135* (9), 3414-3417.
34. Chase, P. A.; Welch, G. C.; Jurca, T.; Stephan, D. W., Metal-Free Catalytic Hydrogenation. *Angew. Chem., Int. Ed.* **2007,** *46* (42), 8050-8053.
35. Spies, P.; Schwendemann, S.; Lange, S.; Kehr, G.; Fröhlich, R.; Erker, G., Metal-Free Catalytic Hydrogenation of Enamines, Imines, and Conjugated Phosphinoalkenylboranes. *Angew. Chem., Int. Ed.* **2008,** *47* (39), 7543-7546.
36. Wang, H.; Fröhlich, R.; Kehr, G.; Erker, G., Heterolytic dihydrogen activation with the 1,8-bis(diphenylphosphino)naphthalene/B(C6F5)3 pair and its application for metal-free catalytic hydrogenation of silyl enol ethers. *Chem. Commun.* **2008,** (45), 5966-5968.
37. Greb, L.; Daniliuc, C.-G.; Bergander, K.; Paradies, J., Functional-Group Tolerance in Frustrated Lewis Pairs: Hydrogenation of Nitroolefins and Acrylates. *Angew. Chem., Int. Ed.* **2013,** *52* (22), 5876-5879.
38. Chernichenko, K.; Madarász, Á.; Pápai, I.; Nieger, M.; Leskelä, M.; Repo, T., A frustrated-Lewis-pair approach to catalytic reduction of alkynes to cis-alkenes. *Nat. Chem.* **2013,** *5* (8), 718-723.
39. Stephan, D. W.; Erker, G., Frustrated Lewis Pair Mediated Hydrogenations. In *Frustrated Lewis Pairs I: Uncovering and Understanding*, Eds. Springer Berlin Heidelberg: Berlin, Heidelberg, 2013; pp 85-110.
40. Piers, W. E.; Marwitz, A. J. V.; Mercier, L. G., Mechanistic Aspects of Bond Activation with Perfluoroarylboranes. *Inorg. Chem.* **2011,** *50* (24), 12252-12262.
41. Bertini, F.; Lyaskovskyy, V.; Timmer, B. J. J.; de Kanter, F. J. J.; Lutz, M.; Ehlers, A. W.; Slootweg, J. C.; Lammertsma, K., Preorganized Frustrated Lewis Pairs. *J. Am. Chem. Soc.* **2012,** *134* (1), 201-204.
42. Mo, Z. B.; Pit, A.; Campos, J.; Kolychev, E. L.; Aldridge, S., Catalytic B-N Dehydrogenation Using Frustrated Lewis Pairs: Evidence for a Chain-Growth Coupling Mechanism. *J. Am. Chem. Soc.* **2016,** *138* (10), 3306-3309.
43. Cui, C.; Roesky, H. W.; Schmidt, H.-G.; Noltemeyer, M.; Hao, H.; Cimpoesu, F., Synthesis and Structure of a Monomeric Aluminum(I) Compound [{HC(CMeNAr)$_2$}Al] (Ar = 2,6–i$Pr_2C_6H_3$): A Stable Aluminum Analogue of a Carbene. *Angew. Chem., Int. Ed.* **2000,** *39* (23), 4274-4276.
44. Hicks, J.; Vasko, P.; Goicoechea, J. M.; Aldridge, S., Synthesis, structure and reaction chemistry of a nucleophilic aluminyl anion. *Nature* **2018,** *557* (7703), 92-95.
45. Segawa, Y.; Yamashita, M.; Nozaki, K., Boryllithium: Isolation, Characterization, and Reactivity as a Boryl Anion. *Science* **2006,** *314* (5796), 113.
46. Semenenko, K. N.; Shilkin, S. P.; Kravchenko, O. V.; Polyakova, V. B., Structure of Hexaammines of Aluminum Borohydride and Chloroborohydrides. *Bull. Acad. Sci. USSR, Div. Chem. Sci.* **1974,** *23* (7), 1379-1383.
47. Dunn, N. L.; Ha, M.; Radosevich, A. T., Main Group Redox Catalysis: Reversible PIII/PV Redox Cycling at a Phosphorus Platform. *J. Am. Chem. Soc.* **2012,** *134* (28), 11330-11333.
48. Martin, D.; Soleilhavoup, M.; Bertrand, G., Stable singlet carbenes as mimics for transition metal centers. *Chem. Sci.* **2011,** *2* (3), 389-399.
49. Bourissou, D.; Guerret, O.; Gabbaï, F. P.; Bertrand, G., Stable Carbenes. *Chem. Rev.* **2000,** *100* (1), 39-92.
50. Igau, A.; Grutzmacher, H.; Baceiredo, A.; Bertrand, G., Analogous α,α′-Bis-Carbenoid Triply Bonded Species: Synthesis of a Stable λ3-Phosphinocarbene-λ5-Phosphaacetylene. *J. Am. Chem. Soc.* **1988,** *110* (19), 6463-6466.
51. Arduengo, A. J.; Harlow, R. L.; Kline, M., A stable crystalline carbene. *J. Am. Chem. Soc.* **1991,** *113* (1), 361-363.

52. Nolan, S. P., *N-Heterocyclic carbenes : effective tools for organometallic synthesis*. Wiley-VCH: Weinheim an der Bergstrasse, Germany, 2014.
53. Díez-González, S., *N-heterocyclic carbenes : from laboratories curiosities to efficient synthetic tools*. Royal Society of Chemistry: Cambridge, 2010.
54. Flanigan, D. M.; Romanov-Michailidis, F.; White, N. A.; Rovis, T., Organocatalytic Reactions Enabled by N-Heterocyclic Carbenes. *Chem. Rev.* **2015,** *115* (17), 9307-9387.
55. Nesterov, V.; Reiter, D.; Bag, P.; Frisch, P.; Holzner, R.; Porzelt, A.; Inoue, S., NHCs in Main Group Chemistry. *Chem. Rev.* **2018,** *118* (19), 9678-9842.
56. Lavallo, V.; Canac, Y.; Präsang, C.; Donnadieu, B.; Bertrand, G., Stable Cyclic (Alkyl)(Amino)Carbenes as Rigid or Flexible, Bulky, Electron-Rich Ligands for Transition-Metal Catalysts: A Quaternary Carbon Atom Makes the Difference. *Angew. Chem., Int. Ed.* **2005,** *44* (35), 5705-5709.
57. Frey, G. D.; Lavallo, V.; Donnadieu, B.; Schoeller, W. W.; Bertrand, G., Facile Splitting of Hydrogen and Ammonia by Nucleophilic Activation at a Single Carbon Center. *Science* **2007,** *316* (5823), 439-441.
58. Lavallo, V.; Canac, Y.; Donnadieu, B.; Schoeller, W. W.; Bertrand, G., CO Fixation to Stable Acyclic and Cyclic Alkyl Amino Carbenes: Stable Amino Ketenes with a Small HOMO–LUMO Gap. *Angew. Chem., Int. Ed.* **2006,** *45* (21), 3488-3491.
59. Braunschweig, H.; Dewhurst, R. D.; Hammond, K.; Mies, J.; Radacki, K.; Vargas, A., Ambient-Temperature Isolation of a Compound with a Boron-Boron Triple Bond. *Science* **2012,** *336* (6087), 1420.
60. Böhnke, J.; Braunschweig, H.; Ewing, W. C.; Hörl, C.; Kramer, T.; Krummenacher, I.; Mies, J.; Vargas, A., Diborabutatriene: An Electron-Deficient Cumulene. *Angew. Chem., Int. Ed.* **2014,** *53* (34), 9082-9085.
61. Sasamori, T.; Tokitoh, N., Encyclopedia of Inorganic Chemistry II. **2005**, 1698-1740.
62. Trinquier, G., Double bonds and bridged structures in the heavier analogs of ethylene. *J. Am. Chem. Soc.* **1990,** *112* (6), 2130-2137.
63. Drahnak, T. J.; Michl, J.; West, R., Dimethylsilylene, $(CH_3)_2Si$. *J. Am. Chem. Soc.* **1979,** *101* (18), 5427-5428.
64. West, R.; Fink, M. J.; Michl, J., Tetramesityldisilene, a Stable Compound Containing a Silicon-Silicon Double Bond. *Science* **1981,** *214* (4527), 1343-1344.
65. West, R., Chemistry of the Silicon-Silicon Double Bond. *Angew. Chem., Int. Ed.* **1987,** *26* (12), 1201-1211.
66. West, R.; Denk, M., Stable silylenes: synthesis, structure, reactions. *Pure Appl. Chem.* **1996,** *68* (4), 785-788.
67. Jutzi, P.; Holtmann, U.; Bögge, H.; Müller, A., Protonation of decamethylsilicocene [bis(pentamethylcyclopentadienyl)silicon]. *J. Chem. Soc., Chem. Commun.* **1988,** (4), 305-306.
68. Denk, M.; Lennon, R.; Hayashi, R.; West, R.; Belyakov, A. V.; Verne, H. P.; Haaland, A.; Wagner, M.; Metzler, N., Synthesis and Structure of a Stable Silylene. *J. Am. Chem. Soc.* **1994,** *116* (6), 2691-2692.
69. Kira, M.; Ishida, S.; Iwamoto, T.; Kabuto, C., The First Isolable Dialkylsilylene. *J. Am. Chem. Soc.* **1999,** *121* (41), 9722-9723.
70. Asay, M.; Inoue, S.; Driess, M., Aromatic Ylide-Stabilized Carbocyclic Silylene. *Angew. Chem., Int. Ed.* **2011,** *50* (41), 9589-9592.
71. Abe, T.; Tanaka, R.; Ishida, S.; Kira, M.; Iwamoto, T., New Isolable Dialkylsilylene and Its Isolable Dimer That Equilibrate in Solution. *J. Am. Chem. Soc.* **2012,** *134* (49), 20029-20032.
72. Kosai, T.; Ishida, S.; Iwamoto, T., A Two-Coordinate Cyclic (Alkyl)(amino)silylene: Balancing Thermal Stability and Reactivity. *Angew. Chem., Int. Ed.* **2016,** *55* (50), 15554-15558.
73. Gau, D.; Kato, T.; Saffon-Merceron, N.; Cossío, F. P.; Baceiredo, A., Stable Phosphonium Silaylide with Reactivity as a Sila-Wittig Reagent. *J. Am. Chem. Soc.* **2009,** *131* (25), 8762-8763.
74. Protchenko, A. V.; Birjkumar, K. H.; Dange, D.; Schwarz, A. D.; Vidovic, D.; Jones, C.; Kaltsoyannis, N.; Mountford, P.; Aldridge, S., A Stable Two-Coordinate Acyclic Silylene. *J. Am. Chem. Soc.* **2012,** *134* (15), 6500-6503.

75. Loh, Y. K.; Ying, L.; Ángeles Fuentes, M.; Do, D. C. H.; Aldridge, S., An N-Heterocyclic Boryloxy Ligand Isoelectronic with N-Heterocyclic Imines: Access to an Acyclic Dioxysilylene and its Heavier Congeners. *Angew. Chem., Int. Ed.* **2019,** *58* (15), 4847-4851.
76. Roy, M. M. D.; Ferguson, M. J.; McDonald, R.; Zhou, Y.; Rivard, E., A vinyl silylsilylene and its activation of strong homo- and heteroatomic bonds. *Chem. Sci.* **2019,** 10, 6476-6481.
77. Martin, D.; Canac, Y.; Lavallo, V.; Bertrand, G., Comparative Reactivity of Different Types of Stable Cyclic and Acyclic Mono- and Diamino Carbenes with Simple Organic Substrates. *J. Am. Chem. Soc.* **2014,** *136* (13), 5023-5030.
78. Rekken, B. D.; Brown, T. M.; Fettinger, J. C.; Tuononen, H. M.; Power, P. P., Isolation of a Stable, Acyclic, Two-Coordinate Silylene. *J. Am. Chem. Soc.* **2012,** *134* (15), 6504-6507.
79. Protchenko, A.; Vasko, P.; Do, D. C. H.; Hicks, J.; Fuentes, M. Á.; Jones, C.; Aldridge, S., Reduction of carbon oxides by an acyclic silylene: reductive coupling of CO. *Angew. Chem., Int. Ed.* **2018,** *58* (6), 1808.
80. Wendel, D.; Reiter, D.; Porzelt, A.; Altmann, P. J.; Inoue, S.; Rieger, B., Silicon and Oxygen's Bond of Affection: An Acyclic Three-Coordinate Silanone and Its Transformation to an Iminosiloxysilylene. *J. Am. Chem. Soc.* **2017,** *139* (47), 17193-17198.
81. Hupf, E.; Kaiser, F.; Lummis, P. A.; Roy, M. M. D.; McDonald, R.; Ferguson, M. J.; Kühn, F. E.; Rivard, E., Linking Low-Coordinate Ge(II) Centers via Bridging Anionic N-Heterocyclic Olefin Ligands. *Inorg. Chem.* **2020,** *59* (3), 1592-1601.
82. Lui, M. W.; Merten, C.; Ferguson, M. J.; McDonald, R.; Xu, Y.; Rivard, E., Contrasting Reactivities of Silicon and Germanium Complexes Supported by an N-Heterocyclic Guanidine Ligand. *Inorg. Chem.* **2015,** *54* (4), 2040-2049.
83. Roy, M. M. D.; Baird, S. R.; Dornsiepen, E.; Paul, L. A.; Miao, L.; Ferguson, M. J.; Zhou, Y.; Siewert, I.; Rivard, E., A Stable Homoleptic Divinyl Tetrelene Series. *Chem. - Eur. J.* **2021,** *27* (33), 8572-8579.
84. Wendel, D.; Porzelt, A.; Herz, F. A. D.; Sarkar, D.; Jandl, C.; Inoue, S.; Rieger, B., From Si(II) to Si(IV) and Back: Reversible Intramolecular Carbon–Carbon Bond Activation by an Acyclic Iminosilylene. *J. Am. Chem. Soc.* **2017,** *139* (24), 8134-8137.
85. Wang, X.; Zhu, Z.; Peng, Y.; Lei, H.; Fettinger, J. C.; Power, P. P., Room-Temperature Reaction of Carbon Monoxide with a Stable Diarylgermylene. *J. Am. Chem. Soc.* **2009,** *131* (20), 6912-6913.
86. Ganesamoorthy, C.; Schoening, J.; Wölper, C.; Song, L.; Schreiner, P. R.; Schulz, S., A silicon–carbonyl complex stable at room temperature. *Nat. Chem.* **2020,** *12* (7), 608-614.
87. Reiter, D.; Holzner, R.; Porzelt, A.; Frisch, P.; Inoue, S., Silylated silicon–carbonyl complexes as mimics of ubiquitous transition-metal carbonyls. *Nat. Chem.* **2020,** *12* (12), 1131-1135.
88. Pearsall, M. A.; West, R., The reactions of diorganosilylenes with carbon monoxide. *J. Am. Chem. Soc.* **1988,** *110* (21), 7228-7229.
89. Arrington, C. A.; Petty, J. T.; Payne, S. E.; Haskins, W. C. K., The reaction of dimethylsilylene with carbon monoxide in low-temperature matrices. *J. Am. Chem. Soc.* **1988,** *110* (18), 6240-6241.
90. Tacke, M.; Klein, C.; Stufkens, D. J.; Oskam, A.; Jutzi, P.; Bunte, E. A., Complexes of decamethylsilicocene: Cp_2*Si(CO) and Cp_2*Si(N_2). *Z. Anorg. Allg. Chem.* **1993,** *619* (5), 865-868.
91. Krasowska, M.; Edelmann, M.; Bettinger, H. F., Electronically Excited States of Borylenes. *J. Phys. Chem. A* **2016,** *120* (32), 6332-6341.
92. Krasowska, M.; Bettinger, H. F., Reactivity of Borylenes toward Ethyne, Ethene, and Methane. *J. Am. Chem. Soc.* **2012,** *134* (41), 17094-17103.
93. Soleilhavoup, M.; Bertrand, G., Borylenes: An Emerging Class of Compounds. *Angew. Chem., Int. Ed.* **2017,** *56* (35), 10282-10292.
94. Kinjo, R.; Donnadieu, B.; Celik, M. A.; Frenking, G.; Bertrand, G., Synthesis and Characterization of a Neutral Tricoordinate Organoboron Isoelectronic with Amines. *Science* **2011,** *333* (6042), 610.
95. Braunschweig, H.; Dewhurst, R. D.; Hupp, F.; Nutz, M.; Radacki, K.; Tate, C. W.; Vargas, A.; Ye, Q., Multiple complexation of CO and related ligands to a main-group element. *Nature* **2015,** *522* (7556), 327-330.
96. Légaré, M.-A.; Bélanger-Chabot, G.; Dewhurst, R. D.; Welz, E.; Krummenacher, I.; Engels, B.; Braunschweig, H., Nitrogen fixation and reduction at boron. *Science* **2018,** *359* (6378), 896-900.

97. Légaré, M.-A.; Rang, M.; Bélanger-Chabot, G.; Schweizer, J. I.; Krummenacher, I.; Bertermann, R.; Arrowsmith, M.; Holthausen, M. C.; Braunschweig, H., The reductive coupling of dinitrogen. *Science* **2019,** *363* (6433), 1329-1332.
98. Légaré, M.-A.; Bélanger-Chabot, G.; Rang, M.; Dewhurst, R. D.; Krummenacher, I.; Bertermann, R.; Braunschweig, H., One-pot, room-temperature conversion of dinitrogen to ammonium chloride at a main-group element. *Nat. Chem.* **2020,** *12* (11), 1076-1080.
99. Dohmeier, C.; Robl, C.; Tacke, M.; Schnöckel, H., The Tetrameric Aluminum(I) Compound [{Al(η^5-C_5Me_5)}$_4$]. *Angew. Chem., Int. Ed.* **1991,** *30* (5), 564-565.
100. Hofmann, A.; Tröster, T.; Kupfer, T.; Braunschweig, H., Monomeric Cp3tAl(i): synthesis, reactivity, and the concept of valence isomerism. *Chem. Sci.* **2019,** *10* (11), 3421-3428.
101. Mellerup, S. K.; Cui, Y.; Fantuzzi, F.; Schmid, P.; Goettel, J. T.; Bélanger-Chabot, G.; Arrowsmith, M.; Krummenacher, I.; Ye, Q.; Engel, V.; Engels, B.; Braunschweig, H., Lewis-Base Stabilization of the Parent Al(I) Hydride under Ambient Conditions. *J. Am. Chem. Soc.* **2019,** *141* (42), 16954-16960.
102. Queen, J. D.; Lehmann, A.; Fettinger, J. C.; Tuononen, H. M.; Power, P. P., The Monomeric Alanediyl :AlAr^{i}Pr$_8$ (Ar^{i}Pr$_8$ = C_6H-2,6-(C_6H_2-2,4,6-^{i}Pr$_3$)2-3,5-^{i}Pr$_2$): An Organoaluminum(I) Compound with a One-Coordinate Aluminum Atom. *J. Am. Chem. Soc.* **2020,** *142* (49), 20554-20559.
103. Zhang, X.; Liu, L. L., A Free Aluminylene with Diverse σ-Donating and Doubly σ/π-Accepting Ligand Features for Transition Metals. *Angew. Chem., Int. Ed.* **2021,** *60* (52), 27062-27069.
104. Hinz, A.; Müller, M. P., Attempted reduction of a carbazolyl-diiodoalane. *Chem. Commun.* **2021,** *57* (93), 12532-12535.
105. Hobson, K.; Carmalt, C. J.; Bakewell, C., Recent advances in low oxidation state aluminium chemistry. *Chem. Sci.* **2020,** *11* (27), 6942-6956.
106. Schmidt, E. S.; Jockisch, A.; Schmidbaur, H., A Carbene Analogue with Low-Valent Gallium as a Heteroatom in a quasi-Aromatic Imidazolate Anion. *J. Am. Chem. Soc.* **1999,** *121* (41), 9758-9759.
107. Cordero, B.; Gómez, V.; Platero-Prats, A. E.; Revés, M.; Echeverría, J.; Cremades, E.; Barragán, F.; Alvarez, S., Covalent radii revisited. *Dalton Trans.* **2008,** (21), 2832-2838.
108. Hicks, J.; Vasko, P.; Goicoechea, J. M.; Aldridge, S., Reversible, Room-Temperature C—C Bond Activation of Benzene by an Isolable Metal Complex. *J. Am. Chem. Soc.* **2019,** *141* (28), 11000-11003.
109. Protchenko, A. V.; Vasko, P.; Fuentes, M. Á.; Hicks, J.; Vidovic, D.; Aldridge, S., Approaching a "Naked" Boryl Anion: Amide Metathesis as a Route to Calcium, Strontium, and Potassium Boryl Complexes. *Angew. Chem., Int. Ed.* **2021,** *60* (4), 2064-2068.
110. Roy, M. M. D.; Hicks, J.; Vasko, P.; Heilmann, A.; Baston, A.-M.; Goicoechea, J. M.; Aldridge, S., Probing the Extremes of Covalency in M−Al bonds: Lithium and Zinc Aluminyl Compounds. *Angew. Chem., Int. Ed.* **2021,** *60* (41), 22301-22306.
111. Schwamm, R. J.; Anker, M. D.; Lein, M.; Coles, M. P., Reduction vs. Addition: The Reaction of an Aluminyl Anion with 1,3,5,7-Cyclooctatetraene. *Angew. Chem., Int. Ed.* **2019,** *58* (5), 1489-1493.
112. Schwamm, R. J.; Coles, M. P.; Hill, M. S.; Mahon, M. F.; McMullin, C. L.; Rajabi, N. A.; Wilson, A. S. S., A Stable Calcium Alumanyl. *Angew. Chem., Int. Ed.* **2020,** *59* (10), 3928-3932.
113. Kurumada, S.; Takamori, S.; Yamashita, M., An alkyl-substituted aluminium anion with strong basicity and nucleophilicity. *Nat. Chem.* **2020,** *12* (1), 36-39.
114. Koshino, K.; Kinjo, R., Construction of σ-Aromatic AlB_2 Ring via Borane Coupling with a Dicoordinate Cyclic (Alkyl)(Amino)Aluminyl Anion. *J. Am. Chem. Soc.* **2020,** *142* (19), 9057-9062.
115. Grams, S.; Eyselein, J.; Langer, J.; Färber, C.; Harder, S., Boosting Low-Valent Aluminum(I) Reactivity with a Potassium Reagent. *Angew. Chem., Int. Ed.* **2020,** *59* (37), 15982-15986.
116. Hicks, J.; Vasko, P.; Goicoechea, J. M.; Aldridge, S., The Aluminyl Anion: A New Generation of Aluminium Nucleophile. *Angew. Chem., Int. Ed.* **2021,** *60* (4), 1702-1713.
117. Martin, D.; Lassauque, N.; Donnadieu, B.; Bertrand, G., A Cyclic Diaminocarbene with a Pyramidalized Nitrogen Atom: A Stable N-Heterocyclic Carbene with Enhanced Electrophilicity. *Angew. Chem., Int. Ed.* **2012,** *51* (25), 6172-6175.
118. Gusel'nikov, L. E.; Nametkin, N. S., Formation and properties of unstable intermediates containing multiple p.pi.-p.pi. bonded Group 4B metals. *Chem. Rev.* **1979,** *79* (6), 529-577.
119. Jutzi, P., New Element-Carbon (p-p)π Bonds. *Angew. Chem., Int. Ed.* **1975,** *14* (4), 232-245.

120. Goldberg, D. E.; Harris, D. H.; Lappert, M. F.; Thomas, K. M., A new synthesis of divalent group 4B alkyls M[CH(SiMe$_3$)$_2$]$_2$(M = Ge or Sn), and the crystal and molecular and molecular strcuture of the tin compound. *J. Chem. Soc., Chem. Commun.* **1976,** (7), 261-262.
121. Brook, A. G.; Abdesaken, F.; Gutekunst, B.; Gutekunst, G.; Kallury, R. K., A solid silaethene: isolation and characterization. *J. Chem. Soc., Chem. Commun.* **1981,** (4), 191-192.
122. Yoshifuji, M.; Shima, I.; Inamoto, N.; Hirotsu, K.; Higuchi, T., Synthesis and structure of bis(2,4,6-tri-tert-butylphenyl)diphosphene: isolation of a true phosphobenzene. *J. Am. Chem. Soc.* **1981,** *103* (15), 4587-4589.
123. Hanusch, F.; Groll, L.; Inoue, S., Recent advances of group 14 dimetallenes and dimetallynes in bond activation and catalysis. *Chem. Sci.* **2021,** *12* (6), 2001-2015.
124. Spikes, G. H.; Fettinger, J. C.; Power, P. P., Facile Activation of Dihydrogen by an Unsaturated Heavier Main Group Compound. *J. Am. Chem. Soc.* **2005,** *127* (35), 12232-12233.
125. Peng, Y.; Brynda, M.; Ellis, B. D.; Fettinger, J. C.; Rivard, E.; Power, P. P., Addition of H_2 to distannynes under ambient conditions. *Chem. Commun.* **2008,** (45), 6042-6044.
126. Trinquier, G.; Malrieu, J. P.; Riviere, P., Unusual bonding in trans-bent digermene. *J. Am. Chem. Soc.* **1982,** *104* (17), 4529-4533.
127. Carter, E. A.; Goddard, W. A., Relation between singlet-triplet gaps and bond energies. *J. Phys. Chem.* **1986,** *90* (6), 998-1001.
128. Trinquier, G.; Malrieu, J. P., Nonclassical distortions at multiple bonds. *J. Am. Chem. Soc.* **1987,** *109* (18), 5303-5315.
129. Nagase, S.; Kobayashi, K.; Takagi, N., Triple bonds between heavier Group 14 elements. A theoretical approach. *J. Organomet. Chem.* **2000,** *611* (1), 264-271.
130. Wedler, H. B.; Wendelboe, P.; Power, P. P., Second-Order Jahn–Teller (SOJT) Structural Distortions in Multiply Bonded Higher Main Group Compounds. *Organometallics* **2018,** *37* (18), 2929-2936.
131. Power, P. P., π-Bonding and the Lone Pair Effect in Multiple Bonds between Heavier Main Group Elements. *Chem. Rev.* **1999,** *99* (12), 3463-3504.
132. Fischer, R. C.; Power, P. P., π-Bonding and the Lone Pair Effect in Multiple Bonds Involving Heavier Main Group Elements: Developments in the New Millennium. *Chem. Rev.* **2010,** *110* (7), 3877-3923.
133. Weetman, C., Main Group Multiple Bonds for Bond Activations and Catalysis. *Chem. - Eur. J.* **2021,** *27* (6), 1941-1954.
134. Braunschweig, H.; Dellermann, T.; Dewhurst, R. D.; Ewing, W. C.; Hammond, K.; Jimenez-Halla, J. O. C.; Kramer, T.; Krummenacher, I.; Mies, J.; Phukan, A. K.; Vargas, A., Metal-free binding and coupling of carbon monoxide at a boron–boron triple bond. *Nat. Chem.* **2013,** *5* (12), 1025-1028.
135. Böhnke, J.; Braunschweig, H.; Dellermann, T.; Ewing, W. C.; Hammond, K.; Jimenez-Halla, J. O. C.; Kramer, T.; Mies, J., The Synthesis of B_2(SIDip)$_2$ and its Reactivity Between the Diboracumulenic and Diborynic Extremes. *Angew. Chem., Int. Ed.* **2015,** *54* (46), 13801-13805.
136. Bag, P.; Porzelt, A.; Altmann, P. J.; Inoue, S., A Stable Neutral Compound with an Aluminum–Aluminum Double Bond. *J. Am. Chem. So.c* **2017,** *139* (41), 14384-14387.
137. Weetman, C.; Porzelt, A.; Bag, P.; Hanusch, F.; Inoue, S., Dialumenes – aryl vs. silyl stabilisation for small molecule activation and catalysis. *Chem. Sci.* **2020,** *11* (18), 4817-4827.
138. Hardman, N. J.; Wright, R. J.; Phillips, A. D.; Power, P. P., Synthesis and Characterization of the Neutral "Digallene" Ar′GaGaAr′ and Its Reduction to Na2Ar′GaGaAr′ (Ar′=2,6-Dipp$_2$C$_6$H$_3$, Dipp=2,6-iPr$_2$C$_6$H$_3$). *Angew. Chem., Int. Ed.* **2002,** *41* (15), 2842-2844.
139. Wright, R. J.; Phillips, A. D.; Allen, T. L.; Fink, W. H.; Power, P. P., Synthesis and Characterization of the Monomeric Imides Ar‘MNAr‘ ‘ (M = Ga or In; Ar‘ or Ar‘ ‘ = Terphenyl Ligands) with Two-Coordinate Gallium and Indium. *J. Am. Chem. Soc.* **2003,** *125* (7), 1694-1695.
140. Wright, R. J.; Phillips, A. D.; Hino, S.; Power, P. P., Synthesis and Reactivity of Dimeric Ar‘TlTlAr‘ and Trimeric (Ar‘ ‘Tl)$_3$ (Ar‘, Ar‘ ‘ = Bulky Terphenyl Group) Thallium(I) Derivatives: Tl(I)−Tl(I) Bonding in Species Ligated by Monodentate Ligands. *J. Am. Chem. Soc.* **2005,** *127* (13), 4794-4799.

141. Zhu, Z.; Wang, X.; Peng, Y.; Lei, H.; Fettinger, J. C.; Rivard, E.; Power, P. P., Addition of Hydrogen or Ammonia to a Low-Valent Group 13 Metal Species at 25 °C and 1 Atmosphere. *Angew. Chem., Int. Ed.* **2009,** *48* (11), 2031-2034.
142. Wendel, D.; Szilvási, T.; Jandl, C.; Inoue, S.; Rieger, B., Twist of a Silicon–Silicon Double Bond: Selective Anti-Addition of Hydrogen to an Iminodisilene. *J. Am. Chem. Soc.* **2017,** *139* (27), 9156-9159.
143. Kosai, T.; Iwamoto, T., Stable Push–Pull Disilene: Substantial Donor–Acceptor Interactions through the Si=Si Double Bond. *J. Am. Chem. Soc.* **2017,** *139* (50), 18146-18149.
144. Majumdar, M.; Omlor, I.; Yildiz, C. B.; Azizoglu, A.; Huch, V.; Scheschkewitz, D., Reductive Cleavage of Carbon Monoxide by a Disilenide. *Angew. Chem., Int. Ed.* **2015,** *54* (30), 8746-8750.
145. Cowley, M. J.; Ohmori, Y.; Huch, V.; Ichinohe, M.; Sekiguchi, A.; Scheschkewitz, D., Carbonylation of Cyclotrisilenes. *Angew. Chem., Int. Ed.* **2013,** *52* (50), 13247-13250.
146. Cowley, M. J.; Huch, V.; Scheschkewitz, D., Donor–Acceptor Adducts of a 1,3-Disila-2-oxyallyl Zwitterion. *Chem. - Eur. J.* **2014,** *20* (30), 9221-9224.
147. Krishnan, R.; Frisch, M. J.; Pople, J. A.; von R. Schleyer, P., The vinylidene-acetylene isomerization barrier. *Chem. Phys. Lett.* **1981,** *79* (3), 408-411.
148. Osamura, Y.; Schaefer, H. F.; Gray, S. K.; Miller, W. H., Vinylidene: a very shallow minimum on the C_2H_2 potential energy surface. *J. Am. Chem. Soc.* **1981,** *103* (8), 1904-1907.
149. Chang, N.-y.; Shen, M.-y.; Yu, C.-h., Extended ab initio studies of the vinylidene–acetylene rearrangement. *J. Chem. Phys.* **1997,** *106* (8), 3237-3242.
150. Stanton, J. F.; Gauss, J., Some predictions relevant to future spectroscopic observation of S1 vinylidene. *J. Chem. Phys.* **1994,** *101* (4), 3001-3005.
151. Bruce, M. I., Organometallic chemistry of vinylidene and related unsaturated carbenes. *Chem. Rev.* **1991,** *91* (2), 197-257.
152. Knorr, R., Alkylidenecarbenes, Alkylidenecarbenoids, and Competing Species: Which Is Responsible for Vinylic Nucleophilic Substitution, [1 + 2] Cycloadditions, 1,5-CH Insertions, and the Fritsch−Buttenberg−Wiechell Rearrangement? *Chem. Rev.* **2004,** *104* (9), 3795-3850.
153. Kutin, Y.; Reitz, J.; Antoni, P. W.; Savitsky, A.; Pantazis, D. A.; Kasanmascheff, M.; Hansmann, M. M., Characterization of a Triplet Vinylidene. *J. Am. Chem. Soc.* **2021,** *143* (50), 21410-21415.
154. Lein, M.; Krapp, A.; Frenking, G., Why Do the Heavy-Atom Analogues of Acetylene E_2H_2 (E = Si−Pb) Exhibit Unusual Structures? *J. Am. Chem. Soc.* **2005,** *127* (17), 6290-6299.
155. Rivard, E., Group 14 inorganic hydrocarbon analogues. *Chem. Soc. Rev.* **2016,** *45* (4), 989-1003.
156. Jana, A.; Huch, V.; Scheschkewitz, D., NHC-Stabilized Silagermenylidene: A Heavier Analogue of Vinylidene. *Angew. Chem., Int. Ed.* **2013,** *52* (46), 12179-12182.
157. Ghana, P.; Arz, M. I.; Das, U.; Schnakenburg, G.; Filippou, A. C., Si=Si Double Bonds: Synthesis of an NHC-Stabilized Disilavinylidene. *Angew. Chem., Int. Ed.* **2015,** *54* (34), 9980-9985.
158. Rit, A.; Campos, J.; Niu, H.; Aldridge, S., A stable heavier group 14 analogue of vinylidene. *Nat. Chem.* **2016,** *8* (11), 1022-1026.

Chapter 2 General Methods

All manipulations were carried out using standard Schlenk line or dry-box techniques under an atmosphere of argon or dinitrogen. Solvents were degassed by sparging with argon and dried by passing through a column of the appropriate drying agent.

2.1 Spectroscopic and analytical techniques

NMR spectra were measured in benzene-d_6 (which was dried over potassium), with the solvent then being distilled under reduced pressure and stored under argon in Teflon valve ampoules. NMR samples were prepared under argon in 5 mm Wilmad 507-PP tubes fitted with J. Young Teflon valves. ^{1}H, $^{31}P\{^{1}H\}$, $^{13}C\{^{1}H\}$, $^{11}B\{^{1}H\}$, ^{19}F NMR spectra were measured on a Bruker Avance III HD nanobay 400 MHz or Bruker Avance 500 MHz spectrometer at ambient temperature and referenced internally to residual protio-solvent (^{1}H) or solvent (^{13}C) resonances and are reported relative to tetramethylsilane (δ = 0 ppm). Assignments were confirmed using two-dimensional ^{1}H-^{1}H and ^{13}C-^{1}H NMR correlation experiments. Chemical shifts are quoted in δ (ppm) and coupling constants in Hz.

UV-Vis samples were prepared by dissolving the compound in chloroform (0.8 mM) and transferring the solution into a cuvette (l = 1.0 mm) fitted with a Teflon valve. UV-Vis spectra were measured on a Perkin Elmer Lambda 19 UV/vis/NIR spectrometer.

Elemental analyses were carried out by Elemental Microanalysis Ltd, Okehampton, Devon, UK.

Single-crystal X-ray diffraction data for all compounds were collected at 150 K on a Oxford Diffraction/Agilent SuperNova diffractometer using Cu-*Kα* radiation (λ = 1.54184 Å), and equipped with a nitrogen gas Oxford Cryosystems cooling unit.[1] Raw-frame data were reduced using CrysAlisPro.[25] The structures were solved using SHELXT[2] and refined to convergence

on F^2 by full-matrix least-squares using SHELXL[3] in combination with the SHELXLE program.[4] Distances and angles were calculated using the full covariance matrix. Restraints were used to maintain sensible geometries for the disordered groups and approximate the displacement parameters to typical values.

For chapters 3 and 4, the computational work was performed using Density Functional Theory (DFT) within the Gaussian09 (Revision D.01) program package.[5] Geometry optimizations of the monoanionic ligand systems were performed with the PBE1PBE hybrid exchange-correlation functional[6-10] using a TZVP basis set.[11] Grimme's empirical dispersion correction (DFT-D3) was included in all geometry optimizations.[12-13] Unless otherwise stated, geometry optimizations were carried out for the full system, and frequency calculations were performed to confirm the nature of the stationary points found (minimum). Graphics were created with the Avogadro program.[14] Natural bond orbital (NBO) analyses were performed using NBO 3.1 as implemented in Gaussian09.[34] For chapters 5 and 6, the specific methods used are described in details in the text.

2.2 References

1. Cosier, J.; Glazer, A. M., A nitrogen-gas-stream cryostat for general X-ray diffraction studies. *J. Appl. Crystallogr.* **1986,** *19* (2), 105-107.
2. Sheldrick, G., Crystal structure refinement with SHELXL. *Acta Crystallogr., Sect. C: Struct. Chem.* **2015,** *71* (1), 3-8.
3. Sheldrick, G., A short history of SHELX. *Acta Crystallogr., Sect. A: Found. Adv.* **2008,** *64* (1), 112-122.
4. Hubschle, C. B.; Sheldrick, G. M.; Dittrich, B., ShelXle: a Qt graphical user interface for SHELXL. *J. Appl. Crystallogr.* **2011,** *44* (6), 1281-1284.
5. Frisch, M. J.; Trucks, G. W.; Schlegel, H. B.; Scuseria, G. E.; Robb, M. A.; Cheeseman, J. R.; Scalmani, G.; Barone, V.; Petersson, G. A.; Nakatsuji, H.; Li, X.; Caricato, M.; Marenich, A. V.; Bloino, J.; Janesko, B. G.; Gomperts, R.; Mennucci, B.; Hratchian, H. P.; Ortiz, J. V.; Izmaylov, A. F.; Sonnenberg, J. L.; Williams; Ding, F.; Lipparini, F.; Egidi, F.; Goings, J.; Peng, B.; Petrone, A.; Henderson, T.; Ranasinghe, D.; Zakrzewski, V. G.; Gao, J.; Rega, N.; Zheng, G.; Liang, W.; Hada, M.; Ehara, M.; Toyota, K.; Fukuda, R.; Hasegawa, J.; Ishida, M.; Nakajima, T.; Honda, Y.; Kitao, O.; Nakai, H.; Vreven, T.; Throssell, K.; Montgomery Jr., J. A.; Peralta, J. E.; Ogliaro, F.; Bearpark, M. J.; Heyd, J. J.; Brothers, E. N.; Kudin, K. N.; Staroverov, V. N.; Keith, T. A.; Kobayashi, R.; Normand, J.; Raghavachari, K.; Rendell, A. P.; Burant, J. C.; Iyengar, S. S.; Tomasi, J.; Cossi, M.; Millam, J. M.; Klene, M.; Adamo, C.;

Cammi, R.; Ochterski, J. W.; Martin, R. L.; Morokuma, K.; Farkas, O.; Foresman, J. B.; Fox, D. J. *Gaussian 16 Rev. B.01*, Wallingford, CT, 2016.
6. Adamo, C.; Barone, V., Toward reliable density functional methods without adjustable parameters: The PBE0 model. *J. Chem. Phys.* **1999,** *110* (13), 6158-6170.
7. Ernzerhof, M.; Scuseria, G. E., Assessment of the Perdew–Burke–Ernzerhof exchange-correlation functional. *J. Chem. Phys.* **1999,** *110* (11), 5029-5036.
8. Perdew, J. P.; Burke, K.; Ernzerhof, M., Generalized Gradient Approximation Made Simple. *Phys. Rev. Lett.* **1997,** *78* (7), 1396-1396.
9. Perdew, J. P.; Burke, K.; Ernzerhof, M., Generalized Gradient Approximation Made Simple. *Phys. Rev. Lett.* **1996,** *77* (18), 3865-3868.
10. Perdew, J. P.; Ernzerhof, M.; Burke, K., Rationale for mixing exact exchange with density functional approximations. *J. Chem. Phys.* **1996,** *105* (22), 9982-9985.
11. Schäfer, A.; Huber, C.; Ahlrichs, R., Fully optimized contracted Gaussian basis sets of triple zeta valence quality for atoms Li to Kr. *J. Chem. Phys.* **1994,** *100* (8), 5829-5835.
12. Grimme, S.; Antony, J.; Ehrlich, S.; Krieg, H., A consistent and accurate ab initio parametrization of density functional dispersion correction (DFT-D) for the 94 elements H-Pu. *J. Chem. Phys.* **2010,** *132* (15), 154104.
13. Grimme, S.; Ehrlich, S.; Goerigk, L., Effect of the damping function in dispersion corrected density functional theory. *J. Comput. Chem.* **2011,** *32* (7), 1456-1465.
14. Hanwell, M. D.; Curtis, D. E.; Lonie, D. C.; Vandermeersch, T.; Zurek, E.; Hutchison, G. R., Avogadro: an advanced semantic chemical editor, visualization, and analysis platform. *J. Cheminf.* **2012,** *4* (1), 17.

Chapter 3 Designing FLPs for small molecule activation

3.1 Introduction

Recent decades have witnessed the rapid development of main group chemistry. Among these developments, Frustrated Lewis Pairs (FLPs) offer potential applications in metal-free catalytic processes on unsaturated organic substrates such as the hydrogenation of bulky imines,[1-2] enamines[3], silyl enol ethers,[4] alkenes and alkynes,[5-6] arenes,[7-8] etc. The activation of H_2 by FLPs has been introduced in Chapter 1, Section 1.2. As another important small molecule for industrial use, the activation and functionalization of CO draws much attention from researchers. Unlike transition metals which have accessible σ and π symmetry frontier orbitals, most *p*-block element compounds do not form tractable complexes with CO, primarily due to the lack of suitable orbitals for π-backbonding. Recently, a number of low-valent main group compounds have been developed with a suitable orbital manifold to allow for 'transition metal like' capabilities in the coordination of CO, including isolable carbenes and phosphinidenes, and transient species such as borylenes and silylenes.[9-13] A number of strongly Lewis acidic boranes can also react with CO to form the corresponding borane-carbonyl complex. $OC{\cdot}BH_3$, for example, can be formed by combining B_2H_6 with a high pressure of CO, although this adduct dissociates when the CO pressure is reduced.[14] Perfluoroalkylboranes,[15] Piers' borane,[16] and electron-deficient boroles,[17] have been shown more recently to form the analogous carbonyl complexes, $OC{\cdot}BR_3$, which have been structurally characterized by X-ray crystallography (e.g. Figure 3.1, A). However, the relatively weak OC–B σ-bonding and lack of π-backbonding in these systems typically leads to low thermodynamic stability: $OC{\cdot}B(C_6F_5)_3$, $OC{\cdot}B(CF_3)_3$ and $OC{\cdot}B(C_6F_5)_2H$ all decompose at room temperature or below, with only the perfluoropentaphenylborole adduct retaining CO at elevated temperatures (up to 60 °C).[18]

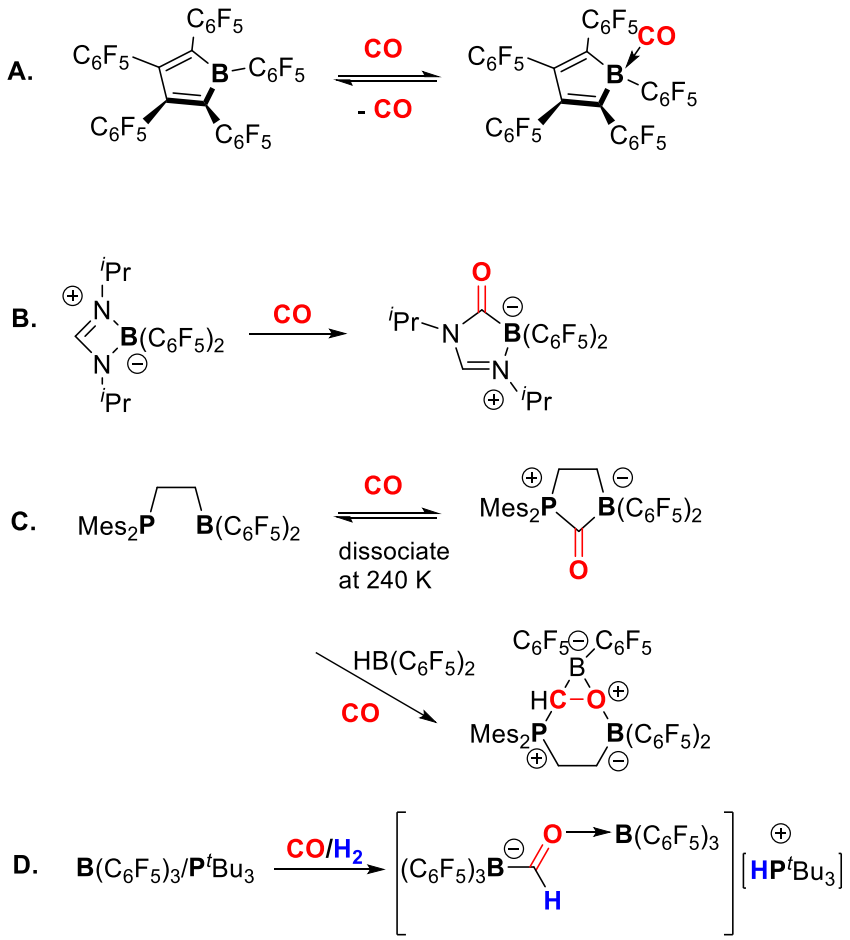


Figure 3.1. *Examples of CO capture by boranes and Frustrated Lewis Pairs.*

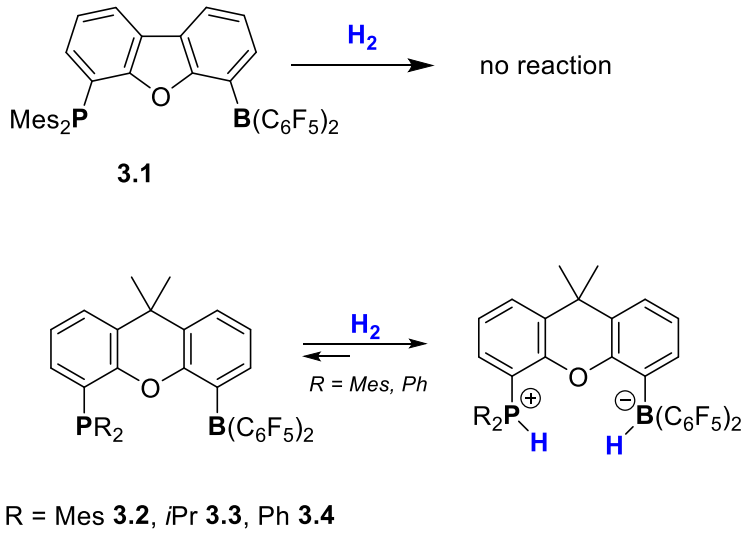
In an alternative to this single-site approach, σ-donation from CO to a Lewis acid and backbonding from a (separate) Lewis base into the CO π^*-orbital offers the potential for carbon monoxide capture by bifunctional systems. As such, CO uptake has been demonstrated by Stephan via ring-opening of a boron amidinate complex to generate a B/N system which acts in cooperative donor-acceptor fashion (Figure 3.1, B).[19] In similar vein, Erker *et al.* have reported a single-component P/B frustrated Lewis pair (FLP) which reacts in solution to give a CO adduct (Figure 3.1, C), albeit one which is only stable up to ca. -30 ^{o}C.[20] Capture can also be combined with chemical modification of the C_1 unit.[21-24] For example, both inter- and intramolecular P/B FLPs have been shown to bind CO and transform it via hydrogenation/hydroelementation to yield formyl-containing products (Figure 3.1, C and D).[21,23]

While these examples illustrate potential strategies for capturing carbon monoxide based on its ambiphilic nature, reversibility in CO uptake is hard to achieve at/close to room temperature due to the intrinsically weak nature of the interactions involved. As mentioned in Chapter 1, Section 1.2.3, reversibility in H_2, CO and other small molecule capture/release needs to be achieved in potential applications of FLPs such as sensing and catalysis.[3, 25-27] In other word, it requires ΔG^o to be close to zero, as well as the activation barriers in both directions ($\Delta G^{\ddagger}$) to be low. By employing a geometrically constrained FLP in which the Lewis acid and base are pre-organized onto a common backbone scaffold, the magnitude of $\Delta S^{\ddagger}$ can be lowered.[28]

Experimentally, our group has experience in applying a xanthene-based backbone, by functionalizing the ortho positions with Lewis bases (-PR_2, R = ^{i}Pr, Ph, Mes) or Lewis acids (-$B(C_6F_5)_2$, -$B(Mes)_2$), to make series of FLPs for small molecule activation.[29] Several key observations were made during the exploration:

(i) The distance between the Lewis acid and Lewis base needs to be within a specified range to make small molecule capture feasible. For example, FLP **3.1** with a wider angle between the P/B functional groups on the carbazole backbone (P-B distance measured as 5.669 Å) shows no reactivity towards H_2. While the xanthene supported P/B FLPs **3.1-3.4** with P-B distances from 4.070-4.487 Å (Table 3.1) readily react with H_2 to form the respective hydrogenated compounds. (Scheme 3.1)

(ii) By tuning the basicity of the phosphine, the activation of H_2 by FLPs can be varied between forming a stable FLP-H_2 compound to a FLP-H_2/FLP equilibrium at room temperature. A more basic phosphine leads to a more stable FLP-H_2 compound. For FLP-H_2 **3.2-H_2** and **3.4-H_2**, the values of ΔH^o and ΔS^o for H_2 loss were measured to be 9.1 kcal mol^{-1}, 24.4 cal mol^{-1} K^{-1} and 8.1 kcal mol^{-1}, 33.0 cal mol^{-1} K^{-1}, respectively.[30]



Scheme 3.1 *Previous examples of carbazole and xanthene based FLPs.*

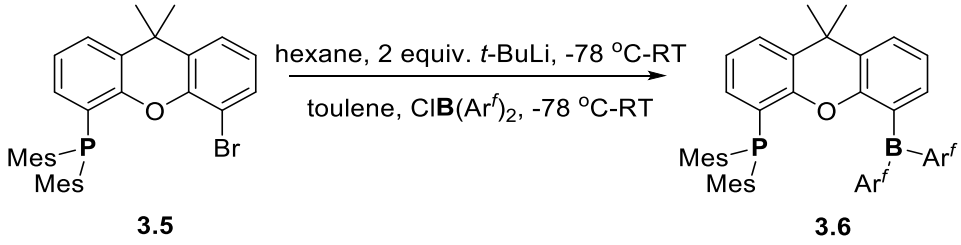
Table 3.1 *P-B distances determined for xanthene-based FLPs* ***3.2-3.4****.*

−PR$_2$	**P−B distances (Å)**
R = Ph	4.070(2)
R = ^{i}Pr	4.487(3)
R = Mes	4.243(3)

3.2 Results and Discussion

Our exploration started by trying to tuning the acidity of the borane on the xanthene based FLP, by using a less acidic borane -B(Ar^{f})$_2$ (Af^{f} = C$_6$H$_3$(CF$_3$)$_2$-3,5). Using the synthetic route developed, mixed phosphine/bromo derivative **3.1** can be synthesized on a scale of up to 10 g in one step.[29] After further lithiation with *t*-BuLi, Xan(PMes$_2$)Li can either be isolated or reacted *in situ* with one equivalent of (Ar^{f})$_2$BCl to form the new FLP **3.6** (Scheme 3.2). This FLP was characterized by standard spectroscopic and analytical techniques, and its molecular structure in the solid state determined by X-ray crystallography. Diagnostic spectroscopic signals in solution are a ^{31}P resonance at δ_p = -36.7 ppm, which is characteristic of an ArPMes$_2$

system and a broad ^{11}B signal at δ_B = 30.5 ppm.[31] Structurally, a key observation is the fact that the non-bonded P···B contact for **3.6** determined by X-ray crystallography (4.404(2) and 4.439(2) Å for the two molecules in the asymmetric unit) is very close to those of **3.2** and **3.3**.



Scheme 3.2 *Synthesis of frustrated Lewis pair* ***3.6****.*

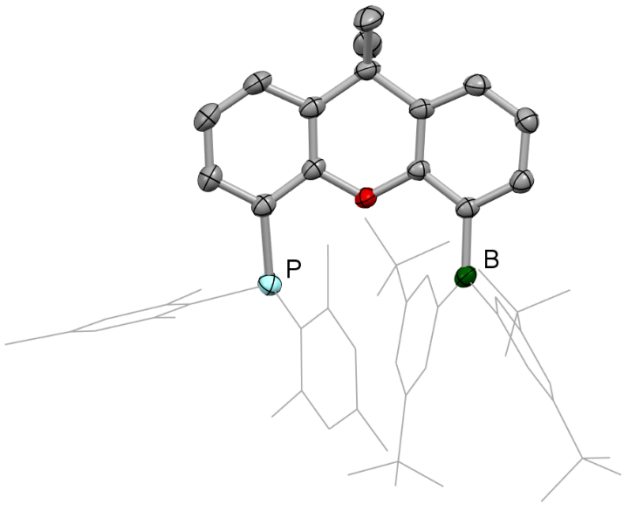
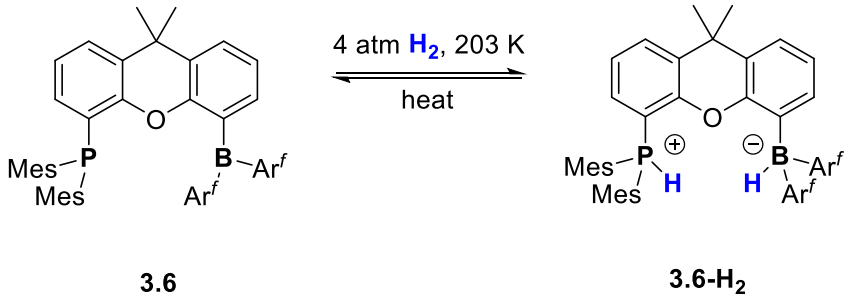


Figure 3.2 *Solid-state structure of* ***3.6*** *determined by X-ray crystallography. Hydrogen atoms and solvent molecule omitted, and selected aryl groups shown in wireframe format for clarity.*

The heterolytic cleavage of dihydrogen by FLP **3.6** is not achieved to form the corresponding phosphonium borate at 295 K and 1 atm H_2 pressure. Increasing the H_2 pressure to 4 atm leads to the appearance of a new peak (about 5% percent of the total composition) at -28.0 ppm in the $^{31}P\{^1H\}$ NMR spectrum. In the (^1H coupled) ^{31}P spectrum, this peak splits into a doublet with $^1J_{PH}$ = 529.1 Hz which is a typical one bond P-H coupling constant. Furthermore, this new P-H bond is evident in the ^1H NMR spectrum which shows a new peak resonance at 7.76 ppm

with the same coupling constant. These results indicate that the FLP **3.6** cleaves H_2 under such conditions, although not quantitatively.



3.6 **3.6-H_2**

Scheme 3.3 *Reversible activation of H_2 by FLP **3.6**.*

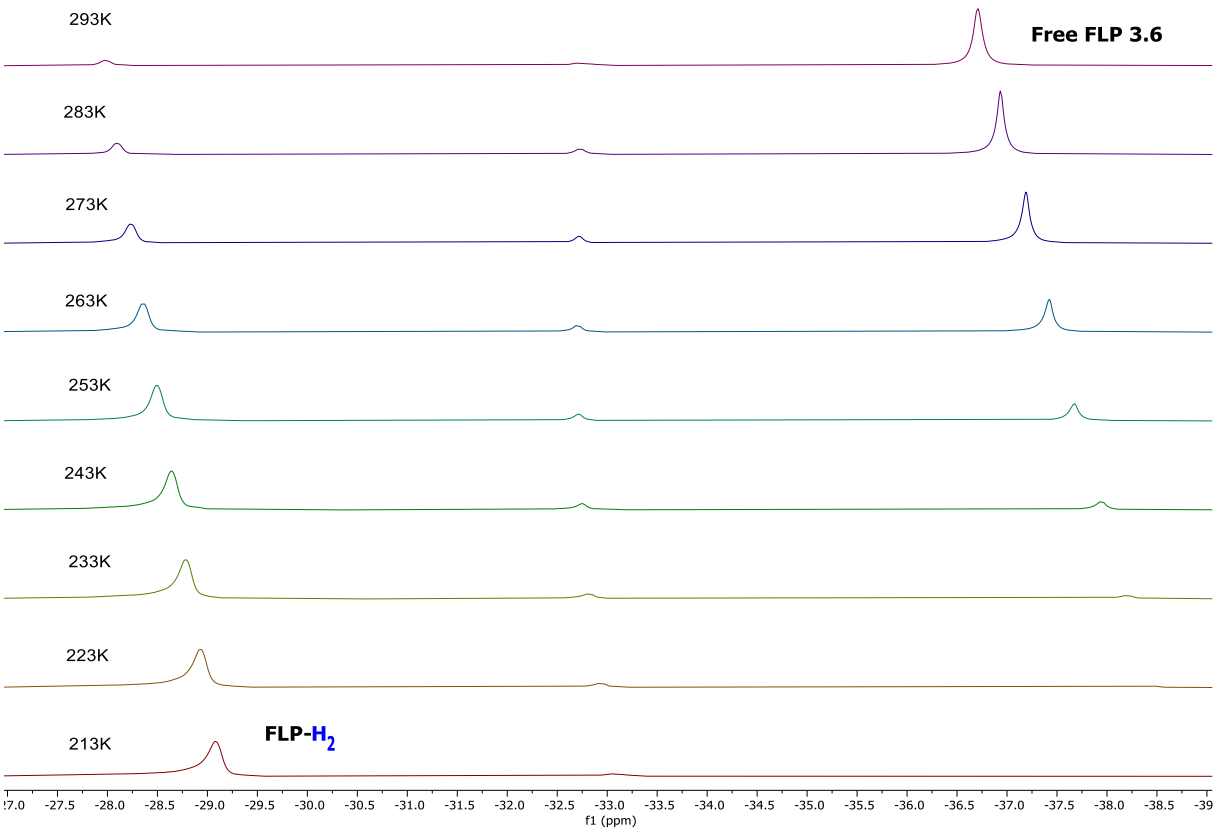


Figure 3.3 *$^{31}P\{^1H\}$ VT-NMR spectra of FLP **3.6** in the presence of H_2 from 213-293 K.*

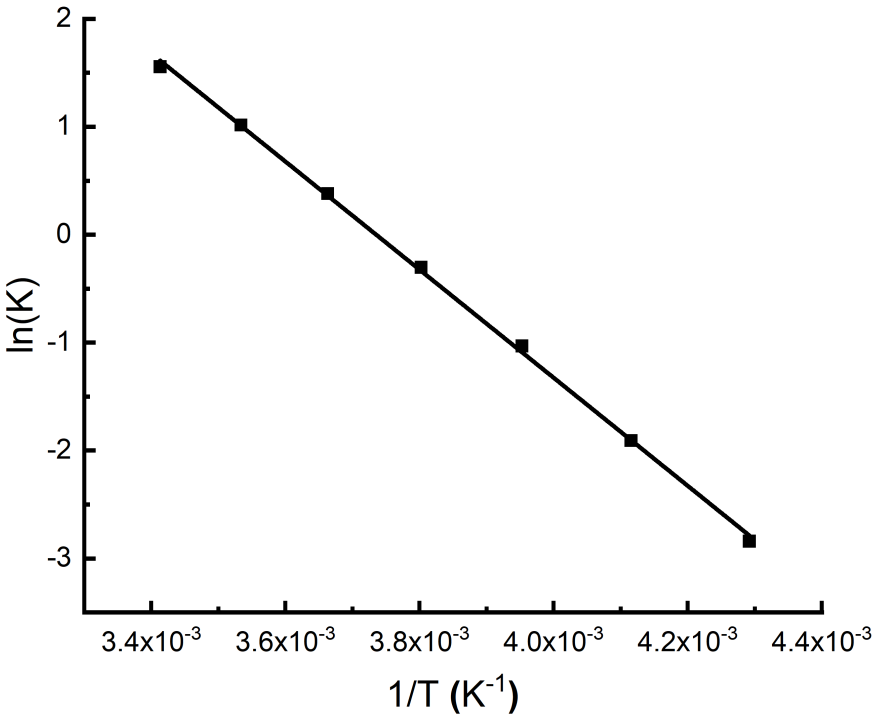


Figure 3.4 *Van't Hoff plot based on the response to temperature of the equilibrium between* ***3.6****-H_2 and* ***3.6*** *(plus H_2) in CD_2Cl_2.*

In order to further monitor the equilibrium **3.6** with H_2, VT-NMR was applied in the temperature range 203 K to 293 K (Figure 3.3). Remarkably, the FLP can be fully converted to the hydrogenated product when cooling down to 203 K. A van't Hoff plot based on the response to temperature of the equilibrium between **3.6**-H_2 and **3.6** (plus H_2) in CD_2Cl_2 can thus be obtained (Figure 3.4). From the linear fit ($R^2 = 0.997$) of ln(K) vs 1/T can be obtained the parameters $\Delta H^o = 42$ kJ mol^{-1} and $\Delta S^o = 155$ J mol^{-1} K^{-1} for the loss of H_2 from **3.6-H_2**. Compared with the values reported previously for Stephan's *para*-$(Mes_2PH)C_6F_4B(C_6F_5)_2H$ and FLP **3.2-H_2** in which the H_2 release process is characterized thermodynamically by the values of $\Delta H^o = 90$ kJ mol^{-1} and $\Delta S^o = 96$ J mol^{-1} K^{-1},[32] the enthalpic term is much smaller for **3.6**, which presumably reflects the lower combined Lewis acidity/basicity of the borane/phosphine components. These data are thus consistent with the instability of the **3.6-H_2** activation product at ambient conditions.

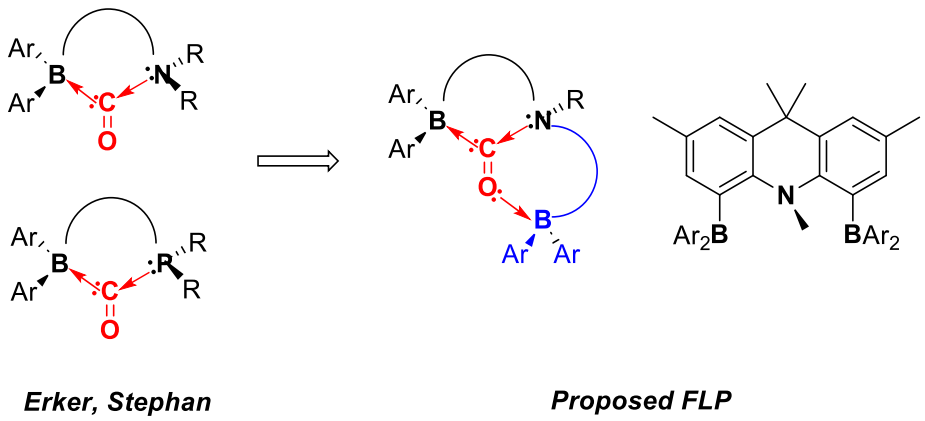
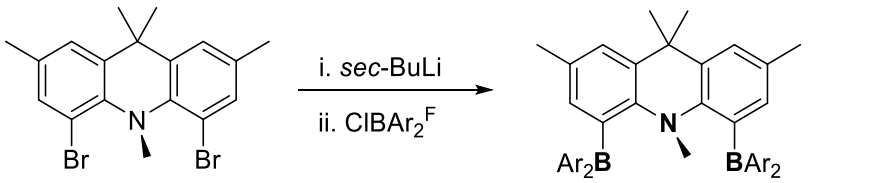


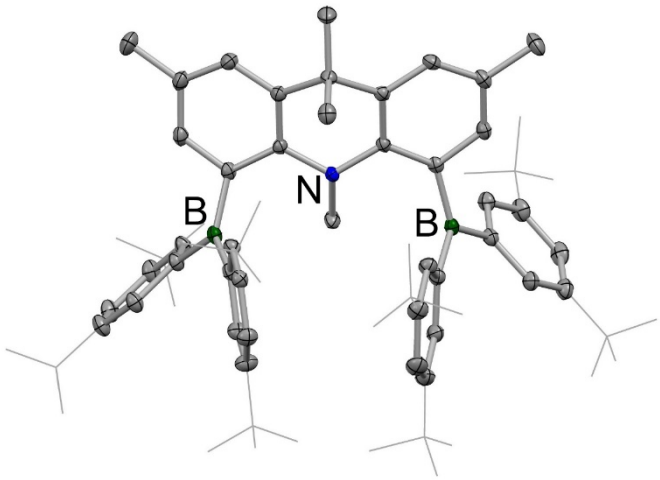
Figure 3.5 *Enhancing CO binding through the inclusion of a second borane function.*

While **3.6** does not react with CO, we hypothesized that a structural modification to simple bifunctional B/P or B/N FLPs involving the incorporation of an additional Lewis acid site to bind the O-terminus of the CO molecule might allow for enhanced binding affinities (Figure 3.5). Frustrated Lewis pairs featuring a BNB arrangement of the acid/base functions can readily be synthesized from acridan dibromide **3.7** via lithiation followed by quenching with the respective chloroborane, $ClBAr^{f}_{2}$ or $ClB(C_6F_5)_2$, yielding strongly coloured **3.8** (orange) or **3.9** (red) in 86-90 % yield. (Scheme 3.4). The symmetrical substitution pattern at the 4 and 5-positions in each compound is reflected in the observation of three singlets (6:6:3) for the backbone and N-bound methyl groups, together with a single signal in the ^{11}B spectrum (at δ_B 60 and 61 ppm, respectively) and a ^{19}F NMR spectrum consistent with only one type of CF_3 or C_6F_5 group. **3.9** is extremely soluble in apolar organic media, making crystallization very difficult; definitive proof of connectivity could be obtained, however, through the isolation of the 1:1 (B-bound) adduct of **3.9** with $^{t}Bu_3PNNO$ (reported by Dr. Ili Zukifly in her DPhil thesis).[34]



3.7

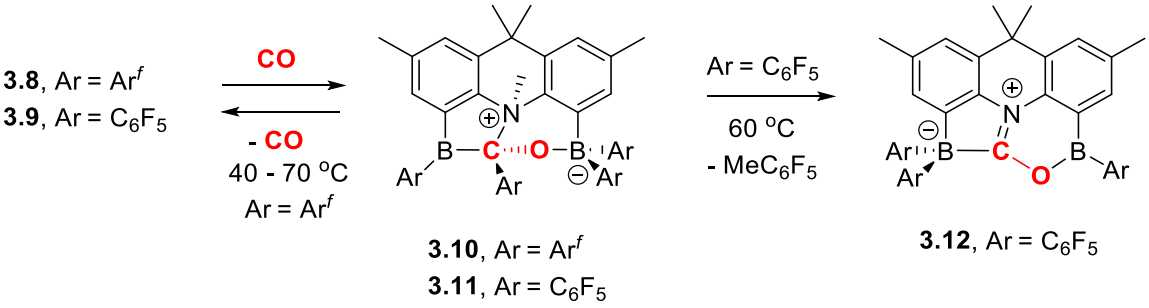
3.8, Ar = Ar^f = $C_6H_3(CF_3)_2$
3.9, Ar = C_6F_5

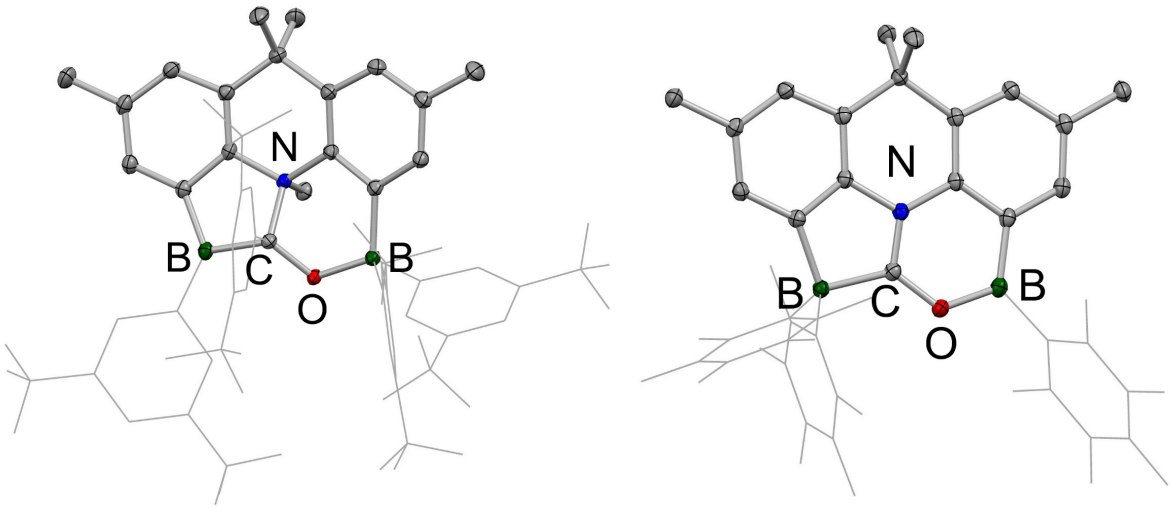


Scheme 3.4 *(upper) Synthesis of BNB-type frustrated Lewis pairs* ***3.8*** *and* ***3.9****, (lower) molecular structure of* ***3.8*** *in the solid state as determined by X-ray crystallography, hydrogen atoms and solvate molecules omitted, and* CF_3 *groups shown in wireframe format for clarity.*

When treated with CO (at room temperature and ca. 1 atm pressure), both BNB systems give similar products **3.10** and **3.11** (Scheme 3.5). In the case of **3.7**, the orange colour of the toluene solution disappears on shaking under a CO atmosphere, and the colourless crystalline product **3.10** precipitates from the reaction mixture after a few minutes in 78 % isolated yield. **3.11** can be synthesized in a similar way (albeit in lower isolated yield due to its very high solubility), in this case using Me_4Si to recrystallize the product. The ^{1}H NMR spectra of the adducts (**3.10** and **3.11**) are very similar, both showing two singlets for the $C(CH_3)_2$ unit and two different aromatic CH_3 resonances, together with a (shifted) lower-field signal associated with the NMe function. The ^{19}F NMR spectra are consistent with the presence of four distinct CF_3 (for **3.10**)

or C_6F_5 environments (for **3.11**), implying a significant reduction in symmetry accompanying the binding of CO. In the case of **3.10**, the nature of the product could be confirmed unambiguously by X-ray crystallography (Scheme 3.5), showing that it results not only from assimilation of carbon monoxide in the BNB FLP pocket, but also from 1,2 aryl group migration from one of the boron centres to the electrophilic carbon derived from the CO molecule. As such, the structure of **3.10** is based on an approximately tetrahedral carbon centre, featuring a significantly lengthened C-O distance (1.365(3) Å, cf. 1.128 Å for CO and ca. 1.23 Å for the C=O bonds in organic carbonyl compounds).[33]





Scheme 3.5 *(upper) Reactions of BNB systems* ***3.8*** *and* ***3.9*** *with carbon monoxide: CO capture and aryl group migration, (lower) Molecular structures of* ***3.10*** *(left) and* ***3.12*** *(right) in the solid state as determined by X-ray crystallography. Hydrogen atoms and solvate molecules omitted, and aryl groups shown in wireframe format for clarity.*

Interestingly, **3.10** and **3.11** undergo different reactions when heated. In the case of the Ar^f derivative **3.10**, CO is re-released at slightly elevated temperatures to regenerate **3.8**. The release of CO can be followed spectroscopically: *in situ* monitoring by ^{1}H NMR spectroscopy in $CDCl_3$ in the temperature range 40 to 70 °C (Figure 3.6) allows for the thermodynamic parameters associated with the regeneration of **3.8** to be determined. A van't Hoff plot yields ΔH^o = 87.1 kJ mol^{-1} and ΔS^o = 257.5 J mol^{-1} K^{-1} for CO loss. The evolution of CO is also accompanied by regeneration of the orange colour characteristic of **3.8** (Figure 3.7), suggesting potential applications of such systems in the sensing of carbon monoxide.

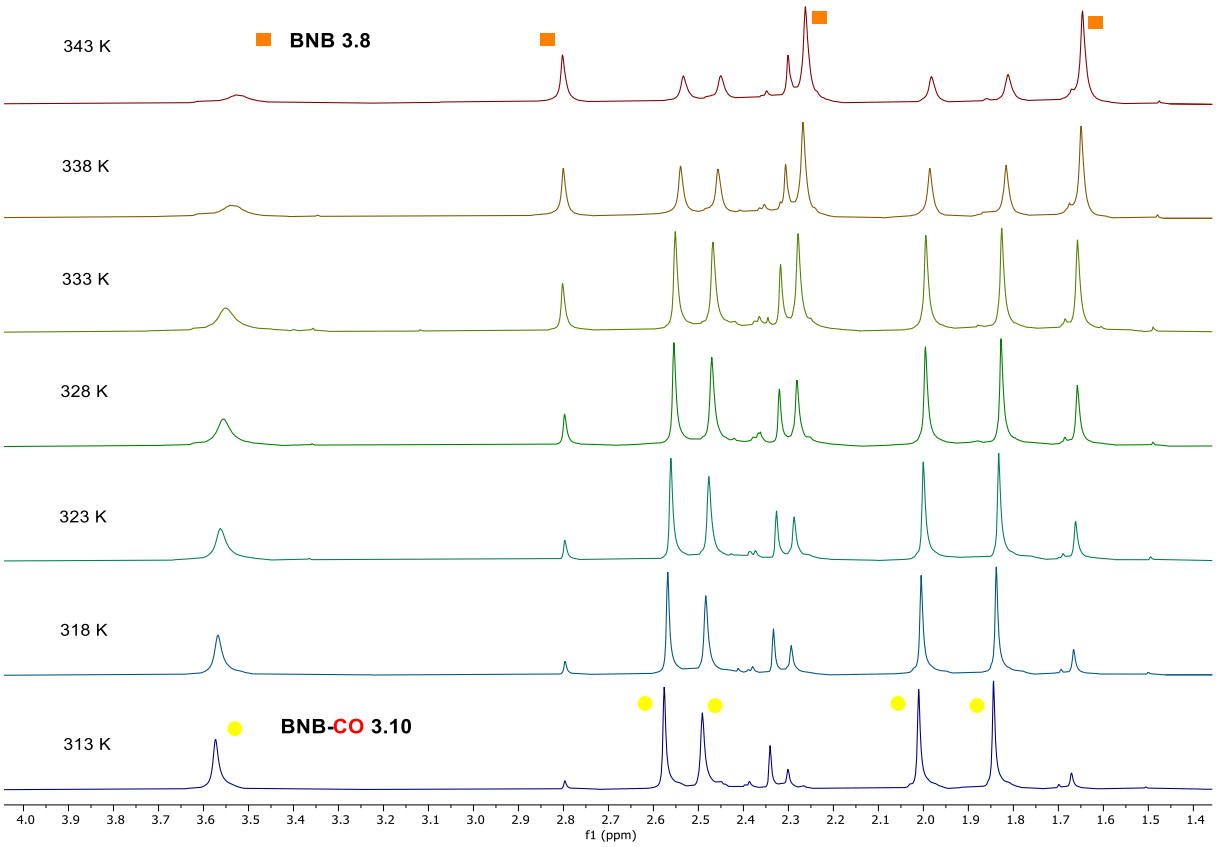


Figure 3.6 *^{1}H VT-NMR of FLP **3.8** in the presence of CO from 313-343 K.*

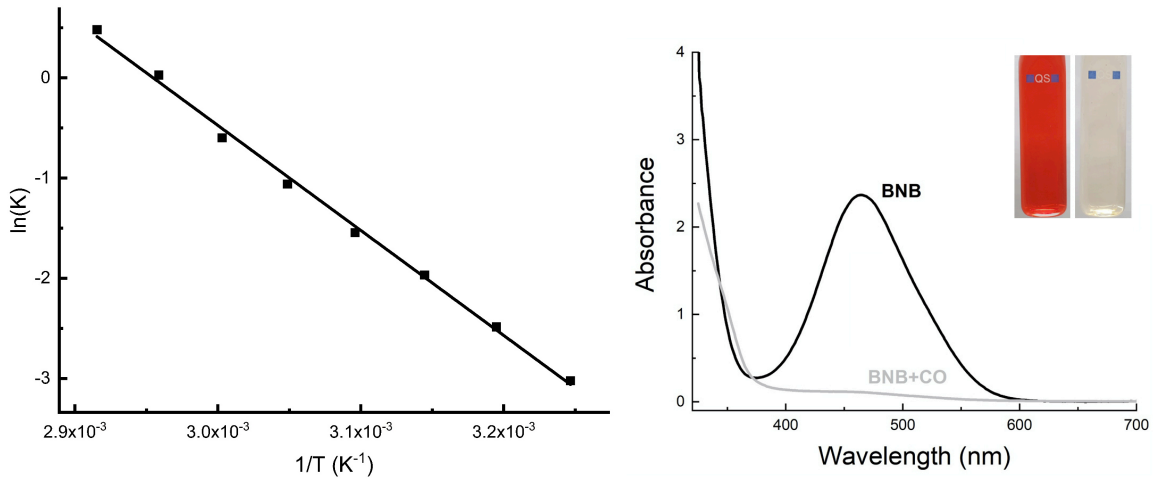
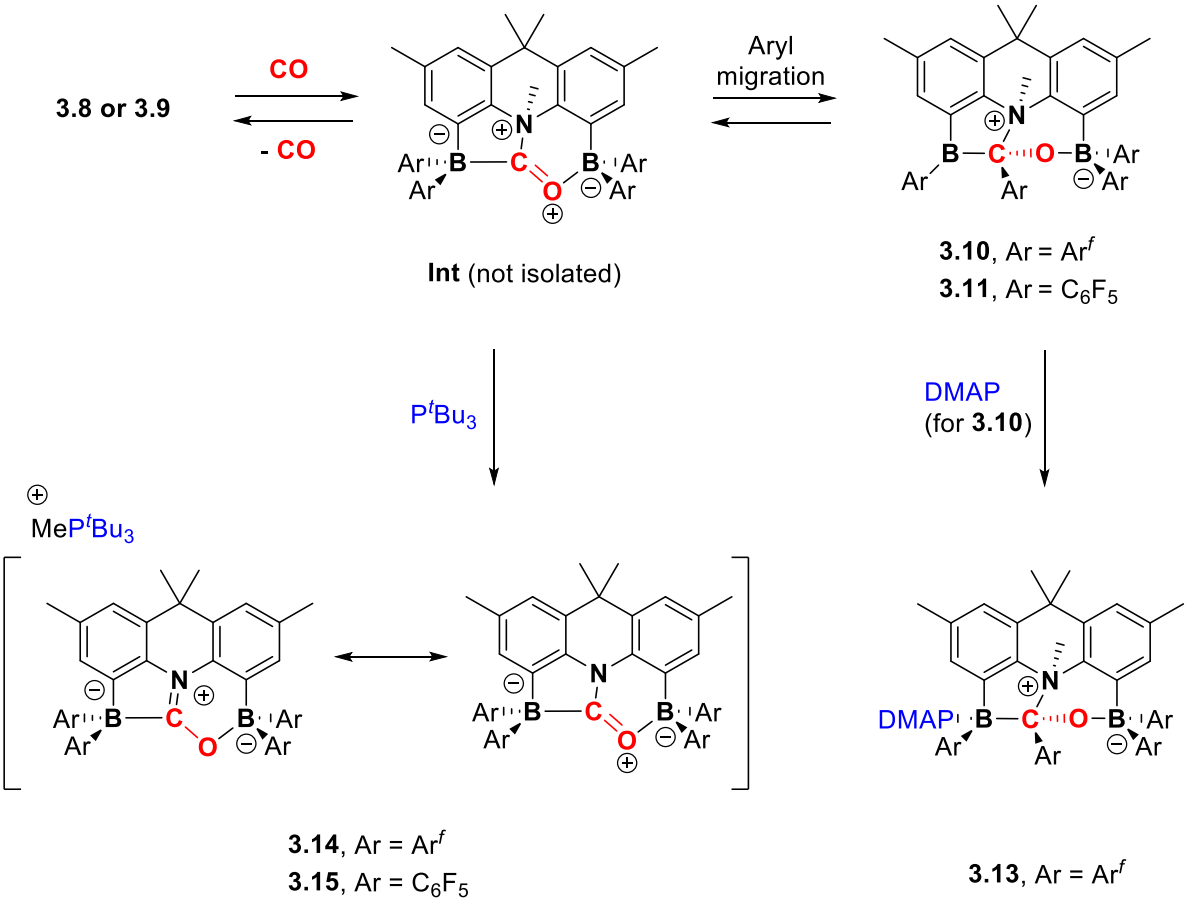


Figure 3.7 *(left) Van't Hoff plot relating to the release of CO from* ***3.10*** *in the temperature range 40 – 70 °C; (right) UV/Vis spectra of* ***3.8*** *(black trace) and* ***3.10*** *(grey trace) in chloroform (ca. 0.8 mM concentration); (inset) photographs: solutions of* ***3.8*** *and* ***3.10*** *in chloroform.*

By contrast, heating **3.11** to 80 °C leads to the elimination of MeC_6F_5 (as shown by ^1H and ^{19}F NMR measurements) to generate zwitterion **3.12** (Scheme 3.5). The ^1H NMR spectrum of **3.12** is consistent with the loss of the N-bound Me group, and the ^{19}F NMR spectrum shows two sets of signals integrating in the ratio 1:2; the associated signals for the *para*-CF units (-146.6 and -159.5 ppm, respectively) are consistent with C_6F_5 units bound to three- and four-coordinate boron centres, respectively. The structure of **3.12** was ultimately determined by X-ray crystallography (Figure 3.5), and confirms that it is formed via formal loss of MeC_6F_5 across the C–N bond of **3.11**. The short C–N distance (1.318(2) Å) and planar arrangement of atoms around carbon (sum of angles = 360.0 °) are consistent with the formation of a C=N double bond, and consequent formulation of **3.12** as an iminium borate species.

We postulate that the differing behaviour of **3.10** and **3.11** at elevated temperatures reflects differences in the Lewis acidities of boranes bearing C_6F_5 and Ar^f functions. Aryl migration is shown to be reversible in both cases (Scheme 3.6), and the more modest Lewis acidity

associated with the Ar^f substituent ultimately translates into weaker binding of the CO molecule, and the ability of **3.8** to *reversibly* capture carbon monoxide. **3.11**, by contrast, is prone to rearrangement before a comparable CO release can occur.



Scheme 3.6 *Trapping of the BNB·CO adduct intermediate for both* ***3.8*** *and* ***3.9*** *via reactions with $^tBu_3P$.*

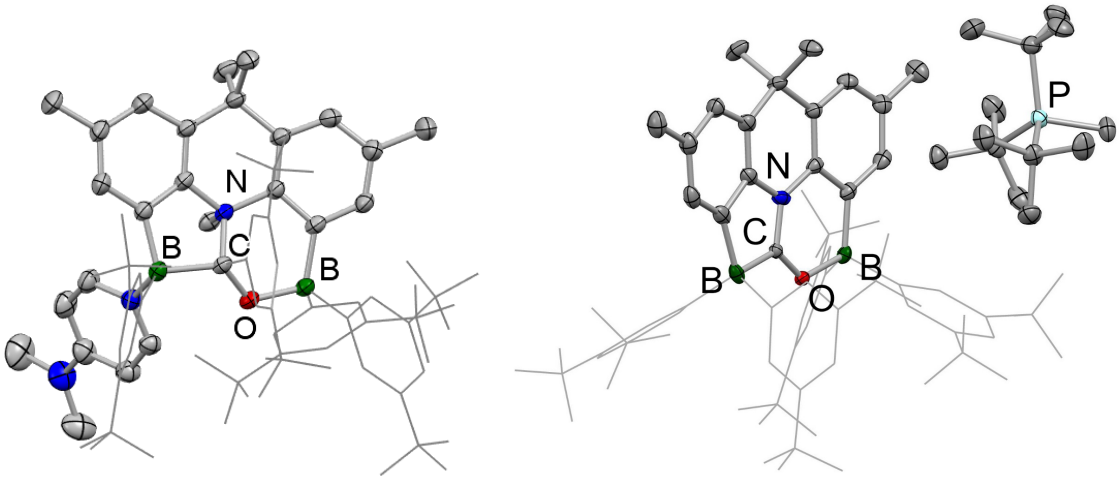


Figure 3.8 *Molecular structure of* ***3.13*** *(left) and* ***3.14*** *(right) in the solid state as determined by X-ray crystallography. Hydrogen atoms and solvate molecules omitted, and aryl groups shown in wireframe format for clarity.*

Although not directly observable in the reaction of either **3.8** or **3.9** with carbon monoxide, we hypothesize that the first-formed species in the uptake of CO is a simple BNB·CO adduct of the form postulated in Scheme 3.6. DFT calculations on the Ar^f systems indicate that the free energy of **3.10** is only marginally lower than that of **Int** (ca. 2 kJ mol^{-1} at the PBE1PBE/TZVP level). With this in mind, we attempted to trap this intermediate (**Int**) via reactions with Lewis bases. While the addition of CO to a solution containing **3.10** and DMAP (*N*,*N*-dimethylaminopyridine) simply leads to the isolation of the corresponding B-bound adduct of **3.10** (**3.13**, Scheme 3.6; X-ray crystal structure shown in Figure 3.8), reactions with more sterically encumbered (and softer) phosphine bases such as P^{t}Bu$_3$ proceed via nucleophilic attack at the N-Me group of **Int**. This demethylation process generates the [MeP^{t}Bu$_3$]$^+$ cation, together with the CO adduct of the corresponding [BNB]$^-$ amidodiboryl moiety. Thus **3.14**, and its C_6F_5 analogue **3.15**, can be accessed in good yield by adding CO to an equimolar mixture of the respective FLP (**3.8** or **3.9**) and P^{t}Bu$_3$.

Spectroscopically, both **3.14** and **3.15** are characterized by the expected resonances corresponding to the $[MeP^tBu_3]^+$ cation (e.g. δ_P ca. 49 ppm), and both compounds feature two signals in the ^{11}B NMR spectrum at $\delta_B < 0$, indicative of O- and C-ligated four-coordinate boron centres (e.g. δ_B = -1.1 and -14.9 ppm for **3.14**). The structures of both salts could also be confirmed crystallographically (Figure 3.8). Of note are (i) the C–N distance measured for **3.14** (1.346(7) Å) which is almost as short as that found in iminium borate **3.12** (1.318(2) Å); and (ii) the C–O separation (1.268(8) Å), which is somewhat shorter than those found in both **3.12** (1.326(2) Å) and **3.10** (1.365(2) Å). Taken together, these structural features suggest that resonance forms incorporating either C=N or C=O double bond character contribute significantly to the overall structure of **3.14** (Scheme 3.6).

From a mechanistic perspective it is important to note that phosphonium salts **3.14** and **3.15** can both also be accessed from the corresponding aryl migrated species (i.e. **3.10** or **3.11**) by the addition of P^tBu_3. This observation is consistent with the idea that the B-to-C aryl migration process is chemically reversible in each case – a factor that, in the case of Ar^f system, ultimately underpins the reversibility of CO uptake.

3.3 Conclusions

In summary, we have synthesized a xanthene-based P/B and two BNB-type frustrated Lewis pairs featuring an acceptor/donor/acceptor functionalized cavity. The P/B FLP can activate H_2 under high pressure (4 atm) and the process was monitored by VT-NMR, which reveals the fact that the less acidic borane leads to weaker binding of H_2 with FLP. The BNB FLP systems are capable of capturing gaseous carbon monoxide; in the case of the $–BAr^f_2$ system CO uptake can be shown by VT-NMR studies to occur reversibly. For both systems, the binding event is accompanied by migration of one of the aryl substituents to the electrophilic carbon of the CO guest. Further experiments employing a bulky tertiary phosphine allow the initially-formed

(non-migrated) CO adducts to be identified and trapped (via demethylation), while also establishing the reversibility of the B-to-C migration process. In conjunction with the slightly less Lewis acidic –BAr^f_2 substituent, this reversibility allows for release of the captured carbon monoxide in the temperature range 40-70 °C, and the possibility for CO sensing, making use of the distinct colourless to orange/red colour change.

3.4 Synthesis and characterization of novel compounds

Xan(PMes$_2$)(BAr^f_2) 3.6

t-BuLi (1.73 ml, 1.7 M, 2.94 mmol) was added into XanPMes$_2$Br (0.82 g, 1.47 mmol) which was dispersed in hexane 30 mL at -78 °C. The mixture was slowly warmed to room temperature and stired over 5-6 h. $ClBAr^f_2$ (0.69 g, 1.47 mmol) was dissolved in toluene 20 mL and added to the mixture at -78 °C and the reaction mixture slowly warmed to room temperature. After stirring overnight, the solvent was removed under vacuum and a small amount of pentane was added to extract the product. The mixture was filtered and the orange yellow colour filtrate was kept at -30 °C until crystals precipitated. Further concentration of the supernatant solution and storage at −30 °C produced a second crop of crystals. Yield: 0.55 g, 41 %.

Anal. Calc. for $C_{49}H_{40}BF_{12}OP$: C 64.35 %, H 4.41 %, found: C 64.00 %, H 4.24 %.

^{1}H NMR (400 MHz, C_6D_6, 25 °C): δ_H 1.47 (s, 6H, $C(CH_3)_2$), 1.92 (s, 6H, *p*-CH_3 of Mes), 1.93 (s, 12H, *o*-CH_3 of Mes), 6.50 (d, J_{PH} = 2.94 Hz, 4H, *m*-Mes), 6.62 (dd, J_{HH} = 1.67 Hz, J_{HH} = 7.35 Hz, 1H, ArH), 6.66 (t, J_{HH} = 7.69 Hz, 1H, ArH), 6.89 (t, J_{HH} = 7.47 Hz, 1H, ArH), 6.93 (ddd, J_{HH} = 1.50 Hz, J_{HH} = 3.61 Hz, J_{HH} = 7.52 Hz, 1H, ArH), 7.04 (dt, J_{HH} = 1.55 Hz, J_{HH} = 7.88 Hz, 1H, ArH), 7.29 (dd, J_{HH} = 1.58 Hz, J_{HH} = 7.79 Hz, 1H, ArH), 7.89 (s, 2H, *p*-ArH of borane), 8.10 (s, 4H, *o*-ArH of borane), ^{13}C {^{1}H} NMR (126 MHz, C_6D_6) δ_C 20.6 (Ar Me), 22.4 and 22.5 (C<u>Me</u>$_2$ of backbone), 30.0 and 34.9 (Ar Me), 120.8, 123.0 (q, $^1J_{CF}$ = 272.6 Hz, CF_3), 124.1, 124.2, 125.1, 125.5, 125.7 (*p*-CH of Ar^f), 126.0, 126.1, 127.3, 127.5, 129.7, 130.3,

130.4, 130.5 (d, J_{CP} = 3.2 Hz),130.7, 130.8 (q, $^{2}J_{CF}$ = 33.1 Hz, *m*-C of Ar^{f}), 131.0, 131.2, 131.5, 132.0, 135.1, 137.9 (*o*-CH of Ar^{f}), 138.0, 142.4, 142.5, 142.6, 154.4 (d, J_{CP} = 19.9 Hz), 154.9. ^{31}P NMR (162 MHz, C_6D_6, 25 ^{o}C): δ_P -36.75. ^{19}F NMR (377 MHz, C_6D_6, 25 ^{o}C): δ_F -62.57.

^{Me}Dibromoacridin 3.7

Dibromoacridin (2.0 g, 5.1 mmol) and KCH_2Ph (0.69 g, 5.4 mmol) were dissolved in toluene (20 mL) at 0 ^{o}C, and the reaction mixture slowly warmed to room temperature with stirring. After 4 h, MeI (0.34 ml, 5.4 mmol) was added and the reaction mixture stirred overnight. The solution was filtered and the filtrate dried under vacuum, affording pale yellow power. Yield: 1.98 g, 96 %.

^{1}H NMR (400 MHz, C_6D_6, 298 K): δ_H 1.17 (s, 3H, CMe_2 of backbone), 1.46 (s, 3H, CMe_2 of backbone), 1.97 (s, 6H, Ar Me), 3.50 (s, 3H, NMe), 6.91 (m, 2H, Ar CH), 7.23 (m, 2H, Ar CH).

^{13}C{^{1}H} (126 MHz, C_6D_6, 298 K): δ_C 20. 6 (Ar Me), 23.8 (C<u>Me</u>$_2$ of backbone), 36.1 (C<u>Me</u>$_2$ of backbone), 38.0 (<u>C</u>Me$_2$ of backbone), 44.4 (NMe), 118.3, 123.8, 132.5, 134.5, 143.3, 143.5.

BNB(Ar^{f}) 3.8

To a suspension of **3.7** (0.36 g, 0.88 mmol) in hexane (20 mL) at -78 ^{o}C was added *sec*-BuLi (1.29 mL of a 1.4 M solution in cyclohexane, 1.8 mmol). The reaction mixture was slowly warmed to room temperature and stirred for 4 h. After cooling back to 78 ^{o}C, a solution of $ClBAr^{f}_2$ (0.67 g, 1.88 mmol) in toluene (10 mL) was then added dropwise, during which time the colour of the solution turned to red orange. After warming to room temperature and stirring overnight, the reaction mixture was allowed to settle and filtered by cannula. The resulting filtrate was dried under vacuum and deep red orange solid was obtained. Yield: 0.85 g, 86 %. **3.7** was further purified by heating the crystals of compound **3.10**, giving an orange crystalline powder.

Anal. Calc. for $C_{56}H_{37}B_2F_{24}N_1$: C 53.46 %, H 2.78 %, N 1.25 %; Meas.: C 52.77 %, H 2.75 %, N 1.39 %.

^{1}H NMR (400 MHz, C_6D_6, 298 K): δ_H 1.55 (s, 6H, CMe_2 of backbone), 2.06 (s, 6H, Ar Me), 2.54 (3H, NMe), 6.66 (d, 2H, J_{HH} = 2.0 Hz, Ar CH), 7.36 (d, 2H, J_{HH} = 2.0, Ar CH), 7.76 (m, 8H, *o*-CH of Ar^f), 7.84 (m, 4H, *p*-CH of Ar^f).

^{13}C{^{1}H} (126 MHz, C_6D_6, 298 K): δ_C 20.6 (Ar Me), 29.3 (C<u>Me</u>$_2$ of backbone), 36.2 (<u>C</u>Me$_2$ of backbone), 46.6 (NMe), 123.6 (q, $^1J_{CF}$ = 272.6 Hz, CF_3), 125.8 (*p*-CH of Ar^f), 128.4, 128.6, 130.8, 131.3, 131.8 (q, $^2J_{CF}$ = 33.3 Hz, *m*-C of Ar^f), 132.7, 137.5 (*o*-CH of Ar^f), 143.1, 145.8.

^{19}F NMR (471 MHz, C_6D_6, 298 K): δ_F -62.8.

^{11}B{^{1}H} NMR (128 MHz, C_6D_6, 25 ^{o}C): δ_B 60.7 (broad).

UV-vis (chloroform, λ_{max}): 464 nm (ε = 29,600 L mol^{-1} cm^{-1})

BNB(C_6F_5) 3.9

3.9 was synthesized in a manner similar to **3.8** using $ClB(C_6F_5)_2$ instead of $ClBAr^f_2$. To a suspension of **3.7** (0.39 g, 0.93 mmol) in hexane (20 mL) at -78 ^{o}C was added *sec*-BuLi (1.39 mL of a 1.4 M solution in cyclohexane, 1.86 mmol). The reaction mixture was slowly warmed to room temperature and stirred for 4 h. After cooling back to -78 ^{o}C a solution of $ClB(C_6F_5)_2$ (0.71 g, 1.86 mmol) in hexane (15 mL) was then added, during which time the colour of the solution turned to red purple. After warming to room temperature and stirring overnight, the reaction mixture was allowed to settle and filtered by cannula. The resulting filtrate was dried under vacuum and deep red orange solid was obtained. Yield: 0.80 g, 90 %. Although we were unable to obtain crystalline samples of **3.9** suitable for microanalysis, we were able to exploit the synthesis of the derived ONNP^{t}Bu$_3$ complex (reported in Dr. Ili Zukifly's thesis)[34] to isolate a crystalline bulk sample for proof of bulk composition.

^{1}H NMR (400 MHz, C_6D_6, 298 K): δ_H 1.45 (s, 6H, CMe_2 of backbone), 2.14 (s, 6H, Ar Me), 3.53 (s, 3H, NMe), 6.96 (d, 2H, J_{HH} = 1.9, Ar CH), 7.31 (d, 2H, J_{HH} = 2.0, Ar CH).

^{13}C{^{1}H} (126 MHz, C_6D_6, 298 K): δ_C 20.7 (Ar Me), 27.3 (C*Me*$_2$ of backbone), 30.7 (C*Me*$_2$ of backbone), 36.4 (*C*Me$_2$ of backbone), 48.0 (NMe), 114.8, 130.4, 130.6, 131.3, 131.4, 137.7 (d, $^{1}J_{CF}$ = 252.3 Hz, CF), 143.8 (d, $^{1}J_{CF}$ = 262.9 Hz, CF), 146.9 (*i*-C of C_6F_5), 148.2 (d, $^{1}J_{CF}$ = 248.7 Hz, CF).

^{11}B{^{1}H} NMR (128 MHz, C_6D_6, 25 ^{o}C): δ_B 61.0 (broad).

^{19}F NMR (471 MHz, C_6D_6, 298 K): δ_F -128.4 (m, 8F, *o*-CF), -145.2 (m, 4F, *p*-CF), -160.4 (m, 8F, *m*-CF).

UV-vis (chloroform, λ_{max}): 500 nm (ε = 43,525 L mol^{-1} cm^{-1})

BNB(Ar^{f})-CO 3.10

3.8 (30 mg, 0.027 mmol) was dissolved in hexane (2 mL) and the solution degassed by the freeze-pump-thaw method, before CO was admitted (ca. 1 atm), at which point the product precipitated from the solution. The reaction mixture was allowed to stand for 10 min before the solvent was decanted. The obtained white crystalline solid was then washed twice with cold hexane (2 x 1 mL) and dried under vacuum. Crystals which were suitable for X-ray crystallography were obtained by dissolving **3.8** in toluene in an NMR tube and charging with 1 atm CO. Yield: 27 mg, 88 %.

Satisfactory microanalytical data were obtained by synthesizing the DMAP adduct of **3.10**. Anal. Calc. for $C_{58}H_{41}B_2F_{24}N_3O_1$: C 54.70 %, H 3.24 %, N 3.30 %; Meas.: C 54.34 %, H 3.16 %, N 3.30 %.

^{1}H NMR (400 MHz, $CDCl_3$, 298 K): δ_H 1.86 (s, 3H, CMe_2 of backbone), 2.02 (s, 3H, CMe_2 of backbone), 2.51 (s, 3H, Ar Me), 2.59 (s, 3H, Ar Me), 3.58 (s, 3H, NMe), 6.76 (s, 2H, Ar CH),

7.11 (s, 2H, Ar CH), 7.15 (s, 1H, Ar CH), 7.36 (s, 1H, Ar CH), 7.42 (s, 1H, Ar CH), 7.53 (s, 1H, Ar CH), 7.65 (s, 1H, Ar CH), 7.87 (s, 1H, Ar CH), 7.92 (s, 1H, Ar CH), 8.31 (overlapping s, 3H, Ar CH), 9.36 (s, 2H, Ar CH).

$^{13}C\{^{1}H\}$ (126 MHz, $CDCl_3$, 298 K): δ_C 22.1 (Ar Me), 29.4 (C<u>Me</u>$_2$ of backbone), 35.4 (C<u>Me</u>$_2$ of backbone), 37.2 (<u>C</u>Me$_2$ of backbone), 69.6 (NMe), 116.4, 119.2, 121.8, 122.2 (q, $^{1}J_{CF}$ = 272.1 Hz, CF_3), 123.1 (q, $^{1}J_{CF}$ = 273.4 Hz, CF_3), 123.9 (q, $^{1}J_{CF}$ = 272. 5Hz, CF_3), 124.1 (q, $^{1}J_{CF}$ = 272.1 Hz, CF_3), 125.3, 129.1, 129.5 (q, $^{2}J_{CF}$ = 32.1 Hz, *m*-C), 130.1 (q, $^{2}J_{CF}$ = 32.1 Hz, *m*-C), 130.7 (q, $^{2}J_{CF}$ = 34.1 Hz, *m*-C), 131.0, 131.5, 132.4, 132.8 (q, $^{2}J_{CF}$ = 33.8 Hz, *m*-C), 134.4, 135.4, 135.9, 136.1, 136.2, 136.3, 138.1, 139.8, 142.5, 148.6, 160.0 (br, NCO).

^{19}F NMR (471 MHz, $CDCl_3$, 298 K): δ_F -62.6 (s, 6F), -63.1 (s, 6F), -63.5 (s, 6F), -63.6 (s, 6F).

$^{11}B\{^{1}H\}$ NMR (128 MHz, $CDCl_3$, 25 ^{o}C): δ_B 31.9 (broad), -0.5.

BNB(C_6F_5)-CO 3.11

3.9 (45 mg, 0.048 mmol) was dissolved in hexane (2 mL), the resulting solution was degassed via the freeze-pump-thaw method and backfilled with 1 atm CO at -40 ^{o}C. The supernatant was decanted and the resulting white powder was further washed with cold hexane (2 x 2 mL) and dried under vacuum. Yield: 10 mg, 22 %.

^{1}H NMR (400 MHz, C_6D_6, 298K): δ = 1.28 (s, 3H, CMe_2 of backbone), 1.32 (s, 3H, CMe_2 of backbone). 2.02 (s, 3H, Ar Me), 2.08 (s, 3H , Ar Me), 2.84 (s, 3H, NMe), 6.98 (m ,1H, Ar CH), 7.10 (m, 1H, Ar CH), 7.23(s, 1H, Ar CH), 7.68 (s, 1H Ar CH).

$^{13}C\{^{1}H\}$ (126 MHz, $CDCl_3$, 298 K): δ_C 21.2 (ArMe), 21.6 (ArMe), 30.9 (C<u>Me</u>$_2$ of backbone), 34.0 (C<u>Me</u>$_2$ of backbone), 37.1 (<u>C</u>Me$_2$ of backbone), 61.2 (NMe), 127.2, 127.5, 129.1, 133.3, 133.8, 134.2, 134.5, 136.5, 136.8 (d, $^{1}J_{CF}$ = 250.5 Hz, CF), 140.2, 140.7, 142.0, 145.9, 147.9

(d, $^{1}J_{CF}$ = 243.5 Hz, CF), 148.2 (d, $^{1}J_{CF}$ = 246.3 Hz, CF), 148.7 (d, $^{1}J_{CF}$ = 248.6 Hz, CF), OCNMe not observed .

$^{19}F\{^{1}H\}$ NMR (471 MHz, C_6D_6, 298 K): 130.1 (s, 4F, *o*-F of Ar^F), -131.8 (s, 2F, *o*-F of Ar^F), -135.7 (m, 2F, *o*-F of Ar^F), -151.9 (t, 1F, J_{FF} = 20.1 Hz, *p*-F of Ar^F), -153.1 (t, 1F, J_{FF} = 21.3 Hz, *p*-F of Ar^F), -155.1 (t, 1F, J_{FF} = 21.1 Hz, *p*-F of Ar^F), -155.5 (t, 1F, J_{FF} = 20.9 Hz, *p*-F of Ar^F), -161.8 (m, 2F, *m*-F of Ar^F), -162.0 (m, 2F, *m*-F of Ar^F), -162.3 (m, 2F, *m*-F of Ar^F), -162.9 (m, 2F, *m*-F of Ar^F).

$^{11}B\{^{1}H\}$ NMR (128 MHz, C_6D_6, 25 °C): δ_B 25.4 (broad), -15.0.

Elimination product of BNB(C_6F_5) 3.12

3.9 (50 mg, 0.053 mmol) was dissolved in pentane (2 mL) and the solution degassed by the freeze-pump-thaw method, before CO was admitted (ca. 1 atm). The reaction mixture was heated at 60 °C for 10 min, cooled to room temperature and filtered by cannula. The resulting filtrate was concentrated to 5 mL and cooled to 4 °C for crystallization. **3.12** was obtained as a colourless crystalline material, which was washed twice with cold pentane (2 x 1 mL) and dried under vacuum. Crystals which were suitable for X-ray crystallography was obtained by slow evaporation of a pentane solution of **3.12.** Yield: 34 mg, 81 %.

Anal. Calc. for $C_{36}H_{16}B_2F_{15}N_1O_1$: C 55.07 %, H 2.05 %, N 1.78 %: Meas.: C 55.40 %, H 2.26 %, N 1.85 %.

^{1}H NMR (400 MHz, $CDCl_3$, 298 K): δ_H 1.82 (s, 6H, CMe_2 of backbone), 2.44 (s, 3H, Ar Me), 2.61 (s, 3H, Ar Me), 7.21 (s, 1H, Ar CH), 7.51 (s, 1H, Ar CH), 7.83 (s, 1H, Ar CH), 8.00 (s, 1H, Ar CH).

$^{13}C\{^{1}H\}$ (126 MHz, $CDCl_3$, 298 K): δ_C 22.1 (Ar Me), 22.2 (Ar Me), 34.2 ($C\underline{Me}_2$ of backbone), 36.9 ($\underline{C}Me_2$ of backbone), 124.7, 130.4, 131.6, 132.3, 133.1, 135.3, 136.7, 137.2 (d, $^{1}J_{CF}$ =

238.1 Hz, CF), 137.7, 138.4 (br), 139.9, 141.0, 146.8 (br), 148.5 (d, $^{1}J_{CF}$ = 260.6 Hz, CF) [O*C*=NMe not observed].

^{19}F NMR (471 MHz, $CDCl_3$, 298 K): δ_F -129.3 (m, 2F, *o*-F of BC_6F_5), -130.9 (m, 4F, *o*-F of $B(C_6F_5)_2$), -146.6 (m, 1F, *p*-F of BC_6F_5), -158.6 (m, 2F, *p*-F of $B(C_6F_5)_2$), -159.5 (m, 2F, *m*-F of BC_6F_5), -163.7 (m, 4F, *m*-F of $B(C_6F_5)_2$).

^{11}B{^{1}H} (128 MHz, $CDCl_3$, 25 ºC): δ_B 37.2 (broad), -14.5.

DMAP adduct of BNB(Ar^f)-CO 3.13

3.10 (124 mg, 0.11 mmol) and DMAP (13 mg, 0.11 mmol) were dissolved in chloroform (1 mL) and layered with pentane. Crystals of **3.13** were obtained after several days. The crystals were isolated, washed with benzene (2 x 1 mL) and pentane (2 x 1 mL), and dried under vacuum. Yield: 45 mg, 33 %.

Anal. Calc. for $C_{58}H_{41}B_2F_{24}N_3O_1$: C 54.70 %, H 3.24 %, N 3.30 %; Meas.: C 54.34 %, H 3.16 %, N 3.30 %.

^{1}H NMR (400 MHz, C_6D_6, 298K): δ = 1.75 (s, 3H, CMe_2 of backbone), 2.00 (s, 3H, CMe_2 of backbone), 2.37 (s, 3H, Ar Me), 2.46 (s, 3H, Ar Me), 3.03 (s, 3H, NMe), 3.24 (s, 3H, NMe_2 of DMAP), 3.40 (s, 3H, NMe_2 of DMAP), 6.26 (s, 1H, Ar CH), 6.45 (s, 2H, Ar CH), 6.57 (s, 1H, Ar CH), 6.66 (dd, 1H, J_{HH} = 7.29, 3.18 Hz, Ar CH), 6.87 (s, 2H, Ar CH), 6.94 (s, 1H, Ar CH), 7.09 (s, 1H, Ar CH), 7.21 (s, 1H, Ar CH), 7.30 (m, 3H, Ar CH), 7.40 (dd, 1H, J_{HH} = 7.29, 3.18 Hz, Ar CH), 7.51 (s, 1H, Ar CH), 8.09 (dd, 1H, J_{HH} = 7.34, 1.26 Hz, Ar CH), 8.21 (s, 2H, Ar CH), 10.23 (dd, 1H, J_{HH} = 7.34, 1.26 Hz, Ar CH).

^{13}C{^{1}H} (126 MHz, $CDCl_3$, 298 K): δ_C 21.9 (Ar Me), 22.0 (Ar Me), 29.9 (C<u>Me</u>$_2$ of backbone), 35.7 (C<u>Me</u>$_2$ of backbone), 36.8 (<u>C</u>Me_2 of backbone), 39.9 (NMe_2 of DMAP), 61.0 (NMe), 107.4, 108.0, 118.9, 119.5, 119.7, 120.0 (q, $^{1}J_{CF}$ = 272.6 Hz, CF_3), 120.4 (q, $^{1}J_{CF}$ = 272.6 Hz,

CF_3), 120.9 (q, $^1J_{CF}$ = 270.8 Hz, CF_3), 121.0, 121.5 (q, $^1J_{CF}$ = 272.6 Hz, CF_3), 123.2, 125.0, 125.4, 126.3, 127.5 (q, $^2J_{CF}$ = 33.4 Hz, *m*-C), 127.9, 128.2 (q, $^2J_{CF}$ = 33.2 Hz, *m*-C), 128.4 (q, $^2J_{CF}$ = 32.0 Hz, *m*-C), 128.5, 128.9, 129.1, 129.2 (q, $^2J_{CF}$ = 32.4 Hz, *m*-C), 129.4, 129.6, 131.7, 131.9, 133.9, 134.0, 135.2, 135.3, 135.6, 137.9, 140.2, 140.9, 143.3, 143.8, 147.1, 155.9, 160.6 (broad, NCO).

^{19}F NMR (471 MHz, $CDCl_3$, 298 K): δ = -61.8 (s, 6F), -62.8 (s, 6F), -63.0 (s, 6F), -63.1 (s, 3F), -63.7 (s, 3F).

$^{11}B\{^1H\}$ NMR (128 MHz, $CDCl_3$, 25 °C): δ_B 30.5 (broad), -0.69.

[MeP^{t}Bu$_3$][BNB(Ar^f)CO] 3.14

Compound **3.14** can be obtained by two methods. Method A: **3.8** (61.0 mg, 0.054 mmol) and P^{t}Bu$_3$ (10.7 mg, 0.054 mmol) were dissolved in benzene, and the solution degassed by the freeze-pump-thaw before CO was admitted (ca. 1 atm). The reaction mixture was then stirred until the colour faded to almost colourless, at which point a crystalline product precipitated from the solution which was suitable for X-ray crystallography. The supernatant was decanted off, and the product washed with cold hexane twice (2 x 5 mL) and dried. Yield: 57.1 mg, 79.6 %. Method B: **3.10** (99.5 mg, 0.086 mmol) and P^{t}Bu$_3$ (17.5 mg, 0.086 mmol) were suspended in benzene (2 mL), and the mixture stirred for 10 min. The solvent was decanted, affording the product as a colourless crystalline material, which was washed with cold hexane (2 x 5 mL) and dried. Yield: 85.0 mg, 73 %).

Anal. Calc. for $C_{63}H_{58}B_2F_{24}NOP$: C 55.90 %, H 4.32 %, N 1.03 %, Meas.: C 55.91 %, H 4.28 %, N 1.10 %.

^{1}H NMR (400 MHz, $CDCl_3$, 298K): δ_H 1.37 (d, 27H, J_{PH} = 14.5 Hz, MeP^t<u>Bu</u>$_3$), 1.44 (d, 3H, J_{PH} = 15.9 Hz, <u>Me</u>P^{t}Bu$_3$), 1.72 (s, 6H, CMe$_2$ of backbone), 2.28 (s, 3H, Ar Me), 2.42 (s, 3H, Ar

Me), 6.82 (d, 1H, J_{HH} = 1.46 Hz, Ar CH), 7.10 (m, 1H, Ar CH), 7.13 (m, 1H, Ar CH), 7.29 (m, 1H, Ar CH), 7.49 (s, 2H, *p*-Ar CH of BAr^{f}_{2}), 7.56 (s, 2H, *p*-Ar CH of BAr^{f}_{2}), 7.62 (s, 4H, *o*-Ar CH of BAr^{F}_{2}), 7.77 (s, 4H, o-Ar*H* of BAr^{f}_{2}). $^{11}B\{^{1}H\}$ NMR (128 MHz, $CDCl_3$, 25 ^{o}C): δ_B 1.81 (s, br, O*B*Ar_2), -10.2 (s, *B*Ar_2CO).

$^{13}C\{^{1}H\}$ (126 MHz, $CDCl_3$, 298 K): δ_C 0.36 (d, $^{1}J_{PC}$ = 45.4 Hz, Me$P^{t}Bu_3$), 21.9 (Ar Me), 22.1 (Ar Me), 28.9 (MePCMe_3), 34.0 (CMe_2 of backbone), 36.3 (CMe_2 of backbone), 37.9 (d, $^{1}J_{PC}$ = 30.8 Hz, MePCMe_3), 118.6 (*p*-CH of Ar^{f}), 119.1 (*p*-CH of Ar^{f}), 123.9, 124.7 (q, $^{1}J_{CF}$ = 272.1 Hz, CF_3), 125.7, 127.2, 128.4, 129.4 (q, $^{2}J_{CF}$ = 32.3 Hz, *m*-C of Ar^{f}), 129.9, 130.9, 131.5, 132.6 (*o*-CH of Ar^{f}),132.9 (*o*-CH of Ar^{f}), 135.1, 136.4, 137.2, 157.3 (NCO).

^{19}F NMR (471 MHz, $CDCl_3$, 298 K): δ = -62.8 (s, 12F), -62.9 (s, 12F).

$^{31}P\{^{1}H\}$ NMR (162 MHz, $CDCl_3$, 298 K): δ_P -49.1.

[MeP^{t}Bu$_3$][BNB(C$_6$F$_5$)CO] 3.15

The synthesis of **3.15** was achieved via a similar method to the synthesis of **3.14** (via method A). **3.9** (16.6 mg, 0.018 mmol) and P^{t}Bu$_3$ (3.6 mg, 0.018 mmol) were dissolved in benzene (1 mL), and the solution degassed by the freeze-pump-thaw method before CO was admitted (ca. 1 atm). The reaction mixture was shaken until the colour faded, at which point crystalline **3.15** precipitated from the solution. The supernatant was then decanted off, and the product washed with cold hexane (2 x 5 mL) and dried. Yield: 11.5 mg, 57%.

Anal. Calc. for $C_{55}H_{46}B_2F_{20}NOP$: C 56.48 %, H 3.96 %, N 1.20 %, Meas.: C 55.99 %, H 4.09 %, N 1.20 %.

^{1}H NMR (400 MHz, CD_2Cl_2, 298K): δ_H 1.52 (d, 27H, J_{PH} = 14.5 Hz, MeP^{t}Bu$_3$), 1.57 (d, 3H, J_{PH} = 11.5 Hz, Me$P^{t}Bu_3$), 1.68 (s, 6H, CMe_2 of backbone), 2.28 (s, 3H, Ar Me), 2.30 (s, 3H, Ar

Me), 6.78 (m, 1H, J_{HH} = 1.46 Hz, Ar CH), 7.06 (m, 1H, Ar CH), 7.10 (m, 1H, Ar CH), 7.18 (m, 1H, Ar CH).

$^{13}C\{^{1}H\}$ (126 MHz, CD_2Cl_2, 298 K): δ_C 0.97 (d, $^{1}J_{PC}$ = 45.9 Hz, MeP^{t}Bu$_3$), 21.7 (ArMe), 21.8 (Ar Me), 29.3 (MePCMe$_3$), 33.7 (CMe$_2$ of backbone), 36.5 (*C*Me$_2$ of backbone), 38.3 (d, $^{1}J_{PC}$ = 31.3 Hz, MePCMe$_3$), 120.7, 122.9, 123.9, 126.0, 127.3, 128.0, 128.2, 128.4, 128.5, 128.7, 130.1, 131.1, 131.6, 135.2, 136.7, 136.8, 136.9 (d, $^{1}J_{CF}$ = 244.6 Hz, CF), 138.7 (d, $^{1}J_{CF}$ = 242.3 Hz, CF), 139.3 (d, $^{1}J_{CF}$ = 246.0 Hz, CF), 148.1 (d, $^{1}J_{CF}$ = 240.3 Hz, CF), O=CNMe not observed.

^{19}F NMR (471 MHz, CD_2Cl_2, 298 K): δ_F -131.7 (m, 4F, *o*-F of BAr$_2$), -134.2 (m, 4F, *o*-F of BAr$_2$), -161.8 (t, 2F, J_{FF} = 19.7 Hz, *p*-F of BAr$_2$), -162.6 (t, 2F, J_{FF} = 20.9 Hz, *p*-F of BAr$_2$), -166.3 (m, 8F, *m*-F of BAr$_2$).

^{11}B NMR (128 MHz, CD_2Cl_2, 25 ^{o}C): δ_B -1.1 (s, br, O*B*Ar$_2$), -15.0 (s, *B*Ar$_2$CO).

$^{31}P\{^{1}H\}$ NMR (162 MHz, CD_2Cl_2, 298 K): δ_P -49.4.

Table 3.2 *Selected crystallographic and refinement data for* ***3.10-3.15****.*

	3.10	**3.12**	**3.13**
Formula	$C_{51}H_{31}B_2F_{24}N_1O_1$	$C_{36}H_{16}B_2F_{15}N_1O_1$	$C_{58}H_{41}B_2F_{24}N_3O_1$
Fw	1123.39	785.13	1245.56
Cryst. System	Monoclinic	Triclinic	Triclinic
Space Group	P 2_1/n	P -1	P -1
Wavelength/Å	1.54184	1.54184	1.54184
a/Å	12.83350(10)	12.2689(5)	12.5944(5)
b/Å	23.3049(2)	13.2274(6)	15.0257(7)
c/Å	17.50850(10)	13.2354(8)	19.6564(6)
α/°	90	105.177(5)	106.987(3)
β/°	92.4850(10)	113.841(5)	92.159(3)
γ/°	90	93.386(4)	112.386(4)
Volume/Å^3	5231.58(7)	1862.75(17)	3242.4(2)
Z	2	2	2
Temp./K	150(2)	150(2)	150(2)
Refls. Collect.	101932	18695	28495
$2\theta_{max}$	153.41	152.268	152.262
R_{int}	0.0491	0.0402	0.0370
Goodness of fit	1.062	1.022	1.058
$R[F^2>2\sigma]$, F	0.0613	0.0480	0.0738
R_w (all data), F^2	0.1616	0.1226	0.2024

	3.14	**3.15**
Formula	$C_{69}H_{58}B_2F_{24}N_1O_1P_1$	$C_{172}H_{146}B_6F_{60}N_3O_3P_3$
Fw	1353.72	3600.68
Cryst. System	Orthorhombic	Monoclinic
Space Group	P n a 2_1	C 2/c
Wavelength/Å	1.54184	1.54184
a/Å	23.8866(3)	12.7828(2)
b/Å	13.0541(2)	21.0733(4)
c/Å	21.7644(3)	59.1848(10)
α/°	90	90
β/°	90	94.540(2)
γ/°	90	90
Volume/$Å^3$	6786.53(16)	16004.8(5)
Z	4	4
Temp./K	150(2)	150(2)
Refls. Collect.	66514	16875
$2\theta_{max}$	153.660	155.538
R_{int}	0.0385	0.0504
Goodness of fit	1.045	1.099
$R[F^2>2\sigma]$, F	0.0562	0.0976
R_w (all data), F^2	0.1508	0.2401

3.5 References

1. Chase, P. A.; Stephan, D. W., Hydrogen and Amine Activation by a Frustrated Lewis Pair of a Bulky N-Heterocyclic Carbene and $B(C_6F_5)_3$. *Angew. Chem., Int. Ed.* **2008,** *47* (39), 7433-7437.
2. Stephan, D. W.; Greenberg, S.; Graham, T. W.; Chase, P.; Hastie, J. J.; Geier, S. J.; Farrell, J. M.; Brown, C. C.; Heiden, Z. M.; Welch, G. C.; Ullrich, M., Metal-Free Catalytic Hydrogenation of Polar Substrates by Frustrated Lewis Pairs. *Inorg. Chem.* **2011,** *50* (24), 12338-12348.
3. Spies, P.; Schwendemann, S.; Lange, S.; Kehr, G.; Fröhlich, R.; Erker, G., Metal-Free Catalytic Hydrogenation of Enamines, Imines, and Conjugated Phosphinoalkenylboranes. *Angew. Chem., Int. Ed.* **2008,** *47* (39), 7543-7546.
4. Wang, H.; Fröhlich, R.; Kehr, G.; Erker, G., Heterolytic dihydrogen activation with the 1,8-bis(diphenylphosphino)naphthalene/$B(C_6F_5)_3$ pair and its application for metal-free catalytic hydrogenation of silyl enol ethers. *Chem. Commun.* **2008,** (45), 5966-5968.
5. Wang, Y.; Chen, W.; Lu, Z.; Li, Z. H.; Wang, H., Metal-Free $HB(C_6F_5)_2$-Catalyzed Hydrogenation of Unfunctionalized Olefins and Mechanism Study of Borane-Mediated σ-Bond Metathesis. *Angew. Chem., Int. Ed.* **2013,** *52* (29), 7496-7499.
6. Greb, L.; Tussing, S.; Schirmer, B.; Oña-Burgos, P.; Kaupmees, K.; Lõkov, M.; Leito, I.; Grimme, S.; Paradies, J., Electronic effects of triarylphosphines in metal-free hydrogen activation: a kinetic and computational study. *Chem. Sci.* **2013,** *4* (7), 2788-2796.
7. Mahdi, T.; Heiden, Z. M.; Grimme, S.; Stephan, D. W., Metal-Free Aromatic Hydrogenation: Aniline to Cyclohexyl-amine Derivatives. *J. Am. Chem. Soc.* **2012,** *134* (9), 4088-4091.
8. Urban, S.; Ortega, N.; Glorius, F., Ligand-Controlled Highly Regioselective and Asymmetric Hydrogenation of Quinoxalines Catalyzed by Ruthenium N-Heterocyclic Carbene Complexes. *Angew. Chem., Int. Ed.* **2011,** *50* (16), 3803-3806.
9. Lavallo, V.; Canac, Y.; Donnadieu, B.; Schoeller, W. W.; Bertrand, G., CO Fixation to Stable Acyclic and Cyclic Alkyl Amino Carbenes: Stable Amino Ketenes with a Small HOMO–LUMO Gap. *Angew. Chem., Int. Ed.* **2006,** *45* (21), 3488-3491.
10. Braunschweig, H.; Dewhurst, R. D.; Hupp, F.; Nutz, M.; Radacki, K.; Tate, C. W.; Vargas, A.; Ye, Q., Multiple complexation of CO and related ligands to a main-group element. *Nature* **2015,** *522* (7556), 327-330.
11. Ganesamoorthy, C.; Schoening, J.; Wölper, C.; Song, L.; Schreiner, P. R.; Schulz, S., A silicon–carbonyl complex stable at room temperature. *Nat. Chem.* **2020,** *12* (7), 608-614.
12. Reiter, D.; Holzner, R.; Porzelt, A.; Frisch, P.; Inoue, S., Silylated silicon–carbonyl complexes as mimics of ubiquitous transition-metal carbonyls. *Nat. Chem.* **2020,** *12* (12), 1131-1135.
13. Hansmann, M. M.; Bertrand, G., Transition-Metal-like Behavior of Main Group Elements: Ligand Exchange at a Phosphinidene. *J. Am. Chem. Soc.* **2016,** *138* (49), 15885-15888.
14. Burg, A. B.; Schlesinger, H. I., Hydrides of Boron. VII. Evidence of the Transitory Existence of Borine (BH_3): Borine Carbonyl and Borine Trimethylammine. *J. Am. Chem. Soc.* **1937,** *59* (5), 780-787.
15. Finze, M.; Bernhardt, E.; Terheiden, A.; Berkei, M.; Willner, H.; Christen, D.; Oberhammer, H.; Aubke, F., Tris(trifluoromethyl)borane Carbonyl, $(CF_3)_3BCO$ Synthesis, Physical, Chemical and Spectroscopic Properties, Gas Phase, and Solid State Structure. *J. Am. Chem. Soc.* **2002,** *124* (51), 15385-15398.

16. Sajid, M.; Kehr, G.; Daniliuc, C. G.; Erker, G., Formylborane Formation with Frustrated Lewis Pair Templates. *Angew. Chem., Int. Ed.* **2014,** *53* (4), 1118-1121.
17. Fukazawa, A.; Dutton, J. L.; Fan, C.; Mercier, L. G.; Houghton, A. Y.; Wu, Q.; Piers, W. E.; Parvez, M., Reaction of pentaarylboroles with carbon monoxide: an isolable organoboron carbonyl complex. *Chem. Sci.* **2012,** *3* (6), 1814-1818.
18. Légaré, M.-A.; Pranckevicius, C.; Braunschweig, H., Metallomimetic Chemistry of Boron. *Chem. Rev.* **2019,** *119* (14), 8231-8261.
19. Dureen, M. A.; Stephan, D. W., Reactions of Boron Amidinates with CO_2 and CO and Other Small Molecules. *J. Am. Chem. Soc.* **2010,** *132* (38), 13559-13568.
20. Sajid, M.; Stute, A.; Cardenas, A. J. P.; Culotta, B. J.; Hepperle, J. A. M.; Warren, T. H.; Schirmer, B.; Grimme, S.; Studer, A.; Daniliuc, C. G.; Fröhlich, R.; Petersen, J. L.; Kehr, G.; Erker, G., N,N-Addition of Frustrated Lewis Pairs to Nitric Oxide: An Easy Entry to a Unique Family of Aminoxyl Radicals. *J. Am. Chem. Soc.* **2012,** *134* (24), 10156-10168.
21. Dobrovetsky, R.; Stephan, D. W., Stoichiometric Metal-Free Reduction of CO in Syn-Gas. *J. Am. Chem. Soc.* **2013,** *135* (13), 4974-4977.
22. Stephan, D. W.; Erker, G., Frustrated Lewis pair chemistry of carbon, nitrogen and sulfur oxides. *Chem. Sci.* **2014,** *5* (7), 2625-2641.
23. Sajid, M.; Elmer, L. M.; Rosorius, C.; Daniliuc, C. G.; Grimme, S.; Kehr, G.; Erker, G., Facile Carbon Monoxide Reduction at Intramolecular Frustrated Phosphane/Borane Lewis Pair Templates. *Angew. Chem., Int. Ed.* **2013,** *52* (8), 2243-2246.
24. Sun, Q.; Daniliuc, C. G.; Mück-Lichtenfeld, C.; Bergander, K.; Kehr, G.; Erker, G., Reductive Cleavage of the CO Molecule by a Reactive Vicinal Frustrated PH/BH Lewis Pair. *J. Am. Chem. Soc.* **2020,** *142* (41), 17260-17264.
25. Chase, P. A.; Welch, G. C.; Jurca, T.; Stephan, D. W., Metal-Free Catalytic Hydrogenation. *Angew. Chem., Int. Ed.* **2007,** *46* (42), 8050-8053.
26. Schwendemann, S.; Fröhlich, R.; Kehr, G.; Erker, G., Intramolecular frustrated N/B lewis pairs by enamine hydroboration. *Chem. Sci.* **2011,** *2* (9), 1842-1849.
27. Piers, W. E.; Marwitz, A. J. V.; Mercier, L. G., Mechanistic Aspects of Bond Activation with Perfluoroarylboranes. *Inorg. Chem.* **2011,** *50* (24), 12252-12262.
28. Bertini, F.; Lyaskovskyy, V.; Timmer, B. J. J.; de Kanter, F. J. J.; Lutz, M.; Ehlers, A. W.; Slootweg, J. C.; Lammertsma, K., Preorganized Frustrated Lewis Pairs. *J. Am. Chem. Soc.* **2012,** *134* (1), 201-204.
29. Mo, Z.; Kolychev, E. L.; Rit, A.; Campos, J.; Niu, H.; Aldridge, S., Facile reversibility by design: tuning small molecule capture and activation by single component frustrated Lewis pairs. *J. Am. Chem. Soc.* **2015,** *137* (38), 12227-30.
30. Mo, Z. B.; Pit, A.; Campos, J.; Kolychev, E. L.; Aldridge, S., Catalytic B-N Dehydrogenation Using Frustrated Lewis Pairs: Evidence for a Chain-Growth Coupling Mechanism. *J. Am. Chem. Soc.* **2016,** *138* (10), 3306-3309.
31. Culcasi, M.; Berchadsky, Y.; Gronchi, G.; Tordo, P., Anodic behavior of crowded triarylphosphines. ESR study of triarylphosphoniumyl radicals, $Ar_3P.bul.+$. *J. Org. Chem.* **1991,** *56* (11), 3537-3542.
32. Welch, G. C.; Juan, R. R. S.; Masuda, J. D.; Stephan, D. W., Reversible, metal-free hydrogen activation. *Science* **2006,** *314* (5802), 1124-1126.
33. Cordero, B.; Gómez, V.; Platero-Prats, A. E.; Revés, M.; Echeverría, J.; Cremades, E.; Barragán, F.; Alvarez, S., Covalent radii revisited. *Dalton Trans.* **2008,** (21), 2832-2838.
34. Zulkifly, I., Frustrated Lewis Pairs derived from xanthene and related backbones. PhD Thesis, University of Oxford, 2020.

Chapter 4 Low valent group 13 species supported by a mono anionic ligand

4.1 Introduction

In recent years, *β*-diketiminate ('Nacnac') ligands have been extensively used in coordination chemistry, to support a wide range of metal complexes from across the Periodic Table.[1-13] Within main group chemistry, a number of landmark compounds have been reported incorporating these chelating monoanionic LX ligand systems. These include Group 13 metal complexes in the +1 oxidation state – systems which are challenging both in terms of their intrinsic tendency to undergo disproportionation and their reactivity towards external reagents.[14] Thus in 2000, the groups of Roesky and Power successfully synthesized the monomeric Al(I) and Ga(I) compounds [HC{(Me)C(Dipp)N}$_2$]E (or (Nacnac)E, **I**, where E = Al, Ga) using sterically encumbered Dipp-substituted β-diketiminate ligands (Figure 4.1; Dipp = 2,6-^{i}Pr$_2$C$_6$H$_3$).[15-16]

In 2018, we employed a chelating dianionic diamido (X_2) ligand, $[NON]^{2-}$, to access *anionic* Al(I) and Ga(I) compounds of the type $K_2[(NON)E]_2$ (Figure 4.1 **II**, E = Al, Ga; NON = 4,5-bis(2,6-diiso-propyl-anilido)-2,7-di-*tert*-butyl-9,9-dimethylxanthene).[17-23] These systems show unusual patterns of reactivity: the aluminyl anion can act as a nucleophile in the formation of C–Al and M–Al bonds,[17, 24] and effect the reversible oxidative addition of the C-C bond in benzene.[25] Given the track record of the Nacnac ligand family in supporting charge neutral E(I) systems, however,[6-13] we targeted related mono-anionic LX donors based on the dimethylxanthene backbone, in which one of the amido groups of the $[NON]^{2-}$ system is formally replaced by a neutral donor. Moreover, given the successful development by Power, and by Jones, of one-coordinate Ga(I) amides (stabilized to a greater or lesser extent by interactions with the flanking aryl substituents, **III**),[26-27] we targeted xanthene systems

featuring L substituents which are known to act as relatively weak donors towards Ga(I). Our aim was to develop amido complexes featuring a weakly interacting (or hemi-labile) L donor that might display the high levels of reactivity associated with genuine one-coordinate systems, while retaining some of the ground state stability of Nacnac compounds. Accordingly, we report in the current manuscript on the development of a mono-anionic [PON]$^-$ ligand (Figure 4.1) and the use of Ga(I) and Ga(III) chemistry to probe its coordination capabilities.

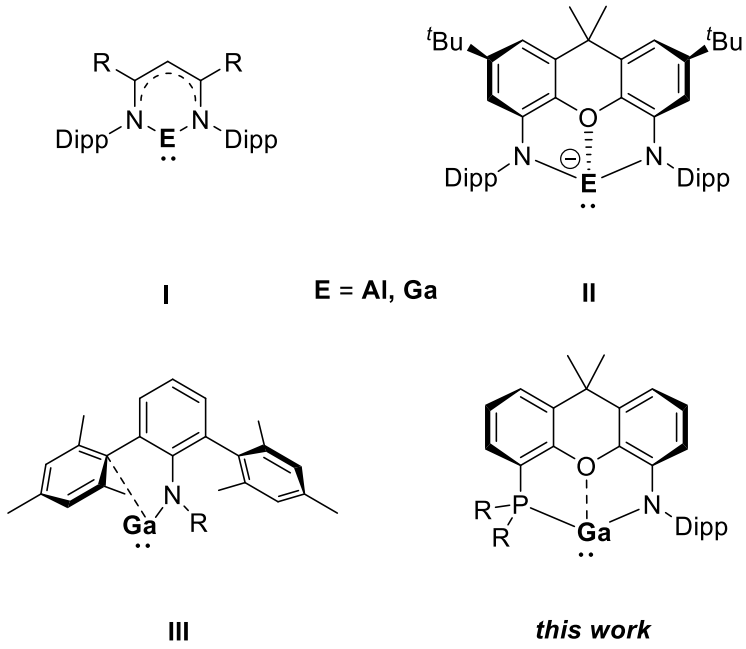
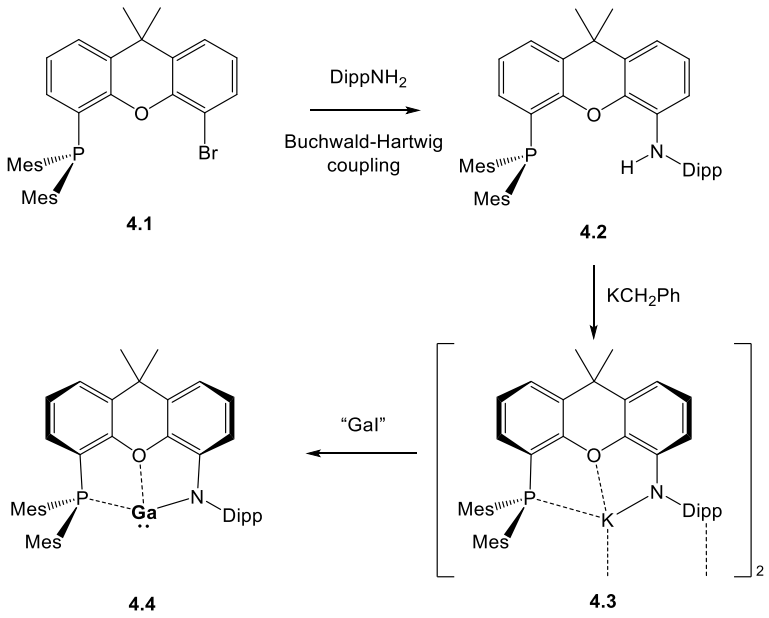


Figure 4.1 *Low valent group 13 metal systems relevant to the work presented in this chapter.*

4.2 Results and Discussion

The H(PON) protio-ligand **4.2** can be synthesized in good yield (ca. 70 %) from the (known) 4-bromo-5-(dimesitylphosphino)-xanthene precursor (**4.1**)[28] and $DippNH_2$ via a Buchwald-Hartwig coupling reaction. Moreover, it is conveniently deprotonated by benzylpotassium, KCH_2Ph, giving the potassiated ligand K(PON) (**4.3**), which can be used for onward reaction chemistry without further purification, or recrystallized from toluene for structural and spectroscopic characterization. **4.3** is thus obtained free of coordinating solvent as dimeric

$K_2(PON)_2$, in which K(PON) monomer units are linked in head-to-tail fashion through close contacts between the potassium centre of one unit and the Dipp aromatic π system of the other (Figure 4.2).



Scheme 4.1. *Synthesis of PON-supported gallylene* ***4.4****.*

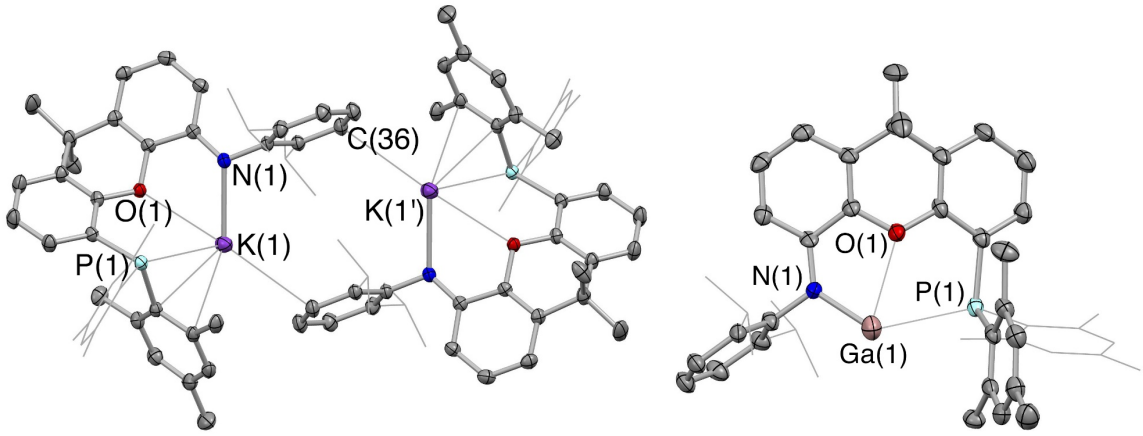


Figure 4.2*. Molecular structures of $K_2(PON)_2$ (****4.3****; left) and (PON)Ga (****4.4****; right) in the solid state as determined by X-ray crystallography. Thermal ellipsoids set at the 40% probability level; Hydrogen atoms and solvate molecules omitted and ^{i}Pr/selected Mes groups shown in wireframe format for clarity. Key bond lengths (Å) and angles (°): (for* ***4.3****) K(1)-N(1) 2.562(2), K(1)-O(1) 3.022(2), K(1)-P(1) 3.351(1), K(1')-C(36) 3.308(3); (for* ***4.4****) Ga(1)-N(1) 1.976(4), Ga(1)-O(1) 2.645(5), Ga(1)-P(1) 3.078(2), N(1)-Ga(1)-P(1) 115.8(2).*

With this new ligand system in hand we set out to probe its coordination chemistry. Accordingly, the Ga(I) system, (PON)Ga, **4.4** can be prepared in ca. 60 % isolated yield via a salt-metathesis reaction between **4.3** and "GaI" (Scheme 4.1),[29] and obtained in crystalline form by recrystallization from benzene. The ^{1}H NMR spectrum of **4.4** features a similar pattern of resonances to those of H(PON) and K(PON), with equivalent phosphorus-bound mesityl substituents, Dipp ^{i}Pr groups and xanthene backbone methyl groups, implying the presence of a plane of symmetry on the NMR timescale. The ^{31}P{^{1}H} resonance of **4.4** (at δ_P = -34.3 ppm) is very close to those of protio-ligand **4.2** (δ_P = -36.9 ppm) and potassiated system **4.3** (δ_P = -34.4 ppm), implying that the interaction of the phosphine donor with the gallium centre in **4.4** is relatively weak. Consistently, the (monomeric) structure of **4.4** in the solid state (Figure 4.2) features a very long Ga···P distance (3.078(2) Å) which is comfortably outside the sum of the respective covalent radii (1.22(4) + 1.07(3) Å),[30] and much longer than that measured for the corresponding Ga(III) system (PON)GaI$_2$ which was synthesized for comparative purposes (2.612(1) Å; Figure 4.6). The Ga-O separation involving the xanthene ether linkage is also relatively long (2.645(5) Å) compared to the sum of the respective covalent radii (1.22(4) + 0.66(2) Å),[30] and is broadly comparable to that measured for the potassium gallyl system K$_2$[(NON)Ga]$_2$, featuring the related [NON]$^{2-}$ diamide ligand (2.542(2) Å).[17] On the other hand, the Ga-N bond is very short (1.976(4) Å) in comparison with those in K$_2$[(NON)Ga]$_2$ (2.093(2) and 2.106(2) Å),[17] presumably reflecting the fact that there is only one Ga–X covalent bond in **4.4**. Indeed, the Ga-N separation in **4.4** is in line with the bond lengths reported by Power and by Jones for Ga(I) amides with geometries which approach mono-coordinate (1.954(2) – 1.985(4) Å),[26-27] consistent with idea that the coordination of the phosphine and ether donors in **4.4** is very weak.

The electronic structure of (PON)Ga (**4.4**) was probed using Density Functional Theory at the PBE1PBE/TZVP level. These calculations suggest that the LUMO+2 (-0.68 eV) is comprised

predominantly of gallium p_z character (Figure 3). The HOMO is ligand-based, with the orbital displaying gallium-centered lone pair character being the HOMO-1 (-5.67 eV). The associated HOMO-LUMO gap (4.99 eV) is very similar to that calculated for (Nacnac)Ga[15] using the same method (4.86 eV). The essentially identical energies of the formally vacant $p\pi$ orbital in each case (-0.66 eV for (Nacnac)Ga) presumably reflect the fact that in **4.4**, the extent of π donation from the (single) amido substituent is markedly enhanced, consistent with the very short crystallographically determined Ga-N bond length. Both of these systems have wider HOMO-LUMO gaps than that determined for the anionic diamido system $[(NON)Ga]^-$. In that case, the narrow HOMO-LUMO gap (4.21 eV) reflects the fact that the LUMO is not destabilized to the same degree by N-to-Ga π donation due to the constraints of the xanthene backbone (which mean that the amido groups cannot attain co-planarity with the GaN_2 unit).[17, 23] The (PON)Ga system can also be compared with Jones' one-coordinate amidogallium(I) system,[27] which is similar in that it features π stabilization from only a single N donor. In that system, the HOMO-LUMO gap (calculated using the same method) is narrower (4.62 eV) and the LUMO somewhat lower than in **4.4** (-0.91 eV). This presumably reflects the fact that the LUMO is orthogonal to the amido π system, and (compared to **4.4**) has less opportunity for interaction with ancillary neutral donors (featuring as it does, only very weak interaction with the flanking arene π system).

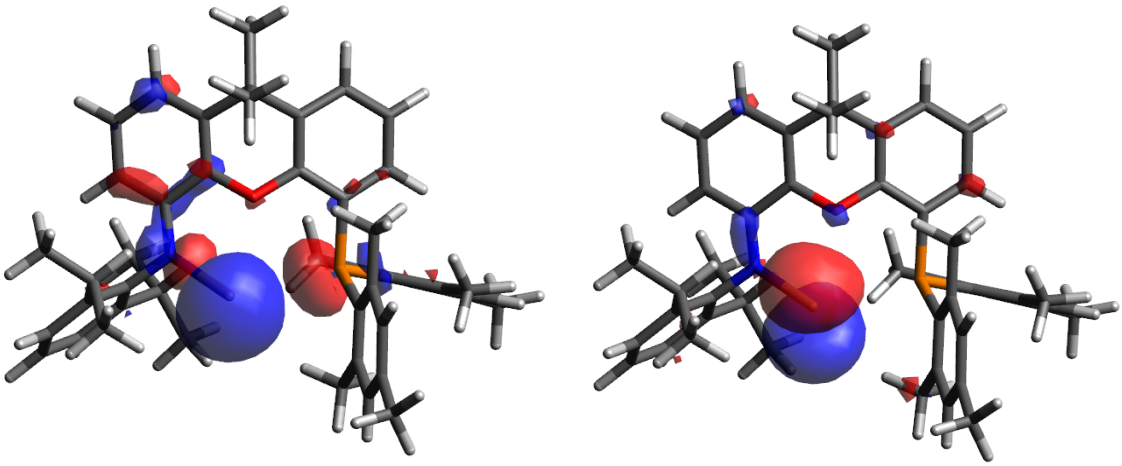


Figure 4.3 *Frontier orbitals of (PON)Ga as determined by Density Functional Theory (isosurface 0.04): (left) HOMO-1 (-5.67 eV); (right) LUMO+2 (-0.68 eV).*

Steric factors are known to be a significant influence on the patterns of reactivity displayed by low-valent main group species. In both (PON)Ga and (Nacnac)Ga, the Ga(I) centre sits in a 'pocket' between flanking aryl substituents: in the *β*-diketiminate system these are the N-bound Dipp groups, which are aligned such that the distances from the arene centroids to the metal are each *ca.* 4.0 Å, and the 'pocket' defined by the open centroid-Ga-centroid angle occupies 189.1° in angular terms (Figure 4.4).[15] In **4.4** the gallium centre is flanked by NDipp and PMes substituents (the centroids of which are also ca. 4.0 Å from the metal centre), and the open 'pocket' by comparison occupies 156.8°. As such, we hypothesized that **4.4** might offer the possibility of a more sterically shielded pocket in which to carry out chemistry at the metal centre.

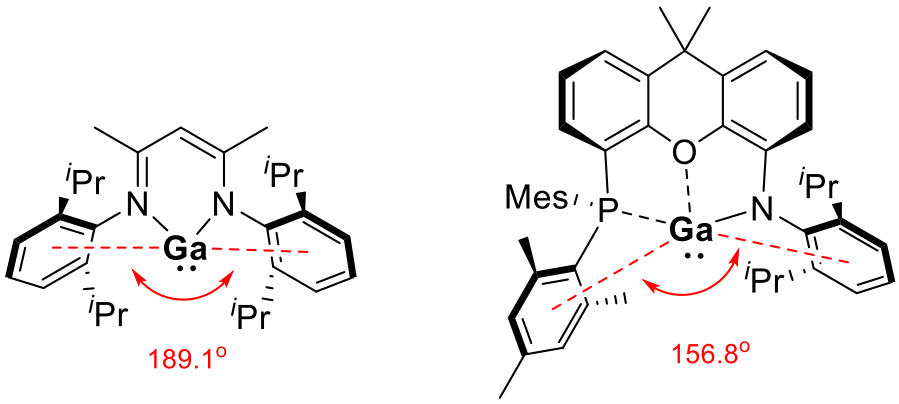
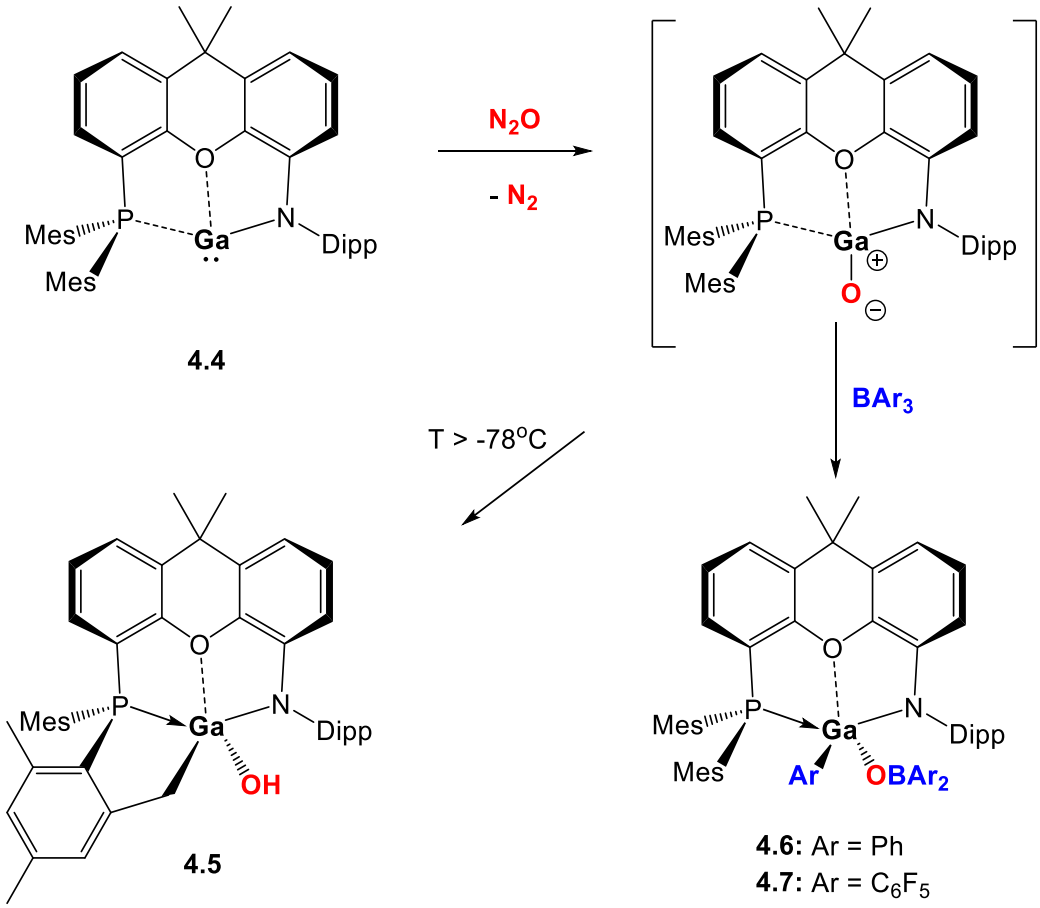


Figure 4.4 *Comparison of the aryl-flanked 'pockets' adjacent to the metal centre in (Nacnac)Ga and (PON)Ga (**4.4**).*

To probe the idea of enhanced steric bulk and encouraged by the finding that the weakly-bound phosphine donor becomes more strongly stabilizing on oxidation of the metal centre (cf. (PON)Ga and (PON)GaI_2), we examined the reactivity of **4.4** towards oxygen atom transfer agents. The isolation of a (hitherto unknown) gallanone complex containing a terminal GaO moiety, would presumably require both very strongly σ-donating and sterically demanding ancillary ligands.[31-32]

Power *et al*. have reported the formation of [(Nacnac)Ga(μ-O)]$_2$ from the reaction of (Nacnac)Ga with N_2O,[33] with the oxo-bridged structure presumably reflecting a steric profile which permits ready dimerization. By contrast, oxidation of **4.4** with N_2O or Me_3NO at room temperature leads to a monomeric product (**4.5**, Scheme 4.2), albeit one which results from intramolecular C-H activation of one of the ortho-methyl groups of the $PMes_2$ substituent across the transient gallium oxo unit.[34] Compound **4.5** has been characterized by spectroscopic methods and its structure in the solid state confirmed crystallographically (Figure 4.5). The formation of **4.5** is signaled by the appearance of a ^{31}P NMR resonance at δp = -41.0 ppm and by increased complexity in the pattern of ^{1}H NMR signals associated with the ortho methyl substituents. Its structure in the solid state is based around an approximately tetrahedral gallium

centre, featuring a significantly shortened Ga-P distance (2.468(1) Å cf. 3.078(2) Å for (PON)Ga), but with a weak Ga···O contact which is essentially unchanged from its precursor (2.578(2) Å vs. 2.645(5) Å). The Ga-C and Ga-OH bond lengths (1.972(4) and 1.828(2) Å) fall within the ranges previously reported for related (Nacnac)Ga-containing compounds.[35-38]



Scheme 4.2 *Oxidation of (PON)Ga by N_2O: formation of products derived from intramolecular C-H or intermolecular B-C bond activation at a putative gallanone intermediate.*

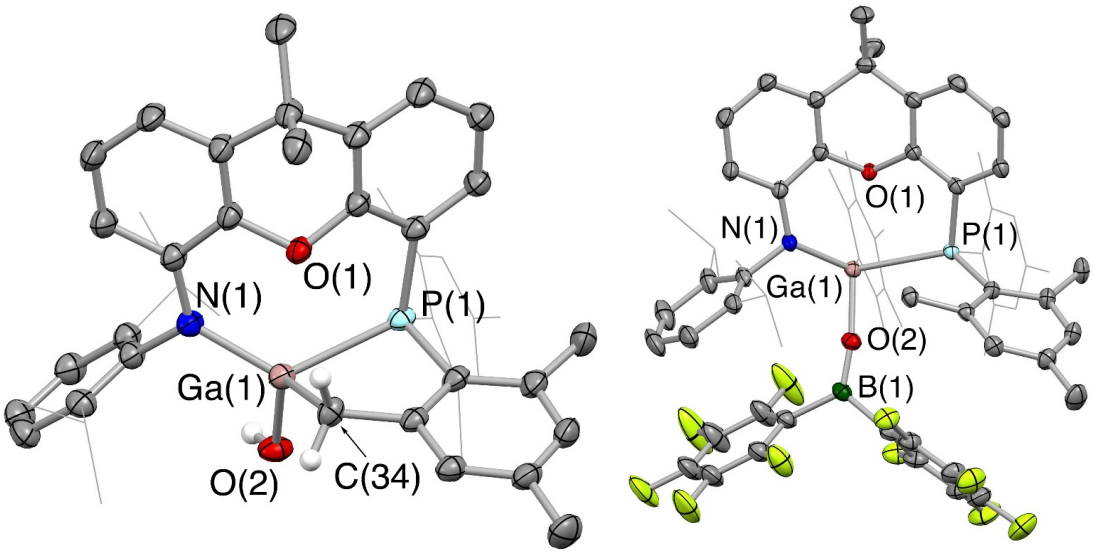


Figure 4.5 *Molecular structures of C-H and B-C activated species* ***4.5*** *(left) and* ***4.7*** *(right) in the solid state as determined by X-ray crystallography. Thermal ellipsoids set at the 40% probability level; most H atoms and solvate molecules omitted and* ^{i}*Pr/selected Mes groups shown in wireframe format for clarity. Key bond lengths (Å) and angles (°): (for* ***4.5****) Ga(1)-N(1) 1.921(3), Ga(1)-P(1) 2.468(1), Ga(1)-O(1) 2.578(2), Ga(1)-O(2) 1.828(2), Ga(1)-C(34) 1.972(4); (for* ***4.7****) Ga(1)-N(1) 1.904(2), Ga(1)-P(1) 2.591(1), Ga(1)-O(1) 2.566(2), Ga(1)-O(2) 1.864(2), B(1)-O(2) 1.297(4), Ga(1)-C(28) 2.015(4).*

Nikonov and co-workers have recently reported the trapping of the monomeric [(Nacnac)GaO] fragment by reactions of (Nacnac)Ga with N_2O in the presence of a range of relatively acidic C-H bonds (e.g. those in sulfoxides and ketones, and at the 2-position of pyridine and related heterocycles).[34] In the case of **4.4**/**4.5**, the fact that C-H activation occurs in the absence of an external trap (and at an unactivated methyl group) suggests that dimerization of the putative [(PON)GaO] monomer is less facile than in the related Nacnac system - in line with estimates of the comparative sizes of the ligand-enforced 'pockets.'

Attempts to identify a labile gallanone intermediate preceding the formation of **4.5** by VT-NMR methods were unsuccessful, so alternative (chemical) trapping methods were pursued

via coordination of either a Lewis acid (at O) or a Lewis base (at Ga). The latter strategy led either to no change in the outcome of the reaction (using IPrMe) or to the precipitation of gallium metal in the presence of the less bulky NHC IMe_4. On the other hand, addition of N_2O in the presence of a borane Lewis acid (either $B(C_6F_5)_3$ or BPh_3) leads to the clean formation of new products which are characterized by ^{31}P NMR signals at -36.1 and -35.6 ppm, respectively. Both products could be unambiguously characterized by X-ray crystallography, and are shown to result from cleavage of a B-C bond in BPh_3 (**4.6**) or $B(C_6F_5)_3$ (**4.7**) across the Ga-O unit formed in the initial reaction of gallylene **4.4** with N_2O (see Scheme 4.2, Figure 4.5). As such, the isolation of compounds **4.6** and **4.7** provides further evidence for the formation of a transient, highly reactive gallanone species by oxygen atom transfer to the gallium centre of **4.4**. It is worth noting that similar reactivity – leading to the cleavage of one of the B-C bonds in $B(C_6F_5)_3$ across a terminal Si=O bond – has been reported by Iwamoto and co-workers in studies of a reactive (but isolable) silanone.[39]

4.3 Conclusions

In summary, the development of a mono-anionic phosphino-amide ligand based on a xanthene backbone is reported, together with the synthesis of the corresponding Ga(I) complex, (PON)Ga (**4.4**), as a probe of its coordination properties in low valent main group chemistry. Structural studies of **4.4** are consistent with very weak O···Ga and P···Ga interactions, and with an R_2NGa fragment that closely resembles those found in one-coordinate amidogallium systems. Strong N-to-Ga π donation from the single amido group leads to a very short N-Ga distance (1.976(4) Å), while the P···Ga contact (3.078(2) Å) is comfortably outside the sum of the respective covalent radii. While the electronic properties of the PON donor are shown to be highly unsymmetrical towards Ga(I), oxidation to Ga(III) leads to stronger coordination of the pendant phosphine arm. From a steric perspective, the profile of the PON ligand is shown

to be significantly larger that those of related *N*,*N*'-chelated *β*-diketiminate systems, and underpins reactivity of (PON)Ga towards O-atom sources that proceeds without oligomerization. However, the enhanced P-donor properties seen on oxidation are not sufficient to quench the reactivity of the highly polar Ga-O unit. Instead, intramolecular benzylic C-H activation is observed across the Ga-O bond of a transient gallanone intermediate.

4.4 Syntheses and characterization of novel compounds

H(PON) 4.2

To a mixture of **4.1** (5.00 g, 9 mmol), NaO^{t}Bu (2.60 g, 27 mmol), $Pd(OAc)_2$ (0.04 g, 0.18 mmol) and DPEPhos (0.15 g, 0.27 mmol), in toluene (50 mL) was added 2,6-diisopropylaniline (1.9 mL, 10 mmol) at room temperature. The reaction mixture was heated to 100 ºC overnight whereupon it was quenched with water and extracted with toluene (3 x 25 mL). After drying over $MgSO_4$ and removal of volatiles under vacuum a brown solid was obtained, which was recrystalized from toluene/ methanol and dried to give **4.2** as a white powder (4.20 g, 72 %). Single crystals suitable for X-ray crystallography were obtained by slow evaporation from a concentrated solution in toluene at room temperature.

^{1}H NMR (400 MHz, C_6D_6, 298 K): δ = 1.05 (d, J_{HH} = 6.9 Hz, 6H, CH(C*H*$_3$)$_2$), 1.14 (d, J_{HH} = 6.9 Hz, 6H, CH(C*H*$_3$)$_2$), 1.46 (s, 6H, C*H*$_3$ of xanthene), 2.09 (s, 6H, *p*-C*H*$_3$ of Mes), 2.33 (s, 12H, *o*-C*H*$_3$ of Mes), 3.33 (sept, J_{HH} = 6.9 Hz, 2H, C*H*(CH$_3$)$_2$), 6.03 (s, 1H, N*H*), 6.19 (dd, J_{HH} = 1.2, 8.0 Hz, 1H, Ar*H*), 6.66 (dd, J_{HH} = 1.2, 8.0 Hz, 1H, Ar*H*), 6.71 (d, J_{HH} = 2.8 Hz, 4H, C*H* of Mes), 6.77 (dd, J_{HH} = 1.0, 7.6 Hz, 1H, Ar*H*), 6.8 (d, J_{HH} = 8.0 Hz, 1H, Ar*H*), 7.07 (m, 1H, Ar*H*), 7.11 (m, 1H, Ar*H*), 7.18 (m, 3H, Ar*H* of Dipp).

^{13}C NMR (126 MHz, C_6D_6, 298 K): δ = 153.5 (d, J_{PC} = 19.3 Hz), 148.4, 143.7 (d, J_{PC} = 16.2 Hz), 138.4, 138.1 (d, J_{PC} = 2.3 Hz), 137.5, 135.6, 130.8, 130.6 (d, J_{PC} = 3.8 Hz), 130.4, 129.9,

129.8, 129.7, 126.4, 126.1 (d, J_{PC} = 13.6 Hz), 124.1, 124.0, 123.8, 113.4, 109.5, 34.7 (d, J_{PC} = 1.8 Hz), 31.5, 28.6, 24.9, 23.2, 22.8, 22.6, 21.0.

^{31}P NMR (162 MHz, C_6D_6, 298 K): δ = -36.9.

[K(PON)]$_2$ 4.3

Toluene (30 mL) was added to a Schlenk flask containing a mixture of **4.2** (1.01 g, 1.50 mmol) and benzylpotassium (0.21 g, 1.60 mmol). The reaction mixture was stirred for 3 h at room temperature, filtered and volatiles removed from the filtrate under vacuum to give **3** as an off-white solid (1.02 g, 95 %). Single crystals suitable for X-ray crystallography were obtained by slow evaporation in toluene.

^{1}H NMR (400 MHz, C_6D_6, 298 K): δ = 1.05 (d, J_{HH} = 6.9 Hz, 6H, CH(C*H*$_3$)$_2$), 1.27 (d, J_{HH} = 6.9 Hz, 6H, CH(C*H*$_3$)$_2$), 1.73 (s, 6H, C*H*$_3$ of xanthene), 2.00 (s, 12H, *o*-C*H*$_3$ of Mes), 2.09 (s, 6H, *p*-C*H*$_3$ of Mes), 3.26 (sept, J_{HH} = 6.9 Hz, 2H, C*H*(CH$_3$)$_2$), 6.17 (dd, J_{HH} = 1.2 Hz, J_{HH} = 8.0 Hz, 1H, Ar*H*), 6.20 (dd, J_{HH} = 1.2, 8.0 Hz, 1H, Ar*H*), 6.66 (d, J_{HH} = 2.8 Hz, 4H, C*H* of Mes), 6.72 (t, J_{HH} = 7.8 Hz, 1H, Ar*H*), 7.05 (m, 2H, Ar*H*), 7.19 (d, J_{HH} = 7.6 Hz, 1H, Ar*H*), 7.30 (d, J_{HH} = 7.7 Hz, 1H, Ar*H*), 7.35 (d, 7.6Hz, 2H, Ar*H*).

^{13}C NMR (126 MHz, C_6D_6, 298 K): δ = 156.6 (d, J_{PC} = 18.6 Hz), 153.6, 149.5, 143.9, 142.7 (d, J_{PC} = 14.7 Hz), 139.2, 138.5, 137.9 (toluene), 133.5 (d, J_{PC} = 2.1 Hz), 132.0, 131.0 (d, J_{PC} = 3.8 Hz), 130.5 (d, J_{PC} 3.7 Hz), 130.2 (d, J_{PC} = 10.3 Hz), 129.3 (toluene), 128.7, 128.6 (toluene), 125.7 (toluene), 125.3, 123.7, 122.4, 120.8 (d, J_{PC} = 6.4 Hz), 120.0, 110.6, 101.2, 34.8 (d, J_{PC} = 2.0 Hz), 32.7, 27.9, 25.2, 24.9, 22.9, 22.8, 21.4 (toluene), 20.9.

^{31}P NMR (162 MHz, C_6D_6, 298 K): δ = -34.4.

(PON)Ga 4.4

To a mixture of Ga metal (0.12 g, 1.70 mmol) and iodine (0.22 g, 0.65 mmol) in a Schlenk flask was added toluene (30 mL). The mixture was sonicated until a green precipitate appeared, and a solution of **3** (1.00 g, 1.50 mmol) in toluene (20 mL) added dropwise. After stirring at room temperature overnight, the reaction mixture was allowed to settle and filtered by cannula. The resulting filtrate was concentrated (to ca. 20 mL) and crystalline product obtained by slow evaporation at room temperature. (0.67 g, 60 %).

Anal. Calc. for $C_{45}H_{51}GaNOP$: 74.80% H 7.11% N 1.94%; Meas.: C 74.47% H 7.06 N 1.80 %.

^{1}H NMR (400 MHz, C_6D_6, 298 K): δ = 1.12 (d, J_{HH} = 7.1 Hz, 6H, CH(CH_3)$_2$), 1.14 (d, J_{HH} = 7.0 Hz, 6H, CH(CH_3)$_2$), 1.50 (s, 6H, CH_3 of xanthene), 2.06 (s, 6H, *p*-CH_3 of Mes), 2.19 (s, 12H, *o*-CH_3 of Mes), 3.40 (sept, J_{HH} = 6.8 Hz, 2H, C*H*(CH$_3$)$_2$), 6.13 (dd, J_{HH} = 1.4, 8.0 Hz, 1H, Ar*H*), 6.55 (dd, J_{HH} = 1.4, 8.0 Hz, 1H, Ar*H*), 6.70 (d, J_{HH} = 2.8 Hz, 4H, C*H* of Mes), 6.76 (m, 1H, Ar*H*), 6.89 (t, J_{HH}=7.8 Hz, 1H, Ar*H*), 7.30 (m, 3H, Ar*H*), 7.36 (m, 2H, Ar*H*).

^{13}C NMR (126 MHz, C_6D_6, 298 K): δ = 157.4 (d, J_{PC} = 22.2 Hz), 148.9, 142.7 (d, J_{PC} = 13.5 Hz), 142.6, 142.4, 138.8, 137.3, 134.1 (d, J_{PC} = 2.8 Hz), 133.8, 131.2, 130.9 (d, J_{PC} = 4.3 Hz), 130.1 (d, J_{PC} = 9.4 Hz), 127.4, 126.4, 125.2, 124.5, 124.0, 122.0 (d, J_{PC} = 8.2 Hz), 112.8, 109.9, 35.1, 30.2, 28.4, 26.5 24.9, 23.2 (d, J_{PC} = 12.5 Hz), 21.0.

^{31}P NMR (162 MHz, C_6D_6, 298 K): δ = -34.3.

Reaction of 4 with N_2O – synthesis of C-H activation product 4.5

A solution of **4.4** (96 mg, 0.13 mmol) in toluene (5 mL) was subjected to three freeze-pump-thaw cycles before backfilling with N_2O (ca. 1 atm) at -78 ^{o}C. The solution was stirred at this

temperature for 4 h, and slowly warmed up to room temperature. The resulting solution was kept at -30 °C for several days to afford colourless crystals of **4.5** (40 mg, 41 %).

Anal. Calc. for $C_{45}H_{51}GaNO_2P$ 73.18 % H 6.96 % N 1.90%; Meas.: C 73.10 % H 6.67 % N 1.86%.

^{1}H NMR (400 MHz, C_6D_6, 298 K): δ = -0.11 (d, J_{PH} = 4.1 Hz, 1H, [Ga]O*H*), 0.97 (d, J_{HH} = 6.6 Hz, 3H, CH(CH_3)$_2$), 1.03 (d, J_{HH} = 6.6 Hz, 3H, CH(CH_3)$_2$), 1.08 (s, 3H, CH_3 of xanthene), 1.28 (d, J_{HH} = 7.0 Hz, 3H, CH(CH_3)$_2$), 1.42 (s, 3H, CH_3 of xanthene), 1.53 (d, J_{HH} = 7.0 Hz, 3H, CH(CH_3)$_2$), 1.97 (s, 3H, *o*-CH_3 of Mes), 2.01 (m, 6H, *o*-CH_3 of Mes), 2.16 (s, 3H, *p*-CH_3 of Mes), 2.25 (s, 3H, *p*-CH_3 of Mes), 2.82 (m, 2H, [Ga]CH_2), 3.48 (sept, J_{HH} = 6.9 Hz, 1H, C*H*(CH$_3$)$_2$), 3.88 (sept, J_{HH} = 6.9 Hz, 1H, C*H*(CH$_3$)$_2$), 6.30 (dd, J_{HH} = 1.3, 8.2 Hz, 1H, Ar*H*), 6.45 (s, 1H, Ar*H*), 6.50 (dd, J_{HH} = 1.3, 7.8 Hz, 1H, Ar*H*), 6.56 (m, 1H, Ar*H*), 6.64 (m, 1H, Ar*H*), 6.82 (td, J_{HH} = 1.2, 7.6 Hz, 1H, Ar*H*), 6.89 (t, J_{HH} = 8.0 Hz, 1H, Ar*H*), 7.13 (m, 3H, Ar*H*), 7.22 (t, J_{HH}=7.6 Hz, 1H, Ar*H*), 7.30 (m, 1H, Ar*H*), 7.45 (td, J_{HH} = 1.3, 7.8 Hz, 1H, Ar*H*).

^{13}C NMR (125.8 MHz, C_6D_6, 298 K): δ = 155.3 (d, J_{PC} = 13.5 Hz), 151.3, 151.1, 148.9, 147.8, 143.8, 143.7 (d, J_{PC} = 8.7 Hz), 143.1, 141.8, 141.2, 141.0, 140.9, 139.7, 136.5 (d, J_{PC} = 3.8 Hz), 133.0, 132.6 (d, J_{PC} = 6.3 Hz), 131.5 (d, J_{PC} = 7.2 Hz), 131.0 (d, J_{PC} = 3.6 Hz), 130.9 (d, J_{PC} = 7.5 Hz), 128.9 (d, J_{PC} = 6.0 Hz), 127.3, 126.7 (t, J_{PC} = 22.0 Hz), 125.2, 124.7 (d, J_{PC} = 16.8 Hz), 123.4 (d, J_{PC} = 5.7 Hz), 121.7 (d, J_{PC} = 31.0 Hz), 119.6, 119.3, 114.1, 109.3, 36.5, 32.0 (Hexane), 31.6, 28.2 (d, J_{PC} = 8.5 Hz), 25.3, 25.2, 25.1, 25.0, 24.5, 24.0 (d, J_{PC} = 5.7 Hz), 23.5, 23.2, 23.1 (Hexane), 21.0, 20.8, 14.4 (Hexane).

^{31}P NMR (162MHz, C_6D_6, 298 K): δ = -41.0.

Reaction of 4.4 with N_2O and BPh_3 – synthesis of B-C activation product 4.6

A mixture of **4.4** (71 mg, 0.098 mmol) and BPh_3 (24 mg, 0.098 mmol) was dissolved in toluene (5 mL) and the resulting solution subjected to three freeze-pump-thaw cycles before backfilling with N_2O (to ca. 1 atm) at -78 °C. The solution was stirred at this temperature for 4 h, and slowly warmed to room temperature. The resulting solution was kept at -30 °C for several days to afford colourless crystals of **4.7** (31 mg, 32 %).

^{1}H NMR (400 MHz, C_6D_6, 298 K): δ = 1.04 (d, J_{HH} = 6.4 Hz, 3H, CH(C*H*$_3$)$_2$), 1.13 (m, 6H, CH(C*H*$_3$)$_2$), 1.47 (m, 12H, *o*-C*H*$_3$ of Mes), 1.81 (s, 3H, C*H*$_3$ of xanthene), 1.95 (s, 3H, C*H*$_3$ of xanthene), 2.09 (m, 3H, CH(C*H*$_3$)$_2$), 2.37 (s, 3H, *p*-C*H*$_3$ of Mes), 3.04 (s, 3H, *p*-C*H*$_3$ of Mes), 3.58 (sept, J_{HH} = 6.8 Hz, 1H, C*H*(CH$_3$)$_2$), 4.16 (sept, J_{HH} = 6.8 Hz, 1H, C*H*(CH$_3$)$_2$), 5.98 (s, 1H, Ar*H*), 6.37 (m, 2H, Ar*H*), 6.55 (m, 1H, Ar*H*), 6.67 (m, 4H, *m-H* of Mes), 6.84 (m, 3H, Ar*H* of Dipp), 7.14 (m, 5H, Ar*H* of [Ga]Ph), 7.22 (m, 5H, Ar*H* of [Ga]OBPh), 7.28 (m, 1H, Ar*H*), 7.37 (m, 5H, Ar*H* of [Ga]OBPh).

^{13}C NMR (125.8 MHz, C_6D_6, 298 K): δ = 155.8 (d, J_{PC} = 12.1 Hz), 149.4, 148.7, 144.4, 143.8, 143.4, 142.9 (d, J_{PC} = 22.1 Hz), 142.5, 142.2, 141.7, 140.5, 140.2, 139.9, 139.3, 136.3, 135.2, 133.8, 131.9, 131.8, 131.5, 130.8, 130.4, 128.8, 128.7, 128.6 (d, J_{PC} = 4.2 Hz), 127.2, 126.4, 125.8, 125.0, 124.5, 119.4, 119.2, 116.1, 109.3, 35.7, 33.3, 32.0 (hexane), 28.7, 28.1, 26.5, 25.8, 25.6 (d, J_{PC} = 11.6 Hz), 24.1, 23.7, 23.4, 23.1 (hexane), 20.9, 20.5, 14.4 (hexane).

^{31}P NMR (162MHz, C_6D_6, 298 K): δ = -36.0.

Reaction of 4.4 with N_2O and $B(C_6F_5)_3$ – synthesis of B-C activation product 4.7

A mixture of **4.4** (69 mg, 0.096 mmol) and $B(C_6F_5)_3$ (49 mg, 0.096 mmol) was dissolved in toluene (5 mL) and the resulting solution subjected to three freeze-pump-thaw cycles before backfilling with N_2O (to ca. 1 atm) at -78 °C. The solution was stirred at this temperature for 4

h and slowly warmed to room temperature. The resulting solution was kept at -30 °C for several days to afford colourless crystals of **4.7** (41 mg, 34 %).

Anal. Calc. for $C_{63}H_{51}BF_{15}GaNO_2P$: C 60.51 % H 4.11 % N 1.12 %; Meas.: C 60.83 % H 3.92 % N 1.26 %.

^{1}H NMR (400 MHz, C_6D_6, 298 K): δ = 0.81 (d, J_{HH} = 6.8 Hz, 3H, CH(C*H*$_3$)$_2$), 0.96 (d, J_{HH} = 6.6 Hz, 3H, CH(C*H*$_3$)$_2$), 1.07 (d, J_{HH} = 6.6 Hz, 3H, CH(C*H*$_3$)$_2$), 1.36 (s, 3H, C*H*$_3$ of Mes), 1.42 (s, 3H, C*H*$_3$ of xanthene), 1.45 (s, 3H, C*H*$_3$ of xanthene), 1.54 (d, J_{HH} = 6.8 Hz, 3H, CH(C*H*$_3$)$_2$), 1.70 (s, 3H, C*H*$_3$ of Mes), 1.74 (s, 3H, C*H*$_3$ of Mes), 1.91 (s, 3H, C*H*$_3$ of Mes), 2.08 (s, 3H, C*H*$_3$ of Mes), 2.70 (s, 3H, C*H*$_3$ of Mes), 3.42 (sept, J_{HH} = 6.8 Hz, 1H, C*H*(CH$_3$)$_2$), 3.64 (sept, J_{HH} = 6.8 Hz, 1H, C*H*(CH$_3$)$_2$, 6.04 (m, 2H, Ar*H*), 6.53 (m, 2H, Ar*H*), 6.55 (dd, J_{HH} = 1.3, 7.9 Hz, 1H, Ar*H*), 6.58 (td, J_{HH} = 1.2, 7.7 Hz, 1H, Ar*H*), 6.68 (t, J_{HH} = 7.7 Hz, 1H, Ar*H*), 6.81 (m, 3H, Ar*H*), 6.88 (dd, J_{HH} = 1.7, 7.7 Hz, 1H, Ar*H*), 7.05 (d, J_{HH} = 7.7 Hz, 1H, Ar*H*), 7.12 (t, J_{HH} = 7.7 Hz, 1H, Ar*H*) .

^{13}C NMR (126 MHz, C_6D_6, 298 K): δ = 154.8 (d, J_{PC} = 9.8 Hz), 148.7, 148.4, 147.7, 145.8, 143.4 (d, J_{PC} = 14.6 Hz), 142.6, 141.9, 141.8, 141.6 (d, J_{PC} = 2.4 Hz), 141.2, 141.0, 140.7, 139.6 (d, J_{PC} = 4.1 Hz), 139.3, 138.3, 136.3, 135.0 (d, J_{PC} = 3.5 Hz), 132.7, 131.5 (d, J_{PC} = 6.8 Hz), 131.2 (d, J_{PC} = 2.8 Hz), 131.2, 131.1 (d, J_{PC} = 2.3 Hz), 129.2, 126.8, 125.4, 125.1, 124.8, 124.7 (d, J_{PC} = 6.2 Hz), 124.1, 122.9 (d, J_{PC} = 33.5 Hz), 116.7, 116.4, 110.8, 35.4, 33.3, 32.0 (Hexane), 28.1, 27.5, 26.8, 25.2, 24.2, 23.9 (d, J_{PC} = 2.8 Hz), 23.9, 23.7, 23.3, 23.1, 23.0 (hexane), 22.5 (d, J_{PC} = 2.8 Hz), 20.7, 20.4, 14.4 (hexane).

^{19}F NMR (471 MHz, C_6D_6, 298 K): δ = -111.8 (s, 1F, *o*-F of [Ga]C_6F_5), -119.3 (d, J_{FF} = 25.6 Hz, 1F, *o*-F of [Ga]C_6F_5), -130.9 (s, 4F, *o*-F of [Ga]OB(C_6F_5)$_2$), -154.5 (t, J_{FF} = 19.5 Hz, 1F, *p*-F of [Ga]C_6F_5), 154.7 (t, J_{FF} = 20.5 Hz, 2F, *p*-F of [Ga]OB(C_6F_5)$_2$), -161.7 (s, 1F, *m*-F of [Ga]C_6F_5), -162.8 (m, 4F, *m*-F of [Ga]OB(C_6F_5)$_2$), -163.7 (s, 1F, *m*-F of [Ga]C_6F_5).

^{31}P NMR (162 MHz, C_6D_6, 298 K): δ = -35.6.

(PON)GaI$_2$

A mixture of Ga metal (12 mg, 0.16 mmol) and iodine (63 mg, 0.25 mmol) in toluene (5 mL) was sonicated until the solution turned colourless. A solution of **4.3** (0.11 g, 0.17 mmol) also in toluene (5 mL) was then transferred dropwise into the GaI_3 solution. After stirring at room temperature overnight, the reaction mixture was allowed to settle and filtered by cannula. The resulting filtrate was concentrated (to ca. 3 mL) and crystalline product obtained from slow evaporation at room temperature. (0.13 g, 81 %).

^{1}H NMR (400 MHz, C_6D_6, 343 K): δ = 1.01 (s, 6H, CH(C*H*$_3$)$_2$), 1.26 (s, 6H, CH(C*H*$_3$)$_2$), 1.56 (s, 6H, C*H*$_3$ of xanthene), 1.99 (s, 6H, *p*-C*H*$_3$ of Mes), 2.26 (br, 12H, *o*-C*H*$_3$ of Mes), 3.14 (s, 2H, C*H*(CH$_3$)$_2$), 6.20 (dd, J_{HH} = 1.1, 8.0 Hz, 1H, Ar*H*), 6.53 (dd, J_{HH} = 1.3, 7.9 Hz, 1H, Ar*H*), 6.60 (s, 4H, C*H* of Mes), 6.71 (m, 1H, Ar*H*), 6.83 (m, 2H, Ar*H*), 7.23 (d, J_{HH} = 7.9 Hz, 1H, *p*-C*H* of Dipp), 7.29 (m, 2H, *m*-C*H* of Dipp).

^{13}C NMR (126 MHz, C_6D_6, 343 K): δ = 149.7 (d, J_{PC} = 6.9 Hz), 149.5, 143.4, 141.6, 141.2, 141.0, 134.0 (d, J_{PC} = 4.2 Hz), 132.6, 131.9 (d, J_{PC} = 7.4 Hz), 131.8, 131.6, 128.6, 127.3, 125.2, 124.7 (d, J_{PC} = 7.4 Hz), 124.6, 116.9, 116.6, 114.6, 112.7, 34.5, 33.4, 29.1, 25.3, 20.7.

^{31}P NMR (162 MHz, C_6D_6, 298 K): δ = -30.8.

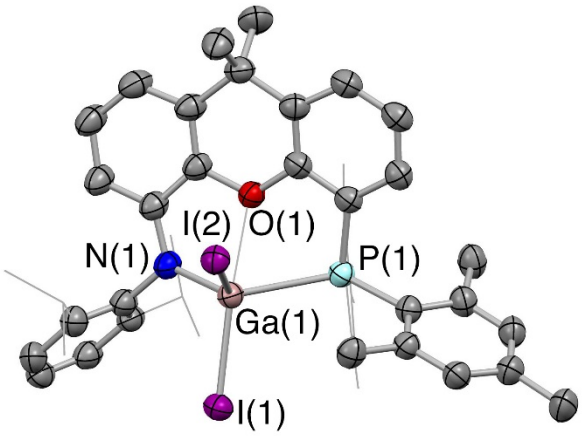


Figure 4.6 *Molecular structure of (PON)GaI_2 in the solid state as determined by X-ray crystallography. Thermal ellipsoids set at the 40% probability level; Hydrogen atoms and solvate molecules omitted and ^{i}Pr/selected Mes groups shown in wireframe format for clarity. Key bond lengths (Å) and angles (°):, Ga(1)-N(1) 1.927(3), Ga(1)-O(1) 2.388(2), Ga(1)-P(1) 2.612(1), Ga(1)-I(1) 2.570(1), Ga(1)-I(2) 2.580(1).*

***Table 4.1**. Selected crystallographic and refinement data for compounds **4.2–4.7** and **PONGaI$_2$**.*

	4.2	**4.3**	**4.4**
Formula	$C_{45}H_{52}NOP$	$C_{52}H_{59}KNOP$	$C_{51}H_{57}GaNOP$
Fw	653.89	784.07	800.66
Crystal System	Triclinic	Triclinic	Triclinic
Space Group	P-1	P-1	P-1
Wavelength/Å	1.54184	1.54184	1.54184
a/Å	11.3306(3)	12.7485(8)	12.8171(3)
b/Å	6.5217(6)	13.7483(9)	13.6400(4)
c/Å	20.7251(4)	14.3199(8)	14.2809(4)
α/°	81.490(2)	78.513(5)	78.240(2)
β/°	84.932(2)	73.380(5)	72.984(2)
γ/°	79.593(2)	65.466(6)	65.459(3)
Volume/Å^3	3766.34(19)	2178.5(3)	2161.97(11)
Z	4	2	2
Temperature/K	150(2)	150(2)	150(2)
Reflections collected	15583	9036	16185
$2\vartheta_{max}$	152.08	154.312	152.654
R_{int}	0.0456	0.0392	0.0356
Goodness of fit	1.017	1.045	1.045
$R[F^2>2\sigma]$, F	0.0499	0.0562	0.0469
R_w(all data), F^2	0.1286	0.1480	0.1554

	4.5	**4.6**	**4.7**	**PONGaI$_2$**
Formula	$C_{60}H_{66}GaNO_2P$	$C_{67}H_{76}BGaNO_3P$	$C_{69}H_{66}BF_{15}GaNO_{3.5}P$	$C_{50}H_{40}Ga_1O_1N_1P_1I_2$
Fw	933.82	1054.78	1361.72	1050.47
Crystal System	Monoclinic	Monoclinic	Triclinic	Monoclinic
Space Group	$P2_1/n$	$P2_1/c$	P-1	$P2_1/n$
Wavelength/Å	1.54184	1.54184	1.54184	1.54184
a/Å	12.6281(4)	21.97110(10)	12.9244(4)	11.77520(10)
b/Å	22.5013(5)	11.79260(10)	16.4616(5)	11.57010(10)
c/Å	18.1528(5)	23.02780(10)	17.5979(5)	34.8107(2)
α/°	90	90	69.507(2)	90
β/°	106.257(3)	106.7600(10)	81.629(2)	95.3600(10)
γ/°	90	90	66.917(3)	90
Volume/Å^3	4951.9(2)	5712.97(7)	3226.18(18)	4721.88(6)
Z	4	4	2	4
Temperature/K	150(2)	150(2)	150(2)	150(2)
Reflections collected	24072	163774	63726	59922
$2\vartheta_{max}$	152.72	152.29	153.95	152.16
R_{int}	0.0411	0.0489	0.0598	0.0542
Goodness of fit	1.035	1.045	1.025	1.121
$R[F^2>2\sigma]$, F	0.0639	0.0749	0.0451	0.0697
R_w(all data), F^2	0.1692	0.1848	0.1278	0.1591

4.5 References

1. Bradley, W.; Wright, I., 129. Metal derivatives of NN′-diarylamidines. *J. Chem. Soc.* **1956,** (0), 640-648.
2. Parks, J. E.; Holm, R. H., Synthesis, solution stereochemistry, and electron delocalization properties of bis(.beta.-iminoamino)nickel(II) complexes. *Inorg. Chem.* **1968,** *7* (7), 1408-1416.
3. McGeachin, S. G., Synthesis and properties of some β-diketimines derived from acetylacetone, and their metal complexes. *Can. J. Chem.* **1968,** *46* (11), 1903-1912.
4. Honeybourne, C. L.; Webb, G. A., Some metal complexes of 1,3-di-imines. *Chem. Commun.* **1968,** (13), 739-740.
5. Bonnett, R.; Bradley, D. C.; Fisher, K. J., Bis-(NN′-diethylbutane-2,4-di-iminato)cobalt(II), a tetrahedral cobalt derivative of a new nitrogen chelate group. *Chem. Commun.* **1968,** (15), 886-887.
6. Bourget-Merle, L.; Lappert, M. F.; Severn, J. R., The Chemistry of β-Diketiminatometal Complexes. *Chem. Rev.* **2002,** *102* (9), 3031-3066.
7. Hill, M. S.; Hitchcock, P. B.; Pongtavornpinyo, R., A Linear Homocatenated Compound Containing Six Indium Centers. *Science* **2006,** *311* (5769), 1904-1907.
8. Green, S. P.; Jones, C.; Stasch, A., Stable Magnesium(I) Compounds with Mg-Mg Bonds. *Science* **2007,** *318* (5857), 1754.
9. Rodriguez, M. M.; Bill, E.; Brennessel, W. W.; Holland, P. L., Nitrogen Reduction and Hydrogenation to Ammonia by a Molecular Iron-Potassium Complex. *Science* **2011,** *334* (6057), 780-783.
10. Asay, M.; Jones, C.; Driess, M., N-Heterocyclic Carbene Analogues with Low-Valent Group 13 and Group 14 Elements: Syntheses, Structures, and Reactivities of a New Generation of Multitalented Ligands. *Chem. Rev.* **2011,** *111* (2), 354-396.
11. Tsai, Y.-C., The chemistry of univalent metal β-diketiminates. *Coord. Chem. Rev.* **2012,** *256* (5), 722-758.
12. Chen, C.; Bellows, S. M.; Holland, P. L., Tuning steric and electronic effects in transition-metal β-diketiminate complexes. *Dalton Trans.* **2015,** *44* (38), 16654-16670.
13. Camp, C.; Arnold, J., On the non-innocence of "Nacnacs": ligand-based reactivity in β-diketiminate supported coordination compounds. *Dalton Trans.* **2016,** *45* (37), 14462-14498.
14. Dohmeier, C.; Loos, D.; Schnöckel, H., Aluminum(I) and Gallium(I) Compounds: Syntheses, Structures, and Reactions. *Angew. Chem., Int. Ed.* **1996,** *35* (2), 129-149.
15. Hardman, N. J.; Eichler, B. E.; Power, P. P., Synthesis and characterization of the monomer Ga{(NDippCMe)$_2$CH} (Dipp = C$_6$H$_3$^{i}Pr$_2$-2,6): a low valent gallium(i) carbene analogue. *Chem. Commun.* **2000,** (20), 1991-1992.
16. Cui, C.; Roesky, H. W.; Schmidt, H.-G.; Noltemeyer, M.; Hao, H.; Cimpoesu, F., Synthesis and Structure of a Monomeric Aluminum(I) Compound [{HC(CMeNAr)$_2$}Al] (Ar=2,6–iPr$_2$C$_6$H$_3$): A Stable Aluminum Analogue of a Carbene. *Angew. Chem., Int. Ed.* **2000,** *39* (23), 4274-4276.
17. Hicks, J.; Vasko, P.; Goicoechea, J. M.; Aldridge, S., Synthesis, structure and reaction chemistry of a nucleophilic aluminyl anion. *Nature* **2018,** *557* (7703), 92-95.
18. Schwamm, R. J.; Anker, M. D.; Lein, M.; Coles, M. P., Reduction vs. Addition: The Reaction of an Aluminyl Anion with 1,3,5,7-Cyclooctatetraene. *Angew. Chem., Int. Ed.* **2019,** *58* (5), 1489-1493.
19. Kurumada, S.; Takamori, S.; Yamashita, M., An alkyl-substituted aluminium anion with strong basicity and nucleophilicity. *Nat. Chem.* **2020,** *12* (1), 36-39.

20. Schwamm, R. J.; Coles, M. P.; Hill, M. S.; Mahon, M. F.; McMullin, C. L.; Rajabi, N. A.; Wilson, A. S. S., A Stable Calcium Alumanyl. *Angew. Chem., Int. Ed.* **2020,** *59* (10), 3928-3932.
21. Koshino, K.; Kinjo, R., Construction of σ-Aromatic AlB_2 Ring via Borane Coupling with a Dicoordinate Cyclic (Alkyl)(Amino)Aluminyl Anion. *J. Am. Chem. Soc.* **2020,** *142* (19), 9057-9062.
22. Grams, S.; Eyselein, J.; Langer, J.; Färber, C.; Harder, S., Boosting Low-Valent Aluminum(I) Reactivity with a Potassium Reagent. *Angew. Chem., Int. Ed.* **2020,** *59* (37), 15982-15986.
23. Hicks, J.; Vasko, P.; Goicoechea, J. M.; Aldridge, S., The Aluminyl Anion: A New Generation of Aluminium Nucleophile. *Angew. Chem., Int. Ed.* **2021,** *60* (4), 1702-1713.
24. Hicks, J.; Mansikkamäki, A.; Vasko, P.; Goicoechea, J. M.; Aldridge, S., A nucleophilic gold complex. *Nat. Chem.* **2019,** 11, 237-241.
25. Hicks, J.; Vasko, P.; Goicoechea, J. M.; Aldridge, S., Reversible, Room-Temperature C-C Bond Activation of Benzene by an Isolable Metal Complex. *J. Am. Chem. Soc.* **2019,** *141* (28), 11000-11003.
26. Wright, R. J.; Brynda, M.; Fettinger, J. C.; Betzer, A. R.; Power, P. P., Quasi-Isomeric Gallium Amides and Imides $GaNR_2$ and RGaNR (R = Organic Group): Reactions of the Digallene, Ar'GaGaAr' (Ar' = C_6H_3-2,6-(C_6H_3-2,6-$^iPr_2$)$_2$) with Unsaturated Nitrogen Compounds. *J. Am. Chem. Soc.* **2006,** *128* (38), 12498-12509.
27. Dange, D.; Li, J.; Schenk, C.; Schnöckel, H.; Jones, C., Monomeric Group 13 Metal(I) Amides: Enforcing One-Coordination Through Extreme Ligand Steric Bulk. *Inorg. Chem.* **2012,** *51* (23), 13050-13059.
28. Mo, Z.; Kolychev, E. L.; Rit, A.; Campos, J.; Niu, H.; Aldridge, S., Facile reversibility by design: tuning small molecule capture and activation by single component frustrated Lewis pairs. *J. Am. Chem. Soc.* **2015,** *137* (38), 12227-30.
29. Green, M. L. H.; Mountford, P.; Smout, G. J.; Speel, S. R., New synthetic pathways into the organometallic chemistry of gallium. *Polyhedron* **1990,** *9* (22), 2763-2765.
30. Cordero, B.; Gómez, V.; Platero-Prats, A. E.; Revés, M.; Echeverría, J.; Cremades, E.; Barragán, F.; Alvarez, S., Covalent radii revisited. *Dalton Trans.* **2008,** (21), 2832-2838.
31. Hicks, J.; Heilmann, A.; Vasko, P.; Goicoechea, J. M.; Aldridge, S., Trapping and Reactivity of a Molecular Aluminium Oxide Ion. *Angew. Chem., Int. Ed.* **2019,** *58* (48), 17265-17268.
32. Anker, M. D.; Coles, M. P., Aluminium-Mediated Carbon Dioxide Reduction by an Isolated Monoalumoxane Anion. *Angew. Chem., Int. Ed.* **2019,** *131* (50), 18429-18433.
33. Hardman, N. J.; Power, P. P., Dimeric Gallium Oxide and Sulfide Species Stabilized by a Sterically Encumbered β-Diketiminate Ligand. *Inorg. Chem.* **2001,** *40* (11), 2474-2475.
34. Kassymbek, A.; Vyboishchikov, S. F.; Gabidullin, B. M.; Spasyuk, D.; Pilkington, M.; Nikonov, G. I., Sequential Oxidation and C−H Bond Activation at a Gallium(I) Center. *A Angew. Chem., Int. Ed.* **2019,** *58* (50), 18102-18107.
35. Hennersdorf, F.; Frötschel, J.; Weigand, J. J., Selective Derivatization of a Hexaphosphane from Functionalization of White Phosphorus. *J. Am. Chem. Soc.* **2017,** *139* (41), 14592-14604.
36. Bernabé-Pablo, E.; Jancik, V.; Moya-Cabrera, M., A Synthetic Route to a Molecular Galloxane Dihydroxide and Its Group 4 Heterobimetallic Compounds. *Inorg. Chem.* **2013,** *52* (12), 6944-6950.
37. Solis-Ibarra, D.; Velásquez-Hernández, M. d. J.; Huerta-Lavorie, R.; Jancik, V., Molecular Gallosilicates and Their Group 4 Multimetallic Derivatives. *Inorg. Chem.* **2011,** *50* (18), 8907-8917.

38. Jancik, V.; Pineda, L. W.; Stückl, A. C.; Roesky, H. W.; Herbst-Irmer, R., Preparation of Monomeric $LGa(NH_2)_2$ and of $LGa(OH)_2$ in the Presence of a N-Heterocyclic Carbene as HCl Acceptor. *Organometallics* **2005,** *24* (7), 1511-1515.
39. Kobayashi, R.; Ishida, S.; Iwamoto, T., An Isolable Silicon Analogue of a Ketone that Contains an Unperturbed Si=O Double Bond. *Angew. Chem., Int. Ed.* **2019,** *58* (28), 9425-9428.

Chapter 5 Low oxidation state boryl-tin compounds

5.1 Introduction

Huckel's rule predicts that the dianion and dication of cyclobutadiene (CBD) should be aromatic with 6π and 2π electrons, respectively. The study of the aromaticity of these systems is intriguing; for example, multiply charged 6π-aromatic cyclic systems behave quite differently from neutral and singly charged systems because of the Coulombic repulsion of the two additional electrons.[1-2] A folded $[CBD]^{2-}$ structure with one localized and one allylic delocalized negative charge,[3] a trapezoid structure with 1,2-localized negative charges and a C=C double bond,[4] and a planar delocalized structure stabilized by coordination of the two Li cations[5-6] were all predicted to be energetic minima by early calculations. Experimentally, there have been studies on the transient cyclobutadiene dianion[7] $[CBD]^{2-}$ and its derivatives stabilized by ester[8] or phenyl groups.[9] The first four-membered cyclic system featuring a delocalized 6π-electron system was synthesized and characterized by Sekiguchi *et al*. in 2000.[10] Later in 2004, the same group managed to isolate $[CBD]^{2-}$ derivatives of the heavier group 14 elements ($[R_4Si_4]^{2-}$ and $[R_4Si_2Ge_2]^{2-}$, where R = $SiMe^tBu_2$)[11] in which the central four-membered ring is significantly folded and has two η^2-1,3-coordinated potassium cations accommodated by the ring. These systems are thought to be non-aromatic on the basis of nucleus-independent chemical shift (NICS) calculations.

Although the dication of cyclobutadiene $[CBD]^{2+}$ was first observed spectroscopically by ionization of 3,4-dichloro-1,2,3,4-tetramethylcyclobutene in SbF_5/SO_2 solution at -75 ^oC by Olah *et al*.,[12] the synthesis of derivatives of this type that are stable at room temperature was not achieved until Driess[13] and Roesky[14] reported two $R_4Si_4^{2+}$ rings which were postulated to be aromatic by NICS studies and which feature the dicationic charge delocalized over the Si_4 core. In addition, a dianionic boryl-substituted In_4 ring-isoelectronic to heavier group 14

cyclobutyldiene dications has also been reported, and postulated to have some aromatic character.[15] (Figure 5.1)

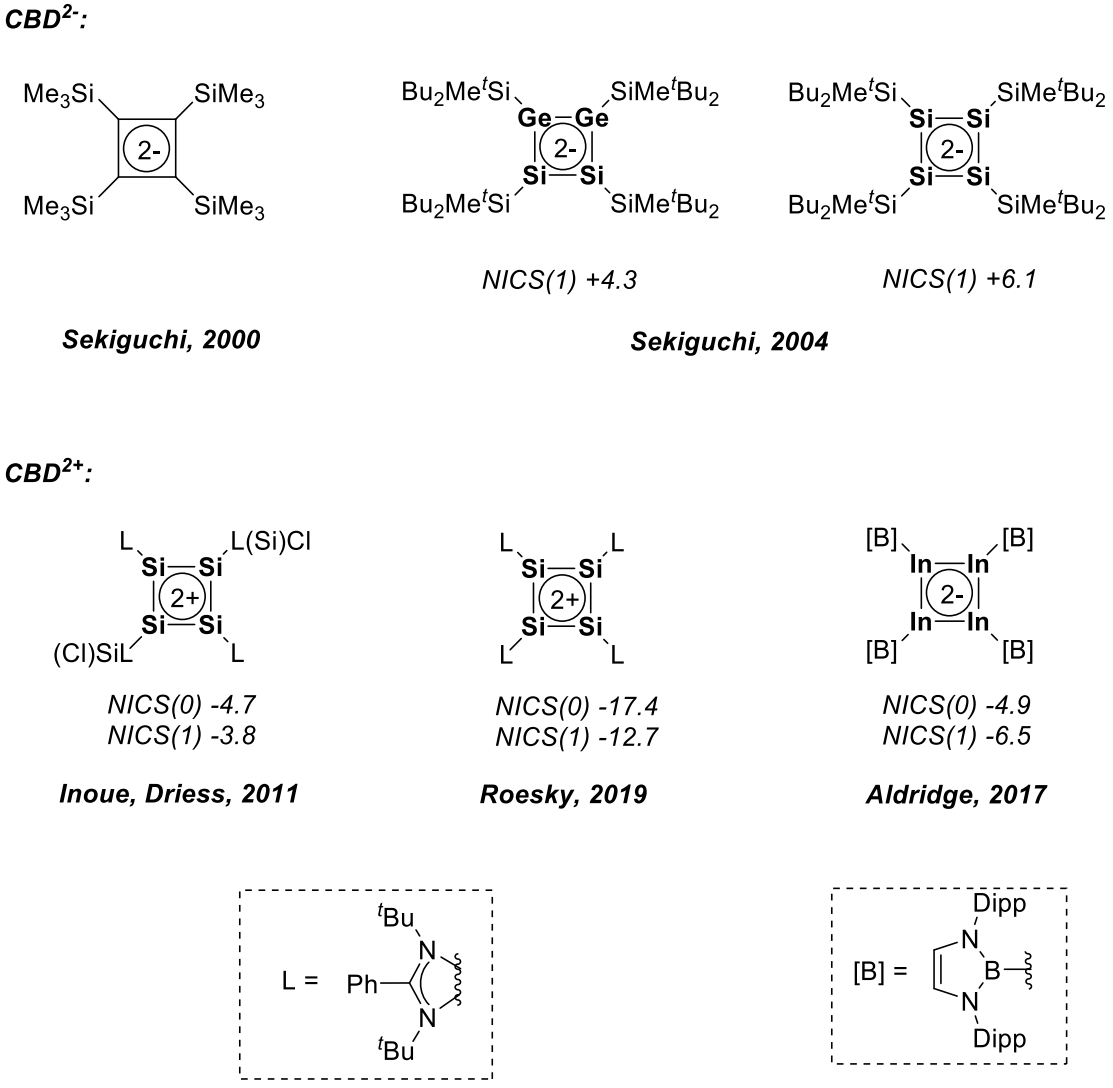
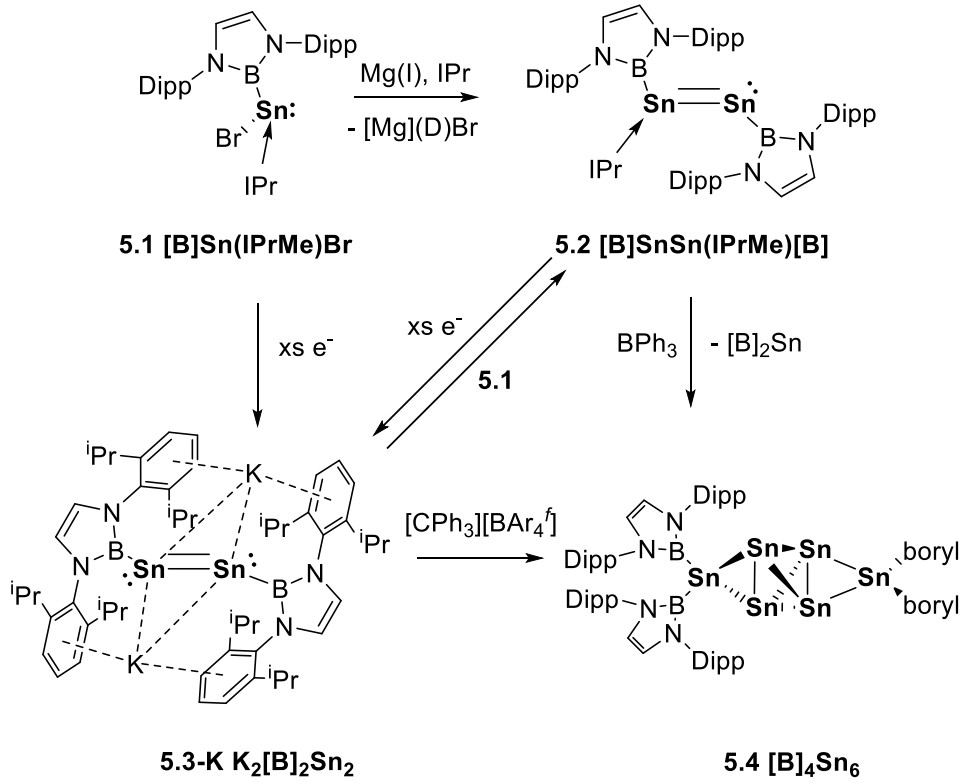


Figure 5.1 *Examples of stable dianions and dications of cyclobutadiene and their heavier analogues.*

5.2 Results and discussion

The N-heterocyclic carbene stabilized (boryl)tin^{II} bromide, [B]Sn(IPrMe)Br **5.1**, ([B] = $(HCNDipp)_2B$, IPrMe = $(NCHMe_2CMe)_2C$) is readily synthesized from (IPrMe)$SnBr_2$ and [B]Li$(thf)_2$ in 61.6 % yield after recrystallization from pentane. The reaction of **5.1** with Jones' reagent [{$HC(MeCMesN)_2$}$Mg]_2$ yields the unsymmetrical mono NHC-stabilized distannyne [B]SnSn(IPrMe)[B] **5.2**, whereas reduction under more forcing conditions with excess KC_8 or potassium naphthalenide generates the more reduced (formally Sn^0) compound $K_2[B]_2Sn_2$ **5.3-K**. **5.2** can also be reduced by KC_8 to generate **5.3-K.** (Scheme 5.1) Both **5.2** and **5.3-K** have been studied crystallographically: the Sn-Sn distances measured by X-ray diffraction were determined to be 2.6508(4) and 2.7489(5) Å, respectively. The longer Sn-Sn distance for **5.3-K** is due to the negative charge on the tin atoms which brings about electronic repulsion between the two metal centres. Both Sn-Sn distances are consistent with formal Sn=Sn double bonds. These distances are compared to ^{Dipp}TerSnSn^{Dipp}Ter (2.6675(4) Å), $K_2(^{Dipp}Ter)_2Sn_2$ (2.7754(3) Å),[16] and $K_2(^{Trip}Ter)_2Sn_2$ (2.7763(9) Å)[17], and are shorter than typical single bonds between tin centres 2.78 Å.[18] **5.3-K** also adopts a *trans* configuration (∠Sn-Sn-B = 96.47(7) °), and the potassium counter-cation is associated with the anion by coordination of the π arene units of the flanking Dipp groups. The reduction of **5.1** to generate **5.2** and **5.3-K** is similar to the related germanium system published earlier by our group.[19]



Scheme 5.1 *Synthesis of boryl substituted tin compounds* ***5.1-5.4****.*

Attempted removal of the remaining carbene donor from **5.2** by employing a Lewis acid (BPh_3) led to the formation of the known bis-boryl stannylene and a new compound, **5.4**, which was characterized by NMR spectroscopy and X-ray crystallography, and shown to feature a neutral bridged tricyclic structure which can be regarded as two bis-boryl stannylene fragments linked to a Sn_4 unit. The Sn-Sn bond lengths (2.8344(7) - 2.8469(7) Å) for **5.4** are noticeably elongated compared to those in **5.2** and **5.3**.

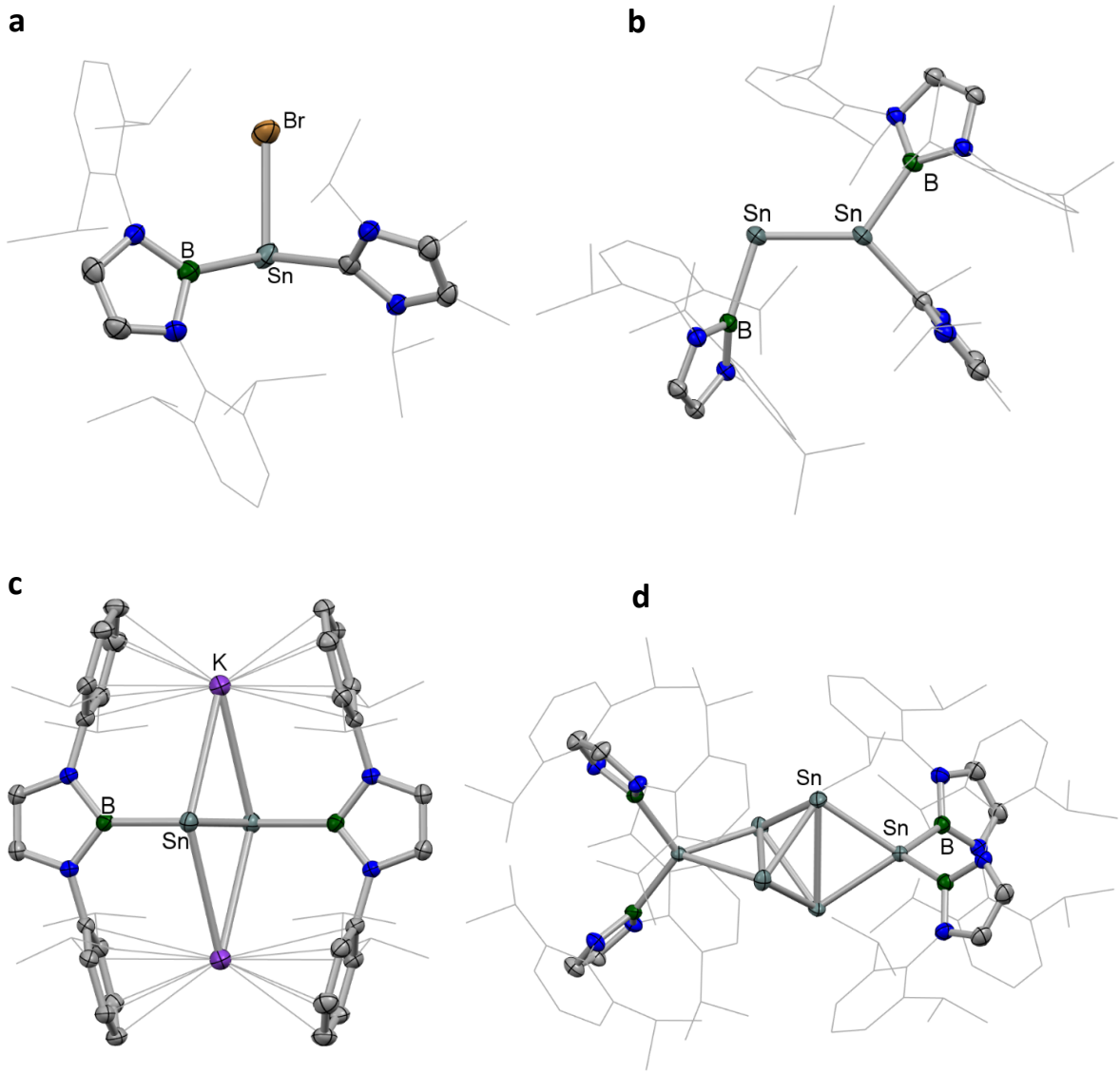


Figure 5.2 *Molecular structures as determined by X-ray crystallography, (a): **5.1**; (b): **5.2**; (c): **5.3**; (d): **5.4**. Thermal ellipsoid plots are at 40% probability level; Hydrogen atoms are omitted and isopropyl groups are drawn in a wireframe format for clarity.*

The conversion of **5.2** to **5.4** has been investigated by quantum chemical and experimental methods (lanl2dz B3LYP D4, Figure 5.3). On this basis, a mechanism is proposed involving initial formation of a diboryldistannyne by removal of the carbene donor from **5.2**, followed by the 1,2-migration of a boryl group from one tin centre to the other to form the distannylvinylidene **Int 1** (ΔG = -5.4 kcal/mol, $\Delta G^{\ddagger}$ = 6.7 kcal/mol). This step is similar to the pathway proposed for the formation of the corresponding digermavinylidene (activation barrier

from diboryldigermyne to digermavinylidene, $\Delta G^{\ddagger}$ = 9.5 kcal/mol),[19] but the tin system **Int 1** cannot be isolated. We propose a subsequent (facile) Sn atom migration between two stannylvinylidene units occurs to produce a second intermediate **Int 2**, which features a transient Sn_3 unit (along with bis-boryl stannylene). This process is endergonic but occurs with a moderate barrier (ΔG = 7.5 kcal/mol, $\Delta G^{\ddagger}$ = 18.3 kcal/mol) and is likely rate limiting. However, subsequent dimerization of **Int 2** to **5.4** is a significantly exergonic process and is the overall driving force of this process (ΔG = -75.5 kcal/mol). Experimentally, **5.4** can also be obtained by two-electron oxidation of the Sn^0 compound K_2[(HCNDipp)$_2$BSnSn(HCNDipp)-$_2$B], a reaction also implies the intermediate formation of distannylvinylidene **Int 1** (Figure 5.3).

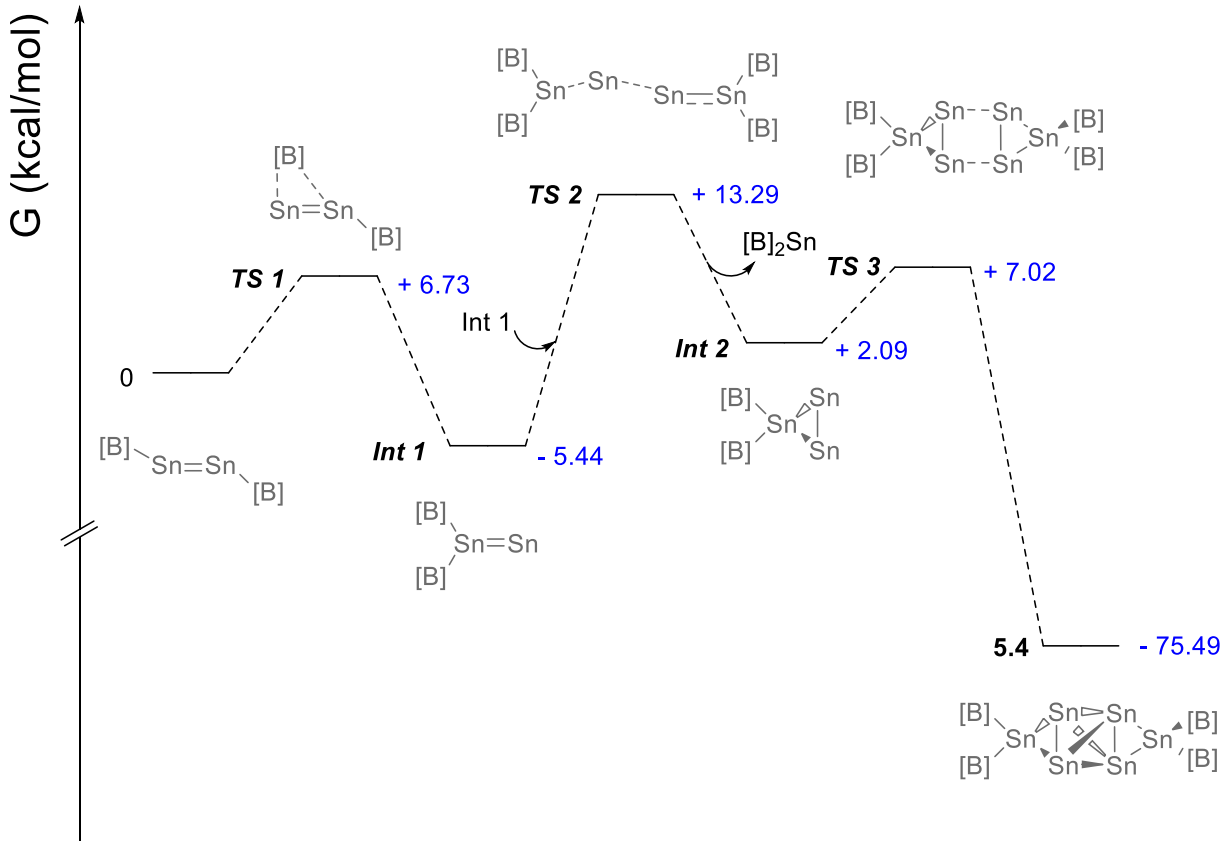


Figure 5.3 *Proposed mechanism for the formation of compound* ***5.4*** *via a distannavinylidene intermediate.*

More interestingly, when monitoring the reduction process of **5.1** with KC_8 or potassium naphthalenide, another species (Figure 5.4, indicated by red star) was observed to be present between the formation of **5.2** (Sn^I) and **5.3** (Sn^0). Moreover, reduction of **5.1** with 1.5 equivalents of KC_8/potassium naphthalenide led to the formation of a dianionic Sn_4 ring **5.5** (Scheme 5.2). The UV-Vis spectrum of **5.5** exhibits a strong absorption peak at 432 nm (ε = 10114 L mol^{-1} cm^{-1}. (Figure 5.6, left) The solid-state structure of $K_2[B]_4Sn_4$ **5.5** features an approximately square array of four (symmetry-related) tin atoms, with each metal centre being additionally bound to a single terminal boryl ligand. The Sn_4 unit is near-planar, with each tin atom lying 0.24 Å out of the least-squares plane, and the internal Sn-Sn-Sn angles being essentially 90° [88.41(3) ° in each case]. The structure is completed by two K^+ counter-ions situated above and below the Sn_4 unit (K···Sn distances: 3.92 and 3.51 Å), which are sandwiched between the flanking Dipp aryl rings of diagonally opposite boryl ligands. A consequence of these K–arene contacts (3.09–3.35 Å) is a slight "puckering" of the ligand envelope of the $[Sn_4[(HCNDipp)_2B]_4]^{2-}$ unit, such that the Sn_4 centroid-Sn-B angles are non-linear (126.7 °), and alternate boron atoms are positioned above/below the approximate Sn_4 plane. (Figure 5.5, left)

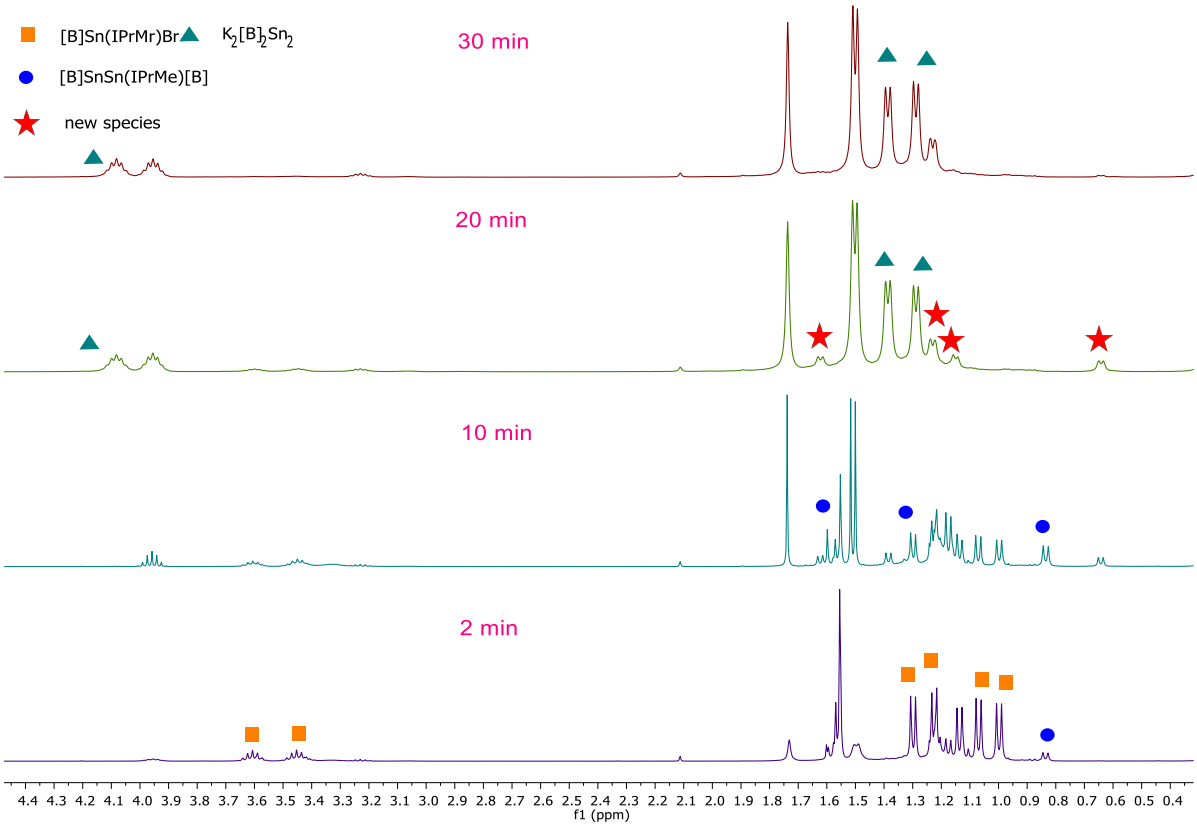
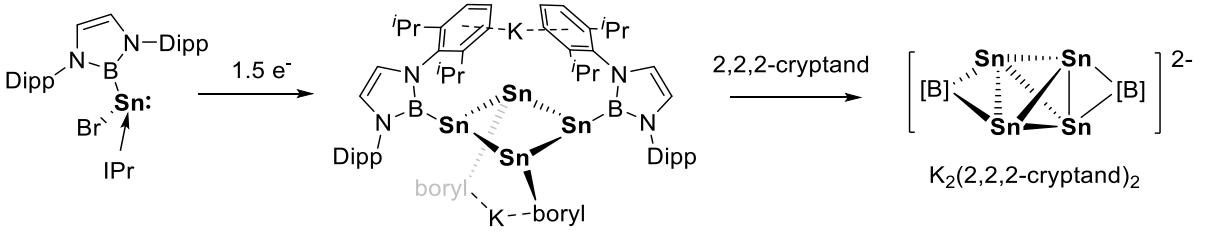


Figure 5.4 *NMR monitoring the reduction process of* ***5.1*** *by* KC_8.



5.1 **5.5 $K_2[B]_4Sn_4$** **5.6 K_2(2,2,2-cryptand)$_2[B]_2Sn_4$**

Scheme 5.2 *Reduction of* ***5.1*** *with 1.5 equivalents of electrons to form* ***5.5****; generation of* ***5.6*** *by the addition of cryptand.*

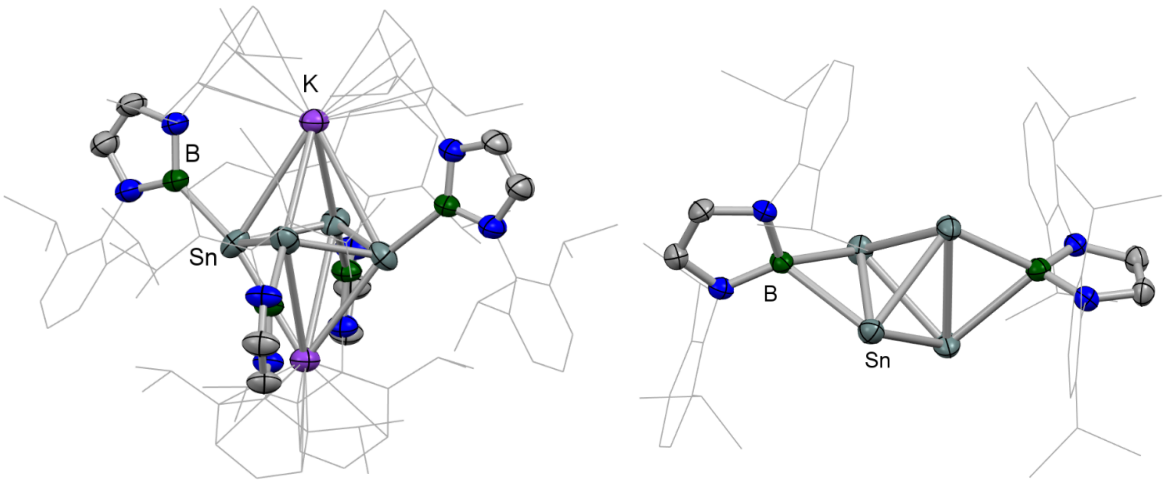


Figure 5.5 *Molecular structures of* ***5.5*** *(left) and* ***5.6*** *(right, cations omitted) as determined by X-ray crystallography. Thermal ellipsoid plots are at 40% probability level; Hydrogen atoms are omitted and isopropyl groups are drawn in a wireframe format for clarity.*

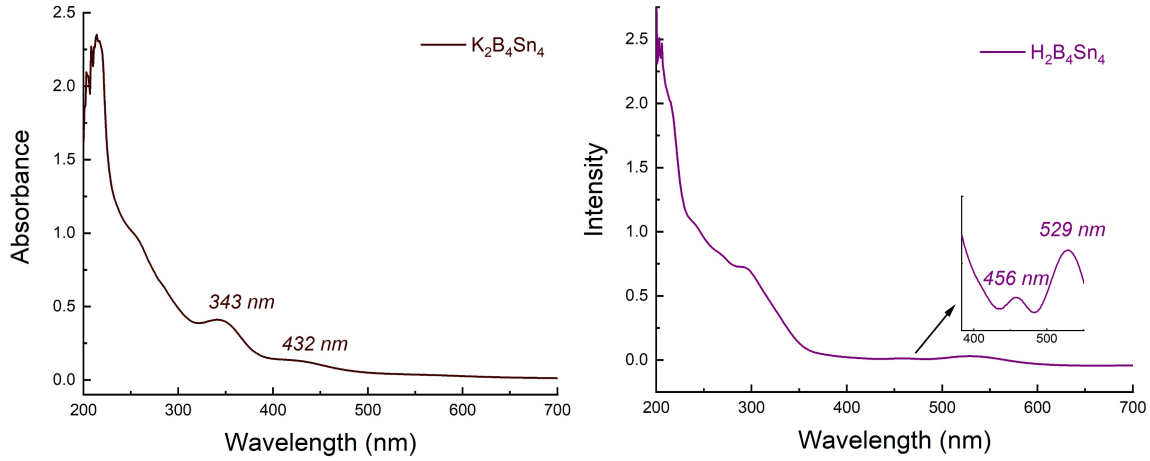


Figure 5.6 *UV-Vis spectra of $K_2[B]_4Sn_4$* ***5.5*** *(left, λ_{max} = 432 nm, ε = 10114 L mol^{-1} cm^{-1}) and $H_2[B]_4Sn_4$* ***5.7*** *(right, λ_{max} = 529 nm, ε = 2242 L mol^{-1} cm^{-1}) in methylcyclohexane.*

As a heavier $[CBD]^{2-}$ analogue, the electronic properties of compound **5.5** were also examined by DFT calculations (r2-scan def2-Tzvp) which revealed that the HOMO and HOMO-1 of the $K_2[B]_4Sn_4$ system are a pair of near-degenerate twisted π orbitals, with the HOMO-2 possessing

Sn−Sn σ-bonding character, and HOMO-5 being mainly comprised of delocalized π orbital (Figure 5.7). Nucleus independent chemical shift (NICS) values have been calculated for $K_2[B]_4Sn_4$ (NICS(0) = −0.28, NICS(1) = −3.17) and can be compared with the values calculated using the same method for benzene (NICS(0) = −7.81, NICS(1) = −9.81), implying non-aromatic character for $K_2[B]_4Sn_4$. In addition, the NICS values for $K_2[B]_4In_4$ were calculated using the same method to be NICS(0) = −7.52, NICS(1) = −8.61, indicating a degree of π aromatic character. (Table 5.1)

Table 5.1 *Nucleus independent chemical shift (NICS) values for selected compounds.*

Compound	NICS(0)	NICS(1)
C_6H_6	-7.81	-9.81
$K_2[B]_4Sn_4$ **5.5**	-0.28	-3.17
$K_2[B]_4In_4$	-7.52	-8.61
$[B]_4Sn_4^{2+}$	-9.46	-11.76

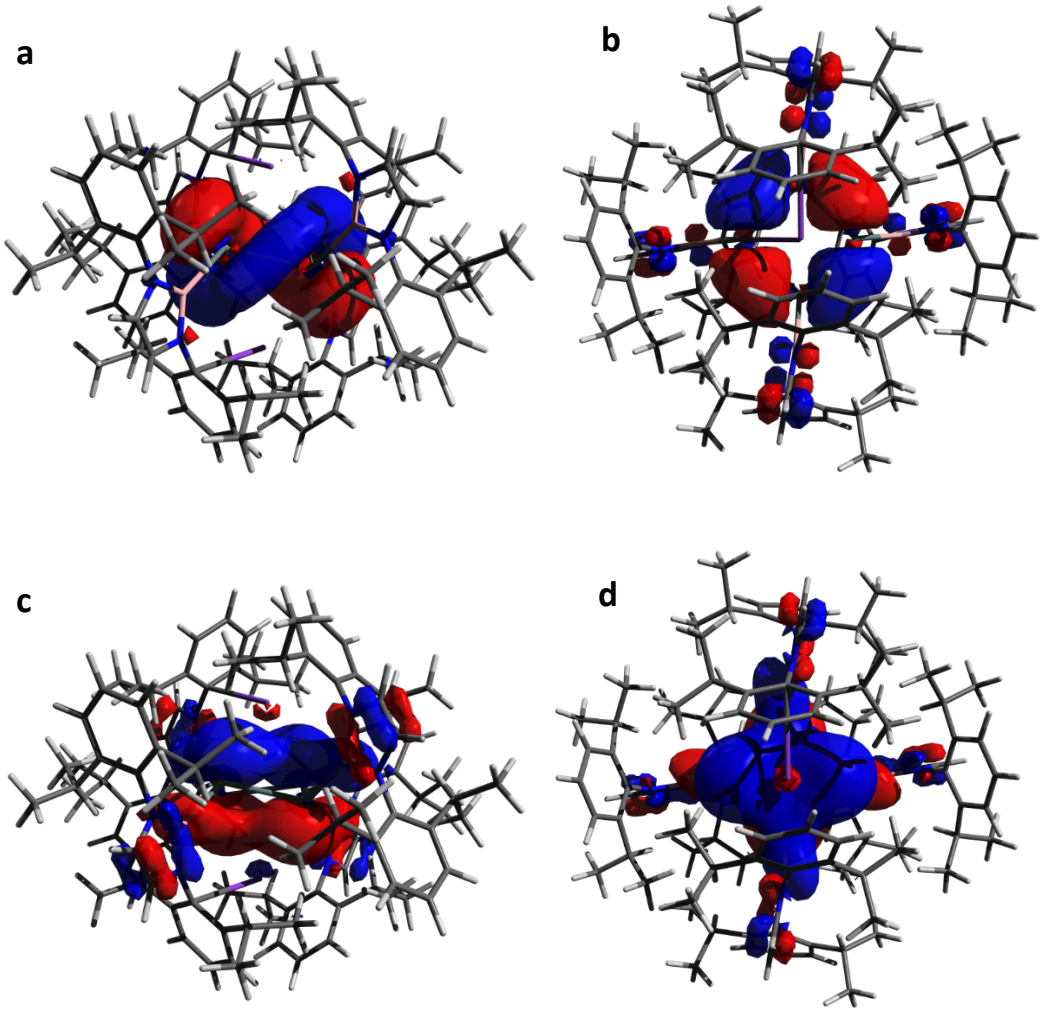
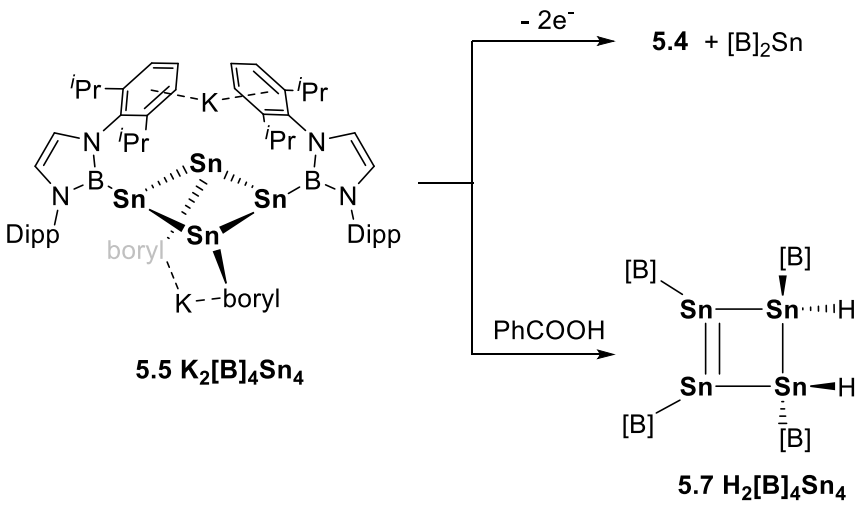


Figure 5.7 *Electron density surfaces and energies of key molecular orbitals for* $K_2[B]_4Sn_4$ ***5.5*** *calculated by Density Functional Theory, a: HOMO, b: HOMO-2 (view from above), c: HOMO-5 (front view), d: HOMO-5 (view from above).*

With **5.5** in hand, we then added 2,2,2-cryptand in an attempt to assess the role of the K^+ ions in maintaining the structural integrity of the Sn_4 unit. Potentially the sequestering of K^+ might break the Sn_4 ring into a pair of [K(2,2,2-cryptand)][$[B]_2Sn_2$] radical anions analogous to Power's [ML_x][(^{Dipp}TerSn)$_2$] (M = Na, K, L = THF, crown ether).[16] However, the reaction gave instead the $[[B]_2Sn_4]^{2-}$ dianion **5.6**. The pyramidal Sn_4 cluster is stabilized by two boryl ligands with each of them bridging across a Sn-Sn bond. This structure can also be interpreted by Wade's Rules: valence electrons = 12, SEP (skeletal electron pairs) = 6, vertices = 4, which

implies a *nido* structure (tetrahedron). The formation for **5.6** demonstrates the importance of potassium cation in stabilizing the Sn_4 fragment in **5.5**.

Oxidation of **5.5** with AgOTf, $[CPh_3][BAr^f_4]$ and $[Cp_2][FeBAr^f_4]$ led only to the cleavage of the Sn_4 unit, which gave **5.4** and bis-borylstannylene as final products. However, by employing benzoic acid, a dihydride derivative of the Sn_4 dianion, $H_2[B]_4Sn_4$ (**5.7**), could be obtained. (Scheme 5.3) The UV-Vis spectrum of **5.7** exhibits a strong absorption peak at 529 nm (ε = 2242 L mol^{-1} cm^{-1}), which accounts for the deep red purple colour of the complex in solution. (Figure 5.6, right) Compound **5.7** was characterized by NMR spectroscopy and X-ray crystallography. The tin-bound hydrides appear at 4.25 ppm with two sets of satellites indicating the coupling between the ^1H and $^{117}Sn/^{119}Sn$ nuclei (J_{HSn119} = 53.9 Hz, J_{HSn117} = 45.6 Hz). **5.7** also shows an unsymmetrical geometry with four doublets for the boryl backbones in the range of 6.03 – 6.24 ppm. The solid state structure (Figure 5.8) shows a shorter Sn(1)-Sn(2) bond (2.6737(7) Å) compared to that of Sn(1)-Sn(4) (2.8333(5) Å), Sn(2)-Sn(3) (2.8232(5) Å) and Sn(3)-Sn(4) (2.8333(5) Å), consistent with a formal Sn=Sn double bond and single bonds, respectively. (Figure 5.8). The B(1)Sn(1)Sn(2)B(2) unit is near coplanar, while the B(3)Sn(3)B(4)Sn(4) adopts a *trans*-bent geometry, with a torsion angle of 125.0 °. The skeletal geometry is completed by two hydrogen atom connected to Sn(3) and Sn(4), respectively. Further experiments are being conducted to try to abstract both hydrides to make a $[[B]_4Sn_4]^{2+}$ dication i.e. a heavier analogue of $[CBD]^{2+}$. Preliminary calculations shown that the NICS values for $[[B]_4Sn_4]^{2+}$ dication are NICS(0) = −9.46, NICS(1) = −11.76, which suggest formal aromaticity for this system (Table 5.1).



Scheme 5.3 *Synthesis of $[B]_4Sn_4H_2$ dihydride **5.7**.*

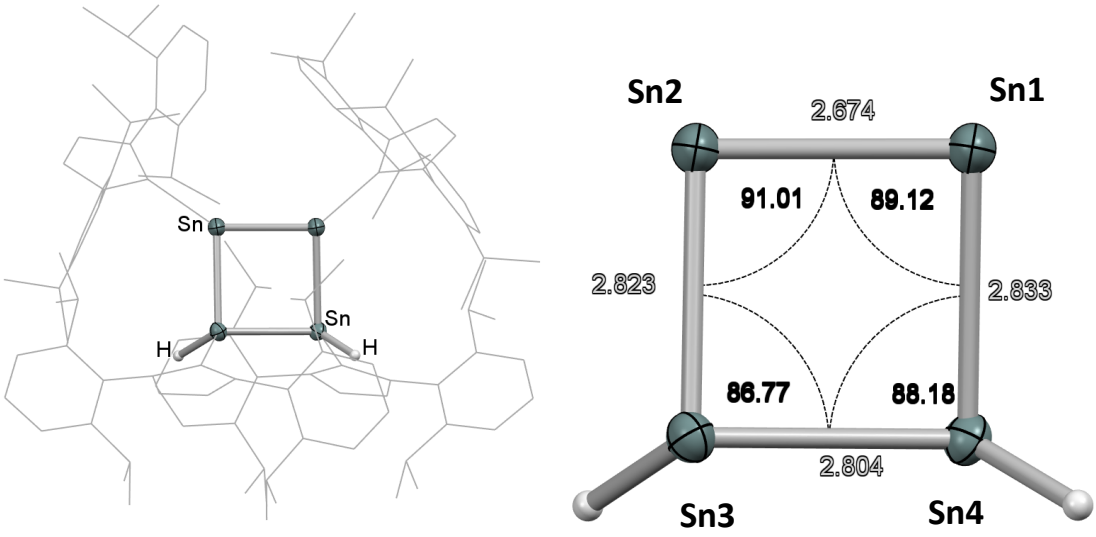


Figure 5.8 *Molecular structure of **5.7** as determined by X-ray crystallography. Left, view perpendicular to the Sn(3)-Sn(4) bond, Right, structure and bonding metrics (distances, Å; angles, °) of the Sn_4 core of **5.7**. Thermal ellipsoid plots are at 40% probability level; most hydrogen atoms are omitted, and boryl groups are drawn in a wireframe format for clarity.*

5.3 Conclusions

The boryl substituted tin halide [B]Sn(IPrMe)Br (**5.1**) has been used as a precursor to synthesize low oxidation state tin compounds. Accordingly, we found the formation of

formally Sn^{I} [B]SnSn(IPrMe)[B] (**5.2**) and Sn^{0} ($K_2[B]_2Sn_2$, **5.3**) compounds and their transformation into $[B]_4Sn_6$ (**5.4**), via a bisborylstannavinylidene intermediate. Moreover, we also isolated a tin cyclobutadiene dianion analogue, $K_2[B]_4Sn_4$, (**5.5**) which can react with benzoic acid to give a neutral Sn_4 ring $H_2[B]_4Sn_4$ (**5.7**). Aromaticity studies show that **5.5** is not aromatic and the potential dication $[[B]_4Sn_4]^{2+}$ could be aromatic.

5.4 Synthesis and characterization of novel compounds

[B]Sn(IPrMe)Br 5.1

To a suspension of (IPrMe)$SnBr_2$ (0.70 g, 1.5 mmol) in Et_2O (20 mL) at -35 ^oC was slowly added a pre-cooled (-35 ^oC) solution of [B]Li·2THF (0.82 g, 1.5 mmol) in Et_2O (10 mL). After stirring at this temperature for 30 min, the reaction mixture was slowly warmed to room temperature and stirred for another 1 h. The solvent was then removed under vacuum and the residue was extracted with toluene. The filtrate was concentrated and triturated with pentane. After storing in the freezer overnight, the pale yellow crystalline solid was isolated and dried under vacuum. Yield: 0.72 g, 62 %.

Anal. Calc. for $C_{37}H_{56}BBrN_4Sn$: C 57.99 %, H 7.37 %, N 7.31 %; Meas.: C 57.68 %, H 7.48 %, N 7.00 %.

^{1}H NMR (400 MHz, C_6D_6, 298K): δ_H 1.00 (d, J_{HH} = 7.0 Hz, 6H, CH(CH_3)$_2$ of carbene), 1.07 (d, J_{HH} = 7.0 Hz, 6H, CH(CH_3)$_2$ of carbene), 1.10 (d, J_{HH} = 6.9 Hz, 6H, CH(CH_3)$_2$ of Dipp), 1.21 (d, J_{HH} = 6.9 Hz, 6H, CH(CH_3)$_2$ of Dipp), 1.30 (d, J_{HH} = 6.9 Hz, 6H, CH(CH_3)$_2$ of Dipp), 1.56 (s, 6H, CCH_3 of carbene), 1.59 (d, J_{HH} = 6.9 Hz, 6H, CH(CH_3)$_2$ of Dipp), 3.42 (sept, , J_{HH} = 6.9 Hz, 2H, CH(CH_3)$_2$ of Dipp), 3.59 (sept, , J_{HH} = 6.9 Hz, 2H, CH(CH_3)$_2$ of Dipp), 5.40 (sept, J_{HH} = 7.0 Hz, 2H, CH(CH_3)$_2$ of carbene), 6.37 (s, 2H, CH of boryl), 7.12 (t, J_{HH} = 4.6 Hz, 2H, *p*-ArH of Dipp), 7.24 (d, J_{HH} = 4.6 Hz, 4H, *m*-ArH of Dipp).

$^{13}C\{^1H\}$ (151 MHz, C_6D_6, 298K): δ_C 10.0 (C<u>C</u>H$_3$ of carbene), 20.9 and 22.3, (CH(<u>C</u>H$_3$)$_2$ of carbene), 23.5, 24.3, 26.2 and 26.6 (CH(<u>C</u>H$_3$)$_2$ of Dipp), 28.7 and 28.9 (<u>C</u>H(CH$_3$)$_2$ of Dipp), 54.4 (<u>C</u>H(CH$_3$)$_2$ of carbene), 122.7 (<u>C</u>H of boryl), 123.6 (*p*-Ar of Dipp), 123.7 (*m*-Ar of Dipp), 126.4 (<u>C</u>CH$_3$ of carbene), 127.5 (*m*-Ar of Dipp), 141.4 (*o*-Ar of Dipp), 146.3 and 146.6 (*i*-Ar of Dipp), 171.0 (R$_2$<u>C</u>: of carbene).

$^{11}B\{^1H\}$ NMR (128 MHz, C_6D_6, 25 °C): δ_B 38.8.

[B]SnSn(IPrMe)[B] 5.2

A mixture of [B]Sn(D)Br (0.20 g, 0.26 mmol), IPrMe (0.047 g, 0.26 mmol) and [{HC(MeCMesN)$_2$}Mg]$_2$ (0.093 g, 0.13 mmol) was dissolved in toluene (5 mL) at room temperature. The colour of the reaction mixture started to change to dark brown. After stirring for 30 min, the reaction mixture was evaporated to dryness and was extracted with pre-cooled (-30 °C) pentane. After concentration, the filtrate was stored at -30 ℃ for ca. 2 d. The obtained black crystalline compound was isolated, washed with a small amount of cold pentane and dried in vacuo. Yield: 0.120 g, 77 %. Crystals for X-ray crystallography structure determination were obtained from a saturated solution in hexane at 4 °C.

Anal. Calc. for $C_{63}H_{94}B_2N_6Sn_2$ + 0.5 C_5H_{12} (([B]SnSn(D)[B]·0.5pentane): C 63.93 %, H 8.19 %, N 6.83 %; Meas.: C 64.50 %, H 7.76 %, N 6.48 %.

^1H NMR (400 MHz, C_6D_6, 298K): δ_H 0.83 (d, J_{HH} = 7.0 Hz, 12H, CH(C*H$_3$*)$_2$ of carbene), 1.17 (d, J_{HH} = 6.8 Hz, 24H, CH(C*H$_3$*)$_2$ of Dipp), 1.20 (br, overlapping, 24H, CH(C*H$_3$*)$_2$ of Dipp), 1.59 (s, 6H, CC*H$_3$* of carbene), 3.32 (br, 4H, C*H*(CH$_3$)$_2$ of Dipp), 3.44 (br, 4H, C*H*(CH$_3$)$_2$ of Dipp), 5.45 (sept, J_{HH} = 7.3 Hz, 2H, C*H*(CH$_3$)$_2$ of carbene), 6.30 (br, 2H, C*H* of boryl), 6.44 (br, 2H, C*H* of boryl), 7.10 (m, 8H, *m*-Ar*H* of Dipp), 7.19 (m, 4H, *p*-Ar*H* of Dipp).

$^{13}C\{^1H\}$ (151 MHz, C_6D_6, 298K): δ_C 10.1 (C<u>C</u>H$_3$ of carbene), 20.4 and 21.3 (CH(<u>C</u>H$_3$)$_2$ of carbene), 24.3, 25.7 and 26.1 (CH(<u>C</u>H$_3$)$_2$ of Dipp), 28.5 and 28.6 (<u>C</u>H(CH$_3$)$_2$ of Dipp), 54.7 (<u>C</u>H(CH$_3$)$_2$ of carbene), 122.3 (<u>C</u>H of boryl), 123.5 and 123.8 (*m*-Ar of Dipp), 126.8 (<u>C</u>CH$_3$ of carbene), 126.7 and 127.4 (*p*-Ar of Dipp), 141.6 and 142.5 (*o*-Ar of Dipp), 146.2 and 146.4 (*i*-Ar of Dipp), 182.1 (R$_2$<u>C</u>: of carbene).

$^{11}B\{^1H\}$ NMR (128 MHz, C_6D_6, 25 ^oC): δ_B 43.5, 54.2.

(IPrMe)$_2$Li$_2$[B]$_2$Sn$_2$ 5.3-Li

A mixture of [B]Sn(IPrMe)Br (0.20 g, 0.26 mmol) and excess KC_8 (0.21 g, 1.6 mmol) was dissolved/suspended in toluene (5 mL) at room temperature. The reaction mixture was sonicated for 2 h with occasional manual stirring, resulting in a dark red coloured solution. The reaction mixture was then filtered into another Schlenk flask filling with LiI (0.035 g, 0.29 mmol). (The filtrate can also be concentrated and stored at -30 ^oC which gave deep red crystals suitable for crystallography; K$_2$[B]$_2$Sn$_2$ **5.3-K** however is not stable at room temperature.) The reaction mixture was stirred for 20 min and filtered. The filtrate was concentrated and layered with hexane (3 mL). Storing at 4 ℃ overnight gave dark purple crystals, which were isolated, washed with a small amount of cold hexane and dried under vacuum. Yield: 0.035 g (0.05 mmol, 19 %).

^1H NMR (400 MHz, C_6D_6, 298K): δ_H 1.21 (m, 6H, CH(C*H*$_3$)$_2$ of carbene overlapping with pentane), 1.28 (d, J_{HH} = 6.9 Hz, 12H, CH(C*H*$_3$)$_2$ of Dipp), 1.35 (d, J_{HH} = 6.9 Hz, 12H, CH(C*H*$_3$)$_2$ of Dipp), 1.69 (s, 6H, CC*H*$_3$ of carbene), 3.94 (sept, J_{HH} = 6.9 Hz , 6H, C*H*(CH$_3$)$_2$ of Dipp overlapping with C*H*(CH$_3$)$_2$ of carbene), 6.58 (s, 2H, C*H* of boryl), 7.19 (m, 2H, *p*-Ar*H* of Dipp), 7.21 (m, 4H, *m*-Ar*H* of Dipp).

$^{13}C\{^1H\}$ (151 MHz, C_6D_6, 298K): δ_C 9.0 (C<u>C</u>H$_3$ of carbene), 24.6 (CH(<u>C</u>H$_3$)$_2$ of carbene), 24.8 (CH(<u>C</u>H$_3$)$_2$ of Dipp), 25.3 (CH(<u>C</u>H$_3$)$_2$ of Dipp), 28.6 (<u>C</u>H(CH$_3$)$_2$ of Dipp), 50.0 (<u>C</u>H(CH$_3$)$_2$ of carbene), 121.3 (<u>C</u>H of boryl), 122.9 (*m*-Ar of Dipp), 125.4 (*p*-Ar of Dipp), 145.9 (*o*-Ar of Dipp), 148.4 (*i*-Ar of Dipp), other peak for carbene cannot be found.

$^{11}B\{^1H\}$ NMR (128 MHz, C_6D_6, 25 ^oC): δ_B 55.2 (br).

[B]$_4$Sn$_6$ 5.4

A mixture of [B]SnSn(IPrMe)[B] (0.10 g, 0.08 mmol) and BPh_3 (20.3 mg, 0.08 mmol) was dissolved in toluene (5 mL) at room temperature. After stirring for 2 h, the reaction mixture was filtered into a layering Schlenk and concentrated (to ca. 1 mL). 15 mL of pentane was then added on top of the filtrate and the mixture left for crystallization for several days. The solution was then decanted and the deep red crystals which were produced were washed with pentane and dried under vacuum. Yield: 20.0 mg, 21 %.

Anal. Calc. for $C_{52}H_{72}B_2N_4Sn_3$ + 0.4 C_5H_{12} ([B]$_2$Sn$_3$·0.4pentane): C 55.93 %, H 6.68 %, N 4.83 %; Meas.: C 56.56 %, H 6.31 %, N 4.78 %.

^1H NMR (400 MHz, C_6D_6, 298K): δ_H 0.77 (d, J_{HH} = 6.8 Hz, 6H, CH(C*H*$_3$)$_2$ of Dipp), 0.98 (d, J_{HH} = 6.8 Hz, 6H, CH(C*H*$_3$)$_2$ of Dipp), 1.16 (m, 12H, CH(C*H*$_3$)$_2$ of Dipp overlapping), 1.23 (d, J_{HH} = 6.8 Hz, 6H, CH(C*H*$_3$)$_2$ of Dipp), 1.26 (d, J_{HH} = 6.8 Hz, 6H, CH(C*H*$_3$)$_2$ of Dipp), 1.49 (d, J_{HH} = 6.8 Hz, 6H, CH(C*H*$_3$)$_2$ of Dipp), 1.57 (d, J_{HH} = 6.8 Hz, 6H, CH(C*H*$_3$)$_2$ of Dipp), 1.61 (d, J_{HH} = 6.8 Hz, 6H, CH(C*H*$_3$)$_2$ of Dipp), 1.57 (d, J_{HH} = 6.8 Hz, 6H, CH(C*H*$_3$)$_2$ of Dipp), 2.48 (sept, J_{HH} = 6.8 Hz, 2H, C*H*(CH$_3$)$_2$ of Dipp), 2.58 and 2.63 (m, 4H, C*H*(CH$_3$)$_2$ of Dipp overlapping), 3.59 (sept, J_{HH} = 6.8 Hz, 2H, C*H*(CH$_3$)$_2$ of Dipp), 6.05 and 6.21 (d, J_{HH} = 2.2 Hz, 4H, C*H* of boryl), 7.19 (m, 4H, *p*-Ar*H* of Dipp), 7.30 (m, 8H, *m*-Ar*H* of Dipp).

$^{13}C\{^1H\}$ (151 MHz, C_6D_6, 298K): δ_C 21.5, 23.8, 27.0, 27.1, 27.2, 27.6 and 27.7 (CH($\underline{C}H_3$)$_2$ of Dipp), 27.9, 28.0, 28.2, 28.6 and 29.0 ($\underline{C}H(CH_3)_2$ of Dipp), 123.8 ($\underline{C}H$ of boryl), 124.2 and 124.6 (*p*-Ar of Dipp), 124.9 (*m*-Ar of Dipp), 139.9, 141.3, 144.9 and 145.8 (*o*-Ar of Dipp), 147.1 and 148.5 (*i*-Ar of Dipp).

$^{11}B\{^1H\}$ NMR (128 MHz, C_6D_6, 25 °C): δ_B 46.6.

$K_2[B]_4Sn_4$ 5.5

A mixture of [B]Sn(IPrMe)Br (0.20 g, 0.26 mmol) and KC_8 (0.055 g, 0.41 mmol) was dissolved/suspended in toluene (5 mL) at room temperature. The reaction mixture was stirred and monitored by ^1H NMR spectroscopy until most of the starting material turned into the desired product. The mixture was then filtered into a Schlenk tube and concentrated. Pentane (5 mL) was then added and the tube stored at 4 °C overnight to yield black crystals suitable for X-ray crystallography. These were isolated, washed with a small amount of cold pentane and dried in vacuo. Yield: 0.051 g, 36 %.

Anal. Calc. for $C_{52}H_{72}B_2KN_4Sn_2$: C 59.41 %, H 6.90 %, N 5.33 %; Meas.: C 59.58 %, H 7.27 %, N 5.34 %.

^1H NMR (400 MHz, C_6D_6, 298K): δ_H 0.64 (d, J_{HH} = 6.8 Hz, 12H, CH(CH_3)$_2$ of Dipp), 1.15 (d, J_{HH} = 6.8 Hz, 12H, CH(CH_3)$_2$ of Dipp), 1.39 (d, J_{HH} = 6.8 Hz, 12H, CH(CH_3)$_2$ of Dipp), 1.62 (d, J_{HH} = 6.8 Hz, 12H, CH(CH_3)$_2$ of Dipp), 3.45 (sept, J_{HH} = 6.8 Hz, 4H, CH(CH$_3$)$_2$ of Dipp), 3.60 (sept, J_{HH} = 6.8 Hz, 4H, CH(CH$_3$)$_2$ of Dipp), 6.04 and 6.36 (d, J_{HH} = 2.2 Hz, 4H, CH of boryl), 6.77 (m, 6H, ArH of Dipp···K), 7.27 (m, 6H, ArH of Dipp).

^{13}C NMR (126 MHz, C_6D_6) δ_C 24.8, 25.3, 25.8 and 26.2 (CH($\underline{C}H_3$)$_2$ of Dipp), 28.6 and 28.8 ($\underline{C}H(CH_3)_2$ of Dipp), 122.6 ($\underline{C}H$ of boryl), 123.5 and 123.6 (*m*-Ar of Dipp), 123.7 and 123.8 (*p*-Ar of Dipp), 144.1 and 144.2 (*o*-Ar of Dipp), 147.0 and 148.7 (*i*-Ar of Dipp).

$^{11}B\{^{1}H\}$ NMR (128 MHz, C_6D_6, 25 °C): δ_B 49.4.

K_2(2,2,2-cryptand)$_2$[B]$_2$Sn$_4$ 5.6

To a mixture of $K_2[B]_4Sn_4$ (5 mg, 0.002 mmol) and 2,2,2-cryptand (1.8 mg, 0.004 mmol) was added C_6D_6 (0.3 mL). The colour of the solution turned pale and dark purple crystals precipitated immediately, which were suitable for X-ray crystallography. The crystals were isolated, washed with pentane and dried under vacuum. Yield: 2.5 mg, 50 %. **5.6** is not soluble in compatible solvents, so NMR spectra could not be obtained.

H_2[B]$_4$Sn$_4$ 5.7

To a mixture of $K_2[B]_4Sn_4$ (20 mg, 0.09 mmol) and PhCOOH (2.3 mg, 0.09 mmol) was added benzene (5 mL). The solution was stirred for 10 min and then dried under vacuum to remove all volatiles. The residue was extracted into pentane and concentrated to about half of the original volume, and stored at – 30 °C to afford small dark purple crystals which were suitable for X-ray crystallography. Yield: 12 mg, 62 %.

^{1}H NMR (500 MHz, C_6D_6, 298K): δ_H 0.40 (d, J_{HH} = 6.8 Hz, 6H, CH(C*H*$_3$)$_2$ of Dipp), 0.57 (d, J_{HH} = 6.8 Hz, 6H, CH(C*H*$_3$)$_2$ of Dipp), 0.99 (d, J_{HH} = 6.8 Hz, 6H, CH(C*H*$_3$)$_2$ of Dipp), 1.10 (dd, J_{HH} = 6.8, 2.0 Hz, 12H, CH(C*H*$_3$)$_2$ of Dipp), 1.21 (m, 48H, CH(C*H*$_3$)$_2$ of Dipp), 1.31 (d, J_{HH} = 6.8 Hz, 6H, CH(C*H*$_3$)$_2$ of Dipp), 1.38 (dd, J_{HH} = 6.8, 2.0 Hz, 12H, CH(C*H*$_3$)$_2$ of Dipp), 2.53, 2.76, 2.78, 2.93, 3.09, 3.14, 3.31 and 3.48 (sept, J_{HH} = 6.8 Hz, 2H, C*H*(CH$_3$)$_2$ of Dipp), 4.25 (t, J_{HSn119} = 53.9 Hz, J_{HSn117} = 45.6 Hz, 2H, Sn*H*), 6.03, 6.15, 6.16 and 6.24 (d, J_{HH} = 2.0 Hz, 2H, C*H* of boryl), 6.85 (d, J_{HH} = 7.6 Hz, 2H, *p*-Ar*H*), 7.13 (m, 6H, *p*-Ar*H*), 7.29 (m, 16H, *m*-Ar*H*).

^{13}C NMR (126 MHz, C_6D_6) δ 23.8, 23.9, 24.4, 24.5, 25.0, 25.2, 25.4 and 25.6 (CH(<u>C</u>H$_3$)$_2$ of Dipp), 25.9, 26.2, 26.6, 26.7, 26.8, 27.0, 27.3, 27.5, 27.9, 27.9, 28.1, 28.4, 28.5, 28.6, 28.7 and 29.3, (<u>C</u>H(CH$_3$)$_2$ of Dipp), 119.8, 122.8, 123.1 and 123.4 (<u>C</u>H of boryl), 123.6, 123.7, 123.8,

123.9, (*p*-Ar of Dipp), 124.0, 124.1, 124.2 and 125.1 , (*m*-Ar of Dipp), 139.8, 140.0, 140.2, 141.4, (*o*-Ar of Dipp), 145.5, 145.7, 145.9, 146.2, 146.6, 146.8, 147.1 and 147.1 (*i*-Ar of Dipp).

$^{11}B\{^{1}H\}$ NMR (128 MHz, C_6D_6, 25 ^{o}C): δ_B 32.2 ([B]SnH), 44.9 ([B]Sn).

Table 5.2 *Selected crystallographic and refinement data for* ***5.1-5.****7.*

	5.1	**5.2·0.5(C_5H_{12})**	**5.3-K·3(C_7H_8)**
Formula	$C_{37}H_{56}BBrN_4Sn$	$C_{68.5}H_{105}B_2N_6Sn_2$	$C_{73}H_{96}B_2N_4Sn_2$
Fw	766.31	1271.58	1366.73
Crystal System	Monoclinic	Triclinic	Monoclinic
Space Group	P 2_1/n	P -1	I 1 2/a 1
Wavelength/Å	1.54184	1.54184	1.54184
a/Å	18.1470(5)	12.4577(4)	14.96230(10)
b/Å	20.7606(6)	12.5564(4)	18.65890(10)
c/Å	30.9665(9)	23.5965(4)	26.1469(2)
α/°	90	80.881(2)	90
β/°	94.478(3)	85.688(5)	103.5010(10)
γ/°	90	73.611(3)	90
Volume/Å^3	11630.8	3495.40(18)	7097.97(9)
Z	8	2	4
Temperature/K	150(2)	150(2)	150(2)
Reflections collected	31256	14452	7426
$2\vartheta_{max}$	61.13	153.956	152.598
R_{int}	0.0824	0.0440	0.0412
Goodness of fit	1.024	1.040	1.032
$R[F^2>2\sigma]$, F	0.0778	0.0358	0.0276
R_w(all data), F^2	0.2078	0.0901	0.0703

	5.4·(C_5H_{12})	**5.5**	**5.6·4.5(C_6H_6)**
Formula	$C_{109}H_{156}B_4N_8Sn_6$	$C_{104}H_{144}B_4K_2N_8Sn_4$	$C_{115}H_{171}B_2K_2N_8O_{12}Sn_4$
Fw	2333.79	2102.46	2432.17
Crystal System	Orthorhombic	Orthorhombic	Monoclinic
Space Group	A e a 2	F d d d	P 1 21/c 1
Wavelength/Å	1.54184	1.54184	1.54184
a/Å	19.3511(2)	17.5175(10)	25.4902(5)
b/Å	18.8118(2)	29.5905(18)	19.9283(5)
c/Å	30.6225(4)	49.558(2)	24.3629(4)
α/°	90	90	90
β/°	90	90	99.856(2)
γ/°	90	90	90
Volume/Å^3	11147.5(2)	25688(2)	12193.1(4)
Z	4	8	4
Temperature/K	150(2)	150(2)	150(2)
Reflections collected	11663	6574	25164
$2\vartheta_{max}$	152.55	154.132	152.828
R_{int}	0.0849	0.0296	0.0604
Goodness of fit	1.033	1.040	1.013
$R[F^2>2\sigma]$, F	0.0286	0.0521	0.0505
R_w(all data), F^2	0.0716	0.1582	0.1297

	5.7·2(C_5H_{12})
Formula	$C_{114}H_{170}B_4N_8Sn_4$
Fw	2170.57
Crystal System	Triclinic
Space Group	P -1
Wavelength/Å	1.54184
a/Å	13.4132(2)
b/Å	16.8095(3)
c/Å	25.9681(5)
α/°	81.535(2)
β/°	81.8910(10)
γ/°	80.3470(17)
Volume/Å^3	5668.42(17)
Z	2
Temperature/K	150(2)
Reflections collected	23399
$2\vartheta_{max}$	152.486
R_{int}	0.0555
Goodness of fit	1.020
$R[F^2>2\sigma]$, F	0.0380
R_w(all data), F^2	0.0980

5.5 References

1. Sommerfeld, T., A Fresh Look at Aromatic Dianions. *J. Am. Chem. Soc.* **2002,** *124* (6), 1119-1124.
2. Feuerbacher, S.; Cederbaum, L. S., Influence of Delocalization on the Stability of Dianions: Study of a Systematic Series of Dianions with Growing Electronic Localization. *J. Am. Chem. Soc.* **2003,** *125* (31), 9531-9537.
3. Hess, B. A.; Ewig, C. S.; Schaad, L. J., An ab initio study of the cyclobutadiene dianion and dication. *J. Org. Chem.* **1985,** *50* (26), 5869-5871.
4. Van Zandwijk, G.; Janssen, R. A. J.; Buck, H. M., 6.pi. Aromaticity in four-membered rings. *J. Am. Chem. Soc.* **1990,** *112* (11), 4155-4164.
5. Kos, A. J.; Schleyer, P. v. R., Cyclic 4.pi. stabilization. Combined Moebius-Hueckel aromaticity in doubly lithium bridged $R_4C_4Li_2$ systems. *J. Am. Chem. Soc.* **1980,** *102* (27), 7928-7929.
6. Balci, M.; McKee, M. L.; Schleyer, P. v. R., Theoretical Study of Tetramethyl- and Tetra-tert-butyl-Substituted Cyclobutadiene and Tetrahedrane. *J. Phys. Chem. A* **2000,** *104* (6), 1246-1255.
7. McKennis, J. S.; Brener, L.; Schweiger, J. R.; Pettit, R., Evidence for the existence of the dianion of cyclobutadiene. *J. Chem. Soc., Chem. Commun.* **1972,** (7), 365-366.
8. Garratt, P. J.; Zahler, R., The dianion of dimethyl cyclobut-3-ene-1,2-dicarboxylate. Aromaticity vs. Coulombic repulsion. *J. Am. Chem. Soc.* **1978,** *100* (24), 7753-7754.
9. Boche, G.; Etzrodt, H.; Marsch, M.; Thiel, W., The Dianion 1,2-Diphenylbenzocyclobutadienediide. *Angew. Chem., Int. Ed.* **1982,** *21* (2), 132-133.
10. Sekiguchi, A.; Matsuo, T.; Watanabe, H., Synthesis and Characterization of a Cyclobutadiene Dianion Dilithium Salt: Evidence for Aromaticity. *J. Am. Chem. Soc.* **2000,** *122* (23), 5652-5653.
11. Lee, V. Y.; Takanashi, K.; Matsuno, T.; Ichinohe, M.; Sekiguchi, A., Cyclobutadiene Dianions Consisting of Heavier Group 14 Elements: Synthesis and Characterization. *J. Am. Chem. Soc.* **2004,** *126* (15), 4758-4759.
12. Olah, G. A.; Bollinger, J. M.; White, A. M., Stable carbonium ions. LXXXIX. Tetramethylcyclobutenium dication, an aromatic 2 .pi.-electron system. *J. Am. Chem. Soc.* **1969,** *91* (13), 3667-3669.
13. Inoue, S.; Epping, J. D.; Irran, E.; Driess, M., Formation of a Donor-Stabilized Tetrasilacyclobutadiene Dication by a Lewis Acid Assisted Reaction of an N-Heterocyclic Chloro Silylene. *J. Am. Chem. Soc.* **2011,** *133* (22), 8514-8517.
14. Sun, X.; Simler, T.; Yadav, R.; Köppe, R.; Roesky, P. W., A Stable Aromatic Tetrasilacyclobutadiene Dication. *J. Am. Chem. Soc.* **2019,** *141* (38), 14987-14990.
15. Protchenko, A. V.; Urbano, J.; Abdalla, J. A. B.; Campos, J.; Vidovic, D.; Schwarz, A. D.; Blake, M. P.; Mountford, P.; Jones, C.; Aldridge, S., Electronic Delocalization in Two and Three Dimensions: Differential Aggregation in Indium "Metalloid" Clusters. *Angew. Chem., Int. Ed.* **2017,** *56* (47), 15098-15102.
16. Pu, L.; Phillips, A. D.; Richards, A. F.; Stender, M.; Simons, R. S.; Olmstead, M. M.; Power, P. P., Germanium and Tin Analogues of Alkynes and Their Reduction Products. *J. Am. Chem. Soc.* **2003,** *125* (38), 11626-11636.
17. Pu, L.; Senge, M. O.; Olmstead, M. M.; Power, P. P., Synthesis and Characterization of $Na_2\{Ge(C_6H_3\text{-}2,6\text{-}Trip_2)\}_2$ and $K_2\{Sn(C_6H_3\text{-}2,6\text{-}Trip_2)\}_2$ (Trip = $-C_6H_2\text{-}2,4,6\text{-}{}^iPr_3$): A New Class of Multiply Bonded Main Group Compounds. *J. Am. Chem. Soc.* **1998,** *120* (48), 12682-12683.
18. Cordero, B.; Gómez, V.; Platero-Prats, A. E.; Revés, M.; Echeverría, J.; Cremades, E.; Barragán, F.; Alvarez, S., Covalent radii revisited. *Dalton Trans.* **2008,** (21), 2832-2838.
19. Rit, A.; Campos, J.; Niu, H.; Aldridge, S., A stable heavier group 14 analogue of vinylidene. *Nat. Chem.* **2016,** *8* (11), 1022-1026.

Chapter 6 Low oxidation state boryl-germanium compounds

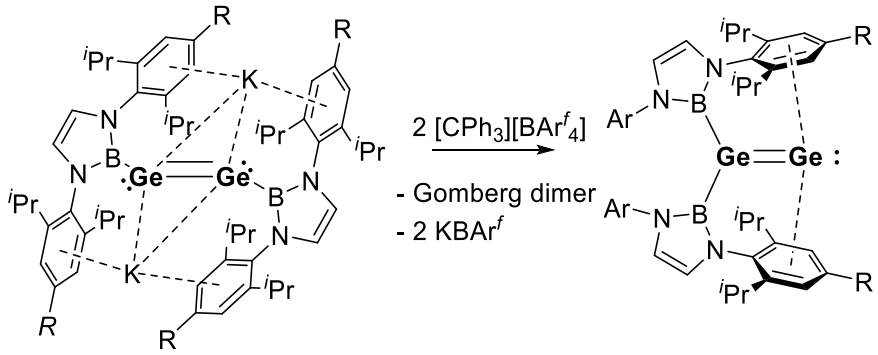
6.1 Introduction

The "double-bond rule" held that heavier *p* block elements could not form stable multiple bonds,[1-3] and was widely accepted until Lappert *et al.* reported the first isolable distannene in 1976,[4] followed rapidly thereafter by West's disilene,[5] Brook's silaethene,[6] and Yoshifuji's diphosphene.[7] The heavier analogues of alkenes, dimetallenes $R_2E{=}ER_2$ (E = Si, Ge, Sn Pb), favour *trans*-bent structures rather than the planar structures found for alkenes. To form a "standard" E-E multiple bond, the significant Pauli repulsion between the occupied orbitals or the excitation energy into the triplet or quartet state needs to be overcome.[8] Therefore a double donor-acceptor interaction is energetically favoured for all but the lighest element, in which the lone pair of electrons from one ER_2 the fragment is donated into the vacant *p* orbital of the other. Calculations based on two monomeric H_2E units (parent dimetallenes) shows that the heavier tetrylenes occupy a singlet ground state (ΔE_{ST} = 16.7 kcal mol^{-1} (Si), 21.8 kcal mol^{-1} (Ge), 24.8 kcal mol^{-1} (Sn), 34.8 kcal mol^{-1} (Pb)), while methylene (H_2C) has a ground state triplet ($\Delta E_{ST} = -14.0$ kcal mol^{-1}),[9] and is capable of forming a planar structure on dimerization, viz C_2H_4. Experimentally, the first ground state triplet silylene was observed via EPR spectroscopy having been generated by the photolysis of a silacyclopropene in a methylcyclohexane glass matrix at 9 K.[10] Similar silyl substituents when applied to germanium led to the formation a highly twisted digermene.[11]

Our target of this part of the project at the outset was to synthesize planar heavier analogues of group 14 metallynes and metallenes by applying strongly electron donating boryl groups, and to explore their reactivity towards small molecules.

6.2 Results and discussions

In order to access heavier analogues of ethyne, we attempted to perturb the geometry of the digermavinylidene $[(HCNDipp)_2B]_2Ge_2$ by employing bulkier substituents on the boryl ligand, in the hope of making the digermyne compound more stable than the vinylidene isomer. It was hypothesized that an additional ^{i}Pr group in the para position of the flanking aryl groups might increase the degree of steric repulsion between the geminal boryl ligands and so promote isomerization to the (1,2) diboryldigermyne isomer. A Trip substituted boryl germanium chloride **6.1** was therefore synthesized by using the corresponding Trip boryl lithium precursor and $(IPrMe)GeCl_2$ (Trip = 2,4,6-$^{i}Pr_3C_6H_2$, IPrMe = $(NCHMe_2CMe)_2$)C. An NMR test reaction aimed at reducing **6.1** with excess KC_8 gave potassium germanide compound **6.2** (not isolated) which was oxidized by one equivalent of $[CPh_3][BAr^{f}_4]$ (per germanium). The tea-coloured solution was then decanted, concentrated, and left for crystallization, leading to the isolation of the ^{Trip}boryl $[(HCNTrip)_2B]$- supported germylvinylidene **6.3** (Scheme 6.1). However, **6.3** has an essentially identical (vinylidene) structure to the Dipp version (**1.71**), in which the four atoms that define the X_2GeGe unit lie within a single plane. The Ge(2)-aryl rings contacts are measured to be 2.901 Å (on average), which are identical to those measured for $[(HCNDipp)_2B]_2Ge_2$ **1.71** (2.904(2) and 2.917(2) Å). The disparate Ge(1)-B(1)-N angles were measured to be 116.1 and 140.3 ^{o} (on average), which indicates the presence of weak stabilizing interactions that involve the flanking arene π systems and the formally vacant in-plane *p* orbital at Ge(2). (Figure 6.1)



1.72 $K_2[B]_2Ge_2$ (R = H)
6.2 $K_2[B]_2Ge_2$ (R = ^{i}Pr, not isolated)

1.71 $[B]_2Ge{=}Ge$ (R = H, Ar = Dipp)
6.3 $[B]_2Ge{=}Ge$ (R = ^{i}Pr, Ar = Trip)

Scheme 6.1 *Synthesis of boryl substituted germanium compounds* ***1.71*** *and* ***6.3****.*

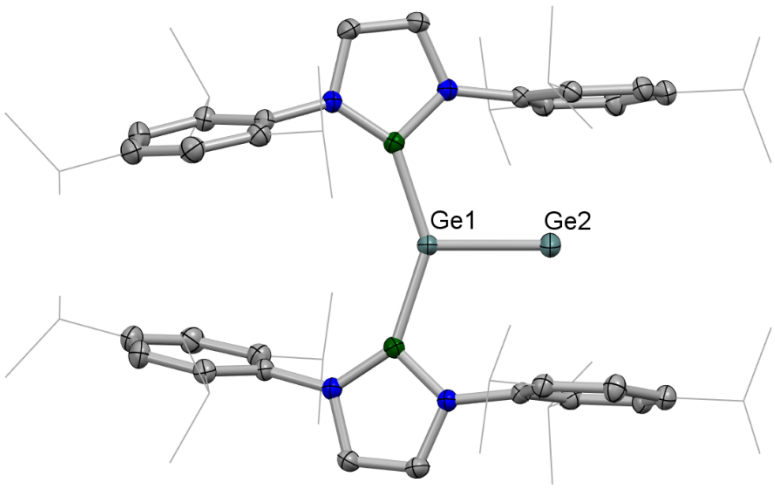
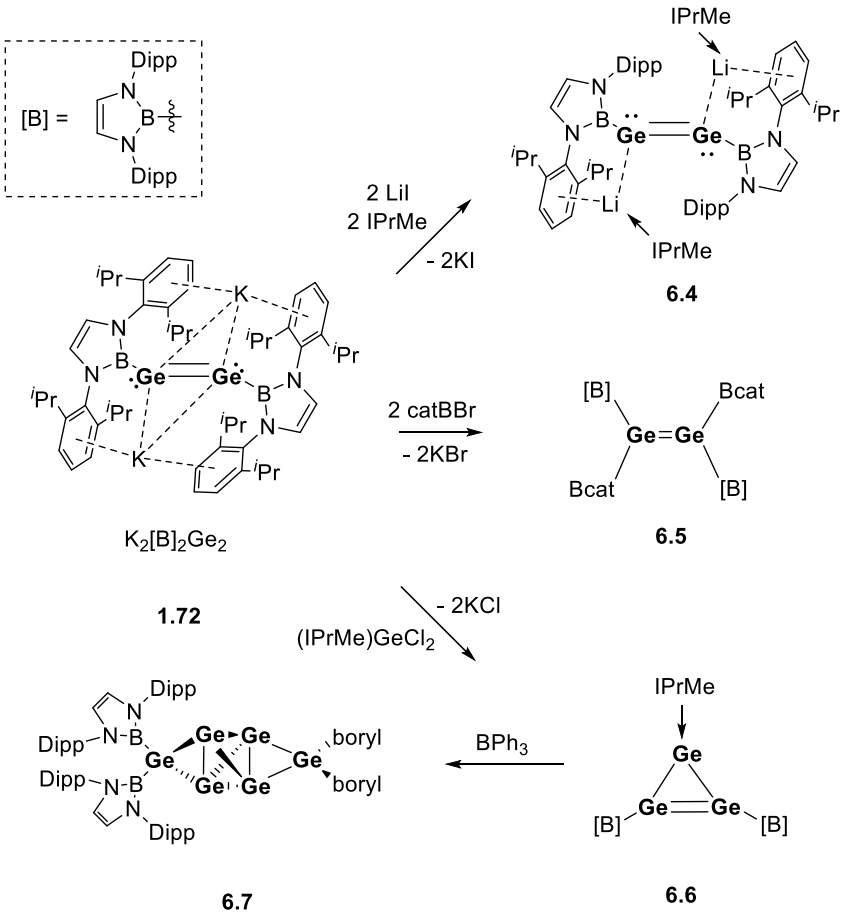


Figure 6.1 *Molecular structure as determined by X-ray crystallography for* ***6.3****. Thermal ellipsoid plots are at the 40% probability level; Hydrogen atoms are omitted, and isopropyl groups are drawn in wireframe format for clarity.*

Given that the use of Trip groups did not yield significantly different results, we returned to studies using the more accessible Dipp-based systems. The related dilithium digermanide $[(IPrMe)Li]_2Ge_2[B]_2$ **6.4** ([B] = $(HCNDipp)_2B$, Scheme 6.2) can be obtained from **1.72** by a salt metathesis reaction with lithium iodide in toluene, in the presence of the carbene IPrMe. **6.4** can be obtained in ca. 30% yield after recrystallization from toluene/hexane. Its solid-state

structure, determined by X-ray crystallography, is based around a Ge_2 unit featuring two boryl groups arranged in 1,2-fashion (and *trans* to one another), with each germanium centre being additionally bound to a single lithium atom. Each lithium centre is also coordinated by a single NHC donor (*d*(Li–C) = 2.133(5) Å) and engages in weaker contacts with two of the carbon atoms of a Dipp group associated with the boryl ligand attached to the other germanium centre (*d*(Li···C) = 2.702(7), 2.743(7) Å). The Ge-Ge bond length of **6.4** 2.3453(5) Å is shorter than that found in **1.72** (2.392(1) Å). However, the carbene-lithium interaction is sufficiently labile that the carbene donor appears to behave as free carbene in solution (^{1}H NMR, 1.29 and 1.70 ppm, see SI). The UV-Vis spectrum of **6.4** in methylcyclohexane shows a longest wavelength absorption maximum at 423 nm (Figure 6.3, left), which is slightly blue-shifted compared with the maximum reported for **1.72** (428 nm).[12]



Scheme 6.2 *Syntheses of low valent germanium compounds* ***6.4*** *to* ***6.7****.*

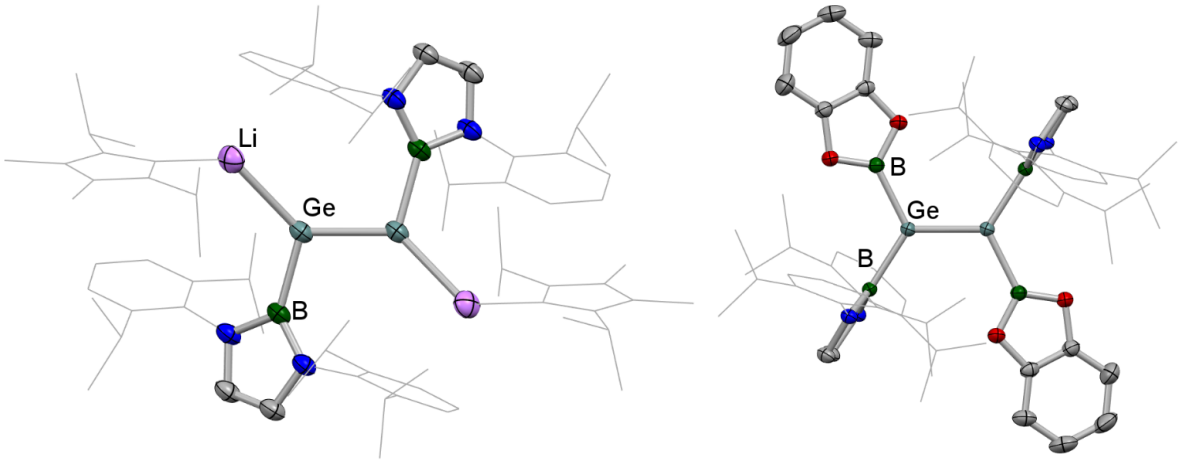


Figure 6.2 *Molecular structures as determined by X-ray crystallography for* ***6.4*** *(left) and* ***6.5*** *(right). Thermal ellipsoid plots are at 40% probability level; Hydrogen atoms are omitted and isopropyl groups are drawn in a wireframe format for clarity; Key bond lengths (Å) and angles (°): (for* ***6.4****) Ge–Ge 2.3453(5), Ge–B 2.091(3), Ge–Li 2.541(7), Li–*C_{NHC} *2.133(5), Li–*C_{aryl} *2.702(7), 2.743(7), B–Ge–Ge–B 166.7(1); (for* ***6.5****) The crystal structure of* ***6.5*** *contains four independent molecules in the asymmetric unit, featuring Ge–Ge distances of 2.234(1), 2.235(1), 2.235(1) and 2.238(1) Å, and B–Ge–Ge–B torsion angles of 180.0(1), 177.3(1), 179.6(1) and 180.0(1)°. The corresponding angles at the germanium centres sum to 358.2 - 360.0°.*

In contrast to the solid-state structure of **1.72** (and related terphenyl-ligated systems) in which the alkali metal cation sits above the centre of the Ge_2 unit and is further encapsulated by π-interactions with the flanking aryl rings, the positioning of the lithium atoms in **6.4** suggests greater directionality in the Ge–Li interactions. The associated Ge–Li distances (2.541(7) Å) are slightly greater than the sum of the respective covalent radii (1.20 + 1.28 Å), and the geometry at each germanium centre defined by the proximal boron, germanium and lithium centres is trigonal planar (Σ(angles at Ge) = 358.83°). In addition, the germanium coordination

planes lie almost parallel, with a torsion angle (166.7(1) °) implying only a small twist between the two.

Viewing **6.4** as a putative digermene featuring boryl and Li(NHC) substituents at each germanium centre, these structural features contrast with other reported examples of R_2GeGeR_2 systems, which typically display *trans*-bent and/or markedly twisted skeletal geometries.[11] Similar heavy atom skeletons are found for digermene of the type $(Si)_2Ge{=}Ge(Si)_2$ (Si $=SiMe_2{}^tBu$, $SiMe{}^iPr_2$, $Si{}^iPr_3$) which are essentially flat.[13-14] This in turn suggests the influence of the strongly electropositive substituents at germanium (boryl, Li(NHC)), and the conceptual formation of **6.4** by the dimerization of two triplet (rather than singlet) germylene fragments via 'conventional' σ and π bond formation. With this in mind, we targeted related system(s) with the Li(NHC) fragments replaced by more covalently bound (but electropositive) substituents, with aim of generating an unambiguous planar digermene.

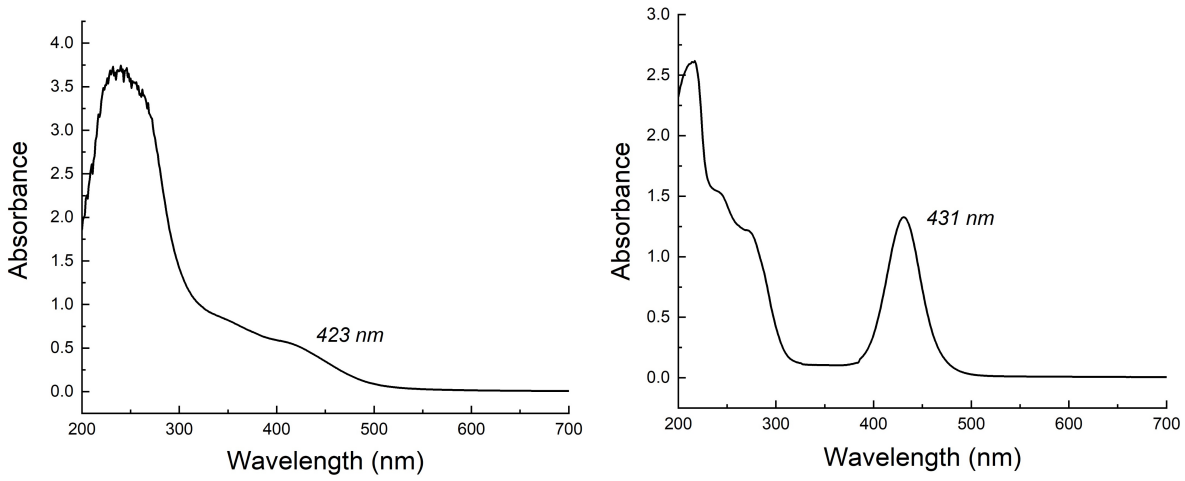
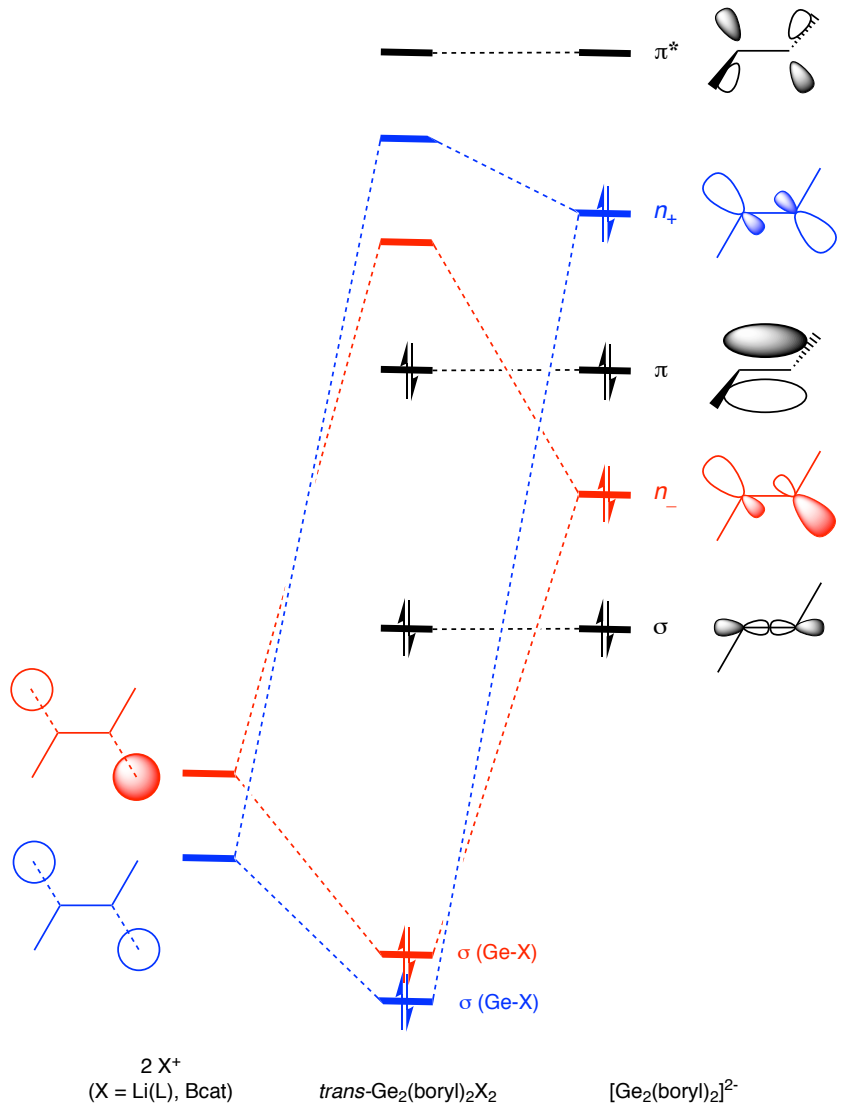


Figure 6.3 *UV-Vis spectra of* ***6.4*** *(left, λ_{max} = 423 nm, ε = 14355 $Lmol^{-1}cm^{-1}$) in methylcyclohexane and* ***6.5*** *(right, λ_{max} = 431 nm, ε = 44659 $Lmol^{-1}cm^{-1}$) in pentane.*

Dipotassium digermanide **1.72** does not react with [B]Br to give a symmetrical tetraboryl digermene under any conditions examined - presumably due to the excessive steric demands of the boryl Dipp substituents. It is of note that the related tin system is a monomeric stannylene,

[B]$_2$Sn, albeit one which has been calculated to possess an unusually small singlet-triplet gap (9.4 kcal mol^{-1}). The use of the much less sterically demanding boron electrophile, catBBr (cat = 1,2-$O_2C_6H_4$), on the other hand, leads to clean conversion in ca. 65 % yield (after recrystallization from pentane) generating the unsymmetrical (*trans*-1,2) tetraboryl digermene, Ge_2[(HCNDipp)$_2$B](Bcat)$_2$ (**6.5**; Scheme 6.2). **6.5** is characterized by two ^{11}B signals at δ_B = 28.9 and 43.6 ppm, and the relative arrangement of the two different sets of boryl ligands has been confirmed by X-ray crystallography (Figure 6.2).

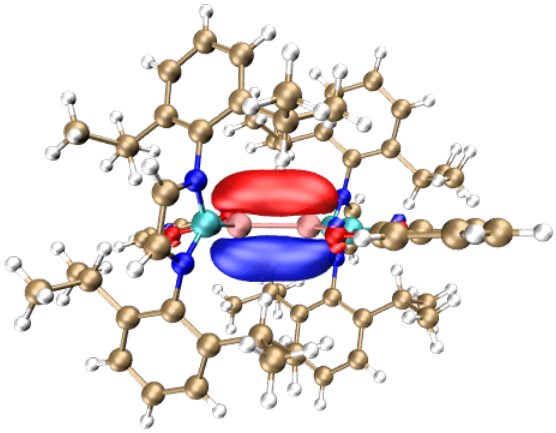
The solid state structure of **6.5** reveals a very short Ge–Ge separation (2.234(1) - 2.238(1) Å for the four molecules in the asymmetric unit), which can be compared to 2.4 Å for the sum of the (single bond) covalent radii,[15] and 2.347(2) and 2.285(1) Å for $Ge_2\{CH(SiMe_3)_2\}_4$ and $Ge_2^{Dipp}Ar_2$ (where ^{Dipp}Ar = 2,6-$C_6H_3Dipp_2$), respectively. Moreover, in contrast to the *trans*-bent structures typically observed for digermenes such as $Ge_2\{CH(SiMe_3)_2\}_4$, **6.5** adopts a planar geometry at each germanium centre (Σ(angles at germanium) = 358.2 - 360.0°) with a B–Ge–Ge–B torsion angle close to 180°. The Ge–Ge distance measured for **6.5** (2.236 Å (mean)) is successively shorter than those determined for dilithium compound **6.4** (2.3453(5) Å) and dipotassium species **1.72** (2.392(1) Å). Notwithstanding the predominantly non-bonding nature of the (a_g, n_+) HOMO in doubly reduced digermyne species such as **1.72**, this sequential shortening presumably reflects a reduction in the partial negative charge at each germanium centre on assimilation of the Li(NHC) and (particularly) the more covalently bound Bcat fragment (Scheme 6.3).



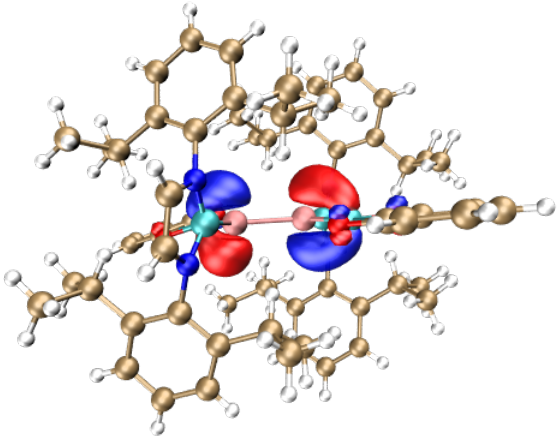
Scheme 6.3 *Molecular Orbital scheme describing the formal combination of Li(NHC)$^+$/Bcat$^+$ fragments with [B]$_2$Ge$_2^{2-}$.*

The UV-Vis spectrum of **6.5** in pentane contains a very strong band at 431 nm that features a significant contribution from the Ge=Ge π-to-π* transition(Figure 6.3), and which suggests retention of the dimeric form in solution. The position of this band is similar to those measured for other species containing Ge=Ge double bonds (e.g. 455 nm for [Ge(IDipp)]$_2$,[16] and 434 nm for (HCNDipp)$_2$BGe=Ge(HCNDipp)$_2$B(IPrMe)).[12] The UV-Vis spectrum of **6.4** in methyl-cyclohexane a similar band with an absorption maximum at 423 nm (cf. 428 nm for **1.72**).[12] For digermene **6.5**, the NTOs for the S1 and S3 transition both involve the Ge-Ge π* orbital. The

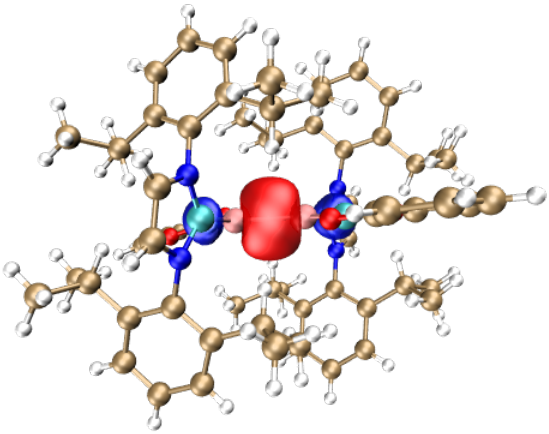
S1 transition (2.932 eV, 423 nm) is calculated to be from the Ge-Ge π to π* orbital (~93 % NTOd_S1 -> NTOa_S1)) with a minor contribution from the Ge-Ge σ to σ* (~4 % NTOd_S1s -> NTOa_S1s). The S3 transition (3.911 eV, 317 nm) also accesses the Ge-Ge π* orbital in this case from the boryl π system (~ 99% NTOd_S3 -> NTOa_S3). (Figure 6.4, M06-2X def2-TZVP D4(dispersion)).



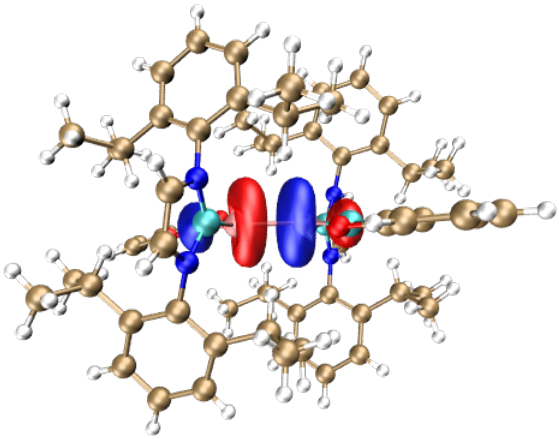
a NTOd_S1



b NTOa_S1



c NTOd_S1s



d NTOa_S1s

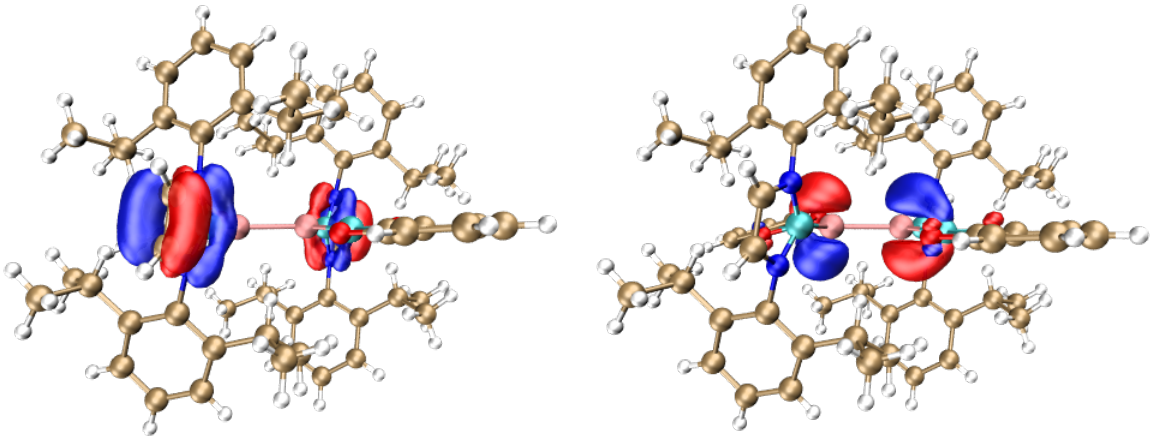
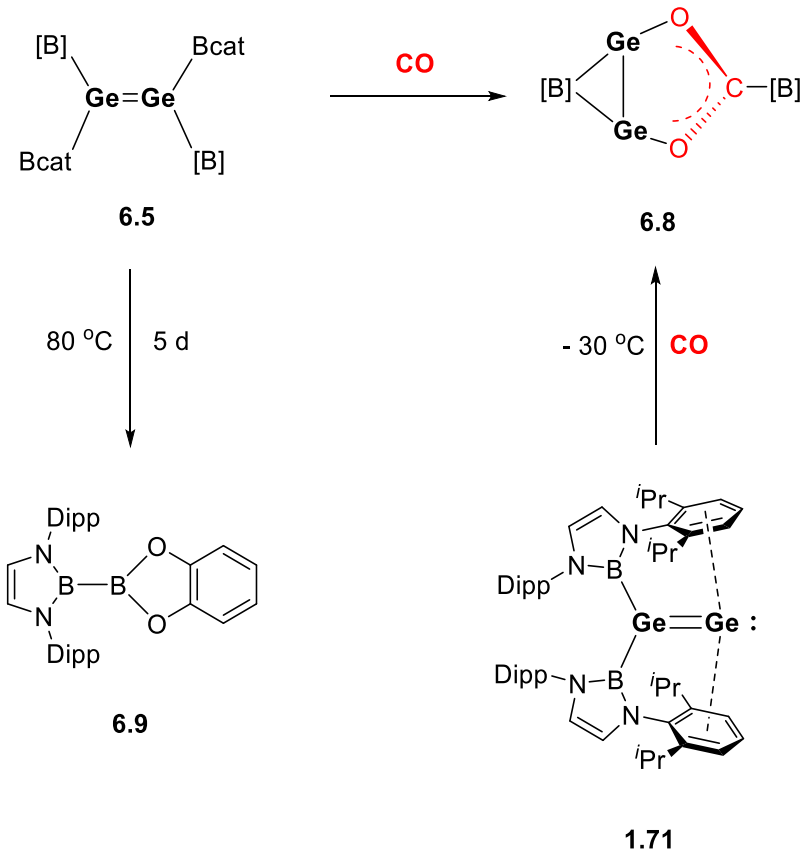


Figure 6.4 *Calculated NTOs of digermene* ***6.5*** *for the S1 and S3 transitions, a (NTOd_S1), b (NTOa_S1), c (NTOd_S1s), d (NTOa_S1s), e (NTOd_S3) and f (NTOa_S3).*

With this planar digermene in hand, we then tried to assess the reactivity of **6.5** with small molecules. Reaction of digermene **6.5** with CO in benzene-d_6 gives a single major product (in ca. 85% yield). ^{1}H and ^{11}B NMR data for the product are consistent with the presence of two different boryl ligand environments (δ_B = 39, 29 ppm); ^{1}H NMR data are also indicative of the loss of the Bcat substituents. Red crystals grown from pentane solution can be analysed by X-ray diffraction and show that the product (**6.8**) features a digermyne unit bridged by boryl and borycarboxylate ligands. The Ge–Ge distance (2.627(1) Å) is consistent with a single bond (*cf.* 2.4 Å for the sum of the respective single bond covalent radii), while the Ge–B contacts (2.313(4) and 2.266(3) Å) are consistent with a bridging mode of interaction. (Figure 6.5)

Although precise details for the formation of compound **6.8** are difficult to establish definitively, some effort has been made to investigate the mechanism of this reaction experimentally. **6.5** was exposed to CO_2 gas because there is a CO_2 unit in **6.8**. However, digermene **6.5** shows no reactivity towards CO_2. We also found that when heated in C_6D_6 for 5 days, digermene **6.5** extrudes the unsymmetrical diborane **6.9** as one product. (Scheme 6.4)

6.9 has an elongated B-B bond (1.688(2) Å, cf. 1.66 Å for a typical B-B single bond),[15] presumably due to the steric factors. This reaction was also monitored by in situ ^{1}H NMR (Figure 6.6) showing the CH of the boryl ligand backbone signal for digermene **6.5** (6.41 ppm) diminishing and the corresponding CH signal for diborane **6.9** (6.31 ppm) growing in.



Scheme 6.4 *Reactivity of* ***6.5*** *towards CO on heating, and* ***1.71*** *towards CO at -30 °C.*

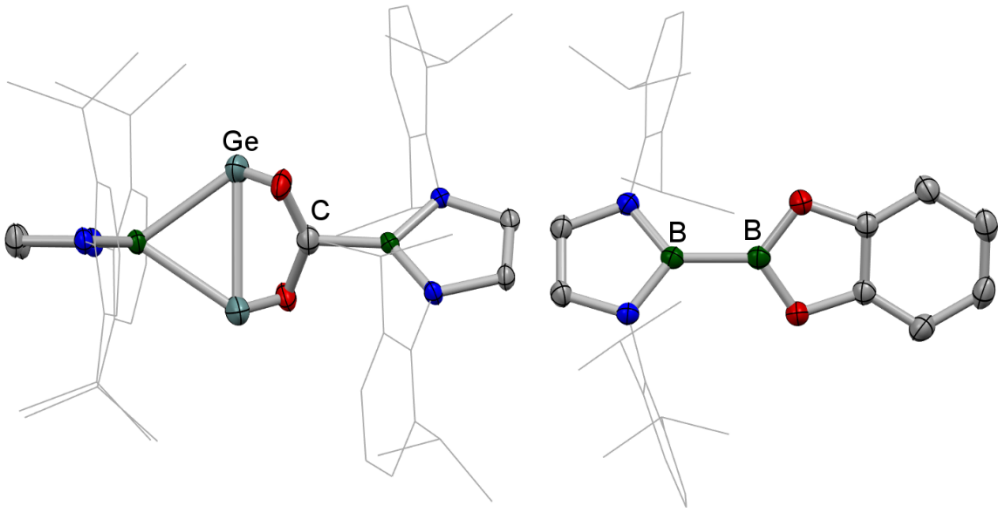


Figure 6.5 *Molecular structures as determined by X-ray crystallography for* ***6.8*** *(left) and* ***6.9*** *(right). Thermal ellipsoid plots are at 40% probability level; Hydrogen atoms are omitted and isopropyl groups are drawn in a wireframe format for clarity.*

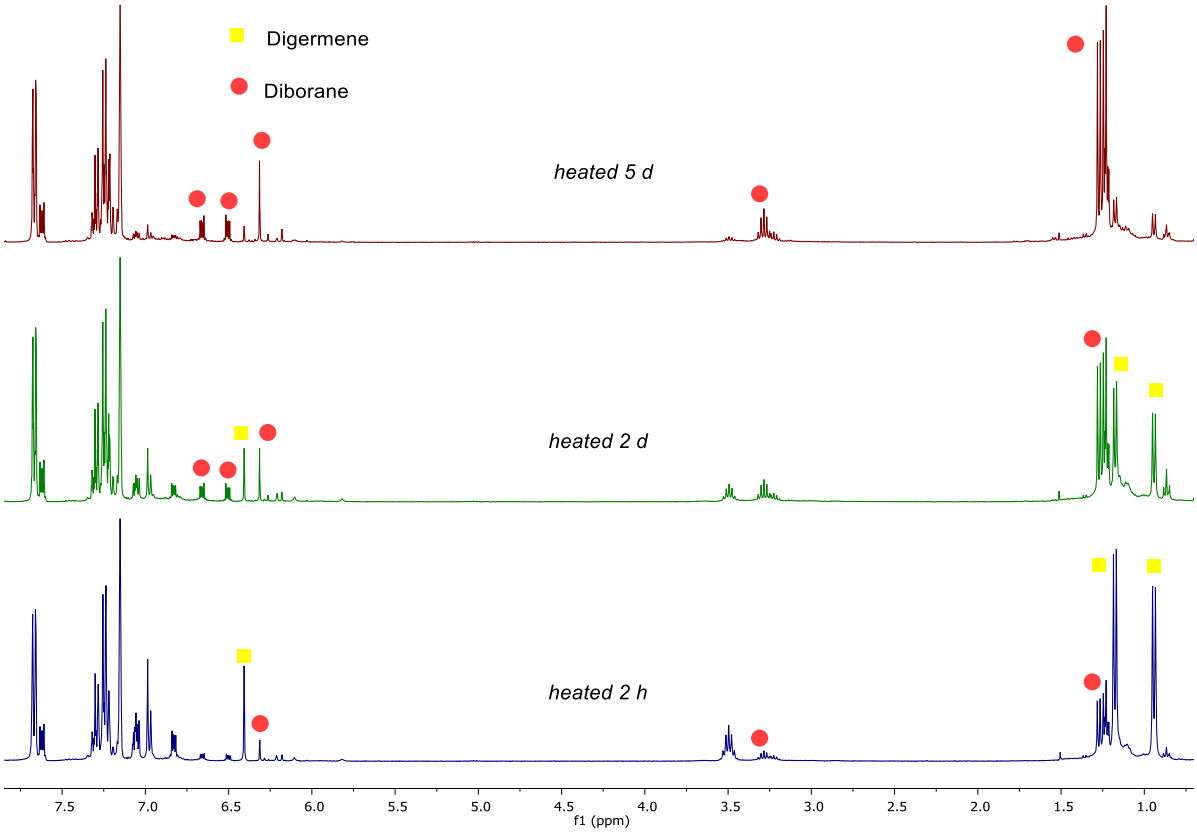


Figure 6.6 *^{1}H NMR Monitoring the thermolysis of digermene* ***6.5*** *to yield diborane* ***6.7****.*

In a related reaction, $[(HCNDipp)_2B]_2Ge_2$ **1.71** and CO were combined at room temperature, giving a product with two different boryl environments (Figure 6.5). However, isolation of this product was not successful due to its unstable nature at ambient temperature. We hypothesize that this initial reaction could give a B-Ge bond insertion product which has precedent in low valent group 14 chemistry. For example, CO can insert into B-Sn bond of $[B]_2Sn$ to give [B]SnC(O)[B] with further boryl group migration generating [B]O([B])C=Sn. We then conducted the reaction of **1.72** with CO at –30 °C, and kept the crystallization tube at –30 °C to try to isolate this new product. Interestingly, the deep red crystals so obtained were found to be $[B]CO_2Ge_2[B]$, **6.8**. (Scheme 6.4) This result has potential implications for the mechanism of the reactivity of digermene **6.5** with CO. We hypothesize that (under reaction conditions) boryl group migration and elimination of the diborane $(Bcat)_2$ are conceivable for digermene **6.5**, yielding $[(HCNDipp)_2B]_2Ge_2$ (**1.71**) as an intermediate. When exposed to CO gas, the low concentration of **1.71** generated can then mimic the reactivity of **1.71** with CO at lower temperature, yielding **6.8** as final product. (Figure 6.6) The mechanism of the conversion of **1.71** to **6.8** is the subject of ongoing DFT calculations in our lab.

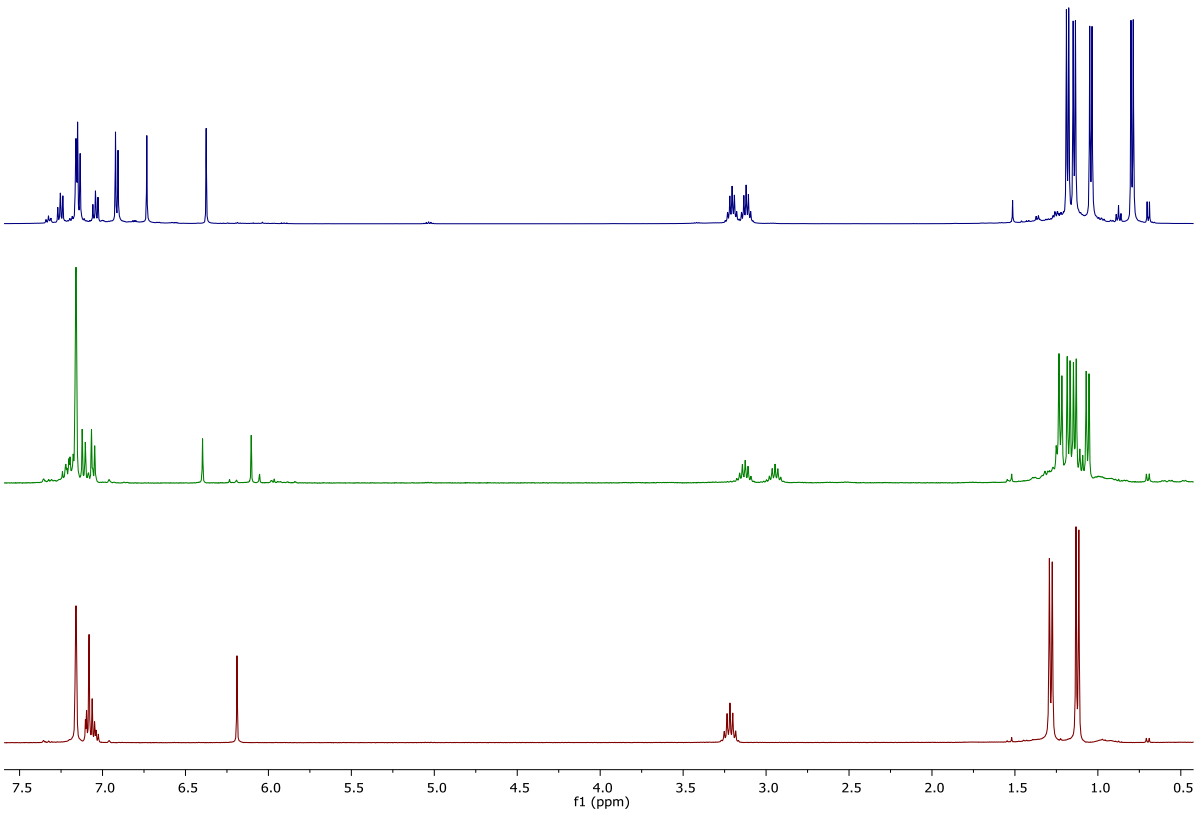


Figure 6.5 *^{1}H NMR comparison between (lower) [(HCNDipp)$_2$B]$_2$Ge$_2$ vinylidene **1.71**, (centre) **1.71** with CO at room temperature and (upper) the product isolated at – 30 ^{o}C.*

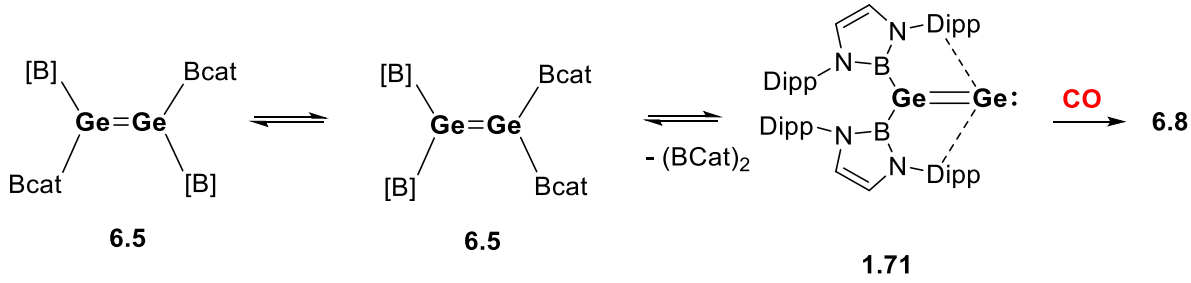


Figure 6.6 *Proposed mechanism for the reactions of digermene **6.5** and [(HCNDipp)$_2$B]$_2$Ge$_2$ vinylidene **1.71** with CO.*

$K_2[B]_2Ge_2$ **1.72** can react with one equivalent of (IPrMe)$GeCl_2$ to form a green compound **6.6** which is postulated to contain a Ge_3 unit. Although crystals suitable for X-ray crystallography of **6.6** could not be obtained, the ^{1}H NMR spectrum shows a 2:1 ratio of two boryl ligands

versus the carbene donor. The shift of the C*H*Me$_2$ unit of carbene to 6.06 ppm also illustrates the coordination of carbene with a germanium centre. More revealingly, **6.6** can also react with BPh_3 to remove the carbene donor to yield a Ge_6 cluster **6.7** (from which can be inferred the composition of **6.6**) (Scheme 6.2). Compound **6.6** was characterized by NMR spectroscopy and X-ray crystallography, and shown to feature a neutral bridged tricyclic structure which can be regarded as two bis-boryl germylene fragments stabilizing a Ge_4 unit. The Ge-Ge bond lengths (2.4635(7) - 2.5012(7) Å) for **6.6** are noticeably stretched compared to those in **1.72**, **6.4** and **6.5**. This $[B]_4Ge_6$ species **6.7** is isostructural with $[B]_4Sn_6$ **5.4** and can serve as a bis-boryl germylene precursor. Initial work attempting to reduce **6.7** in C_6D_6 however only resulted in the formation of protonation product of bisborylgermylene. Future work will focus on using Lewis base donors or small molecules to trap/oxidize the reactive diborylgermylene species. Dienes are not suitable for this case since they can polymerize under reduction conditions. (Scheme 6.5, Figure 6.8)

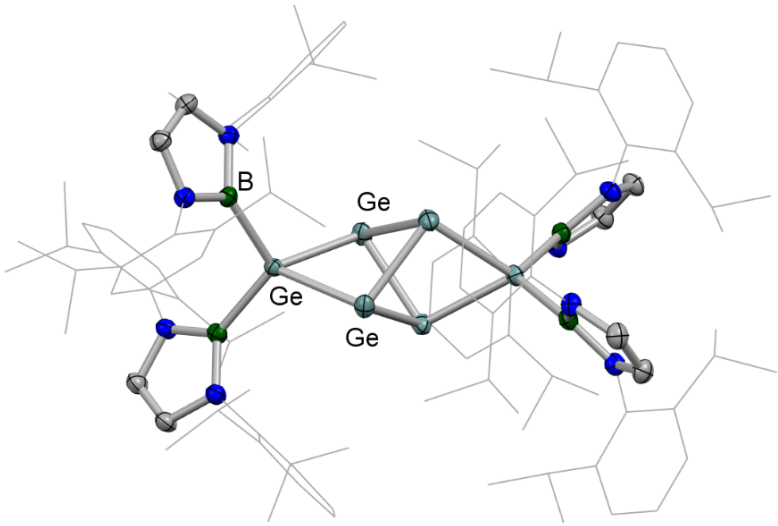
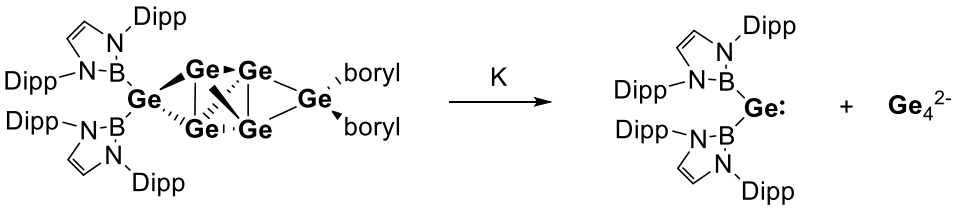


Figure 6.7 *Molecular structure as determined by X-ray crystallography for* ***6.7****. Thermal ellipsoid plots are at 40% probability level; Hydrogen atoms are omitted and isopropyl groups are drawn in a wireframe format for clarity.*



6.7 **6.10**

Scheme 6.6 *Proposed synthesis of bis-boryl germylene from [B]$_4$Ge$_6$ cluster* ***6.7****.*

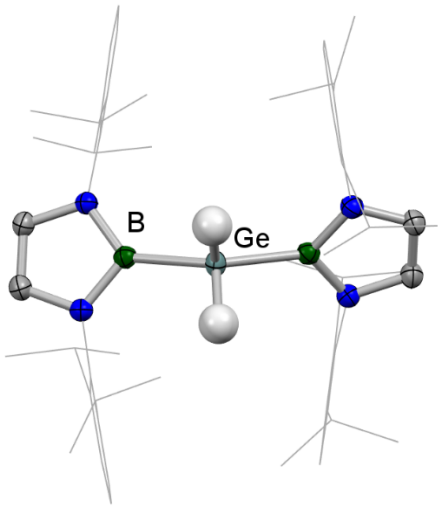


Figure 6.8 *Molecular structures as determined by X-ray crystallography for* ***6.10-H$_2$****. Thermal ellipsoid plots are at 40% probability level; Hydrogen atoms are omitted, and isopropyl groups are drawn in a wireframe format for clarity.*

6.3 Conclusions

In summary, we used $K_2[B]_2Ge_2$ (**1.72**) as nucleophile to react with LiI and catBBr, generating two planar digermene species $Li_2[B]_2Ge_2$ (**6.4**) and [B]BcatGeGeBcat[B] (**6.5**). **6.5** was found to react with CO to form the boryl/borylcarboxylate stabilized digermyne $[B]CO_2Ge_2[B]$ (**6.8**), the mechanism for the formation of which is proposed to go through the bisborylgermavinylidene intermediate. **1.72** can also react with the Ge^{II} electrophile

IPrMeGeCl$_2$ to form a Ge$_3$ unit which leads to the formation of [B]$_4$Ge$_6$ (**6.7**) cluster on abstraction of the carbene.

6.4 Synthesis and characterization of novel compounds

[(HCNTrip)$_2$B]Ge(IPrMe)Cl 6.1

To a suspension of (IPrMe)GeCl$_2$ (0.16 g, 0.48 mmol) in Et$_2$O at -35 ^{o}C was slowly added a pre-cooled (-35 ^{o}C) solution of [(HCNTrip)$_2$B]Li·2THF (0.30 g, 0.48 mmol) in Et$_2$O. After stirring at this temperature for 30 min, the reaction mixture was slowly warmed to room temperature and stirred for another 1 h. The solvent was then removed under vacuum and the residue extracted with toluene. The filtrate was concentrated and triturated with pentane. After storing at -30 ^{o}C overnight, the pale yellow crystalline solid was isolated and dried under vacuum. Yield: 0.28 g, 78 %.

^{1}H NMR (400 MHz, C$_6$D$_6$, 298K): δ_H 1.12 (d, J_{HH} = 5.83 Hz, 6H, CH(C*H$_3$*)$_2$ of carbene), 1.20 (d, J_{HH} = 6.83 Hz, 6H, CH(C*H$_3$*)$_2$ of carbene). 1.28 (m, 24H, *o*-CH(C*H$_3$*)$_2$ and *p*-CH(C*H$_3$*)$_2$ of boryl), 1.38 (d, J_{HH} = 6.83 Hz, 6H, *o*-CH(C*H$_3$*)$_2$ of boryl), 1.57 (s, 6H, CC*H$_3$* of carbene), 1.65 (d, J_{HH} = 6.92 Hz, 6H, *o*-CH(C*H$_3$*)$_2$ of boryl), 2.87 (sept, J_{HH} = 6.88 Hz, 2H, *p*-C*H*(CH$_3$)$_2$ of boryl), 3.49 (sept, J_{HH} = 6.88 Hz, 2H, *o*-C*H*(CH$_3$)$_2$ of boryl), 3.66 (sept, J_{HH} = 6.88 Hz, 2H, *o*-C*H*(CH$_3$)$_2$ of boryl), 5.76 (br, 2H, C*H*(CH$_3$)$_2$ of carbene), 6.30 (s, 2H, C*H* of boryl), 7.11 (d, J_{HH} = 1.97 Hz, 2H, *m*-Ar*H* of Trip), 7.23 (d, J_{HH} = 2.08 Hz, 2H, *m*-Ar*H* of Trip).

^{13}C{^{1}H} NMR (151 MHz, C$_6$D$_6$, 298K): δ_C 9.9 (C$\underline{C}$H$_3$ of carbene), 20.8 (CH($\underline{C}$H$_3$)$_2$ of carbene), 23.5 (C$\underline{C}$H$_3$ of carbene), 24.5 (*p*-CH($\underline{C}$H$_3$)$_2$ of Trip), 26.3 (*o*-CH($\underline{C}$H$_3$)$_2$ of Trip), 26.7 (*o*-CH($\underline{C}$H$_3$)$_2$ of Trip), 28.8 (*o*-$\underline{C}$H(CH$_3$)$_2$ of Trip), 28.9 (*o*-$\underline{C}$H(CH$_3$)$_2$ of Trip), 34.7 (*p*-$\underline{C}$H(CH$_3$)$_2$ of Trip), 52.8 ($\underline{C}$H(CH$_3$)$_2$ of carbene), 121.3 (*m*-Ar), 121.5 (*m*-Ar), 122.4 ($\underline{C}$H of boryl), 126.1

(*C*(CH_3) of carbene), 139.5 (*o*-Ar of Trip), 146.1 (*o*-Ar of Trip), 146.4 (*p*-Ar of Trip), 147.0 (*i*-Ar of Trip), 172.65 (R_2C: of carbene).

$^{11}B\{^1H\}$ NMR (128 MHz, C_6D_6, 25 °C): δ_B 35.8.

For **$K_2[B]_2Ge_2$ 6.2** and **$[B]_2Ge{=}Ge$ 6.3**, the NMR data was not collected due to the small scale of the reaction.

$(IPrMe)_2Li_2[B]_2Ge_2$ 6.4

A mixture of [B]Ge(IPrMe)Cl (0.20 g, 0.29 mmol) and excess KC_8 (0.21 g, 1.6 mmol) was dissolved/suspended in toluene (5 mL) at room temperature. The reaction mixture was sonicated for 2 h with occasional manual agitation, resulting in a brown-coloured solution. The reaction mixture was then filtered into another Schlenk flask filling with LiI (0.04 g, 0.29 mmol). The reaction mixture was stirred for 20 min and filtered. The filtrate was concentrated and layered with hexane (3 mL). Storing at 4 °C overnight gave a dark red crystals suitable for X-ray crystallography, which were isolated, washed with small amount of cold hexane and dried in vacuo. Yield: 0.053 g (0.13 mmol, 28 %).

^1H NMR (400 MHz, C_6D_6, 298K): δ_H 1.24 (d, J_{HH} = 6.9 Hz, 12H, CH(C*H*$_3$)$_2$ of Dipp), 1.29 (24H, CH(C*H*$_3$)$_2$ of Dipp overlapping with CH(C*H*$_3$)$_2$ of carbene), 1.70 (s, 6H, CC*H*$_3$ of carbene), 3.75 (sept, J_{HH} = 6.9 Hz , 4H, C*H*(CH_3)$_2$ of Dipp), 3.89 (sept, J_{HH} = 6.8 Hz , 2H, C*H*(CH_3)$_2$ of carbene), 6.53 (s, 2H, C*H* of boryl), 7.03 (m, 6H, Ar*H* of Dipp).

$^{13}C\{^1H\}$ (151 MHz, C_6D_6, 298K): δ_C 8.9 (C*C*H_3 of carbene), 24.4 (CH(*C*H_3)$_2$ of Dipp), 24.5 (CH(*C*H_3)$_2$ of carbene), 25.1 (CH(*C*H_3)$_2$ of Dipp), 28.7 (*C*H(CH_3)$_2$ of Dipp), 49.2 (*C*H(CH_3)$_2$ of carbene), 120.0 (*C*H of boryl), 122.7 (*m*-Ar of Dipp), 125.3 (*p*-Ar of Dipp), 145.8 (*o*-Ar of Dipp), 148.8 (*i*-Ar of Dipp), other peak for carbene is too broad to be observed.

$^{11}B\{^1H\}$ NMR (128 MHz, C_6D_6, 25 °C): δ_B 43.6.

[B]BcatGeGeBcat[B] 6.5

A mixture of $K_2[B]_2Ge_2$ (20 mg, 0.04 mmol) and (cat)BBr (8.0 mg, 0.04 mmol) in benzene (5 mL) was stirred at room temperature for 1 h. After removal of all volatiles under vacuum, the residuals were extracted with pentane (10 mL) and filtered. Concentration of the filtrate and storage at -30 °C overnight yielded tetraboryldigermene **6.5** as yellow crystals (14 mg, 65 %).

^{1}H NMR (400 MHz, C_6D_6, 298K): δ_H 0.95 (d, J_{HH} = 6.9 Hz, 24H, CH(C*H*$_3$)$_2$ of Dipp), 1.18 (d, J_{HH} = 6.9 Hz, 24H, CH(C*H*$_3$)$_2$ of Dipp), 3.50 (sept, J_{HH} = 6.7 Hz, 8H, C*H*(CH$_3$)$_2$ of Dipp), 6.41 (s, 4H, C*H* of boryl), 6.84 (m, 4H, *p*-Ar*H* of Dipp), 6.98 (m, 8H, *m*-Ar*H* of Dipp), 7.06 (m, 8H, Ar-*H* of BCat)

^{13}C{^{1}H} (151 MHz, C_6D_6, 298K): δ_C 23.2 (CH(*C*H$_3$)$_2$ of Dipp), 26.2 (CH(*C*H$_3$)$_2$ of Dipp), 28.5 (*C*H(CH$_3$)$_2$ of Dipp), 112.6 (OCCH*C*H of BCat), 122.6 (*C*H of boryl), 123.0 (*p*-Ar of Dipp), 123.5 (*m*-Ar of Dipp), 127.7 (OC*C*H of BCat), 139.7 (*i*-Ar of Dipp), 146.3 (*o*-Ar of Dipp), 148.9 (O*C* of BCat).

^{11}B{^{1}H} NMR (128 MHz, C_6D_6, 25 °C): δ_B 28.9, 43.6.

[B]$_2$Ge$_3$(IPrMe) 6.6

To $K_2[B]_2Ge_2$ (0.02 g, 0.02 mmol) in toluene at -35 °C was slowly added a solution of (IPrMe)GeCl (0.006 g, 0.02 mmol) in toluene. After stirring at this temperature for 10 min, the reaction mixture was slowly warmed to room temperature and stirred for another 20 min. The solvent was then removed under vacuum and the residue was extracted with pentane. The filtrate was then dried under vacuum and collected as a brown solid. Yield: 0.015 g, 64 %.

^{1}H NMR (400 MHz, C_6D_6) δ 0.74 (s, 6H, CH(C*H*$_3$)$_2$ of carbene), 1.16, 1.22 and 1.24 (overlapping, 24H, CH(C*H*$_3$)$_2$ of Dipp), 1.44 (CC*H*$_3$ of carbene), 3.58 (br, 4H, C*H*(CH$_3$)$_2$ of

Dipp), 6.06 (br, 1H, C*H*$(CH_3)_2$ of carbene), 6.33 (s, 2H, C*H* of boryl), 7.01 (m, 4H, *m*-Ar*H* of Dipp), 7.11 (m, 2H, *p*-Ar*H* of Dipp).

$^{11}B\{^1H\}$ NMR (128 MHz, C_6D_6, 25 ^oC): δ_B 36.5.

$[B]_4Ge_6$ 6.7

A mixture of $[B]_2Ge_3$(IPrMe) **6.7** (15 mg, 0.013 mmol) and BPh_3 (3.2 mg, 0.013 mmol) was dissolved in C_6D_6 (0.3 mL) at room temperature. After standing for 2 min, the reaction mixture was filtered into a NMR tube and concentrated (to ca. 0.1 mL). 0.5 mL of pentane was then added on top of the filtrate and the mixture left for crystallization overnight. The solution was then decanted and the deep green crystals which were produced were washed with pentane and dried under vacuum. Yield: 7.1 mg, 55.0 %.

Anal. Calc. for $C_{52}H_{72}B_2N_4Ge_3$: C 62.92 %, H 7.31 %, N 5.64 %; Meas.: C 62.34 %, H 7.14 %, N 5.42 %.

^1H NMR (400 MHz, C_6D_6, 298K): δ_H 0.81 (d, J_{HH} = 6.8 Hz, 6H, CH(C*H*$_3$)$_2$ of Dipp), 0.93 (d, J_{HH} = 6.8 Hz, 6H, CH(C*H*$_3$)$_2$ of Dipp), 1.06 (d, J_{HH} = 6.8 Hz, 6H, CH(C*H*$_3$)$_2$ of Dipp), 1.20 (m, 18H, CH(C*H*$_3$)$_2$ of Dipp overlapping), 1.33 (d, J_{HH} = 6.8 Hz, 6H, CH(C*H*$_3$)$_2$ of Dipp), 1.57 (d, J_{HH} = 6.8 Hz, 6H, CH(C*H*$_3$)$_2$ of Dipp), 2.41 (sept, J_{HH} = 6.8 Hz, 2H, C*H*$(CH_3)_2$ of Dipp), 2.53 and 2.57 (m, 4H, C*H*$(CH_3)_2$ of Dipp overlapping), 3.57 (sept, J_{HH} = 6.8 Hz, 2H, C*H*$(CH_3)_2$ of Dipp), 5.83 and 5.91 (d, J_{HH} = 2.3 Hz, 4H, C*H* of boryl), 7.11 (m, 2H, Ar*H* of Dipp), 7.17 (m, 4H, Ar*H* of Dipp overlapping with C_6D_6), 7.30 (m, 6H, Ar*H* of Dipp).

$^{13}C\{^1H\}$ (151 MHz, C_6D_6, 298K): δ_C 22.6, 23.8, 27.1, 27.3 and 27.5 (CH(<u>C</u>H$_3$)$_2$ of Dipp), 27.9, 28.1, 28.8 and 29.2 (<u>C</u>H$(CH_3)_2$ of Dipp), 123.5 and 123.8 (<u>C</u>H of boryl), 124.0 and 124.9 (*p*-Ar of Dipp), 125.0 and 125.1 (*m*-Ar of Dipp), 139.9, 141.7, 145.0 and 145.5 (*o*-Ar of Dipp), 147.2 and 148.7 (*i*-Ar of Dipp).

$^{11}B\{^{1}H\}$ NMR (128 MHz, C_6D_6, 25 ^{o}C): δ_B 33.3.

[B]CO_2Ge_2[B] 6.8

Digermene **6.5** (10 mg, 0.017 mmol) was dissolved in C_6D_6 in a J-Young NMR tube. The resulting solution was subjected to three freeze-pump-thaw cycles before backfilling with CO (ca. 1 atm). The solution was then dried under vacuum and the residue was extracted into pentane. The filtrate was transferred into a crystallization tube which gave deep red crystals after several days. The crystals were separated by filtration, washed with pentane and dried in vacuum to afford the product. Yield: 7.1 mg, 85 %.

^{1}H NMR (400 MHz, C_6D_6, 298K): δ_H 0.79 (d, J_{HH} = 6.8 Hz, 12H, CH(C*H*$_3$)$_2$ of Dipp), 1.04 (d, J_{HH} = 6.8 Hz, 12H, CH(C*H*$_3$)$_2$ of Dipp), 1.15 (d, J_{HH} = 6.8 Hz, 12H, CH(C*H*$_3$)$_2$ of Dipp), 1.18 (d, J_{HH} = 6.8 Hz, 12H, CH(C*H*$_3$)$_2$ of Dipp), 3.12 (sept, J_{HH} = 6.8 Hz, 4H, C*H*(CH$_3$)$_2$ of Dipp), 3.21 (sept, J_{HH} = 6.8 Hz, 4H, C*H*(CH$_3$)$_2$ of Dipp), 6.38 (s, 2H, C*H* of boryl-CO_2),) 6.73 (s, 2H, C*H* of boryl-Ge_2), 6.91 (m, 4H, *m*-Ar*H* of Dipp), 7.04 (m, 2H, *p*-Ar*H* of Dipp), 7.14 (m, 4H, *m*-Ar*H* of Dipp), 7.25 (m, 2H, *p*-Ar*H* of Dipp).

^{13}C NMR (126 MHz, C_6D_6) δ 23.1, 23.9, 25.0 and 26.4 (CH(<u>C</u>H$_3$)$_2$ of Dipp), 28.5 and 28.7 (<u>C</u>H(CH$_3$)$_2$ of Dipp), 119.2 (<u>C</u>H of boryl), 123.8 and 124.0 (*m*-Ar of Dipp), 125.9 (<u>C</u>H of boryl), 127.4 (*p*-Ar of Dipp), 135.8 (*i*-Ar of Dipp), 139.1 and 140.1 (*i*-Ar of Dipp), 146.5 (*o*-Ar of Dipp), peak for <u>C</u>O_2 unit cannot be found.

$^{11}B\{^{1}H\}$ NMR (128 MHz, C_6D_6, 298 K): δ_B 28.9 (B-CO_2) and 39.2 (B-Ge_2).

Table 6.1 *Selected crystallographic and refinement data for* ***6.3-6.10****.*

	6.3	**6.4·(C_5H_{12})**	**6.5**
Formula	$C_{64}H_{96}B_2Ge_2N_4$	$C_{79}H_{124}B_2Ge_2Li_2N_8$	$C_{64}H_{80}B_4Ge_2N_4O_4$
Fw	1088.24	1366.53	1157.74
Crystal System	Orthorhombic	Monoclinic	Triclinic
Space Group	P b c n	I 1 2/a 1	P -1
Wavelength/Å	1.54184	1.54184	1.54184
a/Å	20.5825(3)	21.8726(8)	11.9393(2)
b/Å	15.68147(17)	16.5014(3)	22.4852(2)
c/Å	19.5602(2)	25.3097(7)	36.1463(5)
α/°	90	90	99.1440(10)
β/°	90	114.994(4)	94.3580(10)
γ/°	90	90	92.4280(10)
Volume/Å^3	6313.33(13)	8279.5(5)	9538.1(2)
Z	4	4	6
Temperature/K	150(2)	150(2)	150(2)
Reflections collected	6581	8516	39407
$2\vartheta_{max}$	152.704	148.542	135.368
R_{int}	0.0221	0.0557	0.0403
Goodness of fit	1.053	1.018	1.055
$R[F^2>2\sigma]$, F	0.0323	0.0469	0.0477
R_w(all data), F^2	0.0925	0.1248	0.1261

	6.7·1.5(C_5H_{12})	**6.8**	**6.9**
Formula	$C_{111.5}H_{162}B_4Ge_6N_8$	$C_{53}H_{72}B_2Ge_2N_4O_2$	$C_{32}H_{40}B_2N_2O_2$
Fw	2093.26	963.94	506.28
Crystal System	Monoclinic	Monoclinic	Monoclinic
Space Group	P 1 21/c 1	P 1 21/c 1	P 1 21/c 1
Wavelength/Å	1.54184	1.54184	1.54184
a/Å	25.2248(2)	21.8673(3)	16.5820(2)
b/Å	18.00870(10)	12.3562(2)	11.08990(10)
c/Å	25.7262(2)	19.5602(2)	16.7948(2)
α/°	90	90	90
β/°	109.0900(10)	97.191(2)	105.5900(10)
γ/°	90	90	90
Volume/Å^3	11043.84(15)	5274.52(16)	2974.82(6)
Z	4	4	4
Temperature/K	150(2)	150(2)	150(2)
Reflections collected	22995	10937	6152
$2\vartheta_{max}$	152.53	152.718	152.268
R_{int}	0.0877	0.0425	0.0225
Goodness of fit	1.009	1.091	1.038
$R[F^2>2\sigma]$, F	0.0355	0.0656	0.0408
R_w(all data), F^2	0.0883	0.2045	0.1105

	6.10-H_2O
Formula	$C_{52}\,H_{74}\,B_2\,Ge\,N_4\,O_{0.45}$
Fw	856.64
Crystal System	Monoclinic
Space Group	P 1 21/c 1
Wavelength/Å	1.54184
a/Å	12.63900(10)
b/Å	20.48760(10)
c/Å	19.77430(10)
α/°	90
β/°	94.4480(10)
γ/°	90
Volume/Å^3	5104.99(5)
Z	4
Temperature/K	150(2)
Reflections collected	10635
$2\vartheta_{max}$	152.938
R_{int}	0.0565
Goodness of fit	1.021
$R[F^2>2\sigma]$, F	0.0343
R_w(all data), F^2	0.0963

6.5 Computational Details

All computational work reported here was performed using ORCA (Revision 5.0.3).[17] All computational work was first optimised using the meta-generalized-gradient approximation (mGGA) functional R2-SCAN[18] which was employed in conjunction with the Def2-TZVPPm[19] basis set with the D4 dispersion correction[20] and the employing the geometrical counterpoise correction gCP[21] (together known as the R2SCAN-3c method).[19] Alongside this the Conductor-like Continuum Polarization Model (CPCM) was used to approximate benzene solvation.[22] The nature of the stationary points, minima was confirmed by full frequency calculations, and are characterized by zero imaginary frequencies. Time dependent density functional theory (TDDFT) was performed with the optimized coordinates with the hybrid M062x[23] functional in conjunction with the Def2-TZVP[24] basis set with D30 dispersion correction,[25] Natural transition orbitals (NTO) generated by the ORCA program.

6.6 References

1. Gusel'nikov, L. E.; Nametkin, N. S., Formation and properties of unstable intermediates containing multiple p.pi.-p.pi. bonded Group 4B metals. *Chem. Rev.* **1979,** *79* (6), 529-577.
2. Jutzi, P., New Element-Carbon (p-p)π Bonds. *Angew. Chem., Int. Ed.* **1975,** *14* (4), 232-245.
3. West, R., Chemistry of the Silicon-Silicon Double Bond. *Angew. Chem., Int. Ed.* **1987,** *26* (12), 1201-1211.
4. Goldberg, D. E.; Harris, D. H.; Lappert, M. F.; Thomas, K. M., A new synthesis of divalent group 4B alkyls M[CH(SiMe$_3$)$_2$]$_2$ (M = Ge or Sn), and the crystal and molecular and molecular strcuture of the tin compound. *J. Chem. Soc., Chem. Commun.* **1976,** (7), 261-262.
5. West, R.; Fink, M. J.; Michl, J., Tetramesityldisilene, a Stable Compound Containing a Silicon-Silicon Double Bond. *Science* **1981,** *214* (4527), 1343-1344.
6. Brook, A. G.; Abdesaken, F.; Gutekunst, B.; Gutekunst, G.; Kallury, R. K., A solid silaethene: isolation and characterization. *J. Chem. Soc., Chem. Commun.* **1981,** (4), 191-192.
7. Yoshifuji, M.; Shima, I.; Inamoto, N.; Hirotsu, K.; Higuchi, T., Synthesis and structure of bis(2,4,6-tri-tert-butylphenyl)diphosphene: isolation of a true phosphobenzene. *J. Am. Chem. Soc.* **1981,** *103* (15), 4587-4589.
8. Power, P. P., Main-group elements as transition metals. *Nature* **2010,** *463*, 171.
9. Trinquier, G., Double bonds and bridged structures in the heavier analogs of ethylene. *J. Am. Chem. Soc.* **1990,** *112* (6), 2130-2137.
10. Sekiguchi, A.; Tanaka, T.; Ichinohe, M.; Akiyama, K.; Tero-Kubota, S., Bis(tri-tert-butylsilyl)silylene: Triplet Ground State Silylene. *J. Am. Chem. Soc.* **2003,** *125* (17), 4962-4963.
11. Lee, V. Y.; McNeice, K.; Ito, Y.; Sekiguchi, A., A blue digermene (^{t}Bu$_2$MeSi)$_2$Ge Ge(SiMe^{t}Bu$_2$)$_2$. *Chem. Commun.* **2011,** *47* (11), 3272-3274.
12. Rit, A.; Campos, J.; Niu, H.; Aldridge, S., A stable heavier group 14 analogue of vinylidene. *Nat. Chem.* **2016,** *8* (11), 1022-1026.

13. Iwamoto, T.; Okita, J.; Yoshida, N.; Kira, M., Structure and Reactions of an Isolable Ge=Si Doubly Bonded Compound, Tetra(t-butyldimethylsilyl)germasilene. *Silicon* **2010,** *2* (4), 209-216.
14. Kira, M.; Iwamoto, T.; Maruyama, T.; Kabuto, C.; Sakurai, H., Tetrakis(trialkylsilyl)digermenes. Salient Effects of Trialkylsilyl Substituents on Planarity around the GeGe Bond and Remarkable Thermochromism. *Organometallics* **1996,** *15* (18), 3767-3769.
15. Cordero, B.; Gómez, V.; Platero-Prats, A. E.; Revés, M.; Echeverría, J.; Cremades, E.; Barragán, F.; Alvarez, S., Covalent radii revisited. *Dalton Trans.* **2008,** (21), 2832-2838.
16. Sidiropoulos, A.; Jones, C.; Stasch, A.; Klein, S.; Frenking, G., N-Heterocyclic Carbene Stabilized Digermanium(0). *Angew. Chem., Int. Ed.* **2009,** *48* (51), 9701-9704.
17. (a) Neese, F., The ORCA program system. *WIREs Comput. Mol. Sci.* **2012,** 2, 73-78; (b) Neese, F.; Wennmohs, F.; Becker, U.; Riplinger, C., The ORCA quantum chemistry program package. *J. Chem. Phys.* **2020,** 152, 224108; (c) Neese, F., Software update: the ORCA program system, version 4.0. *WIREs Comput. Mol. Sci.* **2018,** 8, e1327.
18. (a) Furness, J. W.; Kaplan, A. D.; Ning, J.; Perdew, J. P.; Sun, J., Accurate and Numerically Efficient r^{2}SCAN Meta-Generalized Gradient Approximation. *J. Phys. Chem. Lett.* **2020,** 11, 8208-8215; (b) Furness, J. W.; Kaplan, A. D.; Ning, J.; Perdew, J. P.; Sun, J., Correction to "Accurate and Numerically Efficient r^{2}SCAN Meta-Generalized Gradient Approximation". *J. Phys. Chem. Lett.* **2020,** 11, 9248-9248.
19. Grimme, S.; Hansen, A.; Ehlert, S.; Mewes, J.-M., r^{2}SCAN-3c: A "Swiss army knife" composite electronic-structure method. *J. Chem. Phys.* **2021,** 154, 064103.
20. (a) Caldeweyher, E.; Bannwarth, C.; Grimme, S., Extension of the D3 dispersion coefficient model. *J. Chem. Phys.* **2017,** 147, 034112; (b) Caldeweyher, E.; Ehlert, S.; Hansen, A.; Neugebauer, H.; Spicher, S.; Bannwarth, C.; Grimme, S., A generally applicable atomic-charge dependent London dispersion correction. *J. Chem. Phys.* **2019,** 150, 154122.
21. Kruse, H.; Grimme, S., A geometrical correction for the inter- and intra-molecular basis set superposition error in Hartree-Fock and density functional theory calculations for large systems. *J. Chem. Phys.* **2012,** 136, 154101.
22. Barone, V.; Cossi, M., Quantum Calculation of Molecular Energies and Energy Gradients in Solution by a Conductor Solvent Model. *J. Phys. Chem. A.* **1998,** 102, 1995.
23. Weigend, F.; Ahlrichs, R., Balanced basis sets of split valence, triple zeta valence and quadruple zeta valence quality for H to Rn: Design and assessment of accuracy. *Phys. Chem. Chem. Phys.* **2005,** 7, 3297.
24. Weigend, F., Accurate Coulomb-fitting basis sets for H to Rn. *Phys. Chem. Chem. Phys.* **2006,** 8, 1057.
25. Grimme, S.; Antony, J.; Ehrlich, S.; Krieg, H., A consistent and accurate ab initio parametrization of density functional dispersion correction (DFT-D) for the 94 elements H-Pu. *J.Chem.Phys.* **2010,** 132, 154104.